Technical Basis Document No. 1: Climate and Infiltration

Revision 1

CONTENTS

CONTENTS (Continued)

FIGURES

FIGURES (Continued)

TABLES

ACRONYMS

AIN	additional information needed
DOE	U.S. Department of Energy
DRI	Desert Research Institute
ESF	Exploratory Studies Facility
KTI	Key Technical Issue
NRC	U.S. Nuclear Regulatory Commission
TSPA	total system performance assessment
TSPAI	Total System Performance Assessment and Integration
USFIC	Unsaturated and Saturated Flow under Isothermal Conditions
USGS	U.S. Geological Survey

INTENTIONALLY LEFT BLANK

1. INTRODUCTION

1.1 OVERVIEW

This technical basis document is one in a series being prepared for each component of the Yucca Mountain repository system relevant to its design and postclosure performance. The components are illustrated in Figure 1-1.
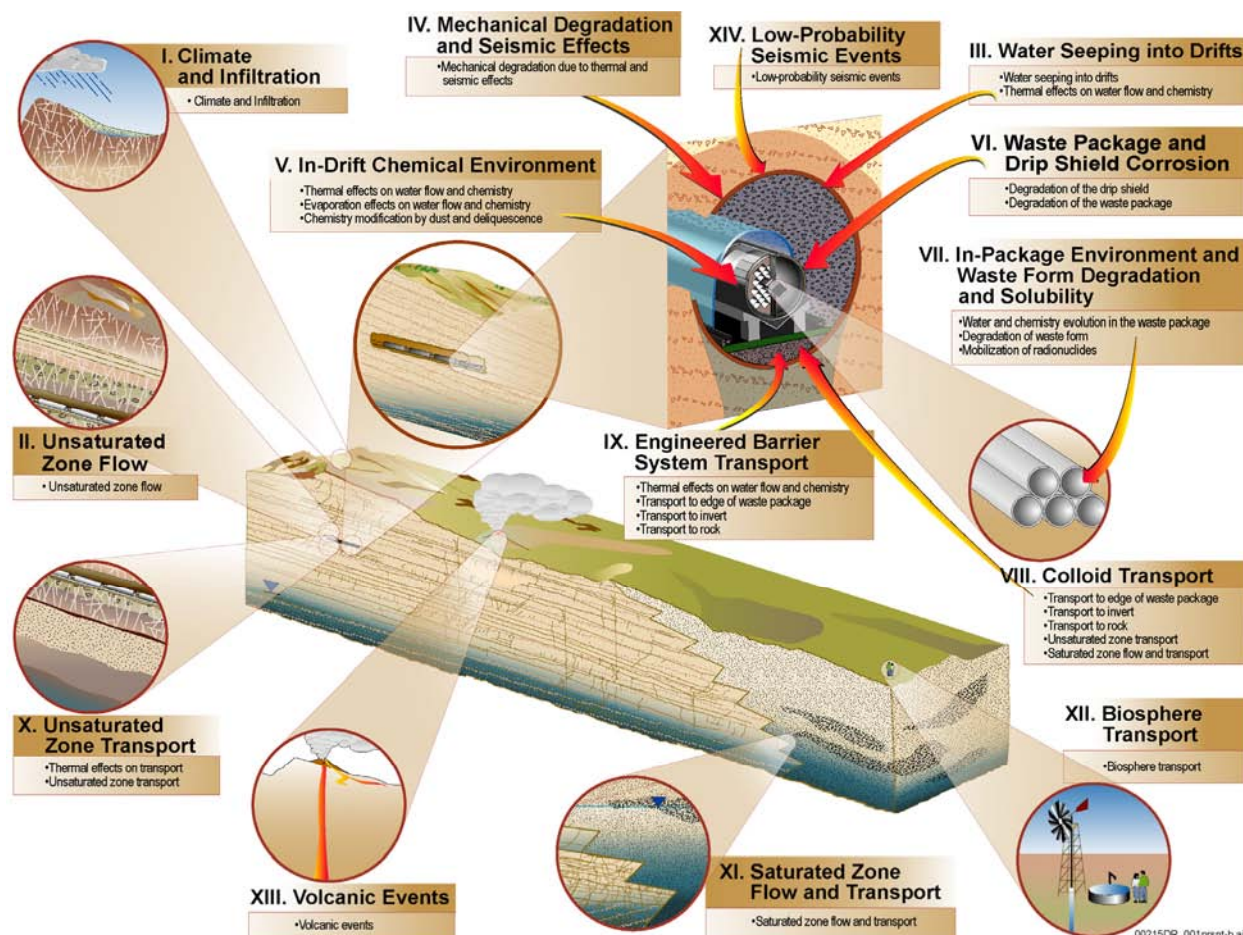
Figure 1-1. Components of the Postclosure Technical Basis for the License Application

Climate controls the range of precipitation and temperature conditions at the land surface. The surface conditions (e.g., runoff, run-on, evapotranspiration) impact the rate of infiltration into the subsurface. Infiltration is defined as the flow of surface water downward across the atmosphere–soil or the atmosphere–bedrock interface (Flint, A.L. et al. 1996, p. 8). Net infiltration, which is the flow of water downward (i.e., drainage) below the root zone, controls deep percolation through the unsaturated zone. Percolation determines seepage that is important to the waste package performance, as well as groundwater recharge. Present-day and future infiltration is a key hydrologic parameter needed for design of the repository in the unsaturated zone at Yucca Mountain. The understanding of present-day infiltration is needed to provide initial conditions for predictions of future hydrologic changes, in association with climate predictions.

To forecast the future climate conditions at Yucca Mountain, the following types of paleoclimate records, representing different time scales, were used: (1) regional records of stable isotope δ^{18}O fluctuations from Devils Hole, Nevada, and microfossil data from Owens Lake, California; (2) vegetation assemblages recovered from local packrat nests (i.e., midden); and (3) global records of an earth-orbital clock of precession and eccentricity and Vostok (Antarctica) ice core isotopic compositions. The stable isotope compositions are typically reported in delta, δ, notation as the parts per million deviation of the ratio of the heavy to light isotopes (^{18}O/^{16}O) in the sample to that of a standard, VSMOW (Vienna standard mean ocean water, for ^{18}O/^{16}O) (USGS 2001a, p. 27). The global records show that climate is cyclic over 400,000-year periods. The estimation of the future climate states at Yucca Mountain for the period from the present to 10,000 years was provided by the U.S. Geological Survey (USGS) (USGS 2001a) and by the Desert Research Institute (DRI) (Sharpe 2002; Sharpe 2003).

Three potential climate states (interglacial, monsoon, and glacial transition) are forecast for the next 10,000 years based on the examination of past proxy climate records, including ostracode and diatom assemblages recovered from the Owens Lake core (USGS 2001a; Sharpe 2003). The interglacial climate state is comparable to the relatively warm present-day climate state. The monsoon climate state is characterized by hot summers with increased summer rainfall relative to the present-day climate. The glacial-transition (or intermediate) climate state has cooler and wetter summers and winters relative to the present-day climate state.

Both USGS (2001a, p. 26) and DRI reports (Sharpe 2003, Table 6-1, p. 56) confirm the existence of a long-term, interglacial climate state similar to modern for at least the last 9,000 years before present. The DRI analysis estimated the duration of interglacial climate from 12,000 years before present (11,600 years before present in Sharpe 2002, Table 6-1, before rounding off) to 1,000 years before present. Within the regulatory period of 10,000 years, no full glacial climate regime is expected.

The timing of the climate intervals for the next 10,000 years is forecast on the basis of theoretically supported assumptions:

- Climate conditions are (USGS 2001a, p. 62): (a) cyclic, (b) can be timed with the earth's orbital clock, and (c) repeat themselves in a predictable way.

- The time of the transition from marine isotope stages 11 and 10 (see Section 2.1) is selected as the analog to estimate climate for the next 10,000 years.

- Ostracode species assemblages from the Owens Lake record for this time period and the sediment accumulation rate are used to determine the nature and timing for the three future climate states (USGS 2001a, p. 67).

Forecasting of climatic data indicates that during the next 10,000 years at Yucca Mountain, the present-day climate should persist for 400 to 600 years, followed by a warmer and wetter monsoon climate for 900 to 1,400 years, followed by a cooler and wetter glacial-transition climate for the remaining 8,000 to 8,700 years (USGS 2001a, p. 76).

Thompson et al. (1999, Table 4, Figures 16 and 17) reported the following for the Yucca Mountain region: (1) a mean annual precipitation of 125 mm and a mean annual temperature of 13.4ºC for the present-day conditions and (2) using analog-based precipitation estimates, the mean annual precipitation for the last glacial maximum was approximated to be from 266 to 321 mm/yr, which is 2 to 2.5 times the modern value, and the mean annual temperature was 7.9ºC to 8.5ºC, which is 4.9ºC to 5.5ºC cooler than the modern value. The glacial-transition climate lower–bound precipitation values exceed the present-day lower-bound values by about 150 mm (USGS 2001a, Section 6.6.2). Thus, much of the future climate (based on this analysis) is wetter and cooler than the present-day climate.

Climatic conditions are key for estimating net infiltration in the unsaturated zone. Net infiltration is defined as water drainage below the bottom of the root system and occurs in the soil or the welded bedrock of the Tiva Canyon Tuff (Tpc), which is the most extensively exposed bedrock unit at Yucca Mountain.

Intensive surface-based investigations at Yucca Mountain started in the early 1980s (Wang and Bodvarsson 2003), which have resulted in a number of conceptual models of infiltration (Flint, A.L. et al. 2001) and infiltration predictions for the present-day and future climates, using time-series data from a number of climate analog sites (Flint, A.L. et al. 2001; Hevesi et al. 2003). To represent the large-scale (volume-averaged) Yucca Mountain infiltration processes, the conceptual and numerical models of infiltration involve a number of simplifications (the validity of these simplifications is discussed in Section 4.2), such as:

- Describing infiltration using the water balance (bucket-type) model for one-dimensional piston-like flow

- Neglecting nonlinear effects in partially saturated soils and fractured rock, lateral flow at the soil–rock interface, preferential flow through heterogeneous soils and fractures, flow under conditions where the soil moisture content is below the field capacity, and redistribution of water caused by fracture–matrix interaction

- Using empirical relationships for saturated and unsaturated hydraulic conductivity and water retention, evapotranspiration, surface runoff, and surface run-on.

Based on the results of numerical simulations, maps were prepared of steady-state net infiltration for the present-day, monsoon, and glacial-transition climate states, including lower-bound, mean, and upper-bound conditions for each of the states, over the Yucca Mountain region. These maps were then used to calculate the steady-state infiltration rates averaged over space and time for each of the climate scenarios (USGS 2001b).

The net infiltration rates obtained for the present-day climate compare reasonably with those from corroborative studies, including geochemical and temperature measurements in the unsaturated zone, as well as groundwater recharge. This comparison provides a validation of net infiltration modeling results.

Experimental and modeling studies show that a spatial and temporal variation in net infiltration at Yucca Mountain is caused by episodic storm and precipitation events (Hevesi et al. 2002), as

well as the heterogeneous nature of topsoil and topography. Near-surface infiltration data (USGS 2001b) suggest that significant infiltration occurs only every few years. In very wet years, infiltration in major drainages (where flow is concentrated) can increase to hundreds of millimeters per year during a relatively short time. Current estimates indicate an average infiltration rate of about 5 mm/yr, with values ranging as high as 20 mm/yr near the ridge top of Yucca Mountain (USGS 2001b).

Because long-term variations in climate occur, changes in net infiltration for future climates will occur as well. Predictions of spatio-temporal distribution of net infiltration for different climate states are likely to contain uncertainties associated with the selection of climate analog sites and corresponding records of precipitation and temperature (NRC 1997). The correlation analysis revealed that net infiltration is mostly dependent on precipitation, soil depth, bedrock permeability, and potential evapotranspiration (BSC 2003a). Because it is not possible to foresee every condition that could occur over the 10,000-year regulatory period, it is necessary to evaluate a range of possible scenarios to ensure that predictions of net infiltration are conservatively bounded within each of the climate scenarios predicted for the Yucca Mountain region (see Section 4.3).

1.2 SIGNIFICANCE OF NET INFILTRATION FOR TOTAL SYSTEM PERFORMANCE ASSESSMENT

The evaluation of net infiltration is needed for assessing the nominal scenario of the repository system in total system performance assessment (TSPA) (DOE 2002a, Vol. II).

The net infiltration is used as input in the prediction of deep percolation flux, the extent of perched-water zones, water transport time through the unsaturated zone, and potential seepage into waste emplacement drifts. Quantitative estimates of net infiltration under present-day and future climatic conditions define the upper-boundary condition of unsaturated zone flow models, which provide input to the TSPA (DOE 1998, Volume 3, Figure 2-1).

The evaluation of net infiltration is also potentially important for the estimation of radiation doses and biosphere dose conversion factors, in the event of using contaminated groundwater for irrigation (Williams 2001) and in the event of the igneous groundwater contamination scenario.

The incorporation of infiltration uncertainty analysis under different climate scenarios is required to support TSPA for the license application, as outlined in the *Total System Performance Assessment-License Application Methods and Approach* (BSC 2002a, Section 3.1).

1.3 OBJECTIVES AND SCOPE

This document summarizes the results of forecasting the climatic conditions and the evaluation of net infiltration at Yucca Mountain, based on the results of field, laboratory, and modeling studies, as well as associated uncertainties for the present-day and future monsoon and glacial-transition climates.

The scope of the document includes:

- Analysis of present-day and future climatic conditions, including the selection of climate analogs (Section 2)

- Analysis of the dominant factors and processes affecting net infiltration (Section 3)

- Basis for the modeling approach, validation of the conceptual model, and the analysis from the results of simulating net infiltration for present-day and potential future climatic conditions (Section 4)

- Discussion of the results of corroborative experimental studies conducted for estimating net infiltration (Section 5)

- The uncertainty analysis of net infiltration (Section 6)

- Conclusions (Section 7).

Appendices to this document include the response to open Key Technical Issues (KTIs) imposed by the U.S. Nuclear Regulatory Commission (NRC), which are related to the evaluation of net infiltration rate (Table 1-1).

Table 1-1. Key Technical Issues Addressed in This Report

KTI Agreement/AIN	Short Description	Appendix
TSPAI 3.18 AIN-1	Water balance, Richards equation	A
TSPAI 3.19 AIN-1	Evapotranspiration	B
TSPAI 3.21 AIN-1	Soil lateral flow	C
USFIC 3.01 AIN-1	Monte Carlo analysis of infiltration uncertainty	D
USFIC 3.02 AIN-1	Parameters of infiltration uncertainty analysis	E

1.4   ENVIRONMENTAL CONDITIONS OF THE YUCCA MOUNTAIN SITE

Physiographic Setting and Topography–Yucca Mountain is located within a transition zone between the northern boundary of the Mojave Desert and the southern boundary of the Great Basin Desert (Flint, A.L. et al. 1996, pp. 43 to 44). Physiographic subdivision of the Yucca Mountain area is shown in Figure 1-2. The topography of the Great Basin is characterized by isolated, long and narrow, roughly north-south-trending mountain ranges and broad intervening valleys. The topography at Yucca Mountain includes: ridge tops (about 7 percent), side slopes (about 47 percent, including footslopes), terraces (about 44 percent), and channels (about 2 percent) (Flint, L.E. and Flint 1995, pp. 2 to 6; Flint, A.L. et al. 1996, pp. 38 and 39). The ridge tops generally are flat to gently sloping, with soils 0.5 to 2 m (1.6 to 6.6 ft) thick. Terraces and channels are located at lower elevations of primary washes and have thin soil cover in the upper washes and thick soils farther down. The surface elevations above the site of the repository are approximately 1,400 m.

Source: Simmons 2004, Figure 8-2.

Figure 1-2. Geographic and Prominent Topographic Features of the Death Valley Region
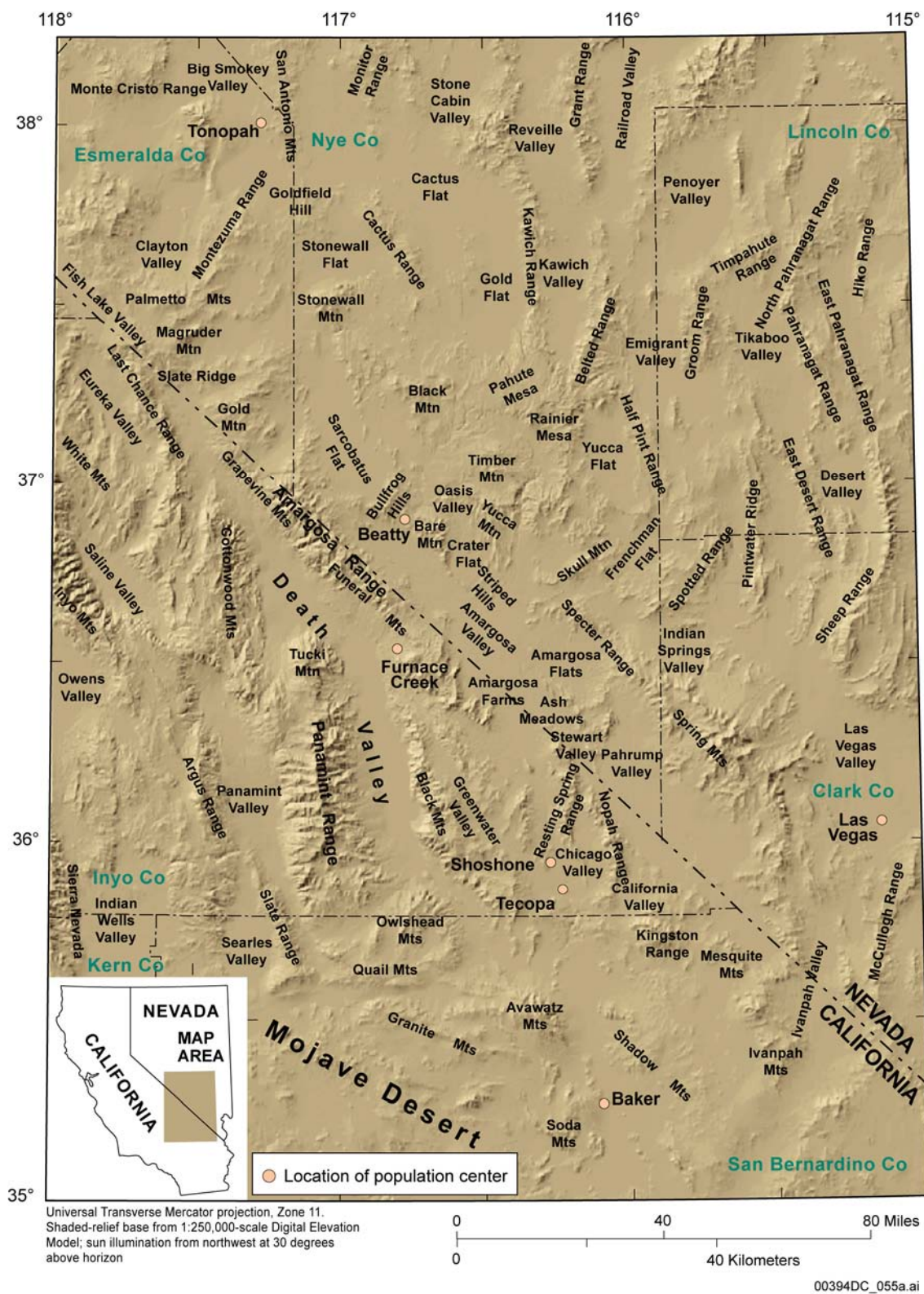
The surface has been shaped by erosional processes on the eastward-sloping ridge of the mountain and along faults and fault scarps that have created a series of washes downcut to varying degrees into different bedrock layers. Slopes are locally steep on the west-facing escarpments eroded along the faults and in some of the valleys that cut into the more gentle eastward-facing dip slopes. Narrow valleys and ravines are cut in bedrock; wider valleys are covered by alluvial deposits with terraces cut by intermittent streams. Locally, small sandy fans extend down the lower slopes and spread out on the valley floors. East of the crest of Yucca Mountain, drainage is into Fortymile Wash; west of the crest, streams flow southwestward down fault-controlled canyons and discharge into Crater Flat (see Figure 1-2).

The topography is different to the south and north of Drill Hole Wash (see Figures 1-3 and 1-4). The washes in the southern area trend eastward, are relatively short (less than 2 km), and have erosional channels with gently sloping sides. The washes north of Drill Hole Wash (e.g., Yucca Wash) trend northwest, are relatively longer (3 to 4 km) because they are controlled by fault features, and have steeper side slopes. The locations of Yucca Mountain watersheds are shown in Figure 1-3.

Climate–In general, the present-day climate of Nevada is characterized as semiarid to arid. Currently, Nevada's climate is being developed under the influence of dry winds entering Nevada and providing reduced precipitation. Mountain systems to the west cause a rain shadow effect. Moisture-laden winds traveling east from the Pacific Ocean rise, cool, and cause precipitation in the mountain systems west of Nevada.

The most important climatic factors affecting water-transport processes in the unsaturated zone are solar radiation flux, diurnal and seasonal temperature cycles, relative humidity, and precipitation, in the form of either rain or snow, as well as extended periods of drought. Current climatic conditions for the site and the Yucca Mountain region are discussed in detail in the *Yucca Mountain Site Description* (Simmons 2004, Section 6). The Yucca Mountain Project environmental program collected site meteorological data using a network of nine automated weather stations (Simmons 2004, Section 6.2).

Average annual precipitation over the area of the Nevada Test Site ranges from a maximum of 370 mm (14.57 in.) in the Belted Range to a minimum of 110 mm (4.33 in.) in the Amargosa Desert. Annual precipitation within the repository area ranges from a minimum of about 100 mm (3.94 in.) at low elevations along the southern boundary to a maximum in excess of 300 mm (11.8 in.) at high elevations in the north (Simmons 2004, Figure 7-6). Based on the analysis of data from 114 precipitation stations in the Yucca Mountain region, which provides at least 8 years of complete record, a strong positive correlation between average annual precipitation and station elevation was found (Simmons 2004, Figure 7-7). These results indicate that the zones of maximum precipitation are likely to correspond to the zones of higher elevations of the mountain ranges.
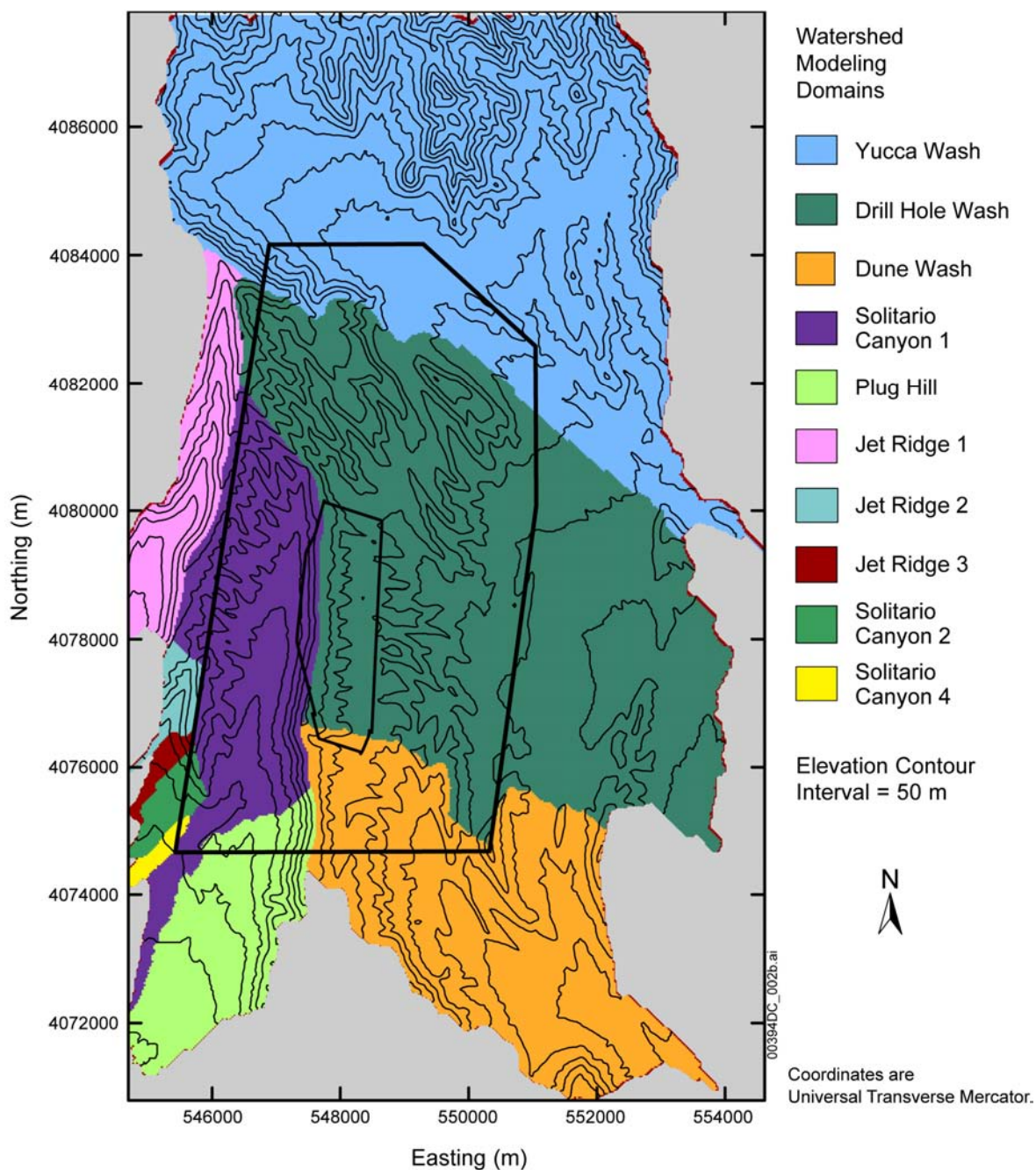
Source: USGS 2001b, Figure 6-12.

NOTE: On this figure and other figures in this document, the inner box is the repository boundary. The outer box is the unsaturated zone flow and transport model simulation area. Both are shown as schematic only and are not to scale.

Figure 1-3.   Location of 10 Watershed Model Domains Included in the Composite Watershed Model Area Overlying the Area of the Unsaturated Zone Flow and Transport Model Presented in *Simulation of Net Infiltration for Modern and Potential Future Climates* (USGS 2001b)
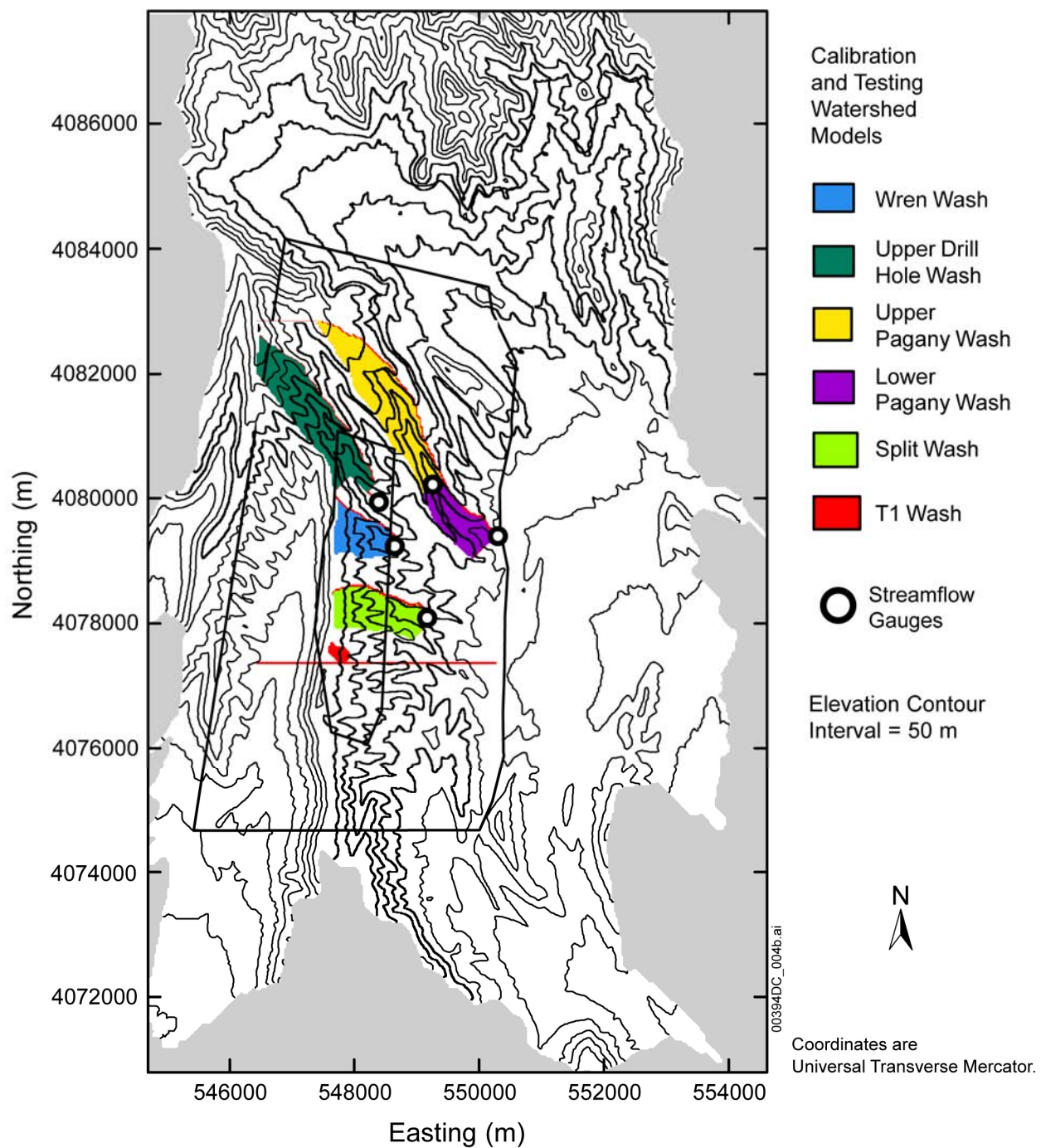
Source: USGS 2001b, Figure 6-19.

Figure 1-4. Location of Stream-Gauging Sites and Calibration Watersheds Defined by the Gauging Sites

Geology–Yucca Mountain is an uplifted, heavily block-faulted ridge of alternating layers of welded and nonwelded volcanic tuffs of Miocene age. The major geologic units at Yucca Mountain are the volcanic tuff formations of the Paintbrush (Tp) Group, the Calico Hills Formation (Tac), and the Crater Flat (Tc) Group. The lithostratigraphic nomenclature divides the Paintbrush Group into the Tiva Canyon (Tpc), Yucca Mountain (Tpy), Pah Canyon (Tpp), and Topopah Spring (Tpt) tuffs. The Crater Flat Group is divided into the Prow Pass (Tcp), Bullfrog (Tcb), and Tram (Tct) tuffs. For purposes of hydrogeologic studies, including infiltration, a separate stratigraphic nomenclature was developed based on the degree of welding and hydrologic property distributions (Simmons 2004, Tables 3-5 and 7-1).

The major hydrogeologic units are divided into the Tiva Canyon welded (TCw), the Paintbrush nonwelded (PTn) (consisting primarily of the Yucca Mountain and Pah Canyon members and the interbedded tuffs), the Topopah Spring welded (TSw), the Calico Hills nonwelded (CHn), and the Crater Flat undifferentiated (CFu) units. Figure 1-5 presents a three-dimensional representation of the block-faulted hydrogeologic units at Yucca Mountain.

For evaluation of net infiltration, only the TCw hydrogeologic unit of the Tiva Canyon Tuff and overlying alluvium are considered. The Tiva Canyon Tuff is a compositionally zoned, generally moderately to densely welded, tuff sequence. The sequence is a highly fractured, variably eroded unit with thicknesses in the repository area varying from 0 to more than 150 m.
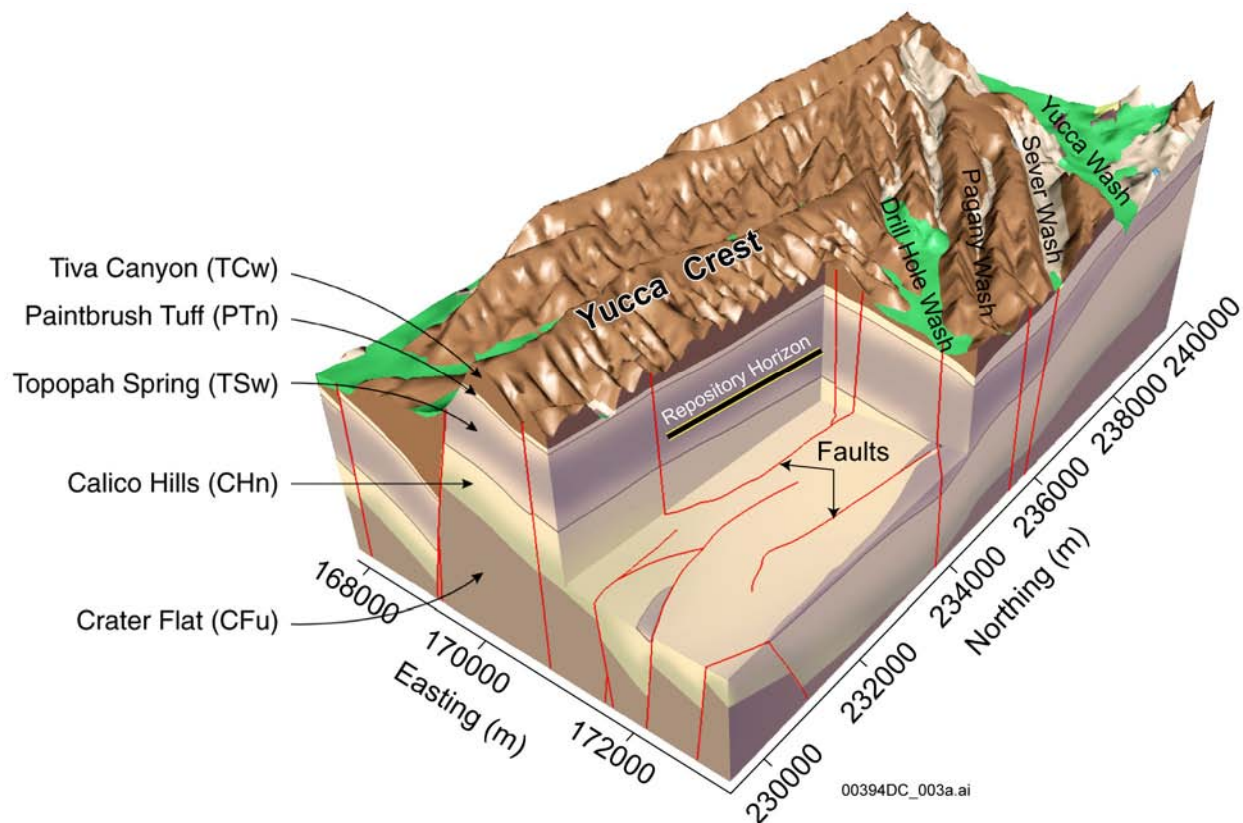
Figure 1-5. Three-Dimensional Geologic Presentation of Yucca Mountain

Hydrogeology–Yucca Mountain is located within the Alkali Flat-Furnace Creek groundwater basin, which is within the larger Death Valley Regional Groundwater System. The groundwater flow system of the Death Valley region is very complex, involving many groundwater systems. In some areas, confining units allow considerable movement between aquifers; in other areas, confining units are sufficiently tight to support artesian conditions. Groundwater below Yucca Mountain and in the surrounding region flows generally south toward discharge areas in the Amargosa Desert and Death Valley. The area around Yucca Mountain is in the central subregion of the Death Valley regional groundwater system, which has three groundwater basins: Pahute Mesa-Oasis Valley, Ash Meadows, and Alkali Flat-Furnace Creek. Figure 1-6 depicts major areas of groundwater recharge and discharge, water level elevations, and flow directions within the Yucca Mountain area. The primary sources of groundwater recharge are infiltration on Pahute Mesa, Rainier Mesa, Timber Mountain, and Shoshone Mountain to the north, and the Grapevine and Funeral Mountains to the west and southwest (see Figure 1-2). Recharge in the immediate Yucca Mountain vicinity is small, consisting of water reaching Fortymile Wash, as well as precipitation that infiltrates into the subsurface (Hevesi et al. 2003).

Surface Hydrology–Yucca Mountain is located in the Amargosa River drainage basin, which is the major tributary drainage area to Death Valley. Streamflow from Yucca Mountain can extend from local drainages to the Amargosa River and then to Death Valley. The Amargosa River and its tributaries are ephemeral streams (i.e., they are dry most of the time), with flow rarely occurring in direct response to precipitation. Along short distances, groundwater discharges at springs into the channel system. During episodic flooding, flow occurs along the Amargosa River, filling much of the Death Valley saltpan to depths of 1 ft (0.3 m) or more (Miller 1977, p. 18). During periods in which the climate has been cooler and wetter, such as 140,000 to 175,000 years ago, Death Valley was filled with water to depths of 175 m (USGS 2001a, p. 27). The entire Death Valley drainage basin and several closed drainage basins are interconnected through the groundwater system (D'Agnese et al. 1997, Figure 9, pp. 20 and 22). About 4,000 mi^2 (10,000 km^2) drain directly into Death Valley (Miller 1977, p. 18). In addition, the Amargosa River drains almost 3,500 mi^2 (9,100 km^2) north and east of Death Valley, and Salt Creek drains about 1,500 mi^2 (3,900 km^2) to the south.

Several artificial lakes (Crystal Reservoir, Lower Crystal Marsh, Horseshoe Reservoir, and Peterson Reservoir) store the collective discharge from various springs located in Ash Meadows. Like the streams, the playas are mainly ephemeral and contain water only after heavy runoff periods. Throughout the Death Valley basin, perennial flow is only observed downgradient from spring discharges and around the margins of playas and saltpans, where the groundwater discharges to the land surface. Surface water flows have been monitored at five sites in the Yucca Mountain region (Figure 1-4).
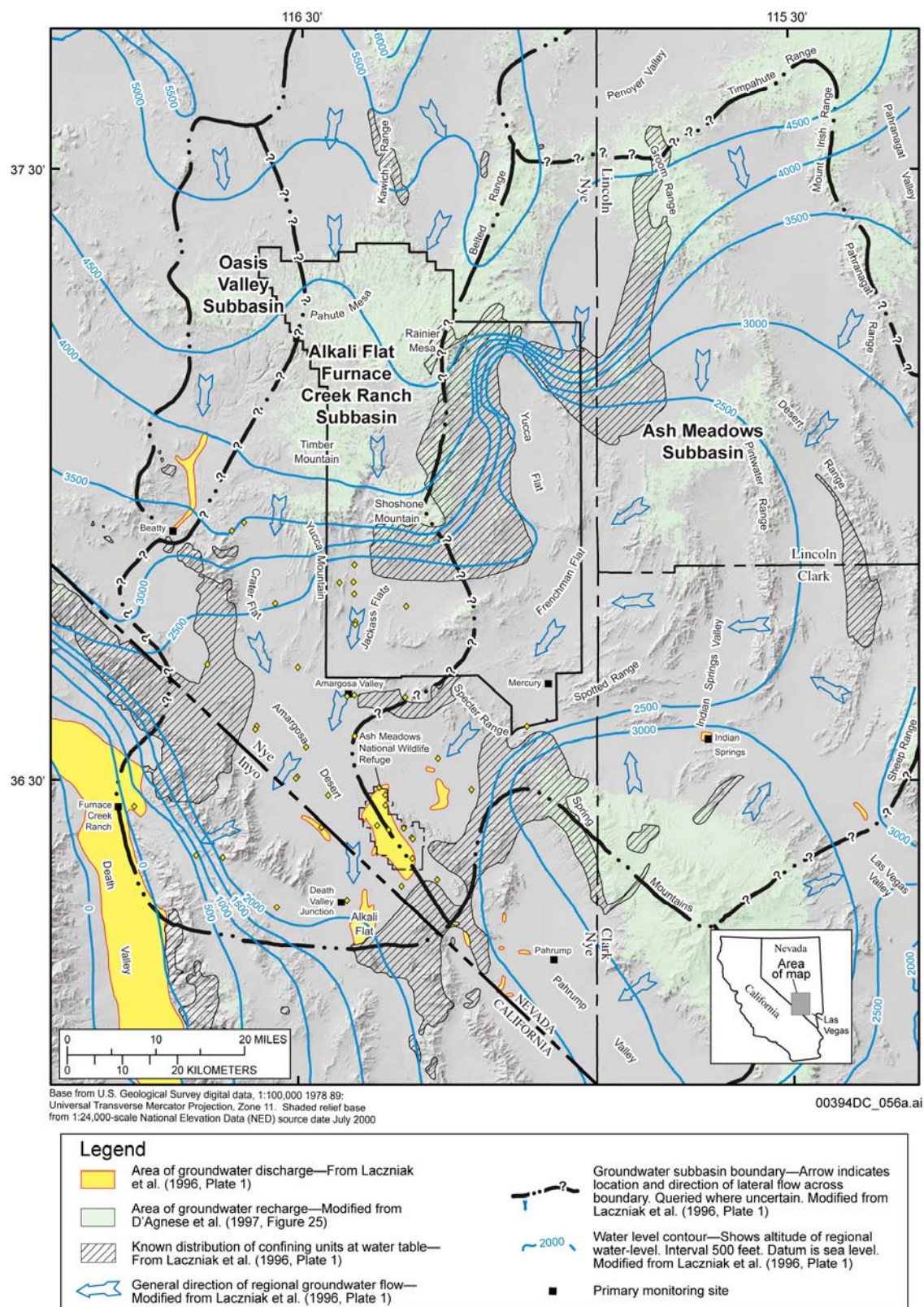
Source: Fenelon and Moreo 2002, Figure 2.

Figure 1-6. Hydrogeologic Map Showing Major Factors Controlling Groundwater Flow in the Yucca Mountain Region, Southern Nevada, and Eastern California

Soils–A soil survey of Midway Valley at the North Portal facilities and the ridges to the west (Resource Concepts 1989) and a more general soil survey of the entire Yucca Mountain region (YMP 1997) identified 17 soil series and seven map units (Table 1-2) (Resource Concepts 1989). Based on a wetlands assessment at the Nevada Test Site (Hansen et al. 1997), there are no hydric soils at the Yucca Mountain site. Yucca Mountain soils are derived from underlying volcanic rocks and mixed alluvium dominated by volcanic material and, in general, have low water-holding capacities.

The shallow soils on ridge tops at Yucca Mountain often consist of a thin hardpan (hardened or cemented soil layer) on top of bedrock and range from well drained to excessively drained, which means that water drains readily to very rapidly. A topsoil layer is typically less than 15 cm thick and, in some instances, has an underlying soil layer 5 to 30 cm thick.

Soils on fan piedmonts and in steep, narrow canyons are relatively deep and well drained (water is drained readily but not rapidly). These soils developed from residues of volcanic parent material, with a component of calcareous eolian sand. Soils formed from the volcanic parent material generally range from moderately shallow (50 to 75 cm) to moderately deep (75 to 100 cm) overlaying a thin hardpan on top of bedrock. The topsoil layers are generally less than 25 cm (10 in.) thick, with an underlying soil layer of 25 to 50 cm. The mixed soils, containing residues from volcanic parent material and calcareous eolian sand, are often deep (100 to 150 cm) or moderately deep, having a well-cemented hardpan. A topsoil layer is less than 15 cm thick, with the underlying layer of soil parent material as deep as 150 cm (60 in.).

Soils on alluvial fans and in stream channels are very deep (greater than 150 cm) and range from well drained to excessively drained. A topsoil layer is generally less than 20 cm (8 in.) thick, with the layer of soil parent material as deep as 150 cm. Soil textures are very gravelly, fine sands, sandy loams, with 35 to 70 percent of rock fragments. The soils are calcareous and moderately alkaline.

Alluvial deposits, consisting of fluvial sediments and debris flows, are present in the valley floors and washes (Rousseau et al. 1999, pp. 10 and 11). These deposits have varying degrees of soil development and thickness and have a gravelly texture, with rock fragments constituting between 20 and 80 percent of the total volume. The alluvial deposits range from 100 m thick in Midway Valley to less than 30 m thick in the mouths of the smaller washes. In the middle of the washes, most alluvial fill (soil) is less than 15 m thick. Side slopes are characterized by a very thin soil cover, with densely welded and highly fractured bedrock.

The erosion of the sediments and exposed bedrock over 10,000 years is expected to be on the order of centimeters (Simmons 2004, Section 3.4.6), which is within the range of existing surface elevation irregularities and would not significantly affect the processes in the hundreds of meters (thousands of feet) of unsaturated zone. Therefore, the effects of soil erosion on infiltration are considered negligible and are reasonably excluded from the TSPA calculations (BSC 2001a, Section 6.4.1).

Table 1-2. Soil Mapping Units at Yucca Mountain

Map Unit	Percent	Geographic Setting	Soil Characteristics
Upspring-Zalda	11	Mountain tops and ridges. Soils occur on smooth, gently sloping ridge tops and shoulders and on nearly flat mesa tops. Rhyolite and tuffs are parent materials for both soil types.	Typically shallow (10 to 51 cm) to bedrock, or to thin duripan (a subsurface layer cemented by silica, usually containing other accessory cements) over bedrock. They are well to excessively drained, have low available water-holding capacity, medium to rapid runoff potential, and slight erosion hazard.
Gabbvally–Downeyville–Talus	8	North-facing mountain side slopes. Talus is stone-sized rock occurring randomly throughout unit in long, narrow, vertically oriented accumulations.	Shallow (10 to 36 cm) to bedrock. Permeability is moderate to moderately rapid. They have moderate to rapid runoff potential, are well drained, and have low available water-holding capacity and moderate erosion hazard.
Upspring–Zalda–Longjim	27	Mountain side slopes. Soils occur on south-, east-, and west-facing slopes, and on moderately sloping alluvial deposits below side slopes.	Shallow (10 to 51 cm) to bedrock or to thin duripan over bedrock. They are well to excessively drained and have moderately rapid to rapid permeability and runoff potential, very low available water-holding capacity, and slight erosion hazard.
Skelon–Aymate	22	Alluvial fan remnants. Soils occur on gently to strongly sloping summits and upper side slopes.	Moderately deep (51 to 102 cm) to indurated (hardened, as in a subsurface layer that has become hardened) duripan or petrocalcic (a subsurface layer in which calcium carbonate or other carbonates have accumulated to the extent that the layer is cemented or indurated) layer with low to very low available water-holding capacity, moderately rapid permeability, slow runoff potential, and slight erosion hazard.
Strozi variant–Yermo–Bullfor	7	Alluvial fan remnants. Soils occur on gently to moderately sloping alluvial fan remnants and stream terraces adjacent to large drainages.	Moderately deep (51 to 102 cm) to deep (102 cm). They are well drained and have rapid permeability, very low available water-holding capacity, slow runoff potential, and slight erosion hazard.
Jonnic variant–Strozi–Arizo	12	Dissected alluvial fan remnants. Soils occur on fan summits, moderately sloping fan side slopes, and inset fans. They are formed in alluvium from mixed volcanic sources.	Moderately deep (36 to 43 cm) to deep (more than 102 cm), sometimes over strongly cemented duripan. They have slow or rapid permeability, slow or moderate runoff potential, very low available water-holding capacity, and slight erosion hazard.
Yermo–Arizo–Pinez	13	Inset fans and low alluvial side slopes in mountain canyons; and drainages between fan remnants. Soils occur on moderately to strongly sloping inset fans near drainages, adjacent to lower fan remnants, and below foothills.	Deep (more than 102 cm), sometimes over indurated duripan. They are well drained and have very low available water-holding capacity, moderately slow to rapid permeability, slow to medium runoff potential, and slight erosion hazard.

Source: CRWMS M&O 1999, pp. 3 and 4.

Vegetation–At Yucca Mountain, Mojave Desert vegetation occurs mostly at lower elevations on bajadas (broad, continuous alluvial slopes) and in washes. Vegetation cover varies from 0 to 90 percent (Hevesi et al. 2003, p. 49; CRWMS M&O 1996). The species most identified over broad areas are *Coleogyne ramosissima* (common name is black bush), located primarily on ridges and canyons. According to *Yucca Mountain Biological Resources Monitoring Program*

Annual Report FY89 & FY90 (EG&G 1991, Section 2.3.1), the most common vegetation association is *Larrea-Lycium-Grayia* (creosote bush-wolfberry-hopsage), which covers approximately 35 percent of the surface area at Yucca Mountain, *Coleogyne* (30 percent), and *Lycium-Grayia* (26 percent). *Larrea-Lycium-Grayia* predominates on the eastern bajadas of central Yucca Mountain, occurring at intermediate elevations in the study area ranging from 1,000 to 1,500 m. *Coleogyne* occurs across the northern third of the study area from the valley floors at elevations of approximately 1,030 m (3,380 ft) to the flat ridge tops at roughly 1,710 m; it generally does not occupy the steep slopes and is present within areas with thin soils.

Evapotranspiration is controlled by the rooting depth and density affecting the amount of water available to the plant (Hevesi et al. 2003). Although Mojave Desert shrubs do not achieve full vegetation cover (CRWMS M&O 1996), the plant systems may extensively exploit soil water in spaces between plants (Levitt et al. 1996).

1.5 TYPES OF INVESTIGATIONS CONDUCTED TO FORECAST FUTURE CLIMATE CONDITIONS AND TO ASSESS NET INFILTRATION

Climatic investigations involved *Future Climate Analysis* (USGS 2000) and other reports (Sharpe 2002; Sharpe 2003) to implement the following:

- Forecasting of climatic conditions based primarily on the analysis of three types of data:

    1. Long-term regional records of stable isotope $\delta^{18}O$ concentrations (Devils Hole, Nevada) and microfossil data (Owens Lake, California)

    2. Local discontinuous vegetation records from packrat nests (middens)

    3. Global records of an earth-orbital clock of precession and eccentricity and Vostok (Antarctica) ice core isotopic compositions.

- Selecting present-day climate analog sites with daily precipitation and temperature records, which can be used for simulating net infiltration.

Understanding of the Yucca Mountain unsaturated zone has evolved from surface-based investigations that began in the early 1980s into rigorous field, laboratory, and modeling studies (USGS 2001b; Flint, A.L. et al. 1996; Flint, A.L. et al. 2001; Wang and Bodvarsson 2003; BSC 2003a). Studies related to the assessment of net infiltration can be grouped as follows:

- Drilling of shallow and deep unsaturated zone boreholes
- Mapping of faults and fractures
- Measurements in boreholes of moisture content and water potential with time and depth
- Determination of unsaturated hydraulic parameters using cores taken from boreholes
- Determination of saturated hydraulic conductivity using air injection tests
- Infiltration tests (e.g., Alcove 1 and Fran Ridge)

- Geochemical and temperature investigations in boreholes
- Numerical modeling of net infiltration, including

  – Calibration and validation of the numerical model
  – Predictions (using 1996 and 2001 models)
  – Uncertainty analysis of net infiltration.

The results of climate and infiltration investigations were also subjected to the expert elicitation projects (DeWispelare et al. 1993; CRWMS M&O 1997a).

1.6 NOTE REGARDING THE STATUS OF SUPPORTING TECHNICAL INFORMATION

This document was prepared using the most current information available at the time of its development. This technical basis document and its appendices providing KTI Agreement/AIN responses reflect the status of the Yucca Mountain Project scientific and design bases at the time of submittal. Information that evolves through subsequent revisions of the analysis and model reports and other references will be reflected in the license application as the approved analyses of record at the time of license application submittal. Consequently, the Yucca Mountain Project will not routinely update either this technical basis document or its KTI Agreement/AIN appendices to reflect changes in the supporting references prior to submittal of the license application.

2. PRESENT-DAY AND FUTURE CLIMATE CONDITIONS

2.1 TECHNICAL BASIS FOR FORECASTING CLIMATES AND SELECTING CLIMATE ANALOG SITES

To forecast the climate conditions at Yucca Mountain, three types of data were used: (1) local records of stable isotope $\delta^{18}O$ concentrations (Devils Hole, Nevada) and microfossil data (Owens Lake, California); (2) local discontinuous vegetation records from packrat nests (middens); and (3) records of an earth-orbital clock (precession and eccentricity) and ice core isotopic compositions. The technical basis for forecasting climate involves four key scientific assumptions (USGS 2001a, p. 19):

- The climate is cyclical; past climates provide insight into potential future climates.

- A relationship exists between the timing of long-term past climate change (i.e., glacial and interglacial cycles) and the timing of changes in certain earth-orbital parameters. This relation establishes a millennial-scale climate-change clock which provides a means to predict the timing of future climate changes.

- A relationship exists between the characteristics of past climates and the sequence of those climates in the long, approximately 400,000-year, earth-orbital cycle. The characteristics of past glacial and interglacial climates within the long earth-orbital cycle differ from each other and do so in a systematic way. This climate-sequence relationship provides a defensible criterion for the selection of a particular past climate as an analog for future climate.

- Long-term, earth-based climate forcing functions, primarily tectonics, have remained relatively unchanged during the last 400,000 years and will likely not change during the next 10,000 years. The potential and practically unpredictable impact of long-term, earth-based forcing functions on climate is not considered for forecasting climate change over the next 400,000 years.

Because direct testing or analysis cannot be used to confirm the first three assumptions, which are interrelated to each other, the validity of a particular past climate as a future-climate analog can be confirmed only through the passage of time (within the 10,000-year period). The assumption that long-term, earth-based forcing functions will not change during the next 10,000 years is consistent with the U.S. Environmental Protection Agency final rule 40 CFR Part 197 with respect to the stability of geologic processes (40 CFR Part 197, pp. 25 and 59).

Earth-orbital parameters and many past climate proxy records show that climate is cyclic over 400,000-year periods. Glacial and interglacial climates can be divided into marine isotope stages as shown in Figure 2-1. The marine isotope stages were first established from studies using marine carbonate $\delta^{18}O$ records and are now applied to many climate proxy records. Even-numbered marine isotope stages represent glacial stages, whereas odd-numbered marine isotope stages represent interglacial stages. Marine isotope stage dates vary with the climate proxy record and location. The examination of time series $\delta^{18}O$ data shown in Figure 2-1 indicate that

the cycling occurs simultaneously with the overall trends of the increase in $\delta^{18}O$ with time. Although the analysis of past climates shows that a strict repetition of climate characteristics is not expected for future climates, the general characteristics (i.e., the greatest effective moisture within the next 400,000 years) of future precipitation and temperature for a particular interglacial–glacial couplet can be inferred from corresponding interglacial–glacial couplets in the past. However, the magnitude or nature of climate states may be altered by positive or negative feedback mechanisms, which are unlikely to happen for the next 10,000 years (USGS 2001a, Section 6.6).
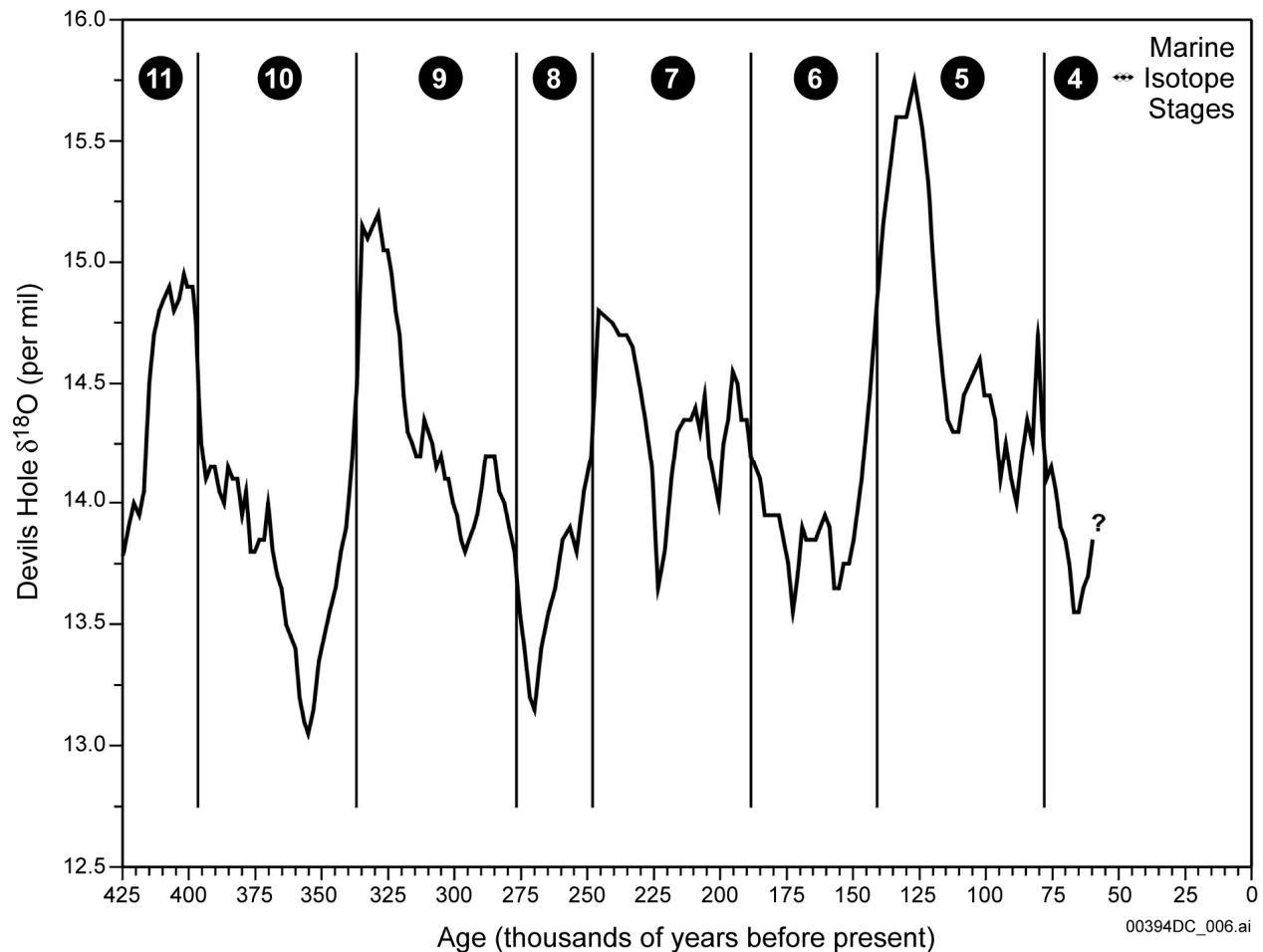
Source: USGS 2001a, p. 28.

NOTE: Stable isotope data are reported relative to VSMOW. High Devils Hole $\delta^{18}O$ values represent warm climates, and low values represent cold climates. Odd numbered marine isotope stages correspond to interglacial climates; even numbered marine isotope stages correspond to glacial climates. The published Devils Hole record stops at approximately 60,000 years before present.

Figure 2-1. Devils Hole Stable Isotope Record Showing the Timing and Cyclical Nature of Climate Change

The estimation of the future climate states at Yucca Mountain was provided by the USGS (2001a) for the period from the present to 10,000 years in the future. The USGS (2001a, p. 26) report confirms the existence of a long-term, present-day interglacial climate state for at least the last 9,000 years before present. The USGS analysis estimates that the present-day climate regime has lasted for about 9,000 to 10,000 years before present. The DRI analysis estimates that the interglacial climate state began about 12,000 years before present (Sharpe 2003, Table 6-1). Within the next 10,000 years no full glacial climate regime is expected. Other features revealed by the ice-core records and high-resolution marine sediment cores indicate that large and abrupt climatic changes occurred in the past.

Although the causes of climate change between glacial and interglacial conditions in the past are not known with certainty (USGS 2001a, p. 21), timing relations between earth-orbital parameters and past climate cycle can be used to forecast the future. Any future climate analysis is uncertain, but perceived relations between measurable cycles provide a reasonable technical basis for forecasting estimated future climate conditions. For the next 10,000 years, three general climate conditions are expected, in order of increasing wetness (USGS 2000):

- Present-day (interglacial) climate for 400 to 600 years
- Monsoon climate for 900 to 1,400 years
- Glacial-transition (intermediate) climate for the balance of the 10,000-year period.

Table 2-1 compares the timing of the USGS and DRI forecasts of future climates. According to Sharpe (2003, p. 56), the difference in timing between the two reports is insignificant, differing by less than 1,800 years.

Table 2-1. Comparison of U.S. Geological Survey and Desert Research Institute Future Climate Forecasts

U.S. Geological Survey		Desert Research Institute	
Climate	Duration	Climate	Duration
Modern	600 years after present	Interglacial	Not applicable.
Monsoon	600 to 2,000 years after present	Monsoon	1,000 years before present to 500 years after present
Glacial Transition	2,000 to 30,000 years after present	Intermediate	500 to 18,500 years after present
		Monsoon	18,500 to 20,000 years after present
		Intermediate	20,000 to 38,000 years after present

Source: Sharpe 2003, Table 6-6.

The range in ages is likely caused by the uncertainty in evaluating sediment accumulation rates in Owens Lake, California, and rounding of values of Sharpe (2003).

To address the future global climate changes in the TSPA, paleoclimatic information (from the records of past climate changes) was used to predict future climate changes. Forecasting of climate states is based on information about past patterns of climates (CRWMS M&O 2000a, pp. 3-38 to 3-42), which is a generally accepted approach, because climate is assumed to be cyclic and largely dependent on repeating patterns of the earth's orbital parameters.

Based on *Future Climate Analysis* (USGS 2000), the Devils Hole, Nevada, stable isotope record (Landwehr et al. 1997) was used to provide the timing and sequence of climate states, and the Owens Lake, California, microfossil record (from sediment cores taken from drilling) is used to reconstruct the magnitude and nature of past climate states for the last 400,000 years.

For the next 10,000 years, each future climate regime is represented by present-day meteorological stations that serve as analog sites (USGS 2000). The map showing the locations of meteorological stations selected as analog sites is shown in Figure 2-2. Table 2-2 summarizes the duration and lists the names and locations of representative present-day meteorological stations characterizing the three climate states. Data from these meteorological stations are, in turn, used to determine precipitation and temperature records, which are then used as inputs to the infiltration model (see Section 4). For each of the climate scenarios (present-day, monsoon, and glacial transition), the lower-bound, mean, and upper-bound states are considered. Table 2-3 presents mean annual temperature and precipitation for these stations, which are discussed in more detail in Section 4.3 (Tables 4-4, 4-6, and 4-7). The daily records and mean annual precipitation and temperature values for each climate regime are then used in numerical simulations to quantify the net infiltration distribution in TSPA models (USGS 2001b; BSC 2003a).
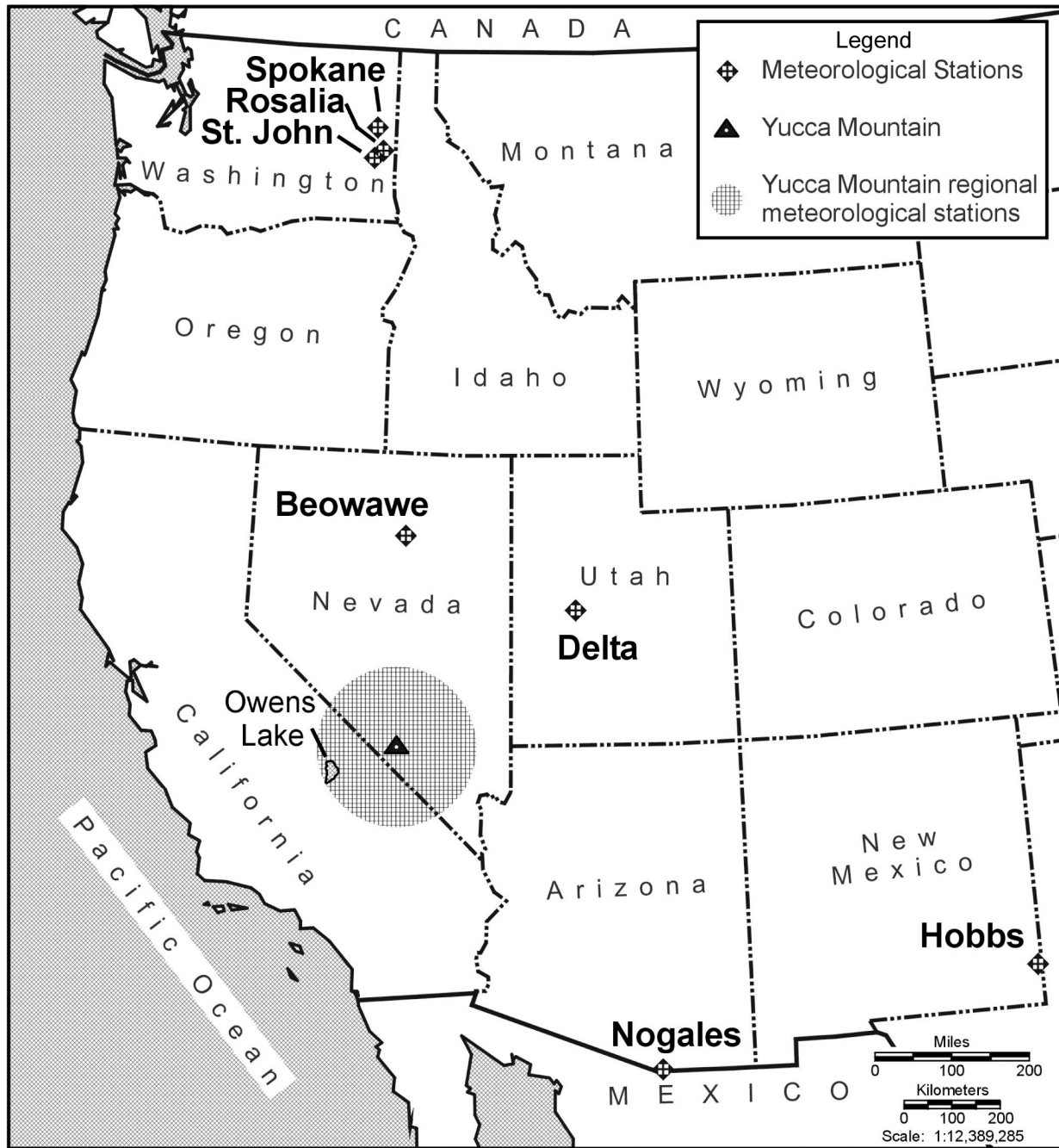
Source: USGS 2001a, p. 70.

Figure 2-2. Map of Meteorological Stations of Climate Analogs

Table 2-2.   Meteorological Stations Selected to Represent 10,000 Years of Future Climate States at Yucca Mountain, Nevada

Climate	Duration	Representative Meteorological Stations	Locations of Meteorological Stations	
Modern Interglacial	400 to 600 years	Site and regional meteorological stations	Yucca Mountain region	
Monsoon	900 to 1,400 years	Average Upper Bound: Nogales, Arizona Hobbs, New Mexico	North Latitude 31° 21' 32° 42'	West Longitude 110° 55' 103° 08'
		Average Lower Bound: Site and regional meteorological stations	Yucca Mountain region	
Glacial Transition	8,000 to 8,700 years	Average Upper Bound: Spokane, Washington Rosalia, Washington St. John, Washington	North Latitude 47° 38' 47° 14' 47° 06'	West Longitude 117° 32' 117° 22' 117° 35'
		Average Lower Bound: Beowawe, Nevada Delta, Utah	North Latitude 40° 35' 25" 39° 20' 22"	West Longitude 116° 28' 29" 112° 35' 45"

Source: USGS 2001a.

Table 2-3. Comparison of Meteorological Characteristics of Climate Analog Sites

Climate Regime	Location	Mean Annual Precipitation (mm)	Mean Annual Temperature (ºC)
Present-Day Lower Bound	Yucca Mountain region	185.8[a]	Range: 15.1 to 18.2[b]
Present-Day Upper Bound	Yucca Mountain region	265.6[a]	Range: 15.1 to 18.2[b]
Monsoon Lower Bound	Yucca Mountain region	188.5[a]	Range: 15.1 to 18.2[b]
Monsoon Upper Bound	Nogales, Arizona Hobbs, New Mexico	414[c] 418[c]	15.8[c] 16.8[c]
Glacial-Transition Lower Bound	Delta, Utah Beowawe, Nevada	198[c] 220[c]	10.1[c] 8.8[c]
Glacial-Transition Upper Bound	Rosalia, Washington Spokane, Washington St. John, Washington	460[c] 410[c] 433[c]	8.4[c] 8.9[c] 9.1[c]

Source: [a] USGS 2001b, Tables 6-8 and 6-12.
          [b] CRWMS M&O 1997b, Tables 2-1 and A-10.
          [c] USGS 2001b, Tables 6-4, 6-5, and 6-6.

2.2 PRESENT-DAY CLIMATE

Certain semipermanent atmospheric pressure features over and near the United States play dominant roles in controlling the present-day synoptic weather patterns that affect the Yucca Mountain area. These are the Bermuda High (western north Atlantic), the Eastern Pacific High (eastern north Pacific), the Aleutian Low (Gulf of Alaska, winter), and the summertime thermal low (southwestern United States) (Ahrens 1994, pp. 288 to 289, Figure 11.3). Seasonal changes in position and strength of these centers of action influence winds and the movement of storms. A generalized view of atmospheric circulation is given in Figure 2-3.
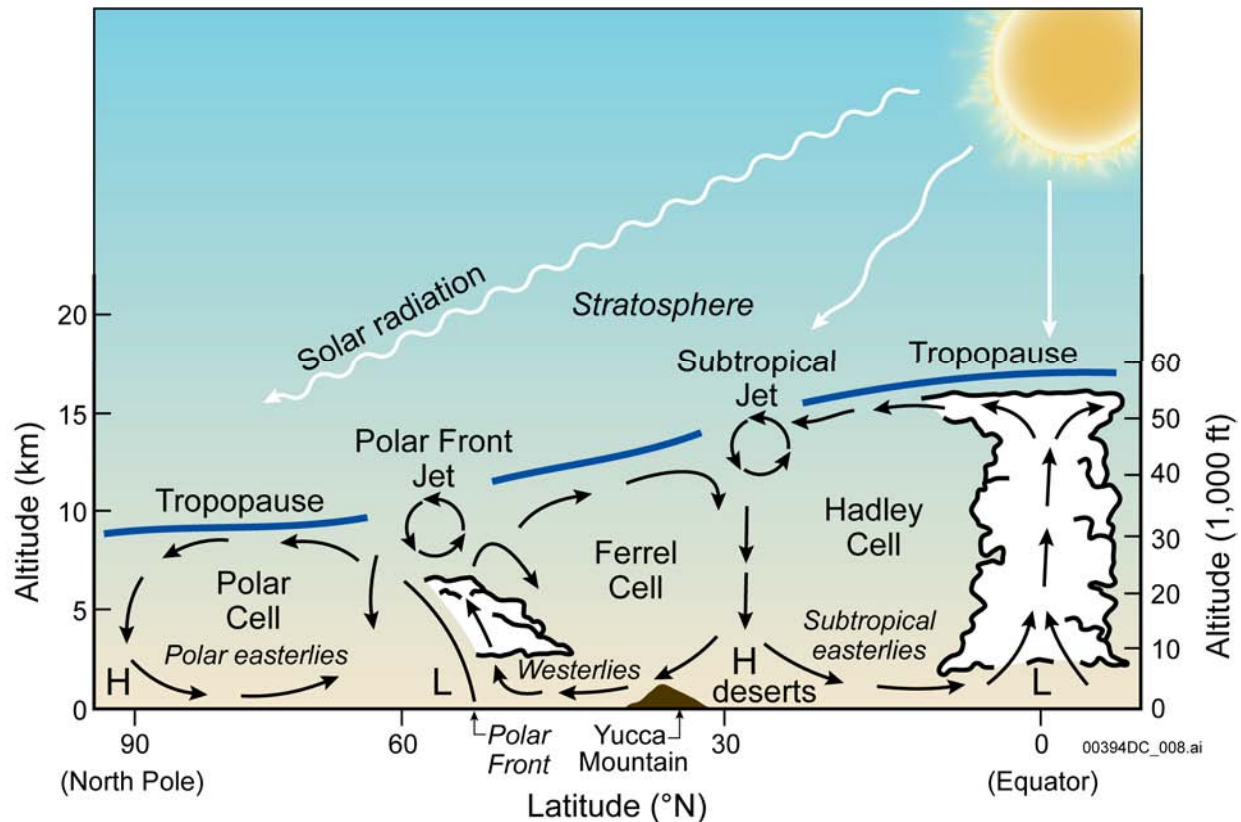
Source: USGS 2001a.

Figure 2-3. Generalized View of Atmospheric Circulation

Great Basin precipitation arises primarily from three airflow trajectories and moisture origins in the Pacific, Gulf of Mexico, and continental regions. The most important to the Yucca Mountain area is the Pacific trajectory. The Sierra Nevada and the transverse mountain ranges of southern California can either block or impede atmospheric moisture transport from the Pacific Ocean to Yucca Mountain, especially during winter, leading to a rain-shadow effect. In summer, moisture usually arrives from the south, where blockage is less effective.

In the winter, the eastward extension of the North Pacific High steers most cyclonic storms away from the southwestern United States by deflecting the jet stream toward more northerly latitudes. Thus, the desert southwest region experiences relatively few storm passages and tends to have mild, dry winter weather. On occasion, the North Pacific High weakens or moves, and the jet

stream shifts to the south to help bring storms, precipitation, and cooler air into the southwest (Mock 1996, pp. 1,111 to 1,113). Though relatively infrequent, these storms are a very important contributor to the annual recharge and stream flow (e.g., at Owens River) in the southwest. Many Pacific cyclones affecting Yucca Mountain form in the vicinity of the Aleutian Low and arrive from the west or northwest, often on a trajectory that curves around or over the southern end of the Sierra Nevada.

In *Simulation of Net Infiltration for Modern and Potential Future Climates* (USGS 2001b), the present-day climate scenario (sometimes referred to as the modern climate scenario) was characterized using the results of observations conducted from 1980 to 1995, with the mean annual precipitation rate of 157.5 mm/yr; and results from the Nevada Test Site Station 4JA 100-year stochastic simulation (mean annual precipitation of 150.19 mm/yr). To represent the lower-bound present-day climate scenario, the driest 10-year period (from 1980 to 1990) from the 100-year observations at the 4JA precipitation station was used. Note that the 4JA Station is located at the elevation of 1,044 m (within the Nevada Test Site) and has a mean annual precipitation of 140 mm (USGS 2001b, Table 6-3). To characterize the present-day climate scenario, the average data for the 1980 to 1995 observations at the Nevada Test Site Station Area 12 Mesa (located within the northern boundary of the Nevada Test Site known as Rainier Mesa) were used, resulting in a mean annual precipitation of 328 mm/yr (USGS 2001b, Table 6-3). These data were intended to represent the wetter conditions resulting from the enhanced El Niño Southern Oscillation activity.

Present-day meteorological data for the upper and lower bounds come from available stations in the region and include both Yucca Mountain project and nonproject data.

2.3 FUTURE CLIMATES

2.3.1 Monsoon Climate

Monsoon climates in the Yucca Mountain area can be characterized by increased summer and annual rainfall relative to today, generated by incursions of moisture from the tropical Pacific or the Gulf of California. Most precipitation would likely be summer-dominated. In addition, monsoon climate states are most likely wetter and warmer than today, with much of the precipitation lost to evapotranspiration and evaporation.

In the region in the United States that currently experiences a strong summer monsoon, two meteorological stations with long-term records were chosen to represent the monsoon climate upper bound: Hobbs, New Mexico (418 mm), and Nogales, Arizona (414 mm). The selection of two meteorological stations was needed to obtain averaged data in order to minimize local meteorological effects. The lower-bound monsoon climate scenario was defined as being equivalent to the average present-day climate stations in southern Nevada (USGS 2001a).

2.3.2 Glacial-Transition Climate

The glacial-transition climate is characterized by displacement of the polar jet from a northerly latitude to the Yucca Mountain area during most, but not all, winters. Continental ice sheets are either in the early stages of growth (interglacial moving toward glacial) or nearing the final stages of retreat (glacial moving toward interglacial). Mountain glaciers most likely exist in the

high Sierra Nevada cirques and may expand or contract on decadal or century scales. During some winters, the polar front resides to the north of Yucca Mountain, but it is still close enough to ensure ample precipitation for regular, seasonal Sierra Nevada stream discharge. Summer seasons are cooler than modern.

The glacial-transition climate occurs during the transition from glacial to interglacial or from interglacial to glacial climate states.

Selecting analog meteorological stations to represent upper and lower bounds of the glacial-transition climate requires identifying sites with cool winter wet seasons, and warm to cool and dry summers (USGS 2001a, Section 6.6.2). Further, the analog sites had to lie on the east side of large mountain ranges and, hence, in the rain shadow of those ranges. Based on the ostracode assemblage in Owens Lake, the absence of cold Canadian-like climate implies that the upper-bound analog should lie within the contiguous United States.

The meteorological stations representing the lower-bound glacial-transition climate should be in a place where mean annual temperature is higher than the upper bound, and thus these stations would be south of the upper bound localities (USGS 2001a, Section 6.6.2). The mean annual temperature, however, should be lower than that for the Owens Lake Basin at present, so that effective moisture is higher, consistent with a full and overflowing lake. The stations should have a lower mean annual precipitation than the upper-bound sites, because the record from the Owens Lake Basin shows episodes of either saline diatoms or ostracodes, implying less surface flow in the Owens River. However, the absence of abundant saline taxa implies effective moisture is higher than at present, reflecting cooler than the present mean annual temperature rather than high mean annual precipitation (USGS 2001a, p. 74). Thus, the lower-bound glacial-transition meteorological sites may have mean annual precipitation values similar to or even lower than present-day Owens Lake Basin (USGS 2001a, p. 74). As with the upper-bound meteorological sites, the region should be winter-precipitation dominated, north of the summer rain regime, and have some or all of the ostracode or diatom species found in the fossil record at Owens Lake. Inspection of meteorological sites that fit lower-bound glacial-transition conditions revealed that there were few choices available (USGS 2001a, Section 6.6.2). The sets of meteorological data that fit all of these criteria and also have long and complete records were found at Delta, Utah, and Beowawe, Nevada.

Because a full and overflowing Owens Lake is related to seasonal and possibly annual residence of the polar front, upper-bound meteorological stations were selected in an area where the polar front currently resides through most or all of the winter season and where its average position prevails for most of the year (USGS 2001a, Section 6.6.2). Given all of the above qualifying conditions, the upper-bound glacial-transition meteorological site was selected in the northwestern United States, east of the Cascades, a high mountain range. The area falls within a rain shadow, as does Yucca Mountain. The regional mean annual precipitation is winter-precipitation dominated and is under the influence of the polar front during the winter, as well as other times throughout the year. Furthermore, unlike localities farther north in Canada, the region does not experience extended dominance by extremely cold, Arctic high pressure, typical of the cold, full-glacial periods. Based on meteorological-station data from eastern Washington state, three stations were selected for the upper-bound glacial-transition climate: Spokane, Rosalia, and St. John (see Figure 2-2). These three stations are close to each other but

do not have identical records, presumably reflecting local differences in mean annual precipitation and mean annual temperature. As in other cases, selection of multiple meteorological stations was intended to minimize local effects on the climate parameters used as input to the infiltration model.

2.4   COMPARISON OF CLIMATE ANALOG SITES

A comparison of the mean annual precipitation and mean annual temperature data from the meteorological analog sites is shown in Table 2-3. The mean annual precipitation for the lower-bound glacial-transition state is only slightly higher than that for the lower-bound present-day and monsoon states. The mean annual precipitation for the upper-bound monsoon and glacial-transition climates exceed that for the present-day climate (Thompson et al. 1999, Figures 16 and 17, Table 4). Thus, future climate, based on the selection of meteorological stations having upper-bound annual mean precipitation in the low 400-mm range is wetter than the present-day climate. The values of mean annual temperature for the glacial-transition analog climate are much lower than the mean annual temperature values in the Yucca Mountain and Owens Lake region today (Thompson et al. 1999).

2.5   ANALYSIS OF FUTURE CLIMATE UNCERTAINTIES

The reasons for the climatic uncertainties can be grouped into two categories (BSC 2002b, Section 4). Epistemic uncertainty arises from the lack of knowledge about the processes and parameters, because the data are limited, or because alternative conceptual interpretations of the available data exist (e.g., DeWispelare et al. 1993); this type of uncertainty can be reduced because the state of knowledge can be improved by further testing or data collection. As a consequence, this type of uncertainty is also referred to as reducible uncertainty. Aleatory uncertainty arises from the existence of spatial and temporal variability of climatic processes and parameters and typically can be accounted for using geostatistical approaches (e.g., using appropriate probability distribution functions); as a consequence, this type of uncertainty is referred to as irreducible uncertainty, which cannot be reduced through further testing or data collection. These two categories of uncertainties are introduced to demonstrate the causes for uncertainties in forecasting climate states, which were identified in reports (USGS 2001a; Sharpe 2003, pp. 40, 57, 61): the timing of future climate, the methodology of climatic forecasting, and the earth's future physical processes.

Uncertainty in the timing is caused by the following factors (Sharpe 2003, p. 40): the determination of age from the Devils Hole records, caused by ambiguity in selecting a precession value that marks the Devils Hole $\delta^{18}O$ inflection points; and the effect of a regional climate on the Devils Hole signal itself, if a primary inflection point precedes or follows a global change. This uncertainty relates, in general, to the issue of correspondence between the orbitally tuned and the terrestrial-based (Devils Hole) records (Winograd et al. 1992, pp. 255, 257 to 258), as well as Owens Lake chronology, based on the ostracode and diatom data (USGS 2001a, Section 6.6).

Mean values of the time for the onset and end of climate states, which are determined based on the precession methodology, are reported to the nearest 500 years (Sharpe 2003, p. 59). Each Devils Hole sample integrates over an average time interval of about 1,800 years (Winograd

et al. 1992, p. 255). The projected duration of the monsoon climate from 900 to 1,400 years (USGS 2001a, p. 76) is less than the Devils Hole age resolution of 1,800 years (Sharpe 2003, p. 56). The Devils Hole timing resolution is likely to have little effect on the duration of the glacial-transition climate (8,000 to 8,700 years) (USGS 2001a, p. 76) within the 10,000-year TSPA regulatory period.

Timing uncertainty is both epistemic and aleatory, because timing is based on the current knowledge and the best available methods of climatic investigations of different data sets. However, timing uncertainty is not significant for the evaluation of net infiltration rate spatial distribution and net infiltration weighting factors for the following reasons:

- Net infiltration was simulated (USGS 2001b) for each of the climate states (present-day, monsoon, and glacial transition) using steady state, cyclic boundary conditions; therefore, the spatially averaged infiltration rates for each of the climate regimes are essentially independent of the duration of the climate state (the same results were obtained for the simulation of percolation in the unsaturated zone) (BSC 2003b, Figures 6.8-3 to 6.8-5). Also, in TSPA simulations of radionuclide transport, the actual transient period during which the unsaturated zone flow system responds to a climate change has been specified as insignificant (DOE 1998, Section 3.6.1.1, p. 3-116).

- The net infiltration weighting factors for the whole period of 10,000 years were evaluated using the meteorological data for the glacial-transition climate state (higher precipitation and lower temperature than modern) (BSC 2003a), granting a conservative estimation of net infiltration needed for the NRC safety analysis (NRC 1997, p. 8).

Uncertainty in the methodology of climate analysis arises from several reasons. It arises from the hypothesis of using the past cyclic climate behavior to forecast the future climate states (USGS 2001a, p. 19; Sharpe 2003, p. 61), which presents epistemic (reducible) uncertainty; however, the validity of this hypothesis about the climate cycling pattern can be confirmed only by the passage of time (USGS 2001a, p. 19). Uncertainty arises from the possibility for earth's orbital parameters to correlate with other factors that cause climate changes (e.g., solar output or other mechanisms) (USGS 2001a, p. 37). The use of a conventional numerical method, including a correlation analysis, is restricted, because even modern science does not know with certainty all reasons for climate changes, so that the change in a climate system cannot be described numerically and long-term time series cannot be constructed (climate change is time-transgressive and climate proxies do not often record climate events in the same manner or with the same magnitude), nor is there a clear knowledge about future boundary conditions needed for numerical modeling; consequently, the climate analysis is based on forecasting future climate (USGS 2001a, p. 62). The second and the third reasons present examples of a combination of both epistemic and aleatory uncertainties.

NRC (Stablein 1997, p. 2; NRC 1997) acknowledged that the paleoclimatic and paleohydrologic methods of analysis can be used to bound the range of past climates in the Yucca Mountain region and to estimate future climatic conditions, and that climatic modeling is not required (NRC 1997, p. 6).

Uncertainty also arises from the well-known fact of the chaotic nature of the climate system (NRC 1997, p. 9; Sharpe 2003, p. 61). The chaotic behavior is caused by a combined effect of several nonlinear dynamic processes, along with positive and negative feedback mechanisms; for example, input of cosmic material (meteorites), changes in solar radiation, ocean salinity, land features (e.g., topography, vegetation, albedo), and atmospheric composition (e.g., fossil fuel emissions, volcanic eruptions). For such a system, precise predictions of long-term climate changes are limited, while the range of long-term changes can be evaluated using stochastic methods, with the aid of probability distributions for such meteorological parameters as precipitation and temperature. Therefore, a modified Monte-Carlo (Latin Hypercube sampling) stochastic approach was used for the evaluation of the spatial distribution of net infiltration and net infiltration weighting factors (BSC 2003a), using analog-site precipitation and temperature records, and probability distributions for daily precipitation and evapotranspiration multipliers (see Section 6).

The effects of anthropogenic physical processes, such as greenhouse effects, acid rain, global warming, and ozone layer depletion, are still unclear and highly uncertain (NRC 1997, pp. 11, 13). Therefore, NRC (1997, p. 13) recommended that for the purposes of evaluating repository performance, it is both pragmatic and conservative to postulate that such changes will be relatively short (several thousands years at most) and that the global cooling (cooler and wetter conditions) will return. Such consideration was implemented in the evaluation of the net infiltration weighting factors for the 10,000-year performance period, using the data for the glacial-transition climate (BSC 2003a). This approach is also consistent with the NRC licensing regulations (10 CFR 63.305(b) and 10 CFR 63.305(c)), requiring the U.S. Department of Energy to vary factors related to the geology, hydrology, and climate based on cautious but reasonable assumptions consistent with present knowledge of factors that could affect the Yucca Mountain disposal system over the next 10,000 years; and assume that all those factors remain constant as they were at the time of submission of the license application (DOE 2002b). Therefore, the effects of human influence on climate are excluded from the TSPA calculations (BSC 2001a, Section 6.5.1 through 6.5.4).

Because various climatic physical processes affecting net infiltration cannot be simulated explicitly for each grid of the regional Yucca Mountain infiltration model, physically based empirical relationships (e.g., the relationship between the precipitation and topographic elevation) were used for simulations of net infiltration (USGS 2001b). To account for the variability of meteorological parameters caused by the effects of relatively small-scale (local) physical processes, such as the effect of topographic features (mountains, valleys, and other terrestrial factors), the Yucca Mountain regional-scale net infiltration predictions were performed using the averaged meteorological data (precipitation and snow rates, temperature) from two or three meteorological stations (USGS 2001b).

Although reports (USGS 2001a; Sharpe 2003, p. 57) identified several types of uncertainties in forecasting climate states, these reports concluded that these uncertainties are adequately addressed by the three climate states, the estimated duration of future climate states (based on the precession methodology) compares favorably with that of past climate states (based on the fossil and isotope records), and that this forecast presents the best possible scientific assessment for future climates. Because there is no simple or objective way of assessing the nature of future climate uncertainties, only future observations could be used to validate the climate forecasting.

3. CONCEPTUAL MODEL OF PROCESSES CONTROLLING NET INFILTRATION

This section comprises the conceptual understanding of dominant factors and processes that control net infiltration at Yucca Mountain. These factors and processes include: surface topography, precipitation, evaporation and transpiration, run-on and runoff, the redistribution of moisture in the shallow subsurface, infiltration, percolation, and groundwater recharge, as well as the types of uncertainty involved in the evaluation of flow parameters and net infiltration. The schematic of the hydrologic cycle involving these factors and processes is shown in Figure 3-1 (Flint, A.L. et al. 1996, p. 9). The mathematical relationships describing the effects of these processes will be presented in Section 4, which is devoted to numerical modeling of net infiltration.
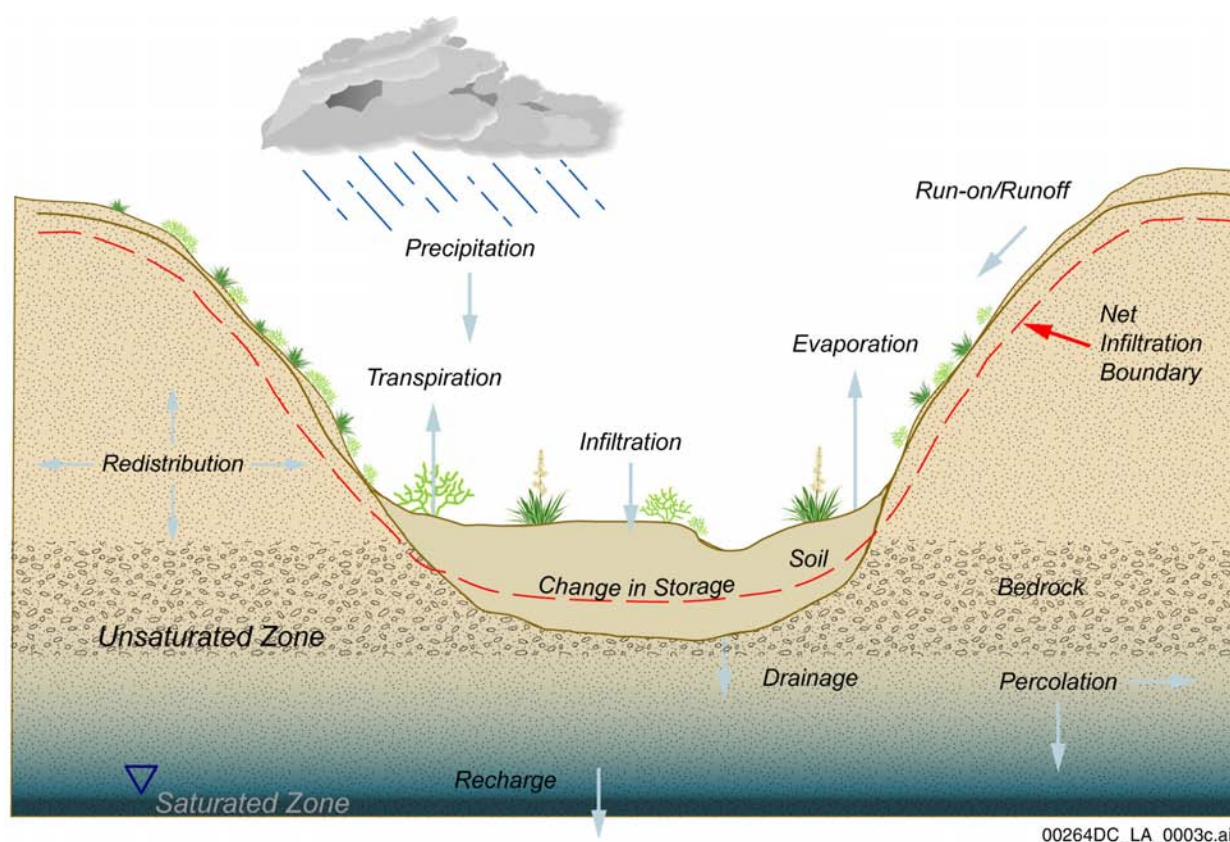
Source: Flint, A.L. et al. 1996, Figure 3.

Figure 3-1. Schematic Illustrating Field-Scale Water Flow Processes Controlling Net Infiltration

3.1 EFFECT OF TOPOGRAPHY

Topography of the land cover is a very important factor affecting both a micro- and macroscale surface and subsurface hydrologic processes. It has direct feedbacks to energy and water systems, and determinations of boundary conditions related to the exchange of momentum, energy and mass between the atmosphere and the subsurface. In particular, the land topography affects the spatial distribution of surface (including surface flow channeling, runoff, and run-on) and subsurface water flow, solar radiation loading, potential evaporation, and evapotranspiration.

Proper land surface characterization is thus crucial for the evaluation of processes controlling net infiltration. Topography may cause the infiltration rate to vary by several orders of magnitude under different geomorphic settings (Scanlon et al. 1999).

3.2 FRACTURE ROCK CHARACTERISTICS

At Yucca Mountain, net infiltration is mostly formed at the bottom of the root zone located within the first 6 m of depth, either within the soil or the fractured tuff of the TCw hydrogeologic unit (Flint, A.L. et al. 1996). The presence of the bedrock is considered to control net infiltration if the bottom of the root zone, where the net infiltration is originated, is located within the TCw hydrogeologic unit, which is significantly fractured. The most important characteristics of fractured rock that could affect net infiltration are fracture length, fracture spacing, fracture connectedness, fracture aperture, and fracture roughness. The degree of tuff welding determines the fracture characteristics, which, in turn, affect how water moves through each particular unit. Small fractures (less than 1 m in length) comprise about 50 percent of the total number of fractures, and the number of fractures less than 2 m comprises about 75 percent of the total number of fractures (Hinds et al. 2003). The effect of small-scale fractures, comprising a significant portion of the total fractures, is incorporated into the large-scale Yucca Mountain numerical model (with gridblock size exceeding 100 m) using calibrated unsaturated hydraulic parameters (Wu et al. 1999). At Yucca Mountain, geologic features such as faults may serve either as capillary barriers or as major conduits, focusing near-surface downward flow, depending on the degree of saturation and hydraulic conductivity of the infilling material.

3.3 SURFACE HYDROLOGY

Surface hydrology is one of the main factors affecting the amount of water entering the subsurface. Overall, the streamflow in the desert terrain of the Amargosa River basin is extremely erratic and sparse. The results of monitoring show that increased streamflow in 1983, 1992, 1993, and 1995 caused groundwater levels to rise in observation boreholes in Fortymile Canyon (Savard 1998, p. 27). The data analysis of streamflow indicates that:

- The flood of February 24 to 25, 1969, was the greatest runoff event since the beginning of streamflow recording in the early 1960s.

- Unit peak discharges typically are greater in small drainage basins than in larger basins.

- Maximum peak discharges do not correlate closely with maximum unit peak discharges.

The types of flooding at Yucca Mountain depend on the amount of precipitation. For example, the 1995 streamflow was dominated by high-magnitude runoff of relatively short duration in Beatty Wash and Fortymile Wash, probably enhanced by localized precipitation on snowpack in the upper altitudes of the Nevada Test Site. In 1998, sustained regional precipitation caused lower magnitude streamflows of longer duration in Fortymile Wash, Amargosa River, and their major tributaries. In both floods, much or all of Fortymile Wash and the Amargosa River flowed simultaneously. In March 1995, water in Fortymile Wash and Beatty Wash flowed off Nevada Test Site; in February 1998, water in Topopah Wash also flowed off Nevada Test Site. In 1995 and 1998, the Amargosa River flowed from its headwaters to its terminus in Death Valley. Both

the 1995 and 1998 floods indicate, therefore, that the Amargosa River, with contributing streamflow from one or more among Beatty, Fortymile, and Topopah Washes, has the potential to transport dissolved and particulate material well beyond the boundary of the Nevada Test Site and Yucca Mountain areas during periods of moderate to severe streamflow. The effects of surface floodings on infiltration and, in particular, preferential flow in the unsaturated zone are discussed in Section 3.8.

3.4   PRECIPITATION

Precipitation at Yucca Mountain can be characterized using the precipitation time series recorded at a number of meteorological stations shown in Figure 3-2. As an example, Figure 3-3 (USGS 2001b, Figure 6-18) shows the daily variations of precipitation over the period from 1980 to approximately 1995 characterizing the present-day climate conditions (these data were used for model calibration—see Section 4). Figure 3-4 shows an example of the Tule Lake, California, precipitation time series used for simulations of the mean glacial-transition climate (DTN: GS000308311221.010).

3.5   TYPES AND DEPTHS OF SOILS

The areal distribution of estimated soil depth in the Yucca Mountain region is shown in Figure 3-5. Soil textures range from gravelly to cobbled, loamy sands to sandy loams. Soils are calcareous (high in calcium carbonate), with lime coatings on the undersides of rocks in the subsoil layer. These soils are moderately to strongly alkaline, with pH ranging from 8.0 to 8.6. Rock fragments ranging in size from gravel to cobbles dominate 45 to 65 percent of the ground surface. Soils include high clay content and thin calcium-carbonate layers, and the underlying bedrock is moderately to densely welded and moderately to highly fractured. The presence of rock fragments in soil layers can impact measured hydraulic properties. Variation of soil hydraulic properties influences the amount, distribution, and routing of overland flow.

3.6   DEPTH OF THE ROOT SYSTEM

The depth of the root zone is determined by vegetation, which controls the depth distribution of both net infiltration and evapotranspiration (i.e., the sum of evaporation and plant transpiration). Vegetation cover can play a major role in hydrologic systems, contributing to recycling of moisture between the atmosphere and soils. Rooting depths for shrubs typically range from 0 to 50 cm (Wallace et al. 1980). Wirth et al. (1999) compiled ranges of maximum rooting depths for various vegetation types under current and future (glacial-transition) climates for a study related to the waste disposal of transuranic waste in greater confinement disposal boreholes at the Nevada Test Site (Cochran et al. 2001). Wirth et al. (1999) report a range of maximum rooting depths of 0.35 to 17.4 m for shrubs under current and future climates, and a range of maximum rooting depths of 0.2 to 30 m for trees under a future climate. Under a future cooler, wetter climate at the Nevada Test Site, areas currently inhabited by shallow rooting shrubs may be replaced by deeper rooting pinon–juniper communities currently found at the upper elevations of the Nevada Test Site (McCurley 2003). Junipers, for example, have a rooting depth ranging from 6 to 60 m.

Easting (ft)
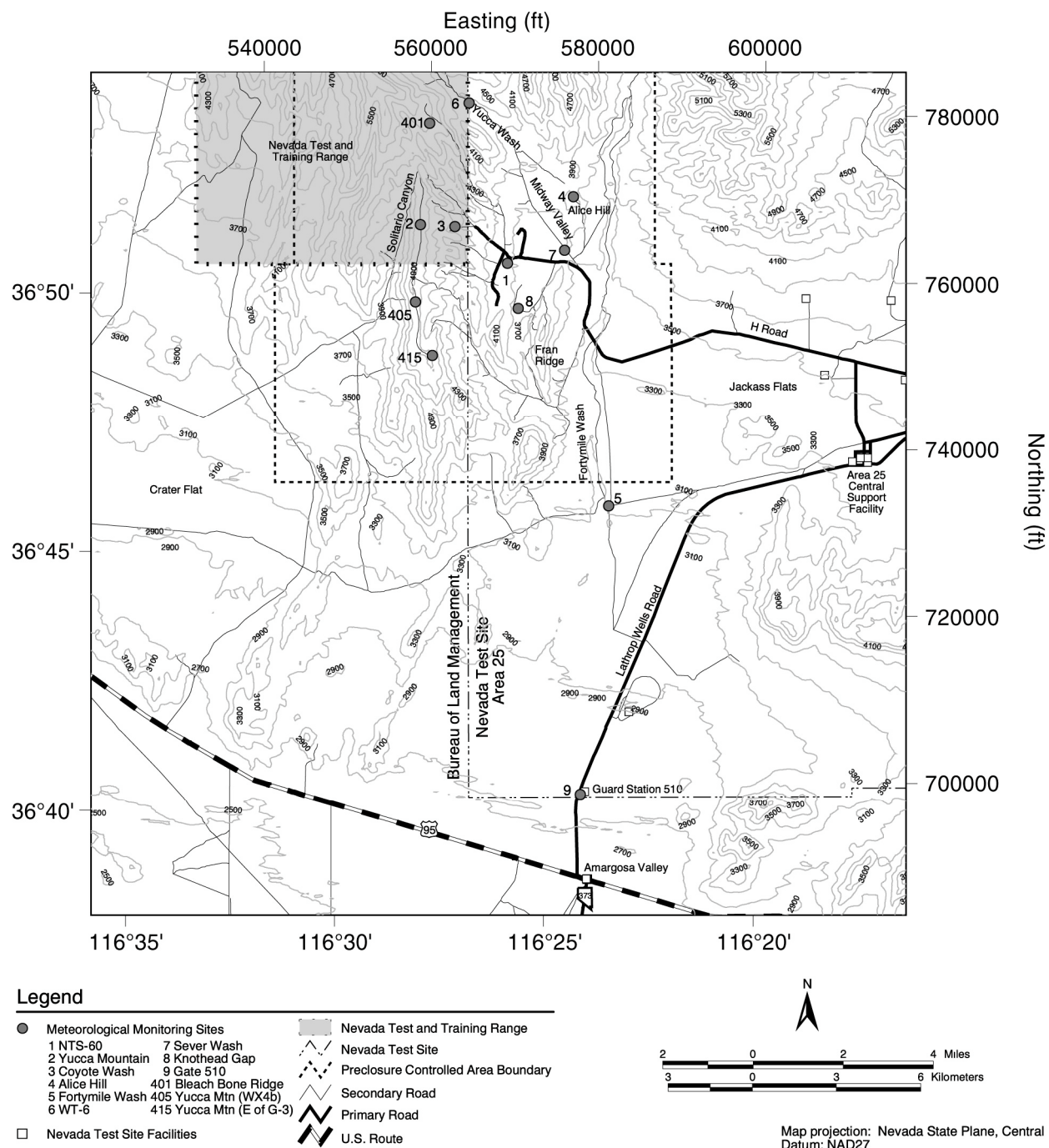
Source: CRWMS M&O 2000b.

Figure 3-2. Locations of Yucca Mountain Site Characterization Project Meteorological Monitoring Sites
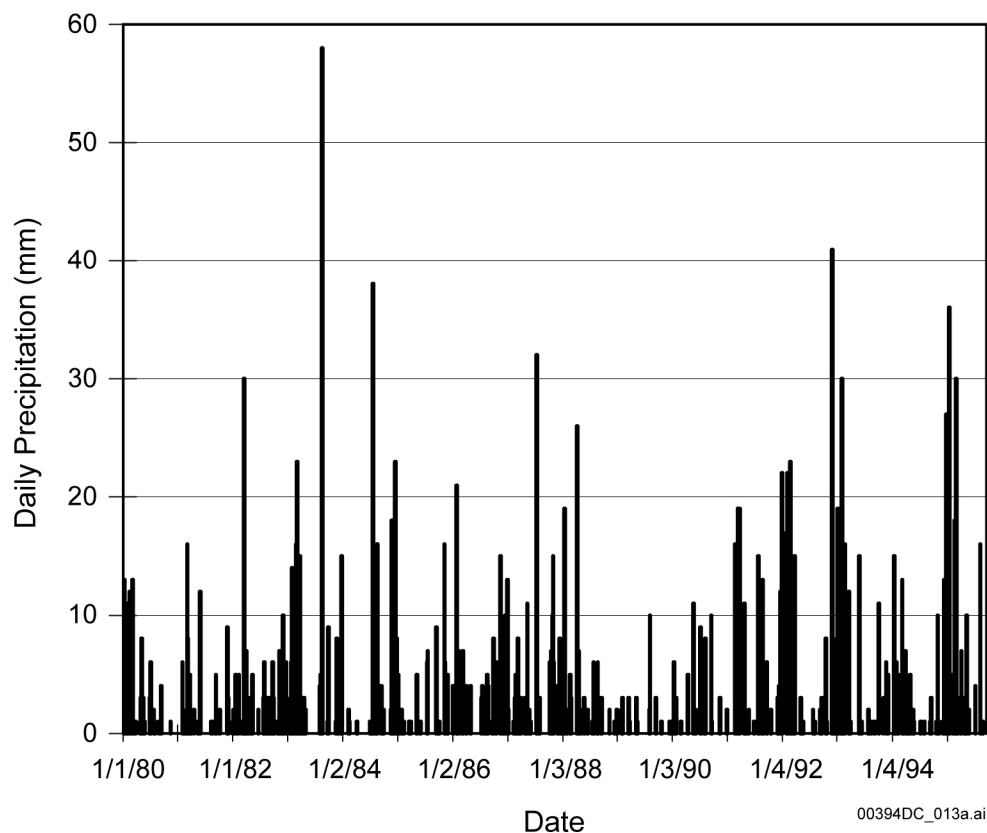
Source: USGS 2001b, Figure 6-18.

Figure 3-3.   Daily Precipitation Record Characterizing Present-Day Precipitation (1980 to Approximately 1995)
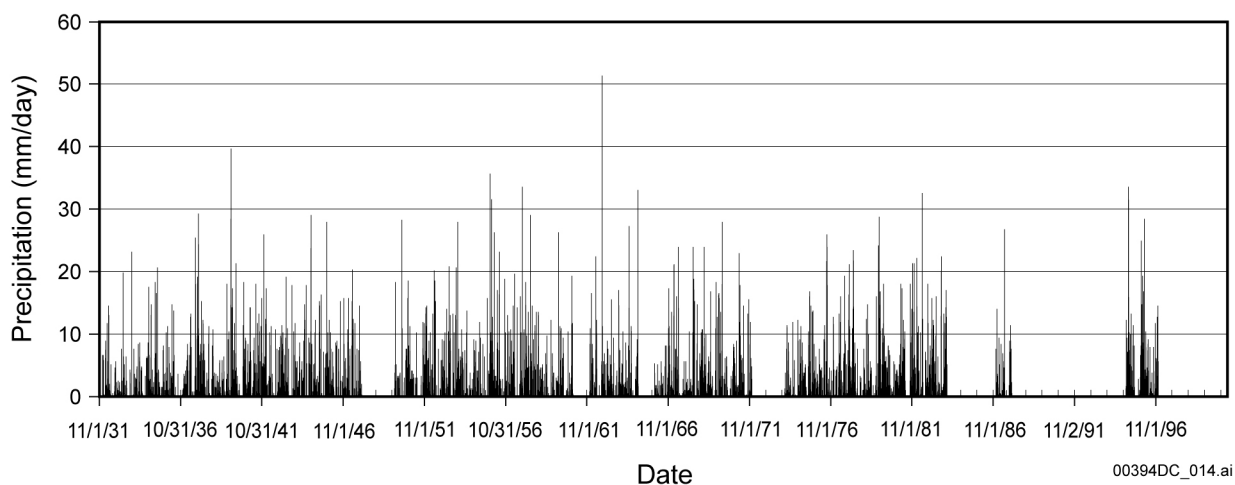
Source: DTN: GS000308311221.010.

Figure 3-4.   Tule Lake, California, Precipitation Time Series Used for Simulations of Net Infiltration for the Glacial-Transition Climate in *Analysis of Infiltration Uncertainty* (BSC 2003a)
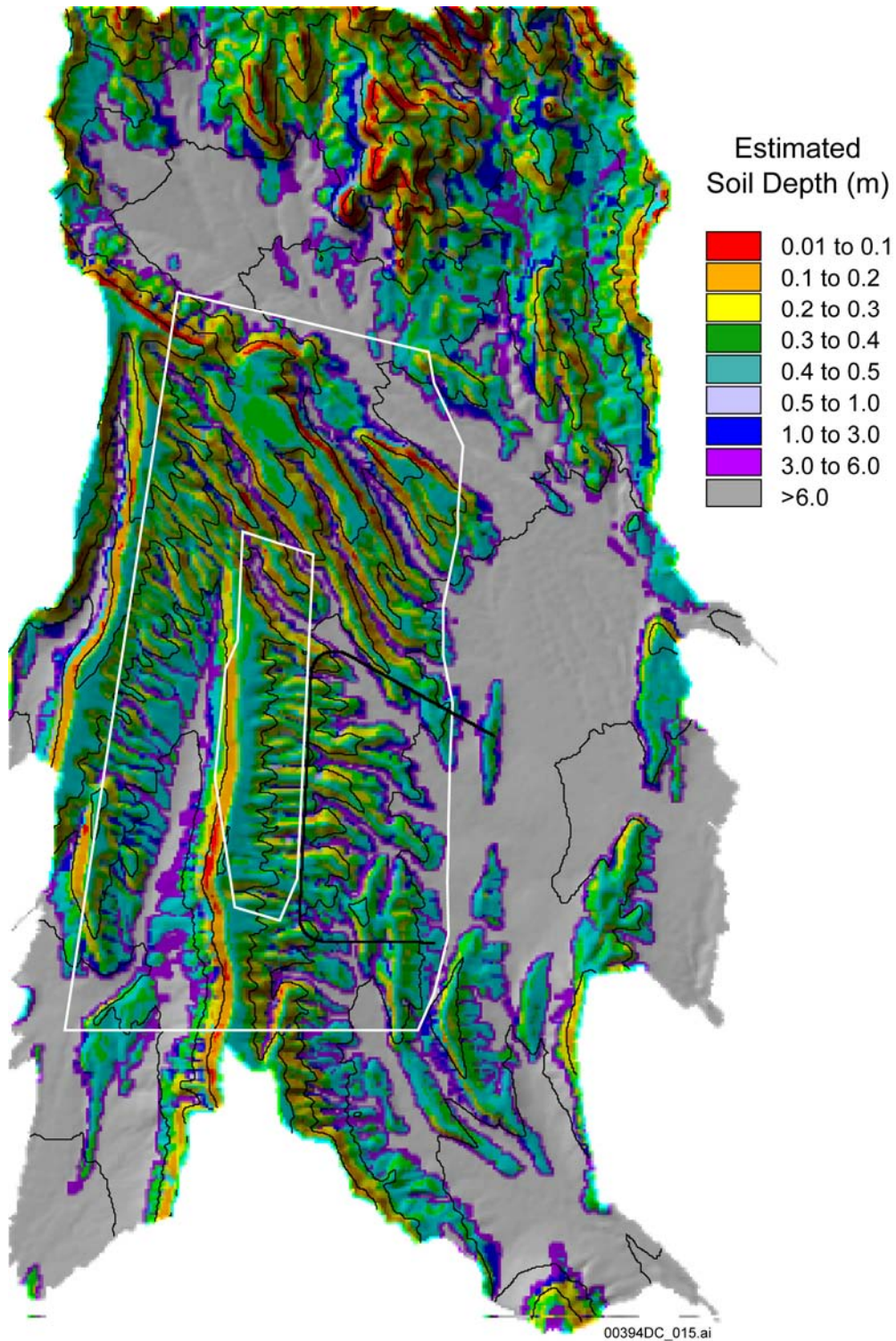
Source: USGS 2001b, Figure 6-16.

Figure 3-5. Estimated Soil Depth in the Yucca Mountain Region

Vegetation root-zone parameters are expected to vary with changes in climate conditions. For example, for the monsoon climate, the root-zone parameters should be modified to reflect greater vegetation density and changes in vegetation type caused by wetter climate conditions (USGS 2001b, Section 6.9.4).

3.7 EVAPOTRANSPIRATION

To assess the evapotranspiration rate, field observations were conducted for several years near Yucca Mountain (Flint, A.L. et al. 1996, p. 59, Figure 29). The data obtained from these observations showed strong advective air transport effects in the arid environment at Yucca Mountain. The data also indicated considerable variability in evaporation, with observed evaporation exceeding calculated potential evaporation by about 100 percent. The data also were used to establish the upper limit of available energy for potential evapotranspiration modeling, given that modeled potential evapotranspiration should not exceed observed evaporation. Potential evapotranspiration rates range from a minimum of 500 mm/yr to a maximum of 900 mm/yr, depending mostly on the land-surface slope and aspect. Minimum values of evapotranspiration occur at steep northerly and northeasterly facing slopes, particularly at locations surrounded by blocking topography.

During winter, potential evapotranspiration is at a minimum because of shorter days, lower sun angle, and lower air temperatures, and root activity is either diminished or dormant. Moreover, after large storm or snowmelt events, water can penetrate deeper and accumulate in the root zone more rapidly than it can be removed by evapotranspiration. Therefore, large values of potential evapotranspiration do not prevent the events of episodic infiltration of precipitated or snowmelt water into the subsurface, causing preferential and transient flow phenomena in the shallow part of the unsaturated zone, as discussed in the following section.

3.8 PREFERENTIAL AND TRANSIENT INFILTRATION PHENOMENA

One of the most important features related to our conceptual understanding of infiltration at Yucca Mountain is the possibility of preferential flow. Field and modeling data provide strong evidence supporting the notion of fast, transient, and preferential flow through rock discontinuities at Yucca Mountain. Figure 3-6 shows a schematic presentation of zones of preferential flow (weeps). Figures 3-7 through 3-9 demonstrate evidence of fast, preferential flow based on the variations of the measured water content in boreholes. For example, Figure 3-7 demonstrates that during the period from 1984 to 1995, episodic events of preferential flow (shown by the increased moisture content) occurred eight times, as measured in UE-25 UZN#1, with propagation of moisture to depths generally between 1 and 2.5 m but reaching 11 m in 1995, following a significant storm event (see Section 3.3). Measurements from USW UZ-N15 demonstrate that water could propagate to a depth of about 10 m, following flooding, even without a noticeable increase in the moisture content within a shallow bedrock layer (Figure 3-8). Figure 3-9 illustrates how a zone of increased moisture content measured in UE-25 UZN#63 (which reached at a depth of 2 m) disappeared within the following 6 months.
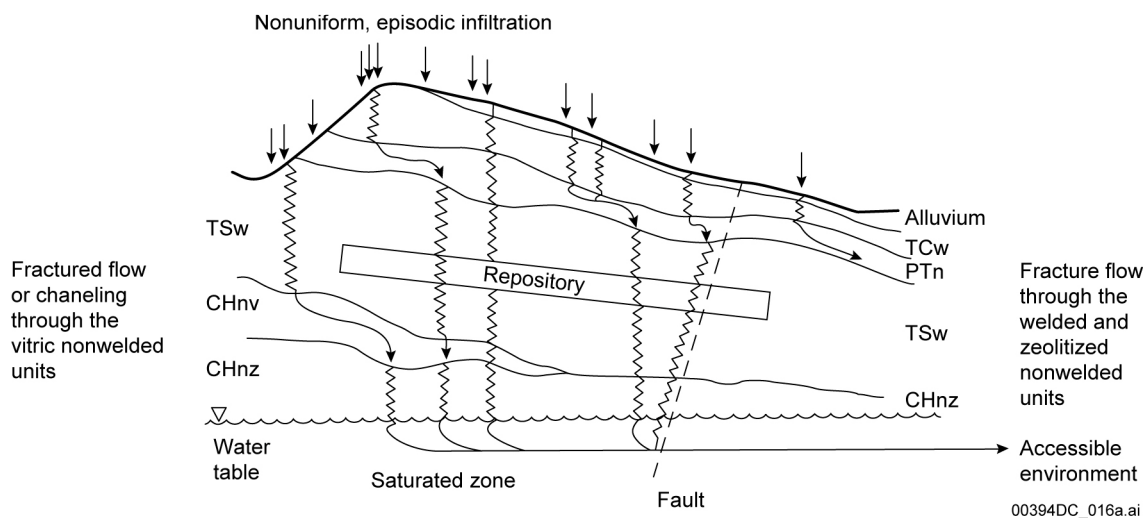
Source: Pruess et al. 1999.

Figure 3-6. Schematic of the Weeps Model for Significant Fracture Flow at Yucca Mountain
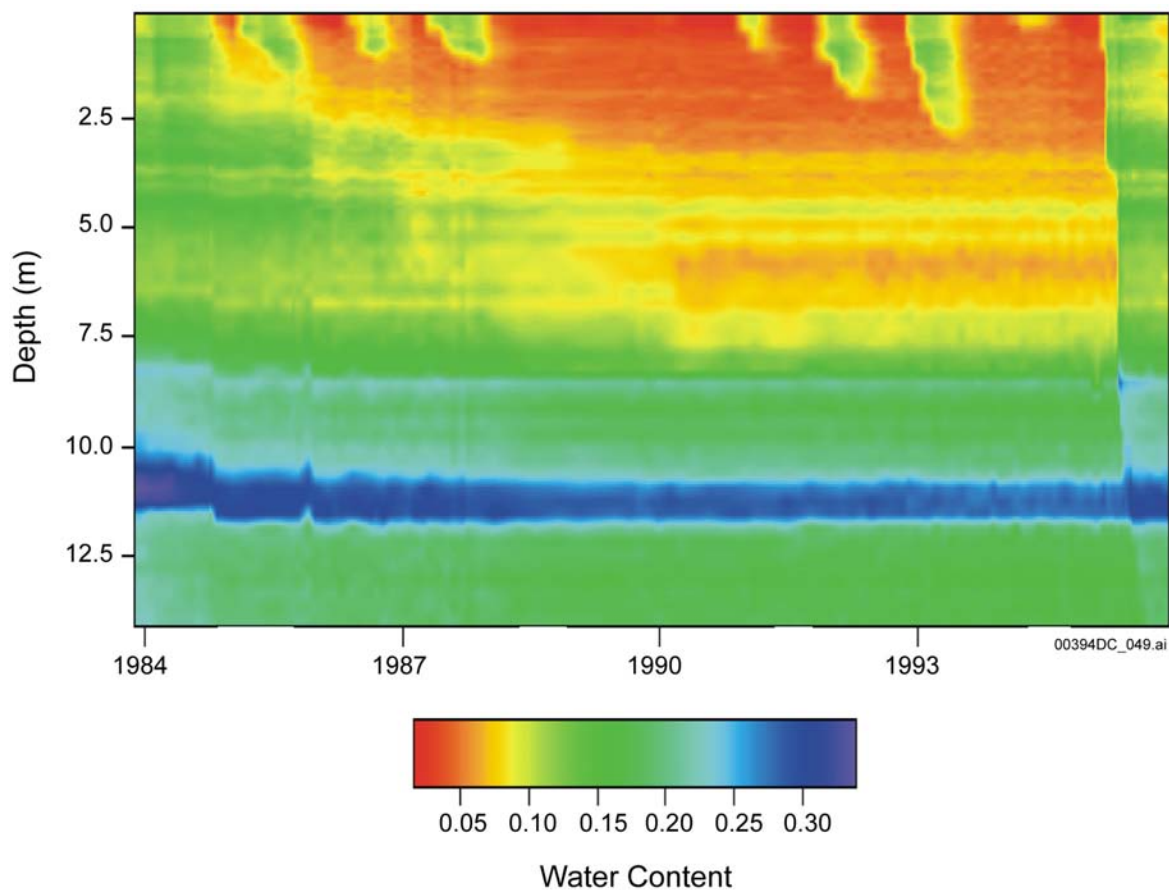
Source: Flint, A.L. et al. 1996, Figure 31.

Figure 3-7.   Measured Water-Content Profiles at Borehole UE-25 UZN#1 from 1984 through Approximately 1995
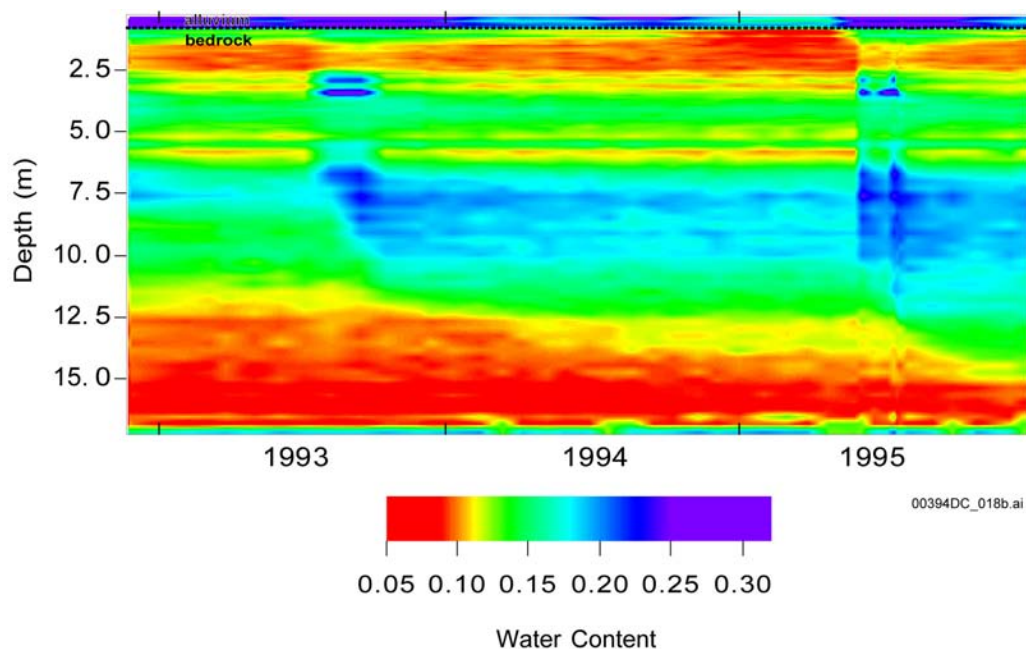
Source: USGS 2001b, Figure 6-4.

Figure 3-8. Measured Water-Content Profiles at Borehole USW UZ-N15 for 1993 to 1995
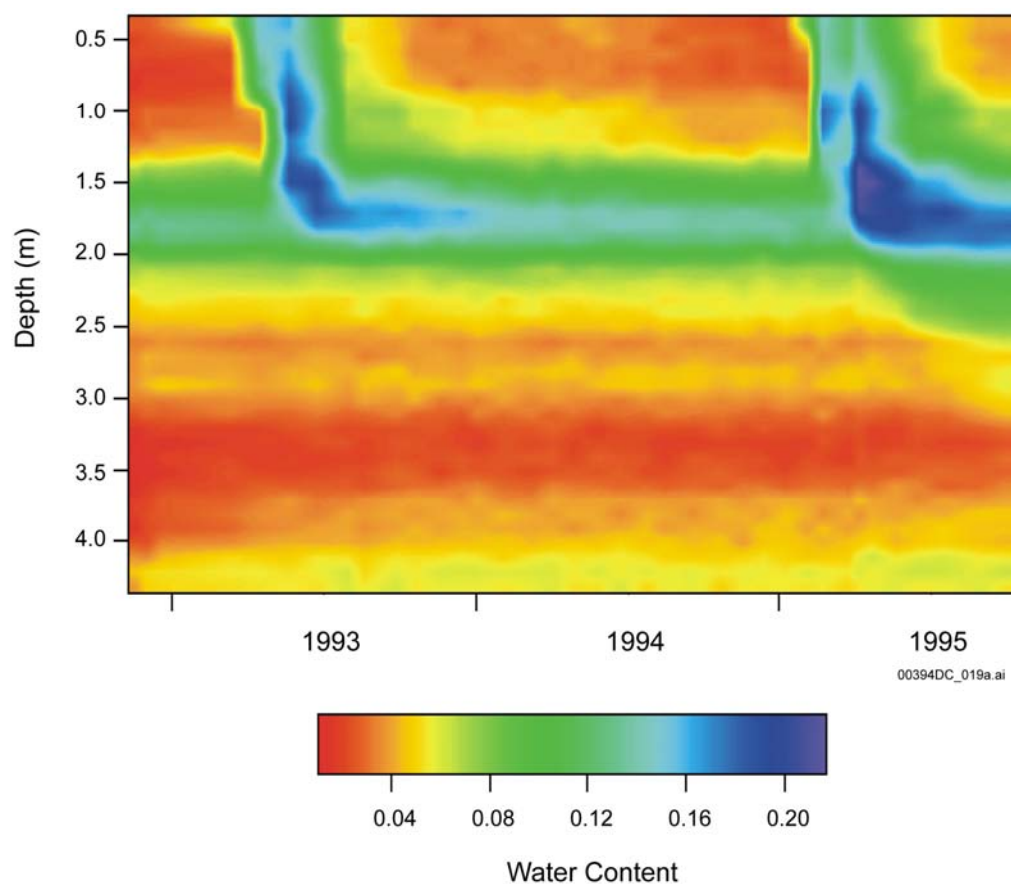
Source: CRWMS M&O 2000b, Figure 8.2-11.

Figure 3-9. Measured Water-Content Profiles in Borehole UE-25 UZN#63 for 1993 through 1995

The presence of preferential flow through a fracture system is also supported by the analysis of estimates of space-averaged net infiltration (Flint, A.L. et al. 1996) and percolation through the mountain. While field estimates indicate that the infiltration rate is on the order of 1 to 10 mm/yr (Bodvarsson and Bandurraga 1996), the calculations based on the flow through the welded tuff matrix show the infiltration rate on the order of one or at most several millimeters per year.

A concept of preferential flow is also supported by environmental isotope data, calcite deposition, and chloride data. For example, the environmental isotopes, in particular ^{36}Cl and ^{99}Tc, have been reported at the repository level in the Exploratory Studies Facility (ESF) by Fabryka-Martin et al. (1996), and elevated concentrations of tritium have been found within the Calico Hills unit (Yang et al. 1996). (Note that based on the results of recent investigations (BSC 2003c), validation studies of the ^{36}Cl data are ongoing (Section 5.2) (Paces et al. 2003).) The presence of these isotopes at the repository level suggests the presence of preferential flow paths within the unsaturated zone.

Calcite coating data show that calcite deposition mostly occurs within the fractures (Paces et al. 1996). Very little evidence of calcite coatings or other similar deposits have been found within the matrix, indicating very low diffusion into the matrix.

The investigations of chloride concentrations within the mountain also confirm the idea of preferential, fracture-dominated infiltration processes (Sonnenthal and Bodvarsson 1999). Chloride concentrations within the shallow Tiva Canyon unit are generally lower than 10 mg/L; they range from 30 to 80 mg/L in the nonwelded Paintbrush unit, and decline again to 5 to 10 mg/L in the deep perched-water bodies found above or within the zeolitic portion of the Calico Hills unit (Yang et al. 1996). This suggests predominant fracture flow within the Tiva Canyon Tuff. Chemical concentrations suggest that the component of matrix flow to the perched-water bodies is rather small.

Significant infiltration into the mountain may occur only every five years or so (Flint, A.L. et al. 1996). In the extra wet years, infiltration in major drainages (where flow is concentrated) can increase to hundreds of millimeters per year during a relatively short time of perhaps not more than one week. Because of the fractured nature of the Tiva Canyon unit, rapid infiltration pulses may not dampen significantly before reaching the bottom of the Tiva Canyon unit. For example, A.L. Flint et al. (1996) reported a water pulse that originated during the 1995 wet winter season and was detected a year later. Neutron borehole data in shallow alluvium and the Tiva Canyon Tuff showed slower movement of the water fronts, with velocities as low as only a few millimeters per year (Flint, A.L. et al. 1996). However, after the water has entered permeable and well-connected fracture pathways, its migration velocity may be on the order of tens or even 100 mm/yr. Flow through isolated fast-flow paths in the near-surface units might have an insignificant attenuation mechanism (even though isolated flow paths carry a small amount of water).

Infiltration tests conducted at Fran Ridge (Nicholl and Glass 2002) also provide clear evidence of preferential flow at Yucca Mountain (Figure 3-10). Moreover, tests demonstrated a flow structure that appears remarkably similar to gravity-driven fingers observed during the experiments conducted by Nicholl et al. (1993).

The Yucca Mountain results related to preferential flow phenomena are similar to those gathered at a number of sites throughout the world, indicating funneling and divergence of highly localized and extremely nonuniform water flow paths (Yamamoto et al. 1993; Nativ et al. 1995; Faybishenko et al. 2000; Nicholl and Glass 2002).

00394DC_020.ai

Source: Nicholl and Glass 2002, Figure 4.10.

NOTE: Maps were referenced to a portable 2.44 × 2.44 m (8′ × 8′) grid subdivided at 0.305 × 0.305 m (1′ × 1′) intervals. The blue tracer clearly marks both vertical and subhorizontal fractures. In the upper left-hand side of the image, tracer clearly extends outside of the area cleaned for mapping and disappears into the rubble-covered region. On the right hand side of the image, drill pipe was left standing in one of the vertical locator holes (blue arrow) used to position the grid. Locator holes were dry drilled following infiltration with the air-driven jackleg seen in the upper right-hand corner of the image.

Figure 3-10.   Photograph Showing the Distribution of Tracer and Fractures That Were Mapped Directly beneath the Infiltration Test Site (Scale of 1:12) at Fran Ridge

INTENTIONALLY LEFT BLANK

4. SIMULATION OF NET INFILTRATION FOR PRESENT-DAY AND POTENTIAL FUTURE (MONSOON AND GLACIAL-TRANSITION) CLIMATIC CONDITIONS

4.1 MODELING APPROACH

4.1.1 Basis of the Modeling Approach

This section describes the basis for the modeling approach used for simulating net infiltration with the INFIL code, including the water balance equation, and describes the concepts of piston-like flow, a bucket-type model, and field capacity. To perform the modeling, meteorological conditions were defined based on the cyclic behavior of precipitation, temperature, and surface water flow for each climate state.

Water Balance Equation–Because of the complexity of processes controlling net infiltration (discussed in Section 3) and the significant size of the Yucca Mountain study area, the evaluation of net infiltration is based on the water-balance approach that requires measurements and lumped (distributed) estimates of basin-wide (averaged over a watershed) precipitation, snowpack depth and density, stream discharge, and evapotranspiration (Lichty and McKinley 1995, pp. 4 to 10; Flint, A.L. et al. 1996). The water-balance model is based on the principle of the conservation of mass for water over a particular time interval (e.g., day or year) and volume (area and depth) of the soil. For a watershed area with depth interval from the surface to the bottom of the root zone (Flint, A.L. et al. 1996, pp. 9 to 11) the water balance equation is given by (USGS 2001b):

$$P + A + U + W_s + S_s + B_s + L_i + R_{on} - R_{off} - I - E - T - L_o - E_x = 0 \qquad \text{(Eq. 4-1)}$$

where P is precipitation, A is applied water (human induced), U is upward flow, W_s is the change in soil-water storage, S_s is the change is surface-water storage, B_s is change in biomass-water storage, L_i is lateral inflow, R_{on} is surface run-on, R_{off} is surface runoff, I is net infiltration (drainage or percolation), E is evaporation, T is transpiration, L_o is lateral outflow, and E_x is water extraction (human induced).

Taking into account the run-on, runoff, and evapotranspiration (ET) (which is the sum of E and T), and neglecting other terms of Equation 4-1, net infiltration (I) can be determined by

$$I = P - SF + IR_{on} + SM + SW - SB - ET - R_{off} \qquad \text{(Eq. 4-2)}$$

where I is net infiltration, P is precipitation (rain and snow), SF is snowfall, SB is sublimation, SM is snowmelt, SW is change in water-content storage within the root zone, ET is evapotranspiration, IR_{on} is infiltrated surface-water run-on, and R_{off} is surface-water runoff generated by excess precipitation, snowmelt, or run-on.

Figure 4-1 schematically depicts the vertical profile discretization used for calculations of net infiltration. The left column of Figure 4-1 illustrates that for a shallow soil–bedrock interface, the bottom of the root zone extends into the bedrock (the propagation of the root zone into the bedrock was calculated using an equation from the USGS (2001b, Equation 17)), and the soil layer is divided into two sublayers (used for calculations of infiltration and evapotranspiration— see the discussion below on the bucket-type model). The middle column of Figure 4-1 indicates that as the depth to soil–rock interface increases, the propagation of the root zone into the

bedrock decreases, and the soil layer is divided into three sublayers. The right column of Figure 4-1 illustrates that net infiltration is formed at a depth of 6 m, within the soil unit, if the bedrock unit is below the 6-m depth.
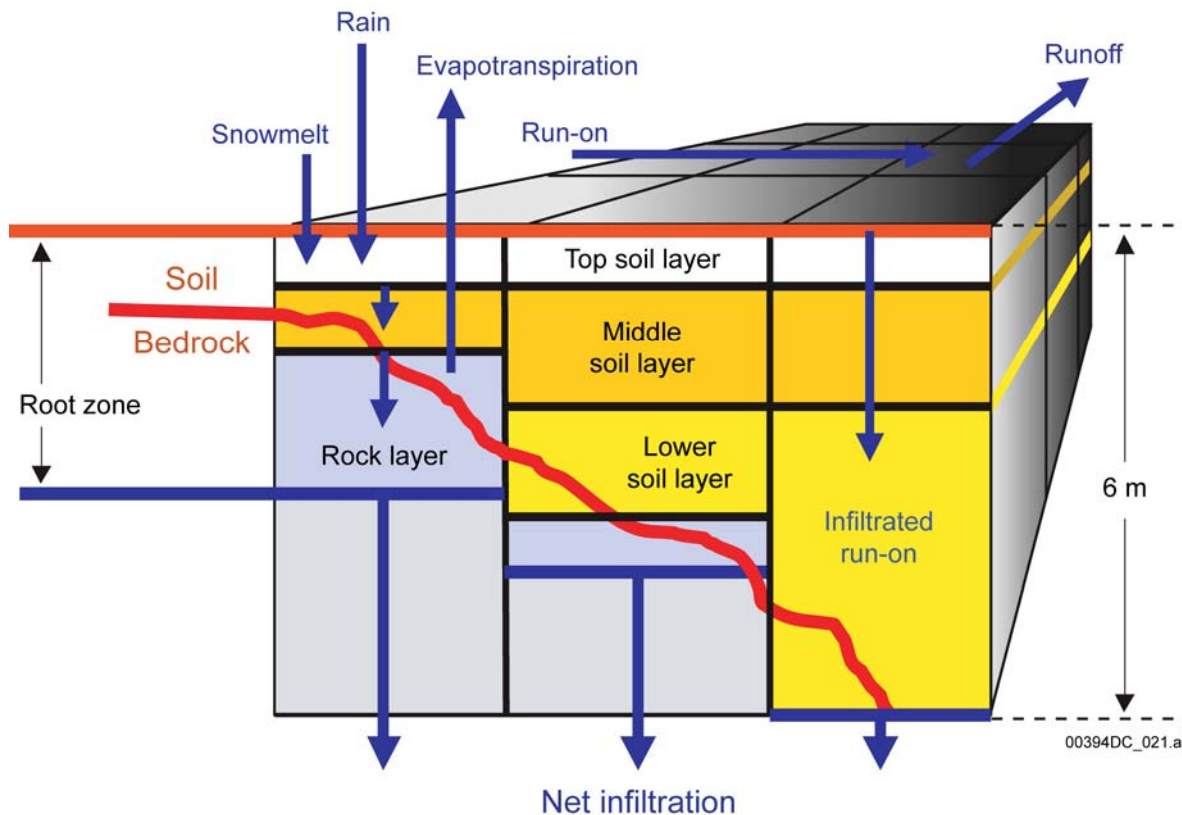
Source: Hevesi et al. 2003.

Figure 4-1.   Conceptual Model of Net Infiltration Illustrating the Layered Root-Zone Water-Balance Model of the Death Valley Region, Nevada and California

Piston-Type Flow–This model assumes the one-dimensional downward progression of a sharp wetting front within a soil profile caused only by advection, with the evaluation of the water transport time for the leading edge of the plume based on the center of mass propagating through diffusion and dispersion. The application of a piston-type flow model is warranted for the evaluation of net infiltration at Yucca Mountain for areas that have root zones in unconsolidated soils and alluvium deposits (see the middle column of Figure 4-1); in these areas, the preferential flow is minimal. The application of this model is also appropriate for the areas that have root systems penetrating into the rock layer (see the left column of Figure 4-1) for the following reasons: episodic events of preferential flow usually occur within small local areas and on a short time scale; however, on a macroscale over sufficiently long times, pulses of preferential flow may average out so that they can be approximated by piston flow (Sukhija et al. 2003). Furthermore, parameters of the model described by Equation 4-2 were calibrated using field observations, as described in Section 4.2.

Bucket Model and the Concept of Field Capacity–To reproduce the interaction between the layers within the soil–rock system, a bucket-type model was used. A "bucket" water-balance model used in calculations presents a series of uniform soil layers from which water is available for evapotranspiration or infiltration. The model assumes that downward infiltration into the lower layer begins when the water content in the upper layer reaches the field capacity. The field capacity is the water-content threshold of the near-surface soil profile (i.e., the root zone), at which drainage becomes negligible (several orders of magnitude less than the saturated flux rate) (Jury et al. 1991, p. 150). Field capacity is an old soil-physics concept intended to provide a characteristic index of how much water may be retained from a rainfall event after redistribution has ceased (Hillel 1982, pp. 243 to 248). In coarse-textured soils, such as those at Yucca Mountain, the drainage rate usually falls to an insignificant level within a few days, after which the water content changes at a slow rate. For thick soils, the saturation corresponding to the field capacity at a depth of 6 m would occur only at areas of localized surface-water flow, such as active stream channels and the base of steep side slopes. Model calibration showed that for upland areas with thin soils, the infiltration rate below the root zone is equal to the saturated hydraulic conductivity of bedrock (for filled fractures with the aperture of 250-µm fractures). The water potential that corresponds to the volumetric water content measured at field capacity is considered to be −0.1 bars (USGS 2001b, Attachment IV). While the use of the field capacity concept reduces the infiltration during dry periods, calculations of net infiltration during the wet periods using the rock saturated hydraulic conductivity overestimates the water flux during the periods of infiltration. As a result, the time-averaged infiltration rate closely matches the experimental data.

Two competing processes affect soil moisture in the bucket model: (1) the model lacks canopy constraints in the release of soil water, leading to rapid evaporation of soil water, and (2) no loss of water from runoff occurs until the soil is saturated, and no rapid evapotranspiration occurs due to canopy interception of precipitation. For a bucket model, the soil water content decreases immediately as evaporation occurs (rapid response scheme), while for a multilayer scheme, water in deep soil layers is reduced through diffusion and then evaporates from the surface.

Although the bucket model and the concept of field capacity present a simplification of the real soil–rock system, the bucket model could be used for regional-scale and long-term predictions to capture the essential features of the regional behavior of soil moisture and infiltration.

Runoff Model–The model used to calculate the runoff is empirical. This model implicitly includes such effects as the two-dimensional surface flow and the differences in types of slopes (converging or diverging (Salvucci and Entekhabi 1995)).

Evapotranspiration Model–Based on a thorough literature review and testing of seven types of models assessing evapotranspiration and bare soil evaporation under arid conditions, Levitt et al. (1996) concluded that the Penman-Monteith and Priestley-Taylor models appear to describe experimental data better than other models for both short- and long-term data sets. These two models require the use of the moisture content of soils. Levitt et al. (1996) also found that these models provide a better description of experimental data for relatively high evapotranspiration (i.e., greater than 1 mm/day). The modified Priestley-Taylor model used in INFIL is based on the empirical relationship for evapotranspiration and the climate analog site temperature data (USGS 2001c).

For the monsoon climate, the evaluation of evapotranspiration was based on modified root-zone parameters reflecting greater vegetation density and changes in vegetation type for the wetter climate conditions (USGS 2001b, Section 6.9.4). For the upper-bound monsoon climate, the root-zone weighting parameters were modified to approximate a 40 percent vegetation cover (as compared to 20 percent for present-day climate) and the maximum thickness of the modeled bedrock root-zone layer was increased from 2 to 2.5 m (6.6 to 8.2 ft).

4.1.2   Unsaturated and Saturated Hydraulic Parameters

The unsaturated hydraulic parameters (used in calculations of the water retention and unsaturated hydraulic conductivity functions) were determined from rock outcrop samples (Flint, L.E. et al. 1996; Flint, L.E. 1998) and through calibration of the INFIL model (USGS 2001b). The hydraulic properties determined using calibrations of the numerical model are fracture and matrix permeability (k_f and k_m), and the fracture and matrix van Genuchten α and m parameters (α_f, α_m, m_f, and m_m). A summary of hydraulic parameters (for soils only) used in these simulations of net infiltration is given in Table 4-1.

Table 4-1. Summary of Soil Properties Used as Input for INFIL V2.0

Soil Unit	Saturated Hydraulic Conductivity (simulated, m/s)	Alpha (1/Pa)	n	Porosity (%)	Rock Fragments (%)	Bulk Density (g/cm³)	Water Content at −0.1 bar Water Potential (%)	Water Content at −60 bars Water Potential (%)
1	5.6×10^{-6}	0.00052	1.24	36.6	10.5	1.60	24.2	5.4
2	1.2×10^{-5}	0.00062	1.31	31.5	11.6	1.73	17.3	2.3
3	1.3×10^{-5}	0.00066	1.36	32.5	18.7	1.70	16.3	1.7
4	3.8×10^{-5}	0.00087	1.62	28.1	21.9	1.81	7.3	0.2
5	6.7×10^{-6}	0.00056	1.28	33.0	15.2	1.69	20.0	3.5
6	2.7×10^{-5}	0.00074	1.40	33.9	11.7	1.66	15.0	1.1
7	5.6×10^{-6}	0.00055	1.26	37.0	17.1	1.58	23.4	4.6
9	5.7×10^{-6}	0.00055	1.30	32.2	19.1	1.72	18.9	2.8

Source: USGS 2001b, Table IV-4.

The saturated hydraulic conductivity (used as a coefficient in the van Genuchten model of unsaturated hydraulic conductivity and direct evaluation of net infiltration) was determined from a series of air-injection tests and the calibration of the INFIL model. The results of field air-injection tests designed to determine the air permeability of rocks could be used to assess the upper limits of the saturated hydraulic conductivity values (needed for the net infiltration uncertainty analysis). For the Tiva Canyon welded unit, the air-permeability values are summarized by Patterson et al. (1996) and Rousseau et al. (1997). Figure 4-2 shows the spatial distribution of the saturated hydraulic conductivity of bedrocks and soils, which was determined from the calibration of the numerical model and was then used in the evaluation of net infiltration.
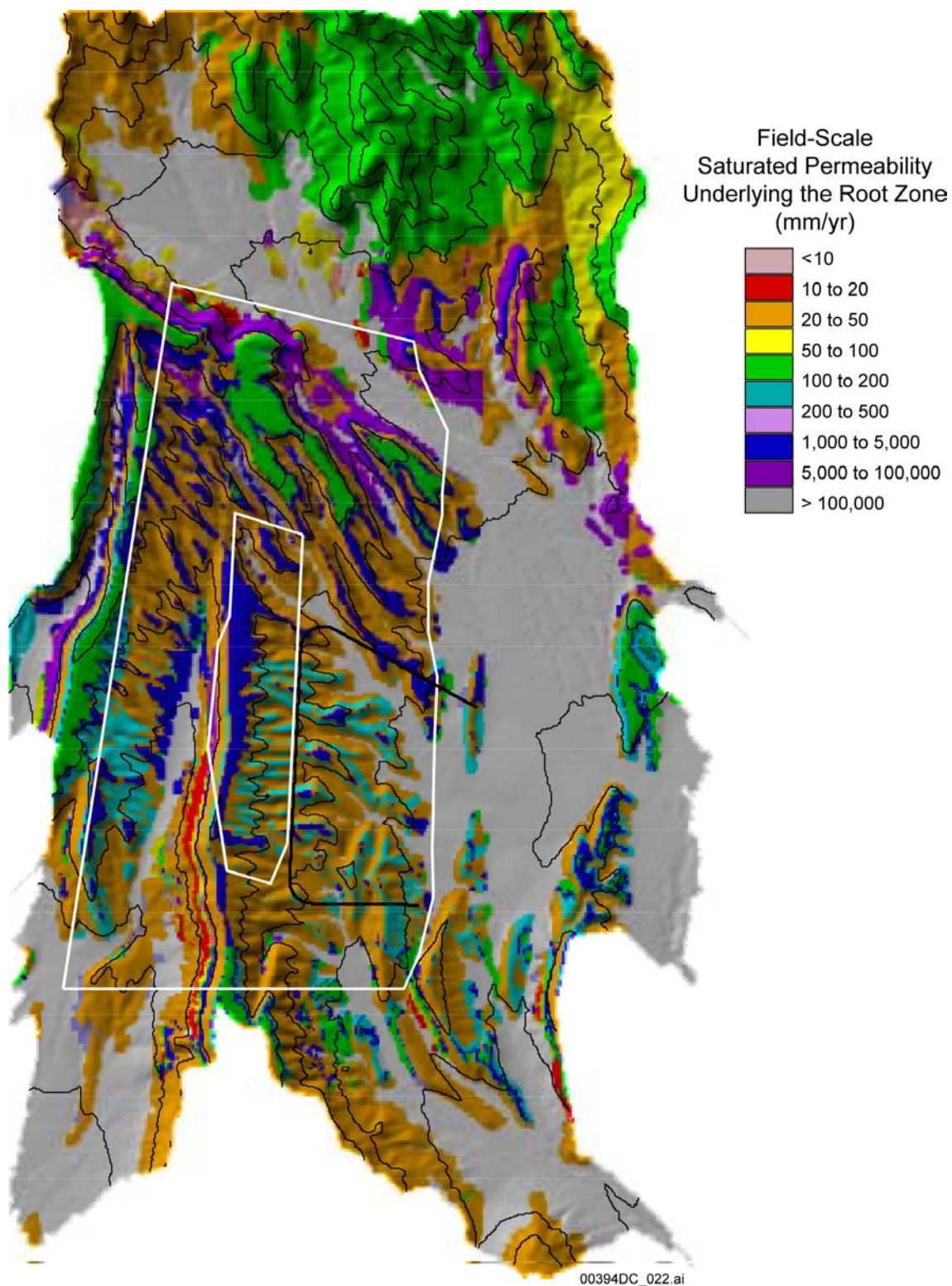
Source: USGS 2001b, Figure 6-15.

Figure 4-2.   Estimated Field-Scale Saturated Hydraulic Conductivity of Bedrock or Soils Underlying the Root Zone

In the TCw hydrogeologic unit, high values of permeability are associated with fractures and major faults (Kwicklis 1999; Ahlers et al. 1996, Section 3). Faults at Yucca Mountain have properties that cause them to function either as highly permeable conduits or as low-permeability barriers (Patterson et al. 1996, pp. 51 and 52), depending on the degree of saturation of infilling material and boundary conditions (e.g., precipitation and run-on). Presumably, the highly fractured breccia zones are very permeable, whereas fault gouge along the base of the faults seems to create low-permeability barriers to flow. Thus, permeability of fractured rock surrounding the monitoring boreholes incorporates the breccia zone effects as larger block permeability and the effects of gouge as smaller block permeability.

The fracture permeabilities are generally in the range of 1 to 10 darcies (LeCain 1997), while fault permeabilities are on the order of 10 to 100 darcies (Ahlers et al. 1996, Section 3). In contrast, the matrix permeabilities of those units are on the order of 1 microdarcy (Flint, A.L. et al. 1996). For comparison, the nonwelded units at Yucca Mountain, including the PTn and CHn hydrogeologic units, have matrix permeabilities on the order of several hundred millidarcies, and these units contain much less fracturing (Flint, A.L. et al. 1996; Ahlers et al. 1996).

To better understand the processes governing flow in the TCw hydrogeologic unit and to determine the TCw hydrogeologic unit hydraulic properties, an infiltration and tracer transport test was performed in the ESF Alcove 1 (BSC 2001b, Section 6.8.1) near the North Portal of the ESF in the upper lithophysal zone of the Tiva Canyon Tuff (Tpcpul) unit (Flint, L.E. 1998, p. 3). The Tpcpul unit extends above the alcove to the ground surface, with the crown of the drift approximately 30 m below the ground surface. The infiltration test was conducted by supplying water at the ground surface directly over Alcove 1. For both phases, the upper boundary condition for water flow remained essentially the same. The seepage into the alcove and the tracer arrival time were recorded. The test consisted of two phases: Phase I was performed from March to August in 1998, and Phase II was performed from January to June in 1999. During Phase II, conservative bromide tracer was also introduced into the infiltrating water. To analyze the Alcove 1 test results, hydraulic properties for fractures and the matrix were assumed to be homogeneously distributed within the model domain (BSC 2001b, Section 6.8.1). Figure 4-3 shows a comparison between observed seepage rate data for Phase I of the test and the simulation result from model calibration with ITOUGH2 (version 3.2) (BSC 2001b, Section 6.8.1). Although arrival times of three major peaks in the Phase I seepage rate data are matched, large differences exist between the simulated and observed seepage rate values at these peaks. The hydraulic parameters calculated from the Alcove 1 test were used in *Analysis of Infiltration Uncertainty* (BSC 2003a). The results of numerical modeling using the results of Alcove 1 observations can also be used for validation of continuum and active-fracture model approaches for modeling flow and transport in unsaturated fractured rock (Liu et al. 1998).
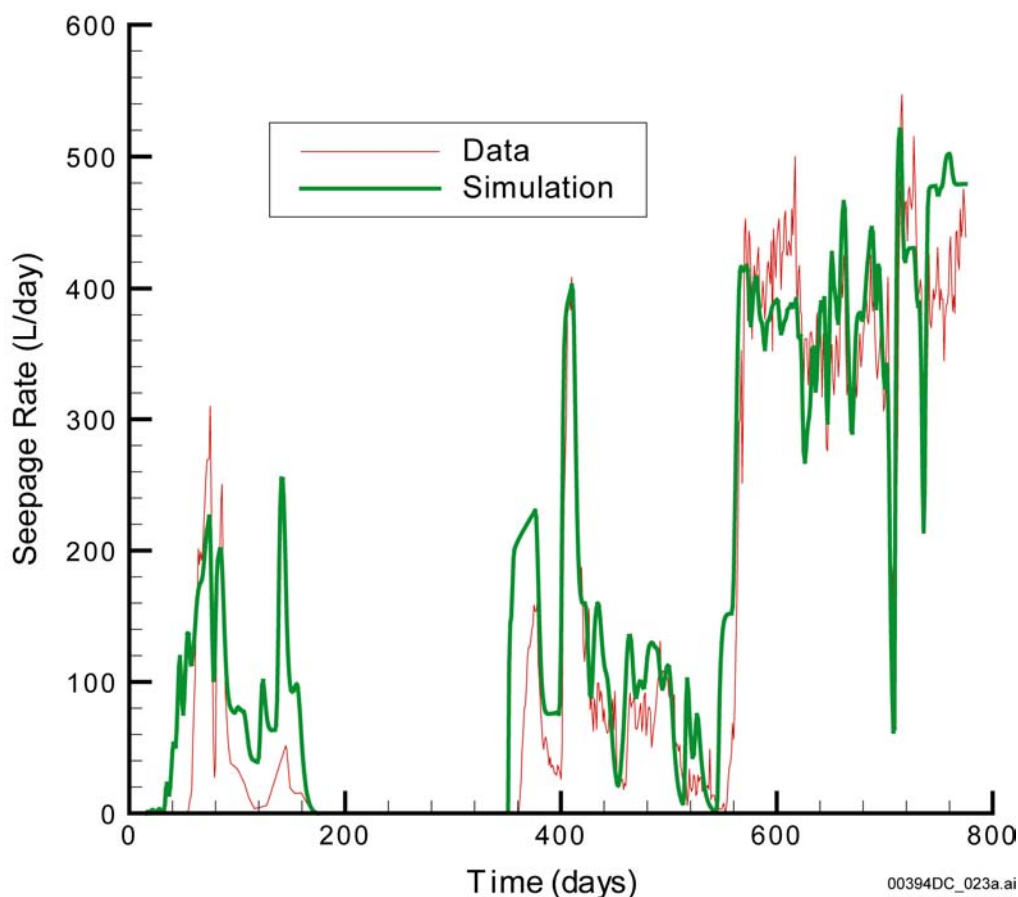
Source: Liu, H-H. et al. 2003.

Figure 4-3. Comparison between Observed Seepage Rate Data for Phase I of the Alcove 1 Test and the Simulation Result from Model Calibration with ITOUGH2

4.1.3 INFIL Model

The INFIL code represents a family of storage routing codes (that assume that gravity is the only driving force in water movement), with approximation of evapotranspiration as a sink. Net infiltration is determined in the INFIL code as water flow below the root zone. The root zone is defined as the zone from the ground surface to a certain depth in soil or bedrock, from which infiltrating water is removed by evapotranspiration (USGS 2001b, p. 20).

The INFIL V2.0 numerical algorithm represents the solution of Equation 4-2. In this model, the downward infiltration rate through the root zone depends primarily on the storage capacity of the root zone, the field capacity, and hydraulic conductivity of the soil and bedrock. The storage capacity of the soil is defined as the porosity minus the residual water content, multiplied by the soil depth.

The INFIL code consists of three main loops for performing a daily simulation of net infiltration over all model cells across a watershed model domain. Figure 4-4 (USGS 2001b, Figure 6-7) provides a flow chart illustration of the general model algorithm and the primary loop, which is driven by the daily climate input file and carries the simulation through the time domain. A

grid-cell loop (nested within the primary loop) performs daily water-balance calculations within each layer of the root zone at each grid cell. The root zone is subdivided into layers based on the estimated maximum depth of bare-soil evaporation and an estimated variation in root density.

The daily root-zone water balance consists of simulating precipitation, snowmelt, sublimation, evapotranspiration, water content for each root-zone layer, net infiltration, and runoff generation. An hourly loop (nested within the water-balance loop) is used for modeling potential evapotranspiration, based on the simulation of incoming solar radiation and effects on total solar radiation resulting from blocking ridges. After the completion of the water-balance loop, a surface-water flow-routing subroutine is called if runoff is generated at any grid cell. Surface-water flow is routed at the end of the day as a time-independent (instantaneous) total daily flow depth across each grid cell. The routing algorithm connects all grid cells horizontally, using surface-water flow-routing parameters included in the geospatial parameter input file. Surface-water flow is coupled to the water-balance calculation by allowing surface water to infiltrate into downstream grid cells according to the available root-zone storage capacity, soil hydraulic conductivity, and estimates for effective surface-water flow area and stream flow duration. Infiltrating water is added to the grid cell's antecedent root-zone water-content term used in the following day's water-balance calculation. The surface-water flow depth routed across the grid cell defining the outflow location of the watershed is converted to a daily mean discharge flow rate, which can be compared to measured stream flow for model calibration.

Water infiltrating and percolating through the multilayered root-zone system is modeled as a cascading piston-flow process. Downward percolation is modeled as a "forward" cascade flow initiated by adding the volume of water into the topsoil root zone to the antecedent water in the topsoil layer. The water content is then compared with the field capacity for each grid cell. The volume of water exceeding the field capacity percolates downward to the underlying layer, and the new water content of the underlying layer is compared against the field capacity of that layer. If the potential percolation rate exceeds the saturated soil hydraulic conductivity (or the saturated bulk bedrock hydraulic conductivity) of the underlying layer, the downward percolation rate is set equal to the saturated hydraulic conductivity of the underlying layer, and the excess water volume is added to a temporary storage term for the overlying layer. The process is repeated for each soil and bedrock layer in the root zone until the bottom layer is reached. (For simulation of net infiltration, a maximum of three soil layers and one bedrock layer were used.) The volume of water exceeding the bedrock storage capacity is the potential net infiltration volume.
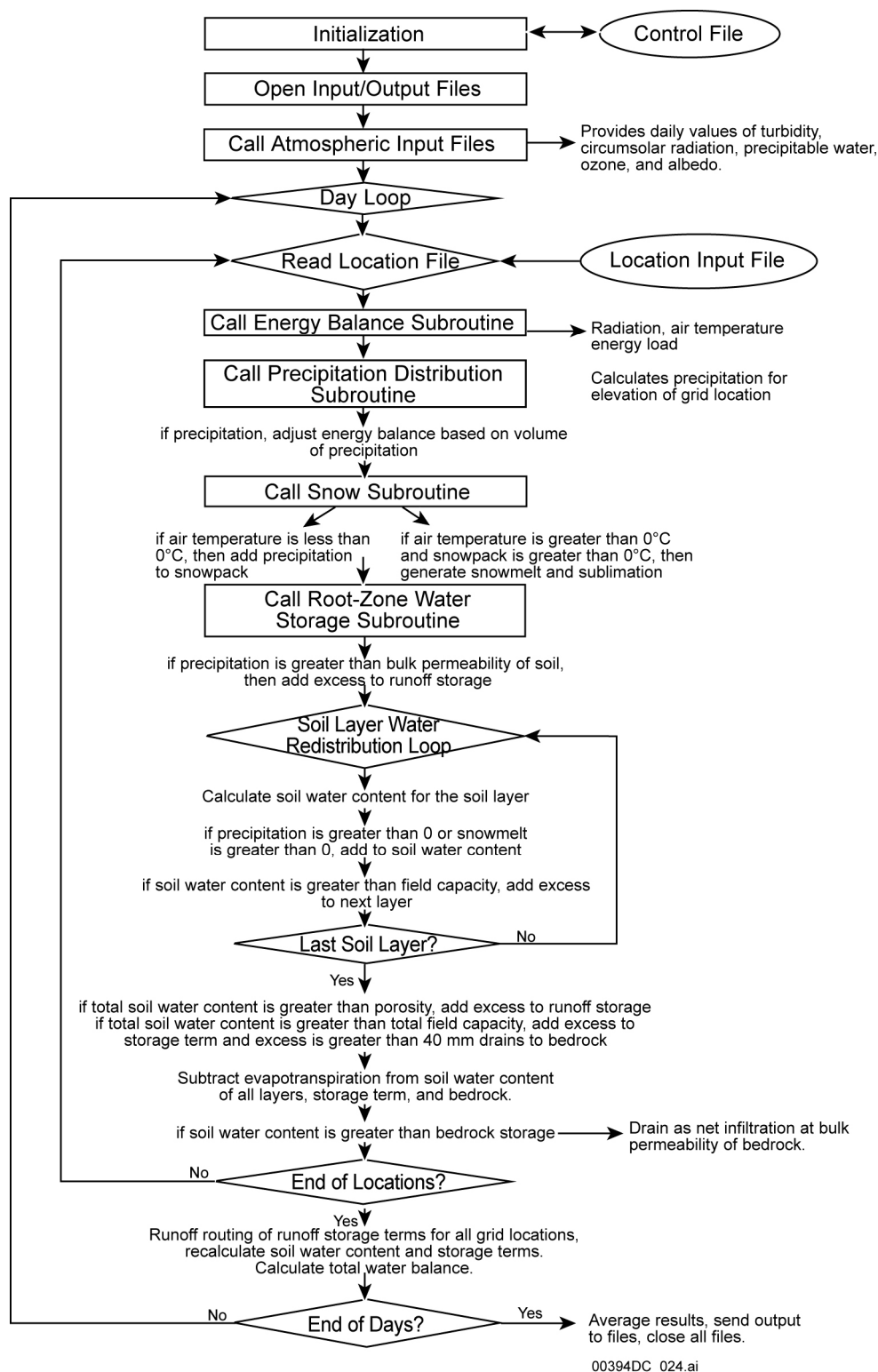
Source: USGS 2001b.

Figure 4-4. Flow Chart of the Model Algorithm Used for Simulating Net Infiltration

For locations with the soil depth of 6 m or greater, the underlying bedrock properties are defined using alluvium–colluvium properties. Based on analysis of neutron moisture meter data (Flint, L.E. and Flint 1995), the maximum depth of infiltration in nonchannel alluvial locations is 6 m; therefore, bedrock properties are not taken into account. The net infiltration is calculated after evapotranspiration is simulated throughout the root zone and limited by the bulk saturated hydraulic conductivity of the underlying rock type. The potential net infiltration volume exceeding the bulk saturated hydraulic conductivity is added to the temporary storage term of the bottom root-zone layer. Starting with the bottom root-zone layer, a reverse cascade is performed to determine if runoff is generated. The volume of water in the temporary storage term is compared against the total storage capacity of each layer defined by the porosity (or effective fracture porosity in the case of bedrock) and layer thickness. If the volume of water in the temporary storage term exceeds the storage capacity, the excess water is added to the temporary storage term of the overlying layer. The process is repeated until the top layer is reached, completing the reverse cascade. The volume of water in the temporary storage term exceeding the storage capacity of the top layer is added to the potential runoff volume calculated for that grid cell. The final runoff volume is calculated following the simulation of evapotranspiration from the root zone.

After the completion of the reverse cascade and the placement of excess water into temporary storage terms, evapotranspiration is simulated for each root-zone layer using a dynamic root-zone weighting function and a modified Priestley-Taylor equation. Evapotranspiration is simulated only for days with air temperature greater than 0°C.

The vegetation characteristics most important for evaluating transpiration are distribution, minimum xylem water potential, and rooting depths (Flint, A.L. et al. 1996, p. 45). The minimum xylem water potential used to calculate the lower limit of plant-available water was −6,000 kPa (60 bar), which is assumed to be equivalent to the wilting point of vegetation. The dynamic weighting is based on calculated relative saturations for each root-zone layer and the relative distribution of water (based on saturation) throughout all layers. The purpose of dynamic weighting is to increase root activity for the wettest layer. Static root density weights are also incorporated into the dynamic weighting function, setting an upper limit on root activity within each layer. For the topsoil layer, the bare-soil evaporation term is added to the transpiration term. Using the calculated weighting terms, evapotranspiration is simulated by applying a form of the modified Priestley-Taylor equation developed by Flint, A.L. and Childs (1991), to each layer of the root zone (USGS 2001b, Section 6.4.6):

$$\text{ET}^k = \alpha' \cdot \text{PET}^k \qquad\qquad (\text{Eq. 4-3})$$

$$\alpha' = \sum_{i} \{ \text{wgt}_i \cdot [a^k (1-\exp(b^k \cdot \text{relsat}_i^k))] \}$$

where ET^k is total root-zone evapotranspiration for grid cell k and PET^k is the adjusted clear-sky simulated equilibrium for grid cell k. (The equilibrium potential evapotranspiration rate is calculated using a α value of 1.0 and is used to represent the nonadvective component of the energy balance.) The term relsat_i^k is the relative saturation calculated for layer i within grid cell k; and a^k and b^k are the Priestley-Taylor model coefficients for grid cell k supplied as soil- and rock-type input parameters in the model control file. (In this analysis, the coefficients were identical for all soil and rock types, but varied between different climate scenarios and between

soils and rocks.) After water contents for each layer are reduced according to the calculated evapotranspiration rates, the final runoff and net infiltration terms are calculated, and the new water-content for each root-zone layer are updated for the following day's water-balance calculation.

4.2 MODEL CALIBRATION AND VALIDATION

4.2.1 Model Calibration

The INFIL model was calibrated using comparisons of simulated streamflow with historical streamflow data from 31 gauging stations in the Death Valley region, and simulated 50-year (1950 to 1999) basinwide average net infiltration with previous estimates of basinwide average recharge for 42 basin areas (defined in previous studies as hydrographic areas and subareas) in the Death Valley region. Model calibration included adjusting the following parameters: bedrock saturated hydraulic conductivity, root density, average storm duration (for summer and winter storms), and soil saturated hydraulic conductivity and wetted area (used to represent stream-channel characteristics).

The numerical model was calibrated by comparing measured volumetric water contents using neutron moisture meters and simulated water-content data (Flint, A.L. et al. 1996). At selected neutron boreholes, water-content data were summed for the soil profile and compared to the model simulation for the same time period by using the developed site precipitation record (USGS 2001b). Two examples are presented: borehole USW UZ-N50, with soil 2.7 m deep (Figure 4-5a), and borehole UE-25 UZN#63, with soil 1.7 m deep (Figure 4-5b).

Changes in water-content profiles through time, measured in boreholes located in active channels with thick soils, were used to develop and calibrate a modified Priestley-Taylor evapotranspiration model (Hevesi et al. 1994). Initial model calibrations conducted using INFIL V1.0 in 1996, and consisting of a generalized (site-wide) calibration of the modified Priestley-Taylor model coefficients, were based primarily on the calculated changes in the measured profiles (USGS 2001b, p. 33; also discussed in Section 6.8.3).

4.2.2 Model Validation Using Comparison of Net Infiltration and Recharge Rates

Because of a deep unsaturated zone, net infiltration is a primary source of groundwater recharge; the results of net infiltration calculations using a water balance model were compared with those from three-dimensional numerical modeling (Wu et al. 1999) and calculations of groundwater recharge rates.
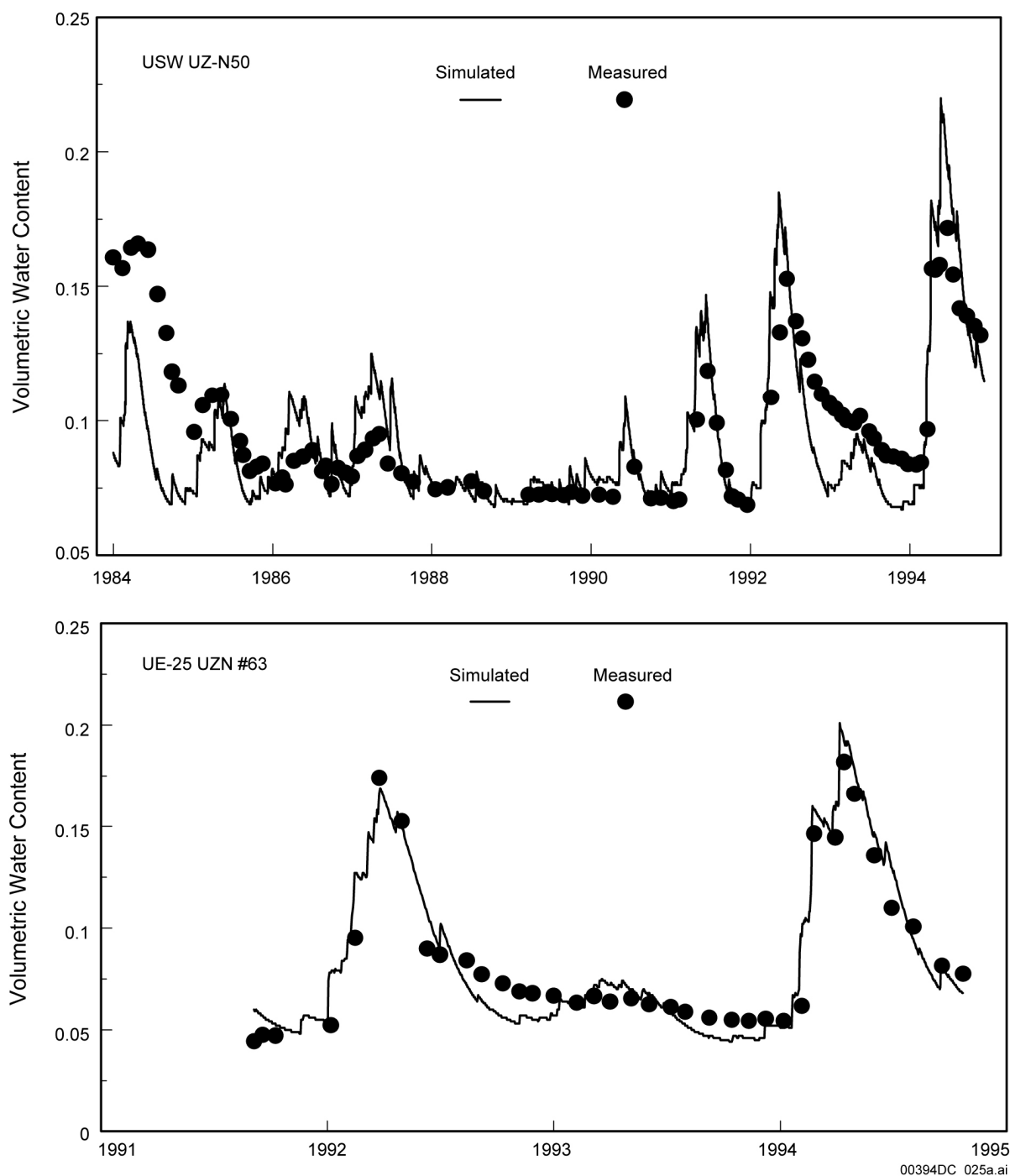
Source: USGS 2001b, Figure 6-20.

Figure 4-5. Simulated and Measured Water Content in Boreholes

Using the water-balance method, Winograd and Thordarson (1975) estimated that 3 percent of precipitation becomes groundwater recharge; their estimate was based on discharge measurements from springs south of Yucca Mountain near the Nevada–California border. The Maxey–Eakin method (Maxey and Eakin 1950) was used in several previous water-balance studies of basins in the Death Valley region to estimate recharge to groundwater basins in

Nevada (Watson et al. 1976; Dettinger 1989; Avon and Durbin 1994; Harrill and Prudic 1998; Donovan and Katzer 2000). Given the average annual precipitation, the Maxey–Eakin method classifies basins into five recharge zones (Maxey and Eakin 1950):

1. No recharge occurs for precipitation less than 203 mm/yr
2. 3 percent recharge for precipitation from 203 to 304 mm/yr
3. 7 percent recharge for precipitation from 305 to 380 mm/yr
4. 15 percent recharged for precipitation from 381 to 507 mm/yr
5. 25 percent recharge for precipitation of 508 mm/yr and greater.

By comparing the Maxey–Eakin estimates with 40 estimates of recharge obtained from the Southern Great Basin using a basinwide water-budget analysis and 27 estimates of recharge obtained using geochemical and numerical modeling approaches, Avon and Durbin (1994) and Harrill and Prudic (1998) concluded that the Maxey–Eakin method provides reasonable estimates of recharge for basins in Nevada (Figure 4-6). Several studies have presented modified and updated versions of the Maxey–Eakin method, based on recent precipitation data, geochemical data, and basinwide water-balance data (D'Agnese et al. 1997; Donovan and Katzer 2000; Hevesi and Flint 1998).
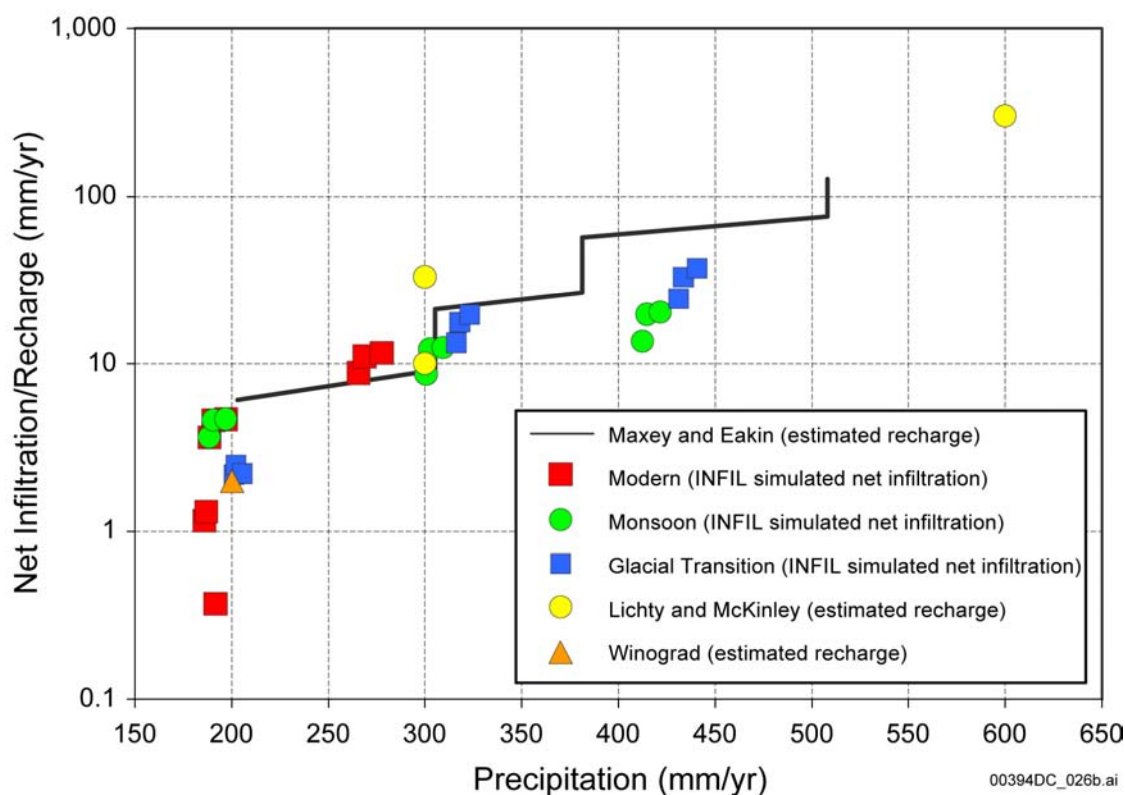
Source: USGS 2001b, Figure 6-41.

NOTE: Estimated recharge data are from Maxey and Eakin 1950, Lichty and McKinley 1995, and Winograd 1981; chloride mass balance data are from CRWMS M&O 2000c.

Figure 4-6.   Comparison of INFIL V2.0 Simulated Average Net Infiltration Rates with an Estimate of the Average Holocene Recharge Rate for the Saturated Zone at Yucca Mountain and with Estimates of Recharge in the Southern Great Basin Obtained Using Alternative Methods

The limitation of the application of the Maxey–Eakin method is that it uses only the average annual precipitation, without considering other factors that can affect recharge (D'Agnese et al. 1997). The problem is that in the Maxey–Eakin method, recharge is estimated by assuming that a zone-specific percentage of precipitation infiltrates to recharge the groundwater. The Maxey–Eakin coefficients were determined by balancing the recharge, which depends on the depth to the water table, with estimates of groundwater discharge for 13 valleys in east-central Nevada (Maxey and Eakin 1950). In the Maxey–Eakin method, the areas with annual precipitation of less than 200 mm are not considered to recharge the groundwater. However, at Yucca Mountain, recharge is known to occur within areas where annual precipitation is less than 200 mm. Therefore, the comparison of the calculated infiltration with that from the Maxey–Eakin coefficients for the annual precipitation that is less than 200 mm is invalid. Moreover, estimates of net infiltration for the Yucca Mountain area may not correspond directly to recharge because of the time lag between the net infiltration and groundwater recharge in the thick unsaturated zone.

Hevesi et al. (2003) conducted numerical modeling of net infiltration for the present-day climatic conditions over the area of Death Valley region in Nevada and California using four types of models. The following parameters were varied in these models: the sublimation rate parameter SUBPAR1, storm duration, bedrock saturated hydraulic conductivity, the stream-channel wetted area, and stream-channel hydraulic conductivity for soils. Hevesi et al. (2003, pp. 96 to 99, Tables 22 and 23) provided a statistical analysis of the results of modeling to compare simulated basinwide average net infiltration and recharge rates to simulated total basinwide net infiltration and recharge volumes. They determined that the simulated net-infiltration volumes are in good agreement with the estimated recharge volumes, and the best fit of simulated and observed data corresponds to the net infiltration model that accounts for streamflow coupled to the root-zone component; this approach was used in the INFIL model for the determination of net infiltration.

4.2.3 Model Validation Using Comparison with Simulations of Percolation in the Unsaturated Zone

The three-dimensional unsaturated flow model (BSC 2003d) was used for simulations of percolation in the unsaturated zone for the mean, lower-bound, and upper-bound present-day, monsoon, and glacial-transition climates. In these simulations, the net infiltration rates for all nine climate state scenarios from *Simulation of Net Infiltration for Modern and Potential Future Climates* (USGS 2001b) were used to assign the upper boundary condition.

The three-dimensional unsaturated flow model is based on using the calibrated soils and rock properties (BSC 2003d; BSC 2003e). The results of modeling were validated using mountain-scale ambient temperature measurements, gas pressure, chloride, calcite, and strontium data. These data were used to constrain infiltration and percolation flux. The field data (matrix liquid saturations, water potentials, and perched-water elevations) were collected from nine boreholes (USW NRG-7a, USW SD-6, USW SD-7, USW SD-9, UE-25 SD-12, USW UZ-14, UE-25 UZ#16, USW WT-24, and USW G-2) (BSC 2003d, Section 6.2-5). The water-potential data were also measured from the Enhanced Characterization of the Repository Block tunnel (BSC 2002c). Perched-water elevations measured in borehole USW WT-24 and pneumatic data measured in boreholes UE-25 SD-12 and UE-25 UZ#7a were used to validate the unsaturated zone model.

Matching the ambient temperature distribution within the unsaturated zone from field measurements and modeling is important to constrain the percolation flux and infiltration rate (Bodvarsson et al. 2003). Temperature data measured in boreholes USW H-5, USW H-4, and UE-25 WT#18 were used to validate the ambient thermal model. The validation criterion was based on matching the observed values with less than 3°C difference (BSC 2002c, Attachment I-1-2-2).

The calcite model is validated by comparing one-dimensional simulation results with the results of field measurements. The validation criterion is that the simulated volume fraction of calcite coating for each unsaturated zone model layer fall within the range of measurements for that layer (BSC 2002c, Attachment I-1-2-4).

^{14}C data from gas samples provide approximate ^{14}C residence time for pore water in the unsaturated zone. The residence time can be interpreted as the tracer transport time from the ground surface to a depth where the gas sample was collected.

Borehole and Enhanced Characterization of the Repository Block strontium concentrations are used to check the unsaturated zone model strontium modeling results. The criterion for validation is a qualitative agreement between the simulated strontium concentrations and the average of the observations at the same elevation, and agreement with the vertical trends (BSC 2002c, Attachment I-1-2-5).

Thus, the results of three-dimensional numerical modeling of flow and transport in the unsaturated zone closely agree with the types of data obtained from field measurements in the unsaturated zone (temperature, gas pressure, chloride and calcite concentrations, saturation, water potential, and perched water levels). These agreements confirm the validity of the upper boundary conditions used for modeling (i.e., the net infiltration rate, which was calculated using the water balance model).

4.3 RESULTS OF MODELING FOR DIFFERENT CLIMATES

4.3.1 Present-Day Climate

For infiltration simulations, using INFIL V2.0, of the present-day climate, lower- and upper-bound mean annual precipitation were 185.8 mm and 265.6 mm, respectively (USGS 2001b, Table 6-8). Mean annual temperatures at Yucca Mountain range from 15.1°C to 18.2°C (CRWMS M&O 1997b, Tables 2-1 and A-10).

Modeling of the present-day climate scenario was provided based on the meteorological data presented in Table 4-2. Results of modeling infiltration for the lower-bound, mean, and upper-bound present-day climate scenarios are summarized in Tables 4-3 and 4-4 (USGS 2001b, Section 7.1.1). For the entire flow domain of 123.7 km^2 (Table 4-3), for the mean present-day climate scenario, average precipitation is estimated to be 188.5 mm/yr, average outflow as streamflow is 0.2 mm/yr (corresponding to an average stream discharge of 0.03 ft^3/s), and average net infiltration is 3.6 mm/yr. Average net infiltration ranges from 1.2 mm/yr for the lower-bound present-day climate to 8.8 mm/yr for the upper-bound present-day climate. Although average annual precipitation for the mean present-day scenario is only 1.4 percent greater than precipitation for the lower-bound present-day scenario, net infiltration for the mean

present-day scenario is 200 percent greater than the net infiltration for the lower bound. This is probably because of greater infiltrated surface-water run-on in channels under mean present-day conditions than under the lower-bound conditions. Maximum rates of infiltrated surface-water run-on for mean present-day conditions are greater than 100 mm/yr in the headwater sections of the primary watersheds such as Solitario Canyon and Yucca, Drill Hole, Pagany, and Abandoned Washes. Results from the upper-bound present-day scenario also indicate that net infiltration is significantly influenced by infiltrated surface-water run-on in channels. In all three present-day climate scenarios, average annual evapotranspiration is greater than 95 percent of average annual precipitation.

For the area of the repository (Table 4-4), for the mean present-day climate scenario, average precipitation is estimated to be 196.9 mm/yr, average outflow as streamflow is 1.4 mm/yr, and average net infiltration is 4.7 mm/yr. For the lower-bound present-day climate, net infiltration is 0.4 mm/yr and outflow is –0.3 mm/yr. (The estimated negative outflow is caused by surface-water inflow from Drill Hole Wash exceeding outflow.) For the upper-bound present-day climate, net infiltration is estimated to be 11.6 mm/yr.

Table 4-2. Summary of Meteorological Data and INFIL Simulation Results Used to Develop Spatially Distributed Net-Infiltration Estimates for Present-Day Scenarios for the 123.7-km^2 Area of the Net Infiltration Model Domain

Parameter		INFIL Simulation Results for the 123.7-km^2 Area of the Net Infiltration Model Domain			
INFIL simulation ID used for developing the present-day scenario		YM1-4ex	4JA1-4ex	4JA1-4ex	A121-4ex
Simulation period (year number)		1980 to 1995	0 to 100	80 to 90	0 to 100
Simulation time (years)		16	100	10	100
Average annual precipitation (mm/yr)	Mean	189.3	187.7	182.8	342.8
	Maximum	282.9	280.6	273.3	512.4
	Minimum	148.0	146.8	143.0	268.1
Average annual evapotranspiration (mm/yr)	Mean	182.7	185.5	181.8	326.8
	Maximum	571.9	652.3	689.1	788.8
	Minimum	61.9	51.1	50.6	83.4
Average annual infiltrated surface water run-on (mm/yr)	Mean	6.0	2.7	1.6	15.1
	Maximum	1,514.4	669.6	599.7	4,343.8
	Minimum	0.0	0.0	0.0	0.0
Average annual outflow (mm/yr)		0.3	0.1	0.0	1.5
Average annual net infiltration (mm/yr)	Mean	5.1	2.2	1.3	14.0
	Maximum	1,486.2	574.4	252.0	4,354.3
	Minimum	0.0	0.0	0.0	0.0

Source: USGS 2001b, Table 6-7.

Table 4-3. Estimation Results for Present-Day Climate Scenarios over the 123.7 km^2 Area of the Infiltration Model Domain

Parameter		Lower Bound	Mean	Upper Bound
Average annual precipitation (mm/yr)	Mean	185.8	188.5	265.6
	Maximum	282.2	281.8	397.1
	Minimum	148.0	147.4	207.8
Average annual evapotranspiration (mm/yr)	Mean	184.8	184.1	255.5
	Maximum	571.9	612.1	700.5
	Minimum	54.7	56.5	71.5
Average annual infiltrated surface water run-on (mm/yr)	Mean	2.1	4.4	9.7
	Maximum	474.2	994.1	2,669.0
	Minimum	0.0	0.0	0.0
Average annual outflow (mm/yr)		0.2	0.2	0.9
Average annual net infiltration (mm/yr)	Mean	1.2	3.6	8.8
	Maximum	252.0	958.9	2,656.6
	Minimum	0.0	0.0	0.0

Source: USGS 2001b, Table 6-8.

Table 4-4. Estimation Results for Present-Day Climate Scenarios over the 4.7 km^2 Area of the 1999 Design Repository Area

Parameter		Lower Bound	Mean	Upper Bound
Average annual precipitation (mm/yr)	Mean	191.6	196.9	277.5
	Maximum	204.1	209.9	295.8
	Minimum	178.2	183.4	258.5
Average annual evapotranspiration (mm/yr)	Mean	191.7	189.9	260.4
	Maximum	252.9	273.3	423.0
	Minimum	155.0	154.7	203.0
Average annual infiltrated surface water run-on (mm/yr)	Mean	1.0	3.4	8.1
	Maximum	59.8	161.1	454.8
	Minimum	0.0	0.0	0.0
Average annual outflow (mm/yr)		−0.3	1.4	4.9
Average annual net infiltration (mm/yr)	Mean	0.4	4.7	11.6
	Maximum	26.6	120.1	387.4
	Minimum	0.0	0.0	0.0

Source: USGS 2001b, Table 6-10.

The greater net infiltration rates are within the higher elevation areas with higher precipitation and thinner soils (USGS 2001b, Section 6.11.1). The spatial distribution for estimated precipitation for the mean present-day climate is presented in Figure 4-7, while the estimated net infiltration is presented in Figure 4-8. Net infiltration of greater than 100 mm/yr occurs throughout the steep, northeast facing slope of The Prow, caused by the combined effect of high precipitation, reduced evapotranspiration, frequent surface-water run-on at the area of very thin soils, and the high permeability of bedrock. High net infiltration also occurs in the upper

channels of Solitario Canyon and Drill Hole, Pagany, and Abandoned Washes. Maximum net infiltration of more than 100 mm/yr occurs within isolated areas on side slopes and in channels with thin soils and high-permeability bedrock. However, total net infiltration within the domain of the unsaturated zone flow and transport model is dominated, by the lower rates of 1 to 20 mm/yr on side slopes and ridge tops, which make up much of the unsaturated zone flow and transport model domain.
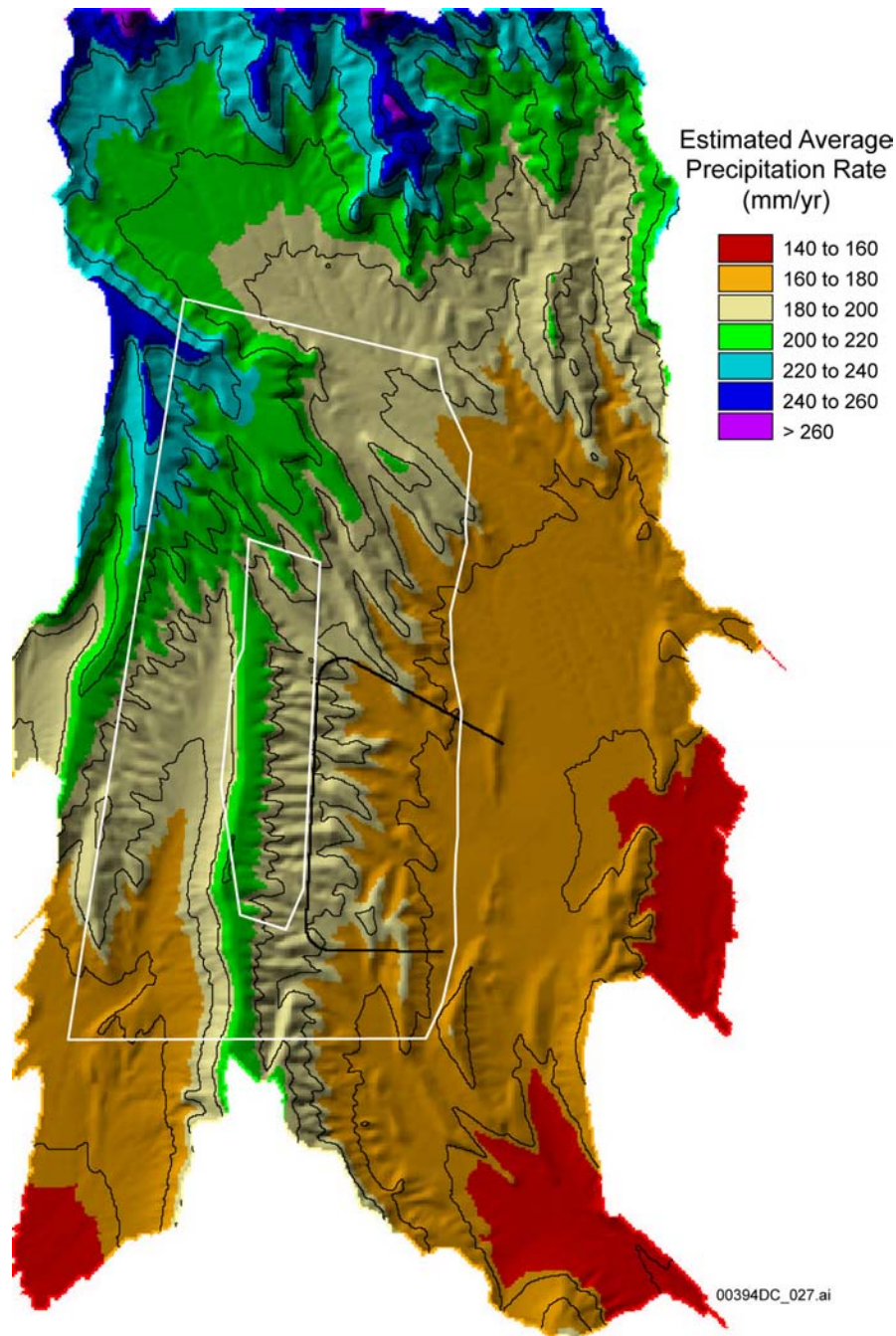
Source: USGS 2001b, Figure 6-23.

Figure 4-7. Estimated Precipitation for the Present-Day Climate Scenario

Mean Modern
Climate Net
Infiltration
(mm/yr)

- 0
- < 1
- 1 to 5
- 5 to 10
- 10 to 20
- 20 to 50
- 50 to 100
- 100 to 500
- 500 to 1,000
- >1,000

00394DC_028.ai
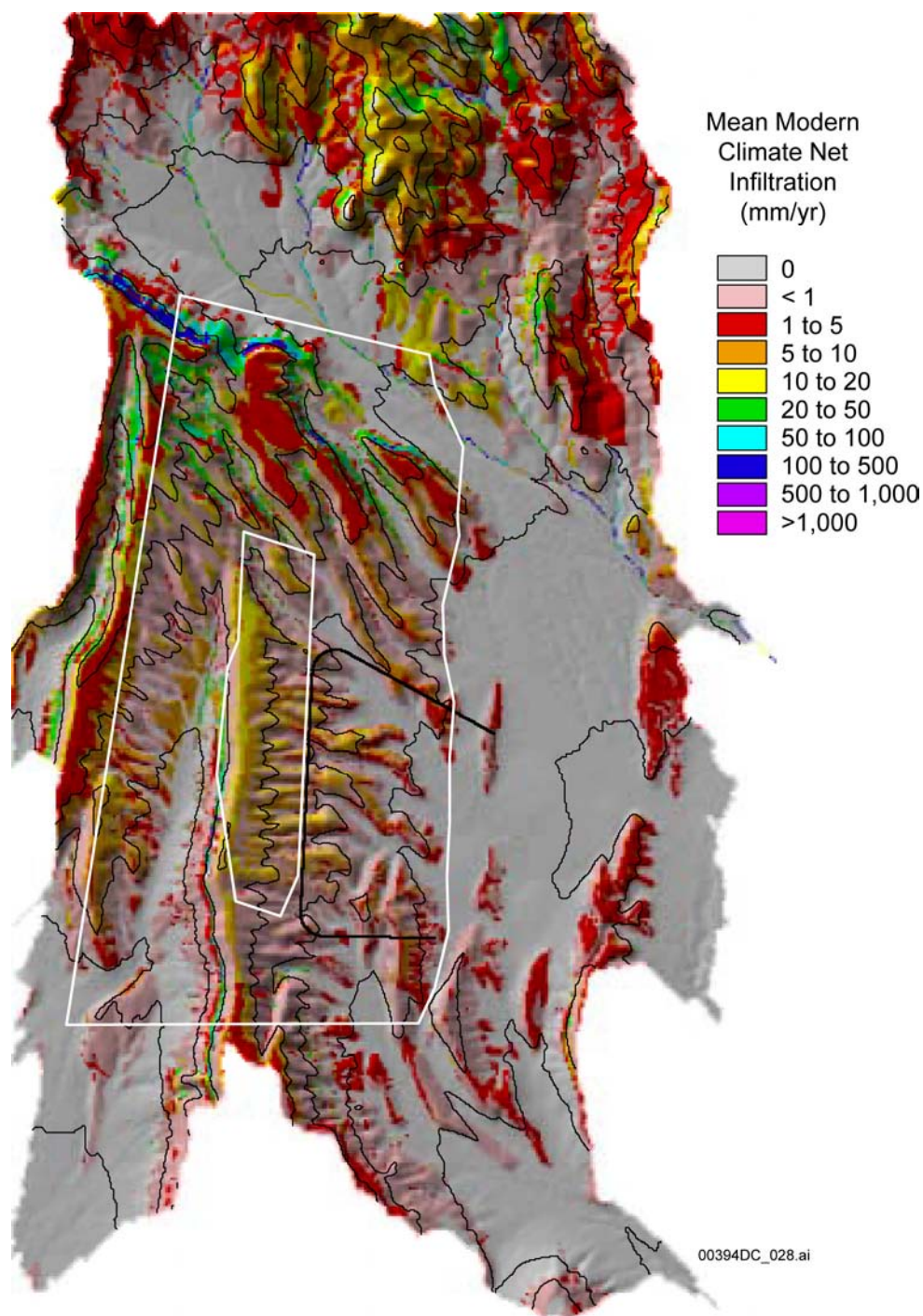
Source: USGS 2001b, Figure 6-26.

Figure 4-8. Estimated Net Infiltration for the Present-Day Climate Scenario

For the lower-bound present-day climate scenario within the repository area, most areas, including the crest, have no net infiltration (USGS 2001b, Section 6.11.1). Areas with net infiltration greater than 5 mm/yr are isolated to north-facing side slopes and along the west-facing slope of Solitario Canyon. For the upper-bound present-day climate scenario, net infiltration along the crest of Yucca Mountain is more than 20 mm/yr, and the relative contribution of net infiltration along channels to the total net infiltration is much greater than that for the mean present-day climate conditions. Maximum net infiltration of nearly 2,700 mm/yr occurs in an active channel in the northern part of Yucca Wash. Within the repository area, maximum net infiltration of between 100 and 500 mm/yr occurs in Drill Hole Wash and along the west-facing slope of Solitario Canyon. In all cases, maximum net infiltration occurs in areas affected by surface-water run-on, and a strong correlation exists between maximum infiltrated surface-water run-on in channels and maximum net infiltration for all areas and all climate scenarios. However, because the areas with relatively high net infiltration (greater than 100 mm/yr) are small, most of the total net infiltration for the entire model domain occurs in upland areas, where net infiltration is less than 20 mm/yr.

4.3.2   Monsoon Climate

The two climate analog sites selected to represent the upper-bound monsoon climate scenario are at Nogales, Arizona, and Hobbs, New Mexico. Meteorological data for the monsoon climate scenario are summarized in Table 4-5. Mean annual temperatures for these two sites are 16.6°C and 17.5°C, respectively, which are within the range of mean annual temperatures at Yucca Mountain—from 15.1°C to 18.2°C. At these sites, the average annual precipitation is 410.5 mm/yr and 414.4 mm/yr, respectively, and average annual net infiltration of 15.1 mm/yr and 12.1 mm/yr, respectively (USGS 2001b, Section 6.9.3, Table 6-4).

Table 4-5.   Summary of Meteorological Data for Nogales and Hobbs Analog Meteorological Stations and INFIL Simulation Results Used to Develop Spatially Distributed Net-Infiltration Estimates for Monsoon Climate Scenarios for the 123.7 km^2 Area of the Net Infiltration Model Domain

Simulation Period (begin date to end date)		Nogales Data for 1/1/49 to 12/31/82	Hobbs Data for 1/1/48 to 12/31/97
Air temperature (ºC)	Mean annual	16.6	17.5
	Maximum daily	33.2	34.0
	Minimum daily	−8.5	−13.7
Average annual precipitation (mm/yr)	Mean	410.5	414.4
	Maximum	511.2	516.0
	Minimum	366.2	369.7
Average annual snow fall (mm/yr)	Mean	1.3	12.2
	Maximum	33.7	44.9
	Minimum	0.0	2.4
Average annual evapotranspiration (mm/yr)	Mean	386.3	386.3
	Maximum	814.7	818.8
	Minimum	107.9	90.8
Average annual infiltrated surface water run-on (mm/yr)	Mean	19.9	16.3
	Maximum	2,884.9	2,306.4
	Minimum	0.0	0.0
Average annual outflow (mm/yr)		5.8	14.3
Average annual net infiltration (mm/yr)	Mean	15.1	12.1
	Maximum	2,900.6	2,330.0
	Minimum	0.0	0.0

Source: USGS 2001b, Table 6-11.

Net infiltration for the Hobbs site was less than that for the Nogales site, even though precipitation was greater—the Hobbs site is warmer and has a higher evapotranspiration rate than the Nogales site. The simulation of infiltration rates for the two analog sites were averaged to obtain net infiltration for the upper-bound monsoon climate scenario (Table 4-6). To define the mean net infiltration for the monsoon climate state, lower- and upper-bound net infiltration simulation results were averaged for each model grid cell (USGS 2001b, Section 6.9.3). In so doing, a uniform distribution of net infiltration was assumed between the lower-bound and upper-bound monsoon scenarios.

Results of infiltration modeling for the lower-bound, mean, and upper-bound monsoon climate scenarios for the entire domain of the infiltration model (123.7 km^2) are summarized in Table 4-6 (USGS 2001b, Section 6.11.2). Results for the lower-bound monsoon scenario are equivalent to the mean present-day climate results. For the mean monsoon climate scenario, average precipitation is 300.5 mm/yr, average outflow as streamflow is 5.1 mm/yr, and average net infiltration is estimated to be 8.6 mm/yr. Calculations for the upper-bound monsoon climate resulted in average precipitation-rate estimates of 412.5 mm/yr, average outflow as streamflow of 10.0 mm/yr, and average net infiltration of 13.6 mm/yr.

Table 4-6. Estimation Results for the Monsoon Climate Scenarios over the 123.7 km^2 Area of the Infiltration Model Domain

Parameter		Lower Bound	Mean	Upper Bound
Mean annual air temperature (ºC)		17.3	17.2	17.0
Average annual precipitation (mm/yr)	Mean	188.5	300.5	412.5
	Maximum	281.8	397.7	513.6
	Minimum	147.4	257.7	368.0
Average annual snow fall (mm/yr)	Mean	n/a	n/a	6.8
	Maximum	n/a	n/a	39.3
	Minimum	n/a	n/a	1.2
Average annual evapotranspiration (mm/yr)	Mean	184.1	285.2	386.3
	Maximum	612.1	714.4	816.7
	Minimum	56.5	77.9	99.3
Average annual infiltrated surface-water run-on (mm/yr)	Mean	4.4	11.2	18.1
	Maximum	994.1	1,794.9	2,595.7
	Minimum	0.0	0.0	0.0
Average annual outflow (mm/yr)		0.2	5.1	10.0
Average annual net infiltration (mm/yr)	Mean	3.6	8.6	13.6
	Maximum	958.9	1,787.1	2,615.3
	Minimum	0.0	0.0	0.0

Source: USGS 2001b, Table 6-12.

Comparison of results from the mean present-day climate conditions to the mean monsoon climate conditions indicates significant changes in the overall water balance, including net infiltration. While average annual precipitation for mean monsoon conditions is about 60 percent greater than that for mean present-day conditions, net infiltration is about 140 percent greater for the monsoon climate. This change in the overall water balance could be caused by the significantly greater infiltration of surface-water run-on during the monsoon climatic conditions (i.e., infiltrated surface-water run-on for mean monsoon conditions is about 155 percent greater than that for mean present-day conditions). Furthermore, the greater influence of infiltrated surface-water run-on in channels is apparent in the substantially greater average annual outflow as streamflow associated with the monsoon climate (i.e., average annual outflow for mean monsoon conditions is 25 times that for mean present-day conditions). Under monsoon conditions, snowfall and surface-water run-on in channels will increase (Table 4-6). Within the area of the repository site (Table 4-7), for the mean monsoon climate scenario, average precipitation is 309.3 mm/yr, average outflow as streamflow is 13.2 mm/yr, and average net infiltration is estimated to be 12.5 mm/yr. For the upper-bound monsoon climate, average precipitation is 421.6 mm/yr, outflow as streamflow is 25.1 mm/yr, and net infiltration is 20.3 mm/yr over the area of the repository.

Table 4-7. Estimation Results for the Monsoon Climate Scenarios over the 4.7 km^2 Area of the 1999 Design Repository Area

Parameter		Lower Bound	Mean	Upper Bound
Average annual precipitation (mm/yr)	Mean	196.9	309.3	421.6
	Maximum	209.9	322.8	435.7
	Minimum	183.4	295.2	407.0
Average annual snow fall (mm/yr)	Mean	n/a	n/a	7.7
	Maximum	n/a	n/a	10.9
	Minimum	n/a	n/a	5.3
Average annual evapotranspiration (mm/yr)	Mean	189.9	281.7	373.5
	Maximum	273.3	466.4	666.0
	Minimum	154.7	217.8	277.1
Average annual infiltrated surface-water run-on (mm/yr)	Mean	3.4	9.1	14.8
	Maximum	161.1	348.6	536.1
	Minimum	0.0	0.0	0.0
Average annual outflow (mm/yr)		1.4	13.2	25.1
Average annual net infiltration (mm/yr)	Mean	4.7	12.5	20.3
	Maximum	120.1	267.0	413.8
	Minimum	0.0	0.0	0.0

Source: USGS 2001b, Table 6-14.

The spatial distribution of estimated net infiltration for the mean monsoon climate scenario (Figure 4-9) indicates that net infiltration along the crest of Yucca Mountain ranges from 20 to 50 mm/yr (USGS 2001b, Section 6.11.2). Within the repository area, maximum net infiltration between 100 and 500 mm/yr occurs in the active channel of Drill Hole Wash and on outcrops of permeable, nonwelded tuff in the middle section of the west-facing slope of Solitario Canyon. Relatively high net infiltration between 100 and 500 mm/yr also occurs on many steep side slopes in the northern part of the unsaturated zone flow and transport model area. In contrast, net infiltration is less than 1 mm/yr in upland areas featuring thin soils underlain by bedrock with low bulk permeability.

The spatial distribution of net infiltration for the upper-bound monsoon climate scenario indicates a greater area with relatively high net infiltration between 100 and 500 mm/yr than for mean monsoon conditions (USGS 2001b, Section 6.11.2). In addition, net infiltration exceeds 50 mm/yr on some parts of the crest of Yucca Mountain. Compared to mean monsoon conditions, the increase in net infiltration for the upper-bound monsoon conditions for areas with relatively high bedrock permeability is much greater than the increase for areas with low bedrock permeability, which remains less than 1 mm/yr. Relatively high run-on rates of 100 to 500 mm/yr occur throughout the active channels of Solitario Canyon and Drill Hole Pagany, Dune, and Yucca Wash.

Mean Monsoon Climate
Net Infiltration (mm/yr)

	0
	0 to 1
	1 to 5
	5 to 10
	10 to 20
	20 to 50
	50 to 100
	100 to 500
	500 to 1,000
	>1,000

N

00394DC_029a.ai
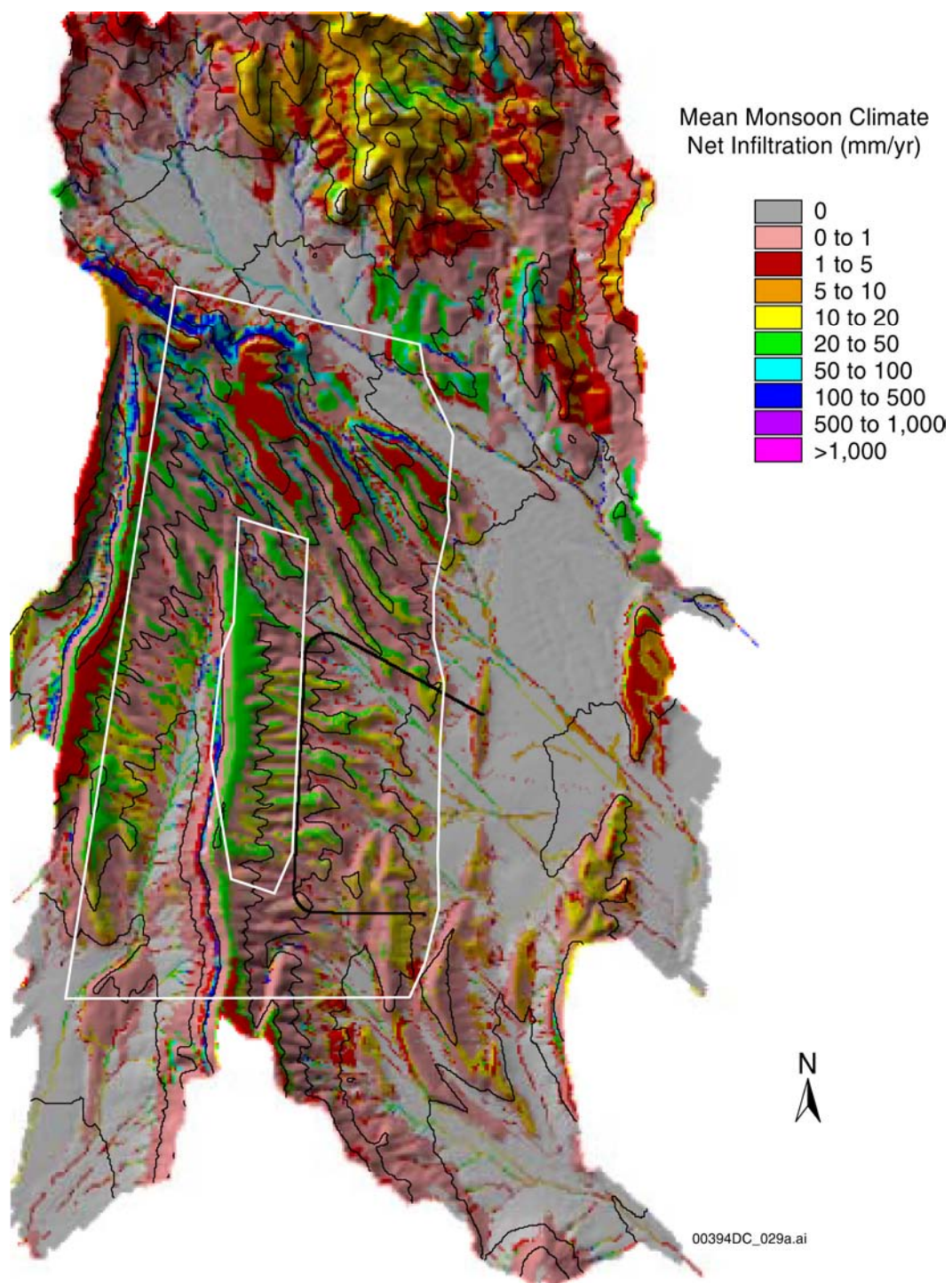
Source: USGS 2001b, Figure 6-29.

Figure 4-9. Estimated Net Infiltration for the Mean Monsoon Climate Scenario

4.3.3   Glacial-Transition Climate

The lower-bound glacial-transition climate scenario is represented by two analog sites (Table 4-8), Beowawe, Nevada, and Delta, Utah (USGS 2001b, Section 6.9.4, Table 6-5). For these sites, mean annual temperatures are 9.6°C and 10.8°C, respectively, which are cooler than current conditions at Yucca Mountain. Average annual precipitation rates are 208.4 mm/yr and 193.7 mm/yr, respectively, and average annual net infiltration rates are 2.9 mm/yr and 1.4 mm/yr, respectively. These lower-bound glacial-transition analog sites represent only slightly wetter, but significantly cooler, climate conditions than the mean present-day conditions.

The upper-bound glacial-transition climate scenario is represented using three analog sites (Table 4-9): Rosalia, Washington; Spokane, Washington; and St. John, Washington. Mean annual temperatures for these three sites are 9.0°C, 9.2°C, and 9.9°C, respectively (USGS 2001b, Section 6.9.4, Table 6-6). For these sites, average annual precipitation rates are 454.9, 406.2, and 432.1 mm/yr, respectively, and average annual net infiltration rates are 29.7, 21.2, and 23.0 mm/yr, respectively.

Meteorological data for simulations of the lower-bound glacial-transition climate are presented in Tables 4-8 and 4-9. To define the mean net infiltration rates for the glacial-transition climate state, the lower-bound and upper-bound net infiltration estimates were averaged for each model grid cell, assuming a uniform distribution of net infiltration between the lower-bound and upper-bound glacial-transition scenarios (USGS 2001b, Section 6.9.1).

In addition to the daily climate input data developed from the analog sites, the glacial-transition climate conditions also were represented by root-zone parameters modified to reflect greater vegetation density and changes in vegetation type for the cooler, wetter glacial-transition climate (USGS 2001b, Section 6.9.4). For the upper-bound glacial-transition climate, the root-zone weighting parameters were adjusted to approximate 60 percent vegetation cover, and the maximum thickness of the bedrock root-zone layer was increased to 3 m (9.8 ft). All adjustments to root-zone parameters were based on estimated root-zone and vegetation characteristics for the future climate conditions.

For the mean glacial-transition climate over the entire flow domain (Table 4-10), average precipitation is 316.1 mm/yr, average snowfall is 45.5 mm/yr, average infiltrated surface-water run-on is 14.6 mm/yr, outflow as streamflow is 1.5 mm/yr, and average net infiltration is estimated to be 13.4 mm/yr. The spatial distribution of estimated precipitation and net infiltration for the mean glacial-transition climate scenario is presented in Figures 4-10 and 4-11, respectively. Net infiltration is between 20 and 50 mm/yr along most of the crest of Yucca Mountain, with isolated areas of net infiltration exceeding 50 mm/yr (USGS 2001b, Section 6.11.3). Within the repository area, maximum net infiltration exceeds 500 mm/yr in the channel of Drill Hole Wash. In comparison, the mean net infiltration is 2.2 mm/yr for the lower-bound glacial-transition climate and 24.6 mm/yr for the upper-bound glacial climate.

Table 4-8. Summary of Meteorological Data for Two Analog Meteorological Stations and INFIL
Simulation Results Used to Develop Spatially Distributed Net Infiltration Estimates for the
Lower Bound Glacial-Transition Climate Scenario for the 123.7 km^2 Area of the Net Infiltration
Model Domain

Parameter		Beowawe Data for 01/1/1951 to 12/31/1997	Delta Data for 01/1/1948 to 12/31/1997
Air temperature (ºC)	Mean annual	9.6	10.8
	Maximum daily	31.0	31.5
	Minimum daily	−31.2	−24.9
Average annual precipitation (mm/yr)	Mean	208.4	193.7
	Maximum	259.5	241.1
	Minimum	185.9	172.8
Average annual snow fall (mm/yr)	Mean	30.7	27.6
	Maximum	118.8	100.0
	Minimum	8.5	9.9
Average annual evapotranspiration (mm/yr)	Mean	201.1	188.1
	Maximum	542.6	508.9
	Minimum	68.1	79.0
Average annual infiltrated surface-water run-on (mm/yr)	Mean	2.9	1.4
	Maximum	735.4	351.2
	Minimum	0.0	0.0
Average annual mean outflow (mm/yr)		0.0	0.0
Average annual net infiltration (mm/yr)	Mean	2.9	1.4
	Maximum	559.7	228.0
	Minimum	0.0	0.0

Source: USGS 2001b, Table 6-15.

Table 4-9. Summary of Meteorological Data for Rosalia, Spokane, and St. John Analog Meteorological Stations and INFIL Simulation Results Used to Develop Spatially Distributed Net-Infiltration Estimates for the Upper Bound Glacial-Transition Climate Scenario for the 123.7 km^2 Area of the Net Infiltration Model Domain

Parameter		Rosalia Data for 01/1/51 to 12/31/97	Spokane Data for 01/1/48 to 12/31/97	St. John Data for 01/1/64 to 12/31/97
Air temperature (ºC)	Mean annual	9.0	9.2	9.9
	Maximum daily	33.5	31.8	30.1
	Minimum daily	−25.4	−26.2	−26.0
Average annual precipitation (mm/yr)	Mean	454.9	406.2	432.1
	Maximum	566.4	505.8	538.0
	Minimum	405.8	362.4	385.5
Average annual snow fall (mm/yr)	Mean	67.5	74.3	44.0
	Maximum	288.0	265.9	209.5
	Minimum	19.1	25.6	13.7
Average annual evapotranspiration (mm/yr)	Mean	411.5	374.4	399.0
	Maximum	773.8	770.4	751.0
	Minimum	122.2	113.8	112.9
Average annual infiltrated surface-water run-on (mm/yr)	Mean	31.4	24.2	25.3
	Maximum	9,092.6	7,044.8	6,308.7
	Minimum	0.0	0.0	0.0
Average annual mean outflow (mm/yr)		3.7	1.8	3.2
Average annual net infiltration (mm/yr)	Mean	29.7	21.2	23.0
	Maximum	9,126.2	7,033.7	6,308.1
	Minimum	0.0	0.0	0.0

Source: USGS 2001b, Table 6-16.

Table 4-10. Estimation Results for the Glacial-Transition Climate Scenarios over the 123.7 km^2 Area of the Infiltration Model Domain

Parameter		Lower Bound	Mean	Upper Bound
Mean annual air temperature (Celsius)		10.2	9.8	9.4
Average annual precipitation (mm/yr)	Mean	201.0	316.1	431.1
	Maximum	250.3	393.5	536.8
	Minimum	179.4	282.0	384.6
Average annual snow fall (mm/yr)	Mean	29.1	45.5	61.9
	Maximum	109.4	181.9	254.5
	Minimum	9.2	14.3	19.5
Average annual evapotranspiration (mm/yr)	Mean	194.6	294.8	395.0
	Maximum	525.7	600.7	751.2
	Minimum	73.6	94.9	116.3
Average annual infiltrated surface-water run-on (mm/yr)	Mean	2.2	14.6	27.0
	Maximum	524.3	3,913.2	7,482.0
	Minimum	0.0	0.0	0.0
Average annual outflow (mm/yr)		0.0	1.5	2.9
Average annual net infiltration (mm/yr)	Mean	2.2	13.4	24.6
	Maximum	370.3	3,902.5	7,489.3
	Minimum	0.0	0.0	0.0

Source: USGS 2001b, Table 6-17.
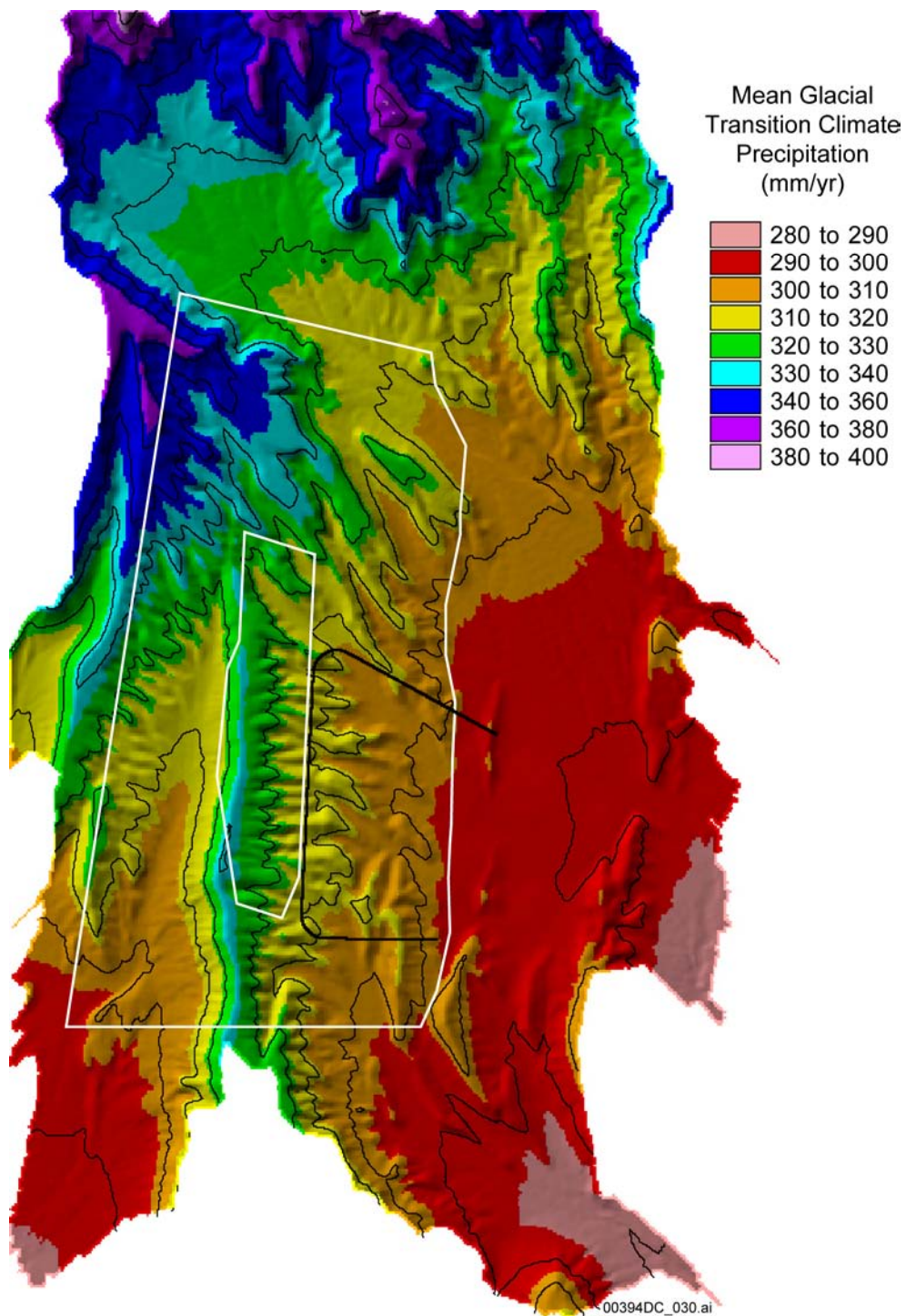
Source: USGS 2001b, Figure 6-32.

Figure 4-10. Precipitation for the Mean Glacial-Transition Climate Scenario
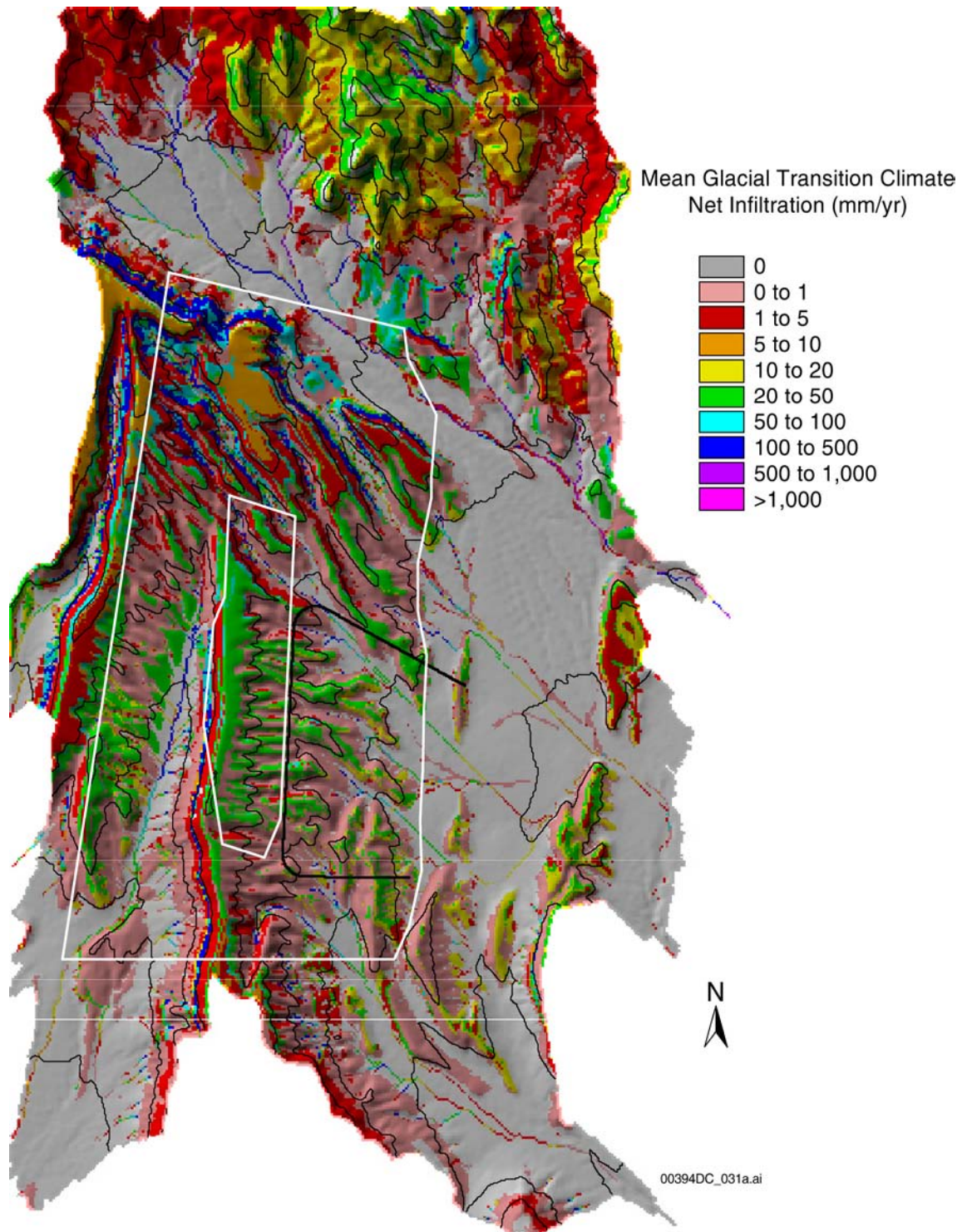
Source: USGS 2001b, Figure 6-36.

Figure 4-11. Estimated Net Infiltration for the Mean Glacial-Transition Climate Scenario

While average annual precipitation for mean glacial-transition conditions is about 68 percent greater, net infiltration is expected to be about 272 percent greater than that for mean present-day. This increase will be caused by the cooler temperature and smaller evapotranspiration. In addition, snowfall is expected to become a significant component of the water balance, accounting for 14 percent of annual precipitation. Infiltrated surface-water run-on is expected to exceed 100 mm/yr throughout most of the upper sections of channels, including Pagany Wash, Drill Hole Wash, Solitario Canyon, and sections of all washes draining the eastern slopes of Yucca Mountain (USGS 2001b, Section 6.11.3). Maximum infiltrated surface-water run-on is expected to exceed 3,000 mm/yr along isolated sections of Yucca Wash.

For the repository area (Table 4-11), average precipitation is estimated to be 323.1 mm/yr, average infiltrated surface-water run-on is 12.0 mm/yr, average outflow as streamflow is 8.0 mm/yr, and average net infiltration is estimated to be 19.8 mm/yr. For the lower-bound glacial-transition climate, net infiltration is 2.2 mm/yr and outflow is 0.3 mm/yr for the repository area, whereas for the upper bound, net infiltration is 37.3 mm/yr and outflow as streamflow is 15.6 mm/yr. The spatial distribution of net infiltration is between 20 and 50 mm/yr along most of the crest of Yucca Mountain, with isolated areas of net infiltration exceeding 50 mm/yr (USGS 2001b, Section 6.11.3). Within the repository area, maximum net infiltration is expected to exceed 500 mm/yr in the channel of Drill Hole Wash.

Table 4-11. Estimation Results for the Glacial-Transition Climate Scenarios for the 4.7 km^2 Area of the 1999 Design Repository Area

Parameter		Lower Bound	Mean	Upper Bound
Average annual precipitation (mm/yr)	Mean	205.5	323.1	440.6
	Maximum	212.4	333.8	455.3
	Minimum	198.4	311.8	425.3
Average annual snow fall (mm/yr)	Mean	32.5	50.3	68.1
	Maximum	42.0	65.2	88.3
	Minimum	24.9	37.8	50.7
Average annual evapotranspiration (mm/yr)	Mean	197.5	287.8	378.1
	Maximum	279.4	477.8	688.6
	Minimum	171.0	219.3	265.3
Average annual infiltrated surface-water run-on (mm/yr)	Mean	1.4	12.0	22.5
	Maximum	100.5	676.6	1,334.8
	Minimum	0.0	0.0	0.0
Average annual outflow (mm/yr)		0.3	8.0	15.6
Average annual net infiltration (mm/yr)	Mean	2.2	19.8	37.3
	Maximum	116.3	591.0	1,181.4
	Minimum	0.0	0.0	0.0

Source: USGS 2001b, Table 6-19.

Overall, net infiltration for the lower-bound glacial-transition climate scenario is significantly less than that of the mean glacial-transition scenario (USGS 2001b, Section 6.11.3). This is caused by a more uniform seasonal distribution of precipitation and a lack of severe storms under the lower-bound glacial-transition climate. The average intensity and frequency of precipitation events for the lower-bound glacial-transition climate is not sufficient to overcome evapotranspiration from the root zone. Maximum net infiltration rates ranging from 100 to 500 mm/yr were obtained on the northeast-facing slope of the Prow Pass Tuff, along isolated sections of the west-facing slope of Solitario Canyon, and along isolated sections of upper Yucca Wash. Within the repository area, net infiltration does not occur in the channel of Drill Hole Wash, and net infiltration along the crest of Yucca Mountain is only 1 to 5 mm/yr. Overall, the distribution and magnitude of net infiltration for the lower-bound glacial-transition scenario is similar to that of the mean present-day scenario, only drier with respect to net infiltration despite having slightly greater annual precipitation. Maximum infiltrated surface-water run-on of more than 100 mm/yr does not occur in channels, but instead is limited to the lower side slopes.

The spatial distribution of net infiltration for the upper-bound glacial-transition climate scenario indicates relatively high net infiltration of 50 to 100 mm/yr throughout the Yucca Mountain crest area (USGS 2001b, Section 6.11.3). In addition, relatively high net infiltration of 100 to 500 mm/yr occurs on most steep side slopes in the northern part of the unsaturated zone flow and transport model domain. Maximum net infiltration of more than 1,000 mm/yr occurs throughout the lower portions of the Yucca Wash channel. Within the repository area, maximum infiltration between 500 and 1,000 mm/yr occurs in isolated sections of the Drill Hole Wash channel.

Table 4-11 shows a comparison of infiltration modeling results for all three glacial-transition climate scenarios for the 4.7 km^2 (1.8 mi^2) repository area. In general, the increase in annual precipitation intensifies the net infiltration, when climate scenarios are compared to one another. However, the relation of net infiltration to precipitation is not linear, because different processes are involved in evapotranspiration, such as temperature, vegetation, and the root-zone distribution.

The increase in the annual precipitation generally intensifies the surface-water runoff, but there are exceptions to this, probably because of differences in the seasonality of precipitation. For comparison, the monsoon climate causes an increase in the surface-water runoff compared to the glacial-transition scenario, even though the glacial-transition scenarios have greater annual precipitation. This is probably because of a higher frequency of severe summer storms during the monsoon climate, resulting in flash runoff in channels before infiltrating into the subsurface.

5. ESTIMATION OF NET INFILTRATION FROM EXPERIMENTAL DATA

Section 5 describes the estimates of net infiltration from corroborative experimental and modeling studies, which are used for model validation.

5.1 FLUX CALCULATIONS USING HYDRAULIC PROPERTIES AND WATER CONTENT MEASUREMENTS

At Yucca Mountain, vertical flux through the near surface unsaturated alluvium deposits was calculated based on Darcy's law, using the estimates of water-potential gradients and unsaturated hydraulic conductivity, and assuming that lateral flow is negligible. Spatially distributed estimates of net infiltration for the repository site, using hydraulic properties of the bedrock matrix underlying the soil, yielded net infiltration ranging from 0.02 to 13.4 mm/yr, representing current meteorological conditions (Flint, A.L. et al. 1996, p. 7). The spatial variability of net infiltration is likely to be caused by the variability of the precipitation, runoff, run-on, and soil and bedrock hydraulic properties.

Using water potential distribution along the soil profile (measured using heat dissipation probes (Flint, A.L. et al. 1996, p. 67)), and the soil moisture-characteristic curves, infiltration was estimated as high as 150 mm per month, following a storm. This estimate agrees with that from changes in the water content in nearby neutron boreholes (Flint, A.L. et al. 1996, p. 68).

Based on the changes in water content measured in neutron-moisture boreholes (located over the repository area), net infiltration ranged from 0 to 45 mm/yr (Flint, A.L. et al. 1996, p. 8).

5.2 GEOCHEMICAL METHODS

The following corroborative geochemical studies can be used to assess the infiltration flux: chloride mass balance, calcite data, ^{36}Cl and tritium isotopes, pore water chemistry, fluid inclusions, oxygen isotopes, chloride mass balance, and calcite data.

A chloride-balance method was used to estimate basin-wide recharge for a 6-year study of two small, upland watersheds in central and south central Nevada (Lichty and McKinley 1995, p. 1). These watersheds were selected as "analog recharge" sites because they represent the possible effects of future, wetter climates at Yucca Mountain. For the smaller of the two basins, the average recharge was 310 mm/yr, or about 50 percent of the estimated average annual precipitation of 639 mm (Lichty and McKinley 1995, Table 15). For the other, more arid basin, average recharge was 33 mm/yr, or 9.8 percent of the average precipitation of 336 mm/yr.

Net infiltration flux estimated at borehole locations within the Yucca Mountain site area, using a chloride mass-balance method, ranged from 0.02 to 5.9 mm/yr (Flint, A.L. et al. 1996, Table 7). The estimates made using the chloride mass-balance flux method vary considerably, depending on the depth of soil or rock samples and the type of material. For example, under a soil terrace at borehole UE-25 UZ#16, the net infiltration flux was 0.02 mm/yr, determined using the soil samples, compared to 3.0 mm/yr and 3.5 mm/yr for the PTn and CHn hydrogeologic unit samples, respectively.

Calcite Data–Based on the USGS-documented hydrogenic calcite abundances in fractures and lithophysal cavities at Yucca Mountain, Xu et al. (2003) calculated percolation fluxes for the

unsaturated zone. They investigated the relationship between percolation flux and measured calcite abundances using reactive transport modeling for the following processes affecting calcite precipitation: (1) infiltration, (2) the ambient geothermal gradient, (3) gaseous CO_2 diffusive transport and partitioning in liquid and gas phases, (4) fracture–matrix interaction for water flow and chemical constituents, and (5) water–rock interaction. Over the bounding range of 2 to 20 mm/yr for infiltration rate, the simulated calcite distributions capture the trend in calcite abundances measured in a deep borehole (USW WT-24) by the USGS. The calcite is found predominantly in fractures in the welded tuffs. Simulations showed that the amount of calcite precipitated in the welded Topopah Spring Tuff is sensitive to the infiltration rate. This dependence decreases at higher infiltration rates, owing to a modification of the geothermal gradient caused by the increased percolation flux. The model also confirms the conceptual model prediction of higher percolation fluxes in the fractures compared to the matrix in the welded units. Based on the calcite data, the infiltration rate is about 2 to 6 mm/yr.

[36]Cl/Cl Ratios–The relationship of [36]Cl/Cl ratios with infiltration rates and soil thickness was investigated for the 66 TSw hydrogeologic unit samples collected within 30 m of a PTn-cutting fault (Campbell et al. 2003). Several types of infiltration tests (point, local average, local maximum) were conducted, based on the infiltration map of A.L. Flint et al. (1996). Although the initial [36]Cl data indicate a possibility for fast flow from the land surface to the repository horizon, more recent attempts to verify this isotopic signature did not corroborate the original findings (Paces et al. 2003). The [36]Cl/Cl ratios lend support to the notions that (1) for a soil layer less than 0.5 m thick, surface runoff reduces the net infiltration rate, which provides the source of water to sustain flow through the PTn hydrogeologic unit, and (2) for a soil layer thicker than about 3 m, the [36]Cl signal has generally not yet reached the top of the bedrock. Investigations into the [36]Cl data for the verification of fast flow paths are ongoing and the results and conclusions will be documented in the final report of *Chlorine-36 Validation Studies at Yucca Mountain, Nevada* (BSC 2003f).

Using Water Potential and Cl Profiles–Scanlon et al. (2002) evaluated the subsurface system response to paleoclimatic forcing using water potential and Cl profiles. They modeled nonisothermal liquid and vapor flow and Cl transport at semiarid sites (High Plains, Texas) and arid sites (Chihuahuan Desert, Texas; Amargosa Desert, Nevada) sites. They showed that infiltration in response to current climatic forcing is restricted to the shallow (about 0.3 to 3 m) subsurface. Lower Cl concentrations at depths were caused by higher water fluxes (0.04 to 8.4 mm/yr) during the Pleistocene and earlier times. Low water potentials and upward gradients indicate current drying conditions. Nonisothermal liquid and vapor flow simulations indicate that upward flow for at least 1,000 to 2,000 years in the High Plains and for 12,000 to 16,000 years at the Chihuahuan and Amargosa Desert sites are required to reproduce measured upward water-potential gradients, and that recharge is negligible (less than 0.1 mm/yr) in these interdrainage areas.

The results of simulation of net infiltration for the present-day conditions (see Figure 4-8) can be compared with those from calculations based on pore-water chloride data (Liu, J. et al. 2003). Figure 5-1 shows the map of calculated infiltration rates for nine regions from Liu, J. et al. (2003, Figure 4), which is superimposed onto the present-day mean infiltration map calculated from the water-balance model (USGS 2001b).

Mean Modern Climate
Net Infiltration

(mm/yr)

⬜	0
🟪	<1
🟥	1 to 5
🟧	5 to 10
🟨	10 to 20
🟩	20 to 50
🟦	50 to 100
🟦	100 to 500
🟪	500 to 1,000
🟪	>1,000

Spatially Averaged
Infiltration Rates

Region	Average Infiltration Rate (mm/yr)
I	10.57
II	2.31
III	7.12
IV	2.32
V	3.05
VI	1.83
VII	1.88
VIII	0.73
IX	1.59

00394DC_051.ai
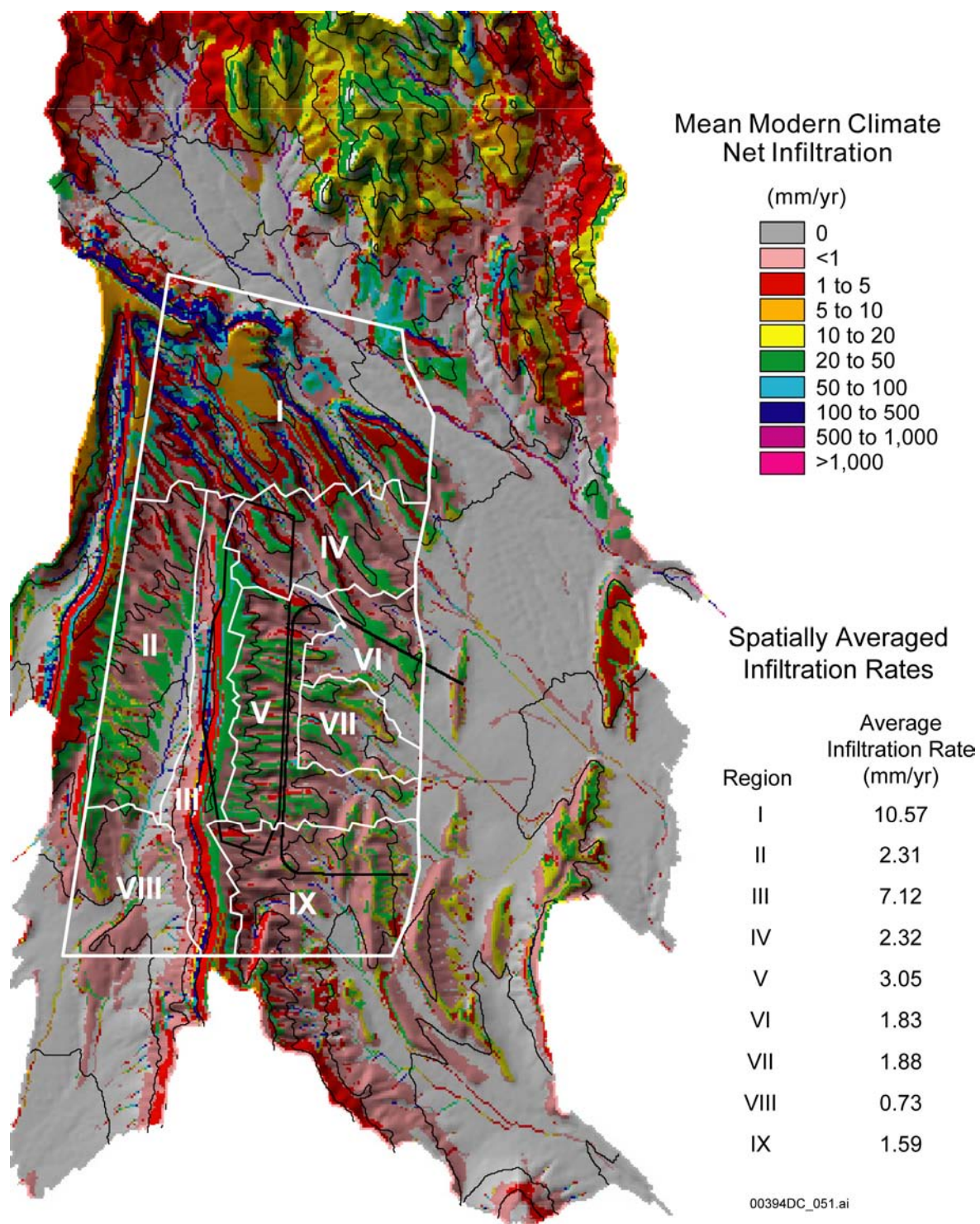
Source: Map of calculated infiltration rates are from Liu, J. et al. (2003, Figure 4, Table 1); present-day mean infiltration map is from the USGS (2001b, Figure 6-26).

Figure 5-1.   Map of Calculated Infiltration Rates for Nine Regions Superimposed onto the Present-Day Mean Infiltration Map

Table 5-1 compares the spatially averaged infiltration rates from the water-balance model simulations (USGS 2001b) with those from the chloride data calculations (Liu, J. et al. 2003). The reasonable comparison of area averaged net infiltration rates illustrated in Table 5-1 supports the validity of water-balance model calculations of net infiltration.

Table 5-1. Infiltration Data by Region

Region	Averaged Net Infiltration (mm/yr)	
	From Water-Balance Simulations	From Chloride Data Simulation
I	10.57	10.57
II	2.31	2.31
III	7.1	7.12
IV	2.43	2.32
V	2.71	3.05
VI	1.14	1.83
VII	1.88	1.88
VIII	0.73	0.73
IX	1.07	1.59
Area averaged	4.58	4.71

Source: Liu, J. et al. 2003, Table 1.

NOTE: Infiltration rates are equal to those from the water-balance model estimates because chloride data are not available for Regions I, II, and VIII.

5.3 ESTIMATION OF PERCOLATION FLUX FROM TEMPERATURE MEASUREMENTS

Temperature measurements taken in boreholes from the Yucca Mountain unsaturated zone were analyzed to estimate percolation-flux rates and overall heat flux. These results are described by Bodvarsson et al. (1999). A multilayer, one-dimensional analytical solution is used for determining percolation flux from temperature data. Case studies have shown that the analytical solution agrees very well with results from the numerical code, TOUGH2. The results of the analysis yield percolation fluxes ranging from 0 to 20 mm/yr for most of the deep boreholes. This range is in good agreement with the results of infiltration studies at Yucca Mountain.

6. UNCERTAINTY ANALYSIS OF NET INFILTRATION ESTIMATES

6.1   CAUSES AND TYPES OF UNCERTAINTY IN ASSESSING NET INFILTRATION

In the report (BSC 2003a), two types of uncertainty in the evaluation of net infiltration were considered: epistemic and aleatoric uncertainties. Epistemic uncertainty can be reduced because the state of knowledge about the processes and parameters can be improved by further characterization and data collection. Aleatoric uncertainty cannot be reduced through further testing and data collection. It can typically be accounted for using geostatistical approaches (e.g., using appropriate probability distribution functions) (Rechard 1996, p. 4-3) with the range of values and a distribution type of model input parameters.

Uncertain input parameters were assigned using known site characterization data, expert judgment, and analog site data records (BSC 2003a). Because both epistemic and aleatoric uncertainties were incorporated into models, the resulting uncertainty is a combined epistemic/aleatoric uncertainty.

The infiltration model provides estimates of infiltration flux, which are used as top boundary conditions in the development of unsaturated zone flow fields in TSPA. The infiltration uncertainty analysis using the Monte Carlo method provides the weighting factors for the glacial-transition climate applied to the unsaturated zone flow fields in TSPA. In addition, the Monte Carlo analyses provide quantitative and qualitative information that supports the description of the surficial soils and topography, one of the natural barriers to downward infiltration. The use of weighting factors developed for the glacial-transition climate for the entire 10,000-year compliance period provides additional conservatism in TSPA for the license application.

6.2   NET INFILTRATION DISTRIBUTION AND CORRELATION ANALYSIS

The uncertainty analysis was performed based on the results of simulation of net infiltration using the INFIL VA_2.a1 code (SNL 2001), which is a modified version of the USGS code INFIL V2.0 (USGS 2001c). The Latin Hypercube sampling technique was used to generate 100 realizations (simulations) of the spatial distribution of net infiltration over the repository area for 12 uncertain input parameters, which are summarized in Tables 6-1 and 6-2.

Precipitation and temperature data, which characterized the glacial-transition climate, were represented by the data set of the Tule Lake, California, meteorological station (see Figure 3-4). The use of the Tule Lake data set was recommended in *Simulation of Net Infiltration for Modern and Potential Future Climates* (USGS 2001b).

Based on *Analysis of Infiltration Uncertainty* (BSC 2003a), Figures 6-1 and 6-2 show frequency histograms of the net infiltration rate distributions for the glacial-transition climate for the modeling domain including and excluding the contingency area—the southern extension of the repository footprint. Using the net infiltration distributions and the mean net infiltration rates for the lower-bound, mean, and upper-bound glacial-transition climate states from the USGS (2001b), weighting factors (i.e., probabilities) for these climate states were determined (BSC 2003a, Section 6). Table 6-3 summarizes the weighting factors for the lower-bound, mean, and upper-bound glacial-transition climate states, which are as follows: 0.22, 0.40, and 0.38,

respectively for the modeling domain including the contingency area, and 0.24, 0.41, and 0.35, respectively, for the modeling domain excluding the contingency area.

Table 6-4 and Figure 6-3 present the results of the correlation analysis between the net infiltration distribution and uncertain input parameters. The results show that the parameters with the most impact on net infiltration are precipitation and bedrock permeability (with positive correlation coefficients, 0.64 and 0.24, respectively), and soil depth and daily potential evapotranspiration (with negative correlation coefficients, −0.49 and −0.34, respectively).

Table 6-1.   Uncertain Input Parameter Distributions Used for the Simulation of Net Infiltration for Glacial-Transition Climate

Parameter Identifier	Mean	Low Range	High Range	Distribution Type	Units
BRPERM	1.00	0.10	10.0	LOGNORMAL	NONE
BRPOROS	0.009	0.002	0.024	NORMAL	NONE
BRZDEPTH	1.50	0.00	3.00	NORMAL	METERS
ETCOEFFA	-10.0	-0.10	-19.9	NORMAL	NONE
ETCOEFFB	1.04	0.54	1.54	NORMAL	NONE
FLAREA	0.25	0.01	0.49	NORMAL	NONE
POTETMUL	1.00	0.60	1.40	NORMAL	NONE
PRECIPM	1.00	0.60	1.40	NORMAL	NONE
SNOPAR1	1.78	0.78	2.78	UNIFORM	NONE
SOILDEPM	1.00	0.10	1.90	NORMAL	NONE
SOILPERM	1.00	0.10	10.0	LOGNORMAL	NONE
SUBPAR1	0.10	0.00	0.20	UNIFORM	NONE

Source: BSC 2003a.

NOTES: Parameter identifiers are defined in Table 6-2.
For lognormal and normal distributions, Latin Hypercube sampling assumes that the low and high values in the range are at the 1.0 and 99.0 percentile (Section 5.1).
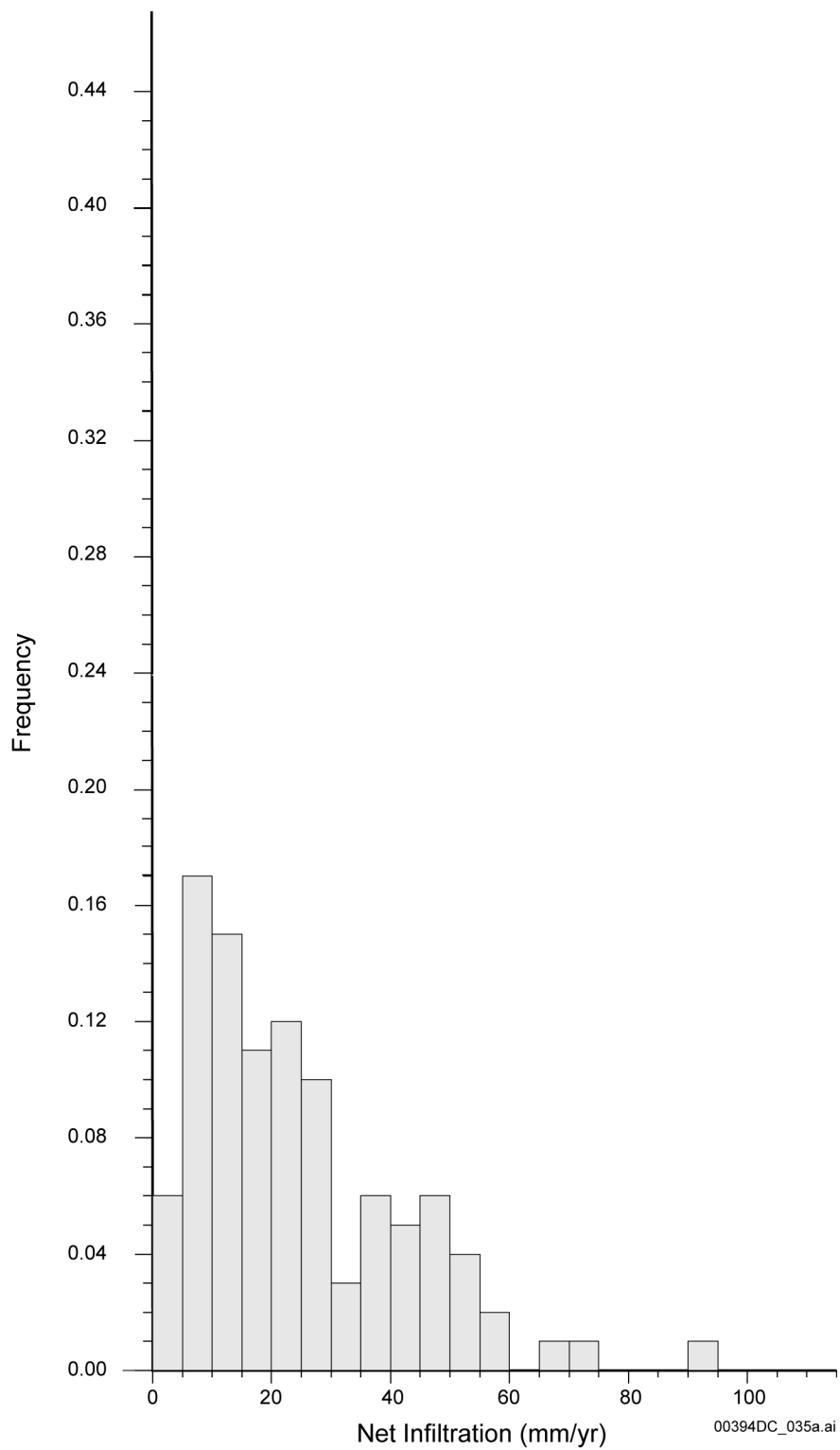
Table 6-2. Description of Uncertain Input Parameters for Glacial-Transition Climate

Parameter Identifier	Parameter
BRPERM	Bedrock bulk saturated hydraulic conductivity (multiplier)
BRPOROS	Bedrock effective root-zone porosity
BRZDEPTH	Bedrock root-zone thickness
ETCOEFFA	First coefficient in expression for evapotranspiration
ETCOEFFB	Second coefficient in expression for evapotranspiration
FLAREA	Surface flow runoff area
POTETMUL	Daily evapotranspiration (multiplier)
PRECIPM	Daily precipitation (multiplier)
SNOPAR1	Snow-melt parameter
SOILDEPM	Soil zone thickness (multiplier)
SOILPERM	Soil saturated hydraulic conductivity (multiplier)
SUBPAR1	First term ("A1") in snow loss (sublimation) equation for temperature regime below freezing (i.e., $T_k \leq 0.0°C$)

Source: BSC 2003a, Figure 6-2a.

Figure 6-1. Histogram of Average Annual Infiltration and Weighting Factors for Glacial-Transition Climate (Including Contingency Area)

Source: BSC 2003a, Figure 6-3a.

Figure 6-2. Histogram of Average Annual Infiltration and Weighting Factors for Glacial-Transition Climate (Excluding Contingency Area)

Table 6-3.   Summary of Analog Infiltration Results and Weighting Factors for Lower-Bound, Mean, and Upper-Bound Glacial-Transition Climate

Glacial-Transition Climate States	Repository Including Contingency Area		Repository Excluding Contingency Area	
	Net Infiltration Analog Value (mm/yr)	Weighting Factor	Net Infiltration Analog Value (mm/yr)	Weighting Factor
Lower Bound	2.0	0.22	2.0	0.24
Mean	17.0	0.40	19.0	0.41
Upper Bound	33.0	0.38	35.0	0.35

Source: BSC 2003a, Table 6-7.

NOTE: Net infiltration analog values are calculated using the infiltration rate maps from the USGS (2001b) for the lower-bound, mean, and upper-bound glacial-transition climates and averaged over the simulated multirectangular region including and excluding the repository contingency area. Weighting factors are calculated as discussed in *Analysis of Infiltration Uncertainty* (BSC 2003a, Section 6.3.1, 6.3.2).

Table 6-4.   Results of the Correlation Analysis of Parameters Used in Calculation of Net Infiltration for the Glacial-Transition State (100 Realizations) for the Repository Domain Approximation, Including the Contingency Area

	BRPOROS	BRZDepth	soildepm	precipm	potermul	brperm	soilperm	etcoeffa	etcoeffb	flarea	snow1	snow2	Net Infiltration
BRPOROS	1	-0.0117	-0.46	0.0047	-0.0014	-0.0106	-0.0985	0.0004	0.0063	0.0036	0.0471	0.0099	-0.091
BRZDepth	-0.0117	1	-0.0126	0.0102	0.0093	0.0551	-0.1101	-0.0006	-0.0059	0.0041	-0.016	-0.0104	-0.0496
soildepm	-0.0046	-0.0126	1	-0.0091	-0.0008	0.0143	0.0322	0.0091	0.0068	-0.0067	-0.0225	0.0154	-0.4931
precipm	0.0047	0.0102	-0.0091	1	-0.0024	-0.0398	-0.0277	0.0075	0.001	0.0083	0.0121	-0.0302	0.638
potermul	-0.0014	0.0093	-0.0008	-0.0024	1	-0.027	-0.0887	0.0036	0.0099	-0.0098	-0.0035	-0.0215	-0.3409
brperm	-0.0106	0.0551	0.0143	-0.0398	-0.027	1	0.0016	0.0053	-0.0452	0.0291	0.076	0.0049	0.2358
soilperm	-0.0985	-0.1101	0.0322	-0.0277	-0.0887	0.0016	1	0.0017	-0.069	-0.0139	0.0209	0.0173	0.009
etcoeffa	0.0004	-0.0006	0.0091	0.0075	0.0036	0.0053	0.0017	1	0.0156	0.0112	-0.0185	-0.0114	-0.098
etcoeffb	0.0063	-0.0059	0.0068	0.001	0.0099	-0.0452	-0.069	0.0156	1	0.0019	0.0141	-0.017	-0.1849
flarea	0.0036	0.0041	-0.0067	0.0083	-0.0098	0.0291	-0.0139	0.0112	0.0019	1	-0.0428	0.0111	-0.0294
snow1	0.0471	-0.016	-0.0225	0.0121	-0.0035	0.076	0.0209	-0.0185	0.0141	-0.0428	1	0.0087	0.0217
snow2	0.0099	-0.0104	0.0154	-0.0302	-0.0215	0.0049	0.0173	-0.0114	-0.017	0.0111	0.0087	1	0.0467
Net Infiltration	-0.091	-0.0496	-0.4931	0.638	-0.3409	0.2358	0.009	-0.098	-0.1849	-0.0294	0.0217	0.0467	1

Source: Net infiltration rate data are from *Analysis of Infiltration Uncertainty* (BSC 2003a, Table 6-5).
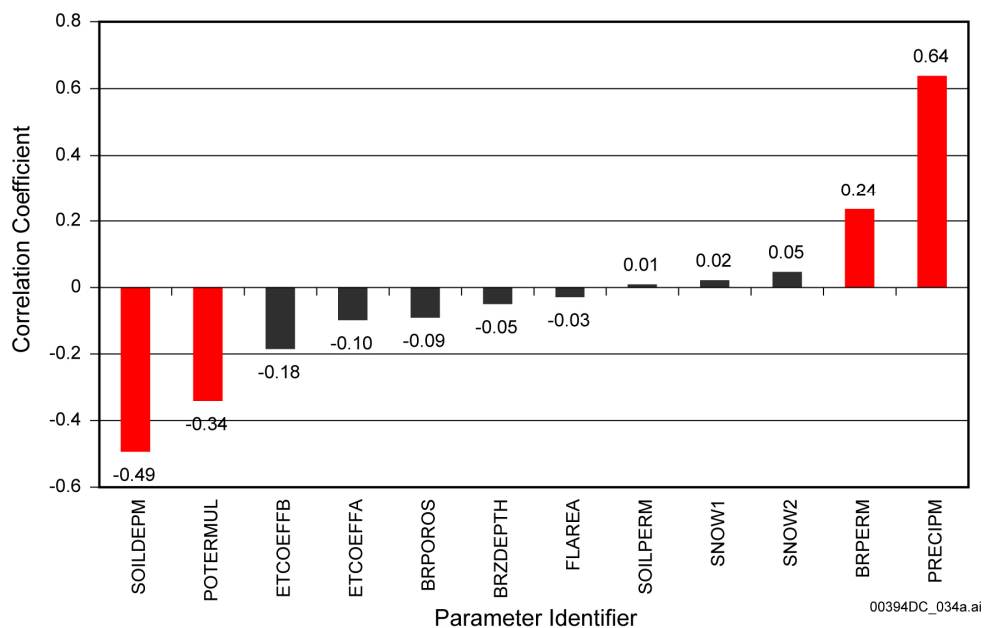
Source: BSC 2003a, Table 6-8.

NOTE: Parameters are defined in Table 6-2.

Figure 6-3.   Correlation Coefficients between Net Infiltration and Uncertain Input Paramenters Used for Simulations of Net Infiltration for the Glacial-Transition Climate (for the Flow Domain, Including the Contingency Area)

7. CONCLUSIONS

For the past 20 years, extensive field, laboratory, and modeling investigations have been performed at Yucca Mountain, which have led to the development of a number of conceptual models of infiltration and climate for the Yucca Mountain region around the repository site (Flint, A.L. et al. 2001; Wang and Bodvarsson 2003). Evaluating the amount of infiltrating water entering the subsurface is important, because this water may affect the percolation flux, which, in turn, controls seepage into the waste emplacement drifts and radionuclide transport from the repository to the water table.

Forecasting of climatic data indicates that during the next 10,000 years at Yucca Mountain, the present-day climate should persist for 400 to 600 years, followed by a warmer and much wetter monsoon climate for 900 to 1,400 years, and by a cooler and wetter glacial-transition climate for the remaining 8,000 to 8,700 years. The analysis of climatic forecasting indicates that long-term climate conditions are generally predictable from a past climate sequence, while short-term climate conditions and weather predictions may be more variable and uncertain. The use of past climate sequences to bound future climate sequences involves several types of uncertainties, such as (1) uncertainty in the timing of future climate, (2) uncertainty in the methodology of climatic forecasting, and (3) uncertainty in the earth's future physical processes. Some of the uncertainties of the climatic forecasting are epistemic (reducible) and aleatoric (irreducible).

Because of the size of the model domain, INFIL treats many flow processes in a simplified manner. For example, uptake of water by roots occurs according to the "distributed model," in which available water in each soil layer is withdrawn in proportion to the root density in that layer, multiplied by the total evapotranspirative demand. Runoff is calculated simply as the excess of precipitation over a sum of infiltration and water storage in the root zone. More significantly, water movement throughout the soil profile is treated according to the bucket model, in which the amount of water that moves down from one layer to the next is equal to the mass of water in excess of field capacity in the upper layer.

The development of a numerical model of infiltration involves a number of abstractions and simplifications to represent the complexity of environmental conditions at Yucca Mountain, such as the arid climate, mountain-type topography, heterogeneous soils and fractured rock, and irregular soil–rock interface. The abstractions and simplifications include:

- Presentation of flow using the water balance, bucket-type model, for one-dimensional, piston-like flow

- Uncertainties associated with neglecting (a) nonlinear effects in partially saturated soils and fractured rock, (b) lateral flow at the soil–rock interface, (c) preferential flow through heterogeneous soils and fractures, (d) flow under the moisture content below the field capacity, (e) redistribution of water caused by fracture–matrix interaction

- Uncertainties in the determination of saturated and unsaturated hydraulic conductivity, water retention, and other parameters controlling water flow in soils and rocks

- Simplifications of models for calculations of evapotranspiration, surface runoff and run-on.

Based on the results of numerical simulations, incorporating the Yucca Mountain region, maps have been generated that predict steady-state net infiltration for the present-day, monsoon, and glacial-transition climate states (including lower-bound, mean, and upper-bound conditions for each of the states). These maps were then used to calculate the space-averaged steady-state infiltration rates for each of the climate scenarios. Experimental and modeling studies conducted at Yucca Mountain show that episodic storm and precipitation events cause net infiltration to occur only every few years (Hevesi et al. 2002; USGS 2001b). In very wet years, infiltration increases to hundreds of millimeters per year within a relatively short time. Current estimates indicate an average infiltration rate of about 5 mm/yr, with highest values greater than 100 mm/yr northwest of the infiltration model area of Yucca Mountain (USGS 2001b, Figure 6-26).

The results of field and modeling investigations over the Yucca Mountain region (BSC 2001c, Section 3.2.2) show that the net infiltration rate varies greatly in space and time, depending on storm amplitudes, durations, and frequencies. In very wet years, infiltration pulses may infiltrate into Yucca Mountain during a relatively short time period (Bodvarsson et al. 1999, p. 10). As the soil thickness decreases and bedrock crops out, net infiltration increases because fast preferential flow through rock fractures exceeds the depth of evapotranspiration (Flint, L.E. and Flint 1995). Spatial and temporal variation in net infiltration at Yucca Mountain is caused by episodic storm and precipitation events, which occur only every few years (USGS 2001b; Hevesi et al. 2002), as well as the heterogeneous nature of a topsoil layer and topography. In very wet years, infiltration increases to hundreds of millimeters per year during a relatively short time.

The data summarized in Table 7-1 illustrate that the net infiltration rates obtained from numerical simulations using the water-balance model compare reasonably well with those from corroborative experimental and modeling studies (geochemical and temperature measurements in the unsaturated zone, as well as groundwater recharge). This comparison validates the results of infiltration studies.

Table 7-1. Comparison of the Estimates of Net Infiltration with the Percolation Flux for Present-Day Climatic Conditions, Determined Using Corroborative Experimental Methods and Numerical Modeling Results

Types of Data	Percolation and Infiltration Rates (mm/yr)	Data Source
Temperature measurements in boreholes	0 to 20	Bodvarsson et al. 1999
Chloride in boreholes	0.02 to 5.9	Flint, A.L. et al. 1996
Chloride simulations	0.73 to 10.57	Liu, J. et al. 2003
Calcite data	2 to 20	Xu et al. 2003
Expert evaluation	3.9 to 12.7	CRWMS M&O 1997a
Averaged calculated net infiltration for the mean present-day climate state from the water balance model	4.7	USGS 2001b

INTENTIONALLY LEFT BLANK

8. REFERENCES

8.1 DOCUMENTS CITED

Ahlers, C.F.; Shan, C.; Haukwa, C.; Cohen, A.B.J.; and Bodvarsson, G.S. 1996. *Calibration and Prediction of Pneumatic Response at Yucca Mountain, Nevada Using the Unsaturated Zone Flow Model.* Milestone OB12M. Berkeley, California: Lawrence Berkeley National Laboratory. ACC: MOL.19970206.0285.

Ahrens, C.D. 1994. *Meteorology Today, An Introduction to Weather, Climate, and the Environment.* 5th Edition. St. Paul, Minnesota: West Publishing. TIC: 237196.

Avon, L. and Durbin, T.J. 1994. "Evaluation of the Maxey-Eakin Method for Estimating Recharge to Ground-Water Basins in Nevada." *Water Resources Bulletin, 30,* (1), 99–111. Herndon, Virginia: American Water Resources Association. TIC: 255352.

Bodvarsson, G.S. and Bandurraga, T.M., eds. 1996. *Development and Calibration of the Three-Dimensional Site-Scale Unsaturated Zone Model of Yucca Mountain, Nevada.* Berkeley, California: Lawrence Berkeley National Laboratory. ACC: MOL.19970211.0176.

Bodvarsson, G.S.; Boyle, W.; Patterson, R.; and Williams, D. 1999. "Overview of Scientific Investigations at Yucca Mountain—The Potential Repository for High-Level Nuclear Waste." *Journal of Contaminant Hydrology, 38,* (1-3), 3-24. New York, New York: Elsevier. TIC: 244160.

Bodvarsson, G.S.; Kwicklis, E.; Shan, C.; and Wu, Y.S. 2003. "Estimation of Percolation Flux from Borehole Temperature Data at Yucca Mountain, Nevada." *Journal of Contaminant Hydrology, 62–63,* 3–22. New York, New York: Elsevier. TIC: 254205.

BSC (Bechtel SAIC Company) 2001a. *Features, Events, and Processes in UZ Flow and Transport.* ANL-NBS-MD-000001 REV 01. Las Vegas, Nevada: Bechtel SAIC Company. ACC: MOL.20010423.0321.

BSC 2001b. *UZ Flow Models and Submodels.* MDL-NBS-HS-000006 REV 00 ICN 01. Las Vegas, Nevada: Bechtel SAIC Company. ACC: MOL.20020417.0382.

BSC 2001c. *FY 01 Supplemental Science and Performance Analyses, Volume 1: Scientific Bases and Analyses.* TDR-MGR-MD-000007 REV 00 ICN 01. Las Vegas, Nevada: Bechtel SAIC Company. ACC: MOL.20010801.0404; MOL.20010712.0062; MOL.20010815.0001.

BSC 2002a. *Total System Performance Assessment—License Application Methods and Approach.* TDR-WIS-PA-000006 REV 00. Las Vegas, Nevada: Bechtel SAIC Company. ACC: MOL.20020923.0175.

BSC 2002b. *Guidelines for Developing and Documenting Alternative Conceptual Models, Model Abstractions, and Parameter Uncertainty in the Total System Performance Assessment for the License Application.* TDR-WIS-PA-000008 REV 00, ICN 01. Las Vegas, Nevada: Bechtel SAIC Company. ACC: MOL.20020904.0002.

BSC 2002c. *Technical Work Plan for: Performance Assessment Unsaturated Zone*. TWP-NBS-HS-000003 REV 02. Las Vegas, Nevada: Bechtel SAIC Company. ACC: MOL.20030102.0108.

BSC 2003a. *Analysis of Infiltration Uncertainty*. ANL-NBS-HS-000027 REV 01. Las Vegas, Nevada: Bechtel SAIC Company. ACC: DOC.20031030.0003.

BSC 2003b. *Abstraction of Drift Seepage*. MDL-NBS-HS-000019 REV 00 ICN 01. Las Vegas, Nevada: Bechtel SAIC Company. ACC: DOC.20031112.0002.

BSC 2003c. *In Situ Field Testing of Processes*. ANL-NBS-HS-000005 REV 02. Las Vegas, Nevada: Bechtel SAIC Company. ACC: DOC.20031208.0001.

BSC 2003d. *UZ Flow Models and Submodels*. MDL-NBS-HS-000006 REV 01. Las Vegas, Nevada: Bechtel SAIC Company. ACC: DOC.20030818.0002.

BSC 2003e. *Calibrated Properties Model*. MDL-NBS-HS-000003 REV 01. Las Vegas, Nevada: Bechtel SAIC Company. ACC: DOC.20030219.0001.

BSC 2003f. *Chlorine-36 Validation Studies at Yucca Mountain, Nevada*. TDR-NBS-HS-000017 REV 00A-Draft. Las Vegas, Nevada: Bechtel SAIC Company. ACC: MOL.20031105.0082.

Campbell, K.; Wolfsberg, A.; Fabryka-Martin, J.; and Sweetkind, D. 2003. "Chlorine-36 Data at Yucca Mountain: Statistical Tests of Conceptual Models for Unsaturated-Zone Flow." *Journal of Contaminant Hydrology, 62-63,* 43-61. New York, New York: Elsevier. TIC: 254205.

Cochran, J.R.; Beyeler, W.E.; Brosseau, D.A.; Brush, L.H.; Brown, T.J.; Crowe, B.M.; Conrad, S.H.; Davis, P.A.; Ehrhorn, T.; Feeney, T.; Fogleman, B.; Gallegos, D.P.; Haaker, R.; Kalinina, E.; Price, L.L.; Thomas, D.P.; and Wirth, S. 2001. *Compliance Assessment Document for the Transuranic Wastes in the Greater Confinement Disposal Boreholes at the Nevada Test Site, Volume 2: Performance Assessment, Version 2.0.* SAND2001-2977. Albuquerque, New Mexico: Sandia National Laboratories. TIC: 254267.

CRWMS M&O (Civilian Radioactive Waste Management System Management and Operating Contractor) 1996. *The Vegetation of Yucca Mountain: Description and Ecology.* B00000000-01717-5705-00030 REV 00. Las Vegas, Nevada: CRWMS M&O. ACC: MOL.19970116.0055.

CRWMS M&O 1997a. *Unsaturated Zone Flow Model Expert Elicitation Project.* Las Vegas, Nevada: CRWMS M&O. ACC: MOL.19971009.0582.

CRWMS M&O 1997b. *Engineering Design Climatology and Regional Meteorological Conditions Report.* B00000000-01717-5707-00066 REV 00. Las Vegas, Nevada: CRWMS M&O. ACC: MOL.19980304.0028.

CRWMS M&O 1999. *Environmental Baseline File for Soils.* B00000000-01717-5700-00007 REV 00. Las Vegas, Nevada: CRWMS M&O. ACC: MOL.19990302.0180.

CRWMS M&O 2000a. *Total System Performance Assessment for the Site Recommendation.* TDR-WIS-PA-000001 REV 00 ICN 01. Las Vegas, Nevada: CRWMS M&O. ACC: MOL.20001220.0045.

CRWMS M&O 2000b. *Yucca Mountain Site Description.* TDR-CRW-GS-000001 REV 01 ICN 01. Las Vegas, Nevada: CRWMS M&O. ACC: MOL.20001003.0111.

CRWMS M&O 2000c. *Analysis of Geochemical Data for the Unsaturated Zone.* ANL-NBS-HS-000017 REV 00. Las Vegas, Nevada: CRWMS M&O. ACC: MOL.20000725.0453.

D'Agnese, F.A.; Faunt, C.C.; Turner, A.K.; and Hill, M.C. 1997. *Hydrogeologic Evaluation and Numerical Simulation of the Death Valley Regional Ground-Water Flow System, Nevada and California.* Water-Resources Investigations Report 96-4300. Denver, Colorado: U.S. Geological Survey. ACC: MOL.19980306.0253.

Dettinger, M.D. 1989. "Reconnaissance Estimates of Natural Recharge to Desert Basins in Nevada, U.S.A., by Using Chloride-Balance Calculations." *Journal of Hydrology, 106,* 55-78. Amsterdam, The Netherlands: Elsevier. TIC: 236967.

DeWispelare, A.R.; Herren, L.T.; Miklas, M.P.; and Clemen, R.T. 1993. *Expert Elicitation of Future Climate in the Yucca Mountain Vicinity, Iterative Performance Assessment Phase 2.5.* CNWRA 93-016. San Antonio, Texas: Center for Nuclear Waste Regulatory Analyses. TIC: 238416.

DOE (U.S. Department of Energy) 1998. *Total System Performance Assessment.* Volume 3 of *Viability Assessment of a Repository at Yucca Mountain.* DOE/RW-0508. Washington, D.C.: U.S. Department of Energy, Office of Civilian Radioactive Waste Management. ACC: MOL.19981007.0030.

DOE 2002a. *Final Environmental Impact Statement for a Geologic Repository for the Disposal of Spent Nuclear Fuel and High-Level Radioactive Waste at Yucca Mountain, Nye County, Nevada.* DOE/EIS-0250. Washington, D.C.: U.S. Department of Energy, Office of Civilian Radioactive Waste Management. ACC: MOL.20020524.0314 through MOL.20020524.0320.

DOE 2002b. *Yucca Mountain Site Suitability Evaluation.* DOE/RW-0549. Washington, D.C.: U.S. Department of Energy, Office of Civilian Radioactive Waste Management. ACC: MOL.20020404.0043.

Donovan, D.J. and Katzer, T. 2000. "Hydrologic Implications of Greater Ground-Water Recharge to Las Vegas Valley, Nevada." *Journal of the American Water Resources Association, 36,* 5, 1,133–1,148. Herndon, Virginia: American Water Resources Association. TIC: 255380.

EG&G (EG&G Energy Measurements) 1991. *Yucca Mountain Biological Resources Monitoring Program Annual Report FY89 & FY90.* EGG 10617-2084. Goleta, California: EG&G Energy Measurements. ACC: NNA.19920131.0206.

Fabryka-Martin, J.; Wolfsberg, A.V.; Dixon, P.R.; Levy, S.; Musgrave, J.; and Turin, H.J. 1996. *Summary Report of Chlorine-36 Studies: Sampling, Analysis, and Simulation of Chlorine-36 in the Exploratory Studies Facility.* Milestone 3783M. Los Alamos, New Mexico: Los Alamos National Laboratory. ACC: MOL.19970103.0047.

Faybishenko, B.; Doughty, C.; Steiger, M.; Long, J.C.S.; Wood, T.R.; Jacobsen, J.S.; Lore, J.; and Zawislanksi, P.T. 2000. "Conceptual Model of the Geometry and Physics of Water Flow in a Fractured Basalt Vadose Zone." *Water Resources Research, 36,* (12), 3,499–3,520. Washington, D.C.: American Geophysical Union. TIC: 250750.

Fenelon, J.M. and Moreo, M.T. 2002. *Trend Analysis of Ground-Water Levels and Spring Discharge in the Yucca Mountain Region, Nevada and California, 1960–2000.* Water-Resources Investigations Report 02-4178. Carson City, Nevada: U.S. Geological Survey. ACC: MOL.20030812.0306.

Flint, A.L. and Childs, S.W. 1991. "Use of the Priestley-Taylor Evaporation Equation for Soil Water Limited Conditions in a Small Forest Clearcut." *Agricultural and Forest Meteorology, 56,* (3–4), 247–260. Amsterdam, The Netherlands: Elsevier. TIC: 241865.

Flint, A.L.; Flint, L.E.; Bodvarsson, G.S.; Kwicklis, E.M.; and Fabryka-Martin, J. 2001. "Evolution of the Conceptual Model of Unsaturated Zone Hydrology at Yucca Mountain, Nevada." *Journal of Hydrology, 247,* (1–2]), 1–30. New York, New York: Elsevier. TIC: 250932.

Flint, A.L.; Hevesi, J.A.; and Flint, L.E. 1996. *Conceptual and Numerical Model of Infiltration for the Yucca Mountain Area, Nevada.* Milestone 3GUI623M. Denver, Colorado: U.S. Geological Survey. ACC: MOL.19970409.0087.

Flint, L.E. 1998. *Characterization of Hydrogeologic Units Using Matrix Properties, Yucca Mountain, Nevada.* Water-Resources Investigations Report 97-4243. Denver, Colorado: U.S. Geological Survey. ACC: MOL.19980429.0512.

Flint, L.E. and Flint, A.L. 1995. *Shallow Infiltration Processes at Yucca Mountain, Nevada— Neutron Logging Data 1984-93.* Water-Resources Investigations Report 95-4035. Denver, Colorado: U.S. Geological Survey. ACC: MOL.19960924.0577.

Flint, L.E.; Flint, A.L.; Rautman, C.A.; and Istok, J.D. 1996. *Physical and Hydrologic Properties of Rock Outcrop Samples at Yucca Mountain, Nevada.* Open-File Report 95-280. Denver, Colorado: U.S. Geological Survey. ACC: MOL.19970224.0225.

Hansen, D.J.; Greger, P.D.; Wills, C.A.; and Ostler, W.K. 1997. *Nevada Test Site Wetlands Assessment*. DOE/NV/11718-124. Las Vegas, Nevada: U.S. Department of Energy. ACC: MOL.20010803.0372.

Harrill, J.R. and Prudic, D.E. 1998. *Aquifer Systems in the Great Basin Region of Nevada, Utah, and Adjacent States - Summary Report.* Professional Paper 1409-A. Denver, Colorado: U.S. Geological Survey. TIC: 247432.

Hevesi, J.A. and Flint, A.L. 1998. "Geostatistical Estimates of Future Recharge for the Death Valley Region." *High-Level Radioactive Waste Management, Proceedings of the Eighth International Conference, Las Vegas, Nevada, May 11-14, 1998.* Pages 173–177. La Grange Park, Illinois: American Nuclear Society. TIC: 237082.

Hevesi, J.A.; Flint, A.L.; and Flint, L.E. 1994. "Verification of a One-Dimensional Model for Predicting Shallow Infiltration at Yucca Mountain." *High Level Radioactive Waste Management, Proceedings of the Fifth Annual International Conference, Las Vegas, Nevada, May 22-26, 1994. 4,* 2323-2332. La Grange Park, Illinois: American Nuclear Society. TIC: 210984.

Hevesi, J.A.; Flint, A.L.; and Flint, L.E. 2002. *Preliminary Estimates of Spatially Distributed Net Infiltration and Recharge for the Death Valley Region, Nevada–California.* Water-Resources Investigations Report 02-4010. Sacramento, California: U.S. Geological Survey. TIC: 253392.

Hevesi, J.A.; Flint, A.L.; and Flint, L.E. 2003. *Simulation of Net Infiltration and Potential Recharge Using a Distributed-Parameter Watershed Model of the Death Valley Region, Nevada and California.* Water-Resources Investigations Report 03-4090. Sacramento, California: U.S. Geological Survey. TIC: 255193.

Hillel, D. 1982. *Introduction to Soil Physics.* New York, New York: Academic Press. TIC: 215629.

Hinds, J.; Bodvarsson, G.S.; and Nieder-Westermann, G.H. 2003. "Conceptual Evaluation of the Potential Role of Fractures in Unsaturated Processes at Yucca Mountain." *Journal of Contaminant Hydrology, 62–63,* 111–132. New York, New York: Elsevier. TIC: 254205.

Jury, W.A.; Gardner, W.R.; and Gardner, W.H. 1991. *Soil Physics.* 5th Edition. New York, New York: John Wiley & Sons. TIC: 241000.

Kwicklis, E.M. 1999. "Determination of Pneumatic Diffusivity." *Hydrogeology of the Unsaturated Zone, North Ramp Area of the Exploratory Studies Facility, Yucca Mountain, Nevada.* Rousseau, J.P.; Kwicklis, E.M.; and Gillies, D.C., eds. Water-Resources Investigations Report 98-4050. Denver, Colorado: U.S. Geological Survey. ACC: MOL.19990419.0335.

Laczniak, R.J.; Cole, J.C.; Sawyer, D.A.; and Trudeau, D.A. 1996. *Summary of Hydrogeologic Controls on Ground-Water Flow at the Nevada Test Site, Nye County, Nevada.* Water-Resources Investigations 96-4109. Carson City, Nevada: U.S. Geological Survey. TIC: 226157.

Landwehr, J.M.; Coplen, T.B.; Ludwig, K.R.; Winograd, I.J.; and Riggs, A.C. 1997. *Data for Devils Hole Core DH-11.* Open-File Report 97-792. Reston, Virginia: U.S. Geological Survey. TIC: 245712.

LeCain, G.D. 1997. *Air-Injection Testing in Vertical Boreholes in Welded and Nonwelded Tuff, Yucca Mountain, Nevada.* Water-Resources Investigations Report 96-4262. Denver, Colorado: U.S. Geological Survey. ACC: MOL.19980310.0148.

Levitt, D.G.; Sully, M.J.; and Lohrstorfer, C.F. 1996. *Modeling Evapotranspiration from Arid Environments: Literature Review and Preliminary Model Results.* Las Vegas, Nevada: Bechtel Nevada. TIC: 254273.

Lichty, R.W. and McKinley, P.W. 1995. *Estimates of Ground-Water Recharge Rates for Two Small Basins in Central Nevada.* Water-Resources Investigations Report 94-4104. Denver, Colorado: U.S. Geological Survey. ACC: MOL.19960924.0524.

Liu, H.-H.; Doughty, C.; and Bodvarsson, G.S. 1998. "An Active Fracture Model for Unsaturated Flow and Transport in Fractured Rocks." *Water Resources Research, 34,* (10), 2633-2646. Washington, D.C.: American Geophysical Union. TIC: 243012.

Liu, H.-H.; Haukwa, C.B.; Ahlers, C.F.; Bodvarsson, G.S.; Flint, A.L.; and Guertal, W.B. 2003. "Modeling Flow and Transport in Unsaturated Fractured Rock: An Evaluation of the Continuum Approach." *Journal of Contaminant Hydrology, 62-63,* 173-188. New York, New York: Elsevier. TIC: 254205

Liu, J.; Sonnenthal, E.L.; and Bodvarsson, G.S. 2003. "Calibration of Yucca Mountain Unsaturated Zone Flow and Transport Model Using Porewater Chloride Data." *Journal of Contaminant Hydrology, 62–63,* 213–235. New York, New York: Elsevier. TIC: 254205.

Maxey, G.B. and Eakin, T.E. 1950. *Ground Water in White River Valley, White Pine, Nye, and Lincoln Counties, Nevada.* Water Resources Bulletin No. 8. Carson City, Nevada: State of Nevada, Office of the State Engineer. TIC: 216819.

McCurley, R. 2003. " 'Evaluation of the Occurrence of Termite Species and Potential Termite Burrowing Depths in the Area of the Nevada Test Site: Present Day and for the Next 10,000 Years' by Myles, T.G. and Hooten, M.M." Memorandum from R. McCurley (SNL) to Records Processing Center (RPC), October 22, 2003, with attachment. ACC: MOL.20031023.0116.

Miller, G.A. 1977. *Appraisal of the Water Resources of Death Valley, California-Nevada.* Open-File Report 77-728. Menlo Park, California: U.S. Geological Survey. ACC: HQS.19880517.1934.

Mock, C.J. 1996. "Climatic Controls and Spatial Variations of Precipitation in the Western United States." *Journal of Climate, 9,* 1111-1125. Boston, Massachusetts: American Meteorological Society. TIC: 237443.

Nativ, R.; Adar, E.; Dahan, O.; and Geyh, M. 1995. "Water Recharge and Solute Transport Through the Vadose Zone of Fractured Chalk Under Desert Conditions." *Water Resources Research, 31*, (2), 253-261. Washington, D.C.: American Geophysical Union. TIC: 233563.

Nicholl, M.J. and Glass, R.J. 2002. *Field Investigation of Flow Processes Associated with Infiltration into an Initially Dry Fracture Network at Fran Ridge, Yucca Mountain, Nevada: A Photo Essay and Data Summary.* SAND2002-1369. Albuquerque, New Mexico: Sandia National Laboratories. ACC: MOL.20031124.0211.

Nicholl, M.J.; Glass, R.J.; and Nguyen, H.A. 1993. "Small-Scale Behavior of Single Gravity-Driven Fingers in an Initially Dry Fracture." *High Level Radioactive Waste Management, Proceedings of the Fourth Annual International Conference, Las Vegas, Nevada, April 26-30, 1993.* 2, 2023–2032. La Grange Park, Illinois: American Nuclear Society. TIC: 208542.

NRC (U.S. Nuclear Regulatory Commission) 1997. *Issue Resolution Status Report on Methods to Evaluate Climate Change and Associated Effects at Yucca Mountain (Key Technical Issue: Unsaturated and Saturated Flow Under Isothermal Conditions).* Washington, D.C.: U.S. Nuclear Regulatory Commission. ACC: MOL.19980219.0880.

Paces, J.B.; Neymark, L.A.; Marshall, B.D.; Whelan, J.F.; and Peterman, Z.E. 1996. *Letter Report: Ages and Origins of Subsurface Secondary Minerals in the Exploratory Studies Facility (ESF).* Milestone 3GQH450M, Results of Sampling and Age Determination. Las Vegas, Nevada: U.S. Geological Survey. ACC: MOL.19970324.0052.

Paces, J.B.; Peterman, Z.E.; Neymark, L.A.; Nimz, G.J.; Gascoyne, M.; and Marshall, B.D. 2003. "Summary of Chlorine-36 Validation Studies at Yucca Mountain, Nevada." *Proceedings of the 10th International High-Level Radioactive Waste Management Conference (IHLRWM), March 30-April 2, 2003, Las Vegas, Nevada.* 348–356. La Grange Park, Illinois: American Nuclear Society. TIC: 254253.

Patterson, G.L.; Weeks, E.P.; Rousseau, J.P.; and Oliver, T.A. 1996. *Interpretation of Pneumatic and Chemical Data from the Unsaturated Zone Near Yucca Mountain, Nevada.* Milestone 3GGP605M. Denver, Colorado: U.S. Geological Survey. ACC: MOL.19970324.0058.

Pruess, K.; Faybishenko, B.; and Bodvarsson, G.S. 1999. "Alternative Concepts and Approaches for Modeling Flow and Transport in Thick Unsaturated Zones of Fractured Rocks." *Journal of Contaminant Hydrology, 38,* (1–3), 281–322. New York, New York: Elsevier. TIC: 244160.

Rechard, R.P. 1996. *An Introduction to the Mechanics of Performance Assessment Using Examples of Calculations Done for the Waste Isolation Pilot Plant Between 1990 and 1992.* SAND93-1378 Revised. Albuquerque, New Mexico: Sandia National Laboratories. TIC: 245715.

Resource Concepts 1989. *Soil Survey of Yucca Mountain Study Area, Nye County, Nevada.* NWPO EV 003-89. Carson City, Nevada: Resource Concepts. TIC: 206227.

Rousseau, J.P.; Kwicklis, E.M.; and Gillies, D.C., eds. 1999. *Hydrogeology of the Unsaturated Zone, North Ramp Area of the Exploratory Studies Facility, Yucca Mountain, Nevada.* Water-Resources Investigations Report 98-4050. Denver, Colorado: U.S. Geological Survey. ACC: MOL.19990419.0335.

Rousseau, J.P.; Loskot, C.L.; Thamir, F.; and Lu, N. 1997. *Results of Borehole Monitoring in the Unsaturated Zone Within the Main Drift Area of the Exploratory Studies Facility, Yucca Mountain, Nevada.* Milestone SPH22M3. Denver, Colorado: U.S. Geological Survey. ACC: MOL.19970626.0351.

Salvucci, G.D. and Entekhabi, D. 1995. "Hillslope and Climatic Controls on Hydrologic Fluxes." *Water Resources Research., 31,* (7), 1725–1739. Washington, D.C.: American Geophysical Union. TIC: 252318.

Savard, C.S. 1998. *Estimated Ground-Water Recharge from Streamflow in Fortymile Wash Near Yucca Mountain, Nevada.* Water-Resources Investigations Report 97-4273. Denver, Colorado: U.S. Geological Survey. TIC: 236848.

Scanlon, B.R.; Christman, M.; Reedy, R.C.; Porro, I.; Simunek, J.; and Flerchinger, G.N. 2002. "Intercode Comparisons for Simulating Water Balance of Surficial Sediments in Semiarid Regions." *Water Resources Research, 38,* 12, 1323. Washington, D.C.: American Geophysical Union. TIC: 255363.

Scanlon, B.R.; Langford, R.P.; and Goldsmith, R.S. 1999. "Relationship Between Geomorphic Settings and Unsaturated Flow in an Arid Setting." *Water Resources Research, 35,* 983–999. Washington, D.C.: American Geophysical Union. TIC: 252295.

Sharpe, S. 2002. *Future Climate Analysis—10,000 Years to 1,000,000 Years After Present.* MOD-01-001 REV 00. Reno, Nevada: Desert Research Institute. ACC: MOL.20020422.0011.

Sharpe, S. 2003. *Future Climate Analysis—10,000 Years to 1,000,000 Years After Present.* MOD-01-001 REV 01. Reno, Nevada: Desert Research Institute. ACC: MOL.20030407.0055.

Simmons, A.M. 2004. *Yucca Mountain Site Description.* TDR-CRW-GS-000001 REV 02. Two volumes. Las Vegas, Nevada: Bechtel SAIC Company. ACC: DOC.20040120.0004.

SNL (Sandia National Laboratories) 2001. Software Code: INFIL. VA_2.a1. DEC Alpha, OpenVMS V7.2-1. 10253-A_2.a1-00.

Sonnenthal, E.L. and Bodvarsson, G.S. 1999. "Constraints on the Hydrology of the Unsaturated Zone at Yucca Mountain, NV from Three-Dimensional Models of Chloride and Strontium Geochemistry." *Journal of Contaminant Hydrology, 38,* (1–3), 107–156. New York, New York: Elsevier. TIC: 244160.

Stablein, N.K. 1997. "Issue Resolution Status Report on Methods to Evaluate Climate Change and Associated Effects at Yucca Mountain (Key Technical Issue: Unsaturated and Saturated Flow Under Isothermal Conditions)." Letter from N.K. Stablein (NRC) to S. Brocoum (DOE/YMSCO), June 30, 1997, with enclosure. ACC: MOL.19980219.0879; MOL.19980219.0880.

Sukhija, B.S.; Reddy, D.V.; Nagabhushanam, P.; and Hussain, S. 2003. "Recharge Processes: Piston Flow vs. Preferential Flow in Semi-Arid Aquifers of India." *Hydrogeology Journal, 11,* (3), 387–395. Berlin, Germany: Springer-Verlag. TIC: 255333.

Thompson, R.S.; Anderson, K.H.; and Bartlein, P.J. 1999. *Quantitative Paleoclimatic Reconstructions from Late Pleistocene Plant Macrofossils of the Yucca Mountain Region.* Open-File Report 99-338. Denver, Colorado: U.S. Geological Survey. ACC: MOL.19991015.0296.

USGS (U.S. Geological Survey) 2000. *Future Climate Analysis*. ANL-NBS-GS-000008 REV 00. Denver, Colorado: U.S. Geological Survey. ACC: MOL.20000629.0907.

USGS 2001a. *Future Climate Analysis.* ANL-NBS-GS-000008 REV 00 ICN 01. Denver, Colorado: U.S. Geological Survey. ACC: MOL.20011107.0004.

USGS 2001b. *Simulation of Net Infiltration for Modern and Potential Future Climates.* ANL-NBS-HS-000032 REV 00 ICN 02. Denver, Colorado: U.S. Geological Survey. ACC: MOL.20011119.0334.

USGS 2001c. Software Code: INFIL. V2.0. PC. 10307-2.0-00.

Wallace, A.; Romney, E.M.; and Cha, J.W. 1980. "Depth Distribution of Roots of Some Perennial Plants in the Nevada Test Site Area of the Northern Mojave Desert." *Great Basin Naturalist Memoirs, 4,* 201–207. Provo, Utah: Brigham Young University. TIC: 254271.

Wang, J.S.Y. and Bodvarsson, G.S. 2003. "Evolution of the Unsaturated Zone Testing at Yucca Mountain." *Journal of Contaminant Hydrology, 62–63,* 337–360. New York, New York: Elsevier. TIC: 254205.

Watson, P.; Sinclair, P.; and Waggoner, R. 1976. "Quantitative Evaluation of a Method for Estimating Recharge to the Desert Basins of Nevada." *Journal of Hydrology, 31,* (3/4), 335-357. Amsterdam, The Netherlands: Elsevier. TIC: 234481.

Williams, N.H. 2001. "Contract No. DE-AC08-01RW12101 – Total System Performance Assessment – Analyses for Disposal of Commercial and DOE Waste Inventories at Yucca Mountain – Input to Final Environmental Impact Statement and Site Suitability Evaluation REV 00 ICN 02." Letter from N.H. Williams (BSC) to J.R. Summerson (DOE/YMSCO), December 11, 2001, RWA:cs-1204010670, with enclosure. ACC: MOL.20011213.0056.

Winograd, I.J. 1981. "Radioactive Waste Disposal in Thick Unsaturated Zones." *Science, 212,* (4502), 1457–1464. Washington, D.C.: American Association for the Advancement of Science. TIC: 217258.

Winograd, I.J.; Coplen, T.B.; Landwehr, J.M.; Riggs, A.C.; Ludwig, K.R.; Szabo, B.J.; Kolesar, P.T.; and Revesz, K.M. 1992. "Continuous 500,000-Year Climate Record from Vein Calcite in Devils Hole, Nevada." *Science, 258,* 255-260. Washington, D.C.: American Association for the Advancement of Science. TIC: 237563.

Winograd, I.J. and Thordarson, W. 1975. *Hydrogeologic and Hydrochemical Framework, South-Central Great Basin, Nevada-California, with Special Reference to the Nevada Test Site.* Geological Survey Professional Paper 712-C. Washington, D.C.: United States Government Printing Office. ACC: NNA.19870406.0201.

Wirth, S.; Brown, T.; and Beyeler, W. 1999. *Native Plant Uptake Model for Radioactive Waste Disposal Areas at the Nevada Test Site*. SAND98-1789. Albuquerque, New Mexico: Sandia National Laboratories. TIC: 254423.

Wu, Y-S.; Haukwa, C.; and Bodvarsson, G.S. 1999. "A Site-Scale Model for Fluid and Heat Flow in the Unsaturated Zone of Yucca Mountain, Nevada." *Journal of Contaminant Hydrology, 38,* (1-3), 185–215. New York, New York: Elsevier. TIC: 244160.

Xu, T.; Sonnenthal, E.; and Bodvarsson, G. 2003. "A Reaction-Transport Model for Calcite Precipitation and Evaluation of Infiltration Fluxes in Unsaturated Fractured Rock." *Journal of Contaminant Hydrology, 64,* (1-2), 113–127. New York, New York: Elsevier. TIC: 254008.

Yamamoto, H.; Kojima, K.; and Tosaka, H. 1993. "Fractal Clustering of Rock Fractures and Its Modeling Using Cascade Process." *Scale Effects in Rock Masses, Proceedings of the Second International Workshop on Scale Effects in Rock Masses, Lisbon, Portugal, June 25, 1993.* da Cunha, P., ed. Pages 81-86. Rotterdam, The Netherlands: A.A. Balkema. TIC: 253608.

Yang, I.C.; Rattray, G.W.; and Yu, P. 1996. *Interpretation of Chemical and Isotopic Data from Boreholes in the Unsaturated Zone at Yucca Mountain, Nevada.* Water-Resources Investigations Report 96-4058. Denver, Colorado: U.S. Geological Survey. ACC: MOL.19980528.0216.

YMP (Yucca Mountain Site Characterization Project) 1997. *Soil Types within the Busted Butte USGS 7.5 Min. Quadrangle*. YMP-97-008.1. Las Vegas, Nevada: Yucca Mountain Site Characterization Office. ACC: MOL.19990610.0224.

8.2   CODES, STANDARDS, REGULATIONS, AND PROCEDURES

10 CFR Part 63. Energy: Disposal of High-Level Radioactive Wastes in a Geologic Repository at Yucca Mountain, Nevada. Readily available.

40 CFR Part 197. Protection of Environment: Public Health and Environmental Radiation Protection Standards for Yucca Mountain, Nevada. Readily available.

8.3   DATA, LISTED BY DATA TRACKING NUMBER

GS000308311221.010. Developed Daily Climate Data from Tule Lake, California Used for Infiltration Uncertainty Analysis. Submittal date: 03/07/2000.

APPENDIX A

**TECHNICAL BASIS FOR THE WATER-BALANCE PLUG-FLOW MODEL
ADEQUATELY REPRESENTING THE NONLINEAR FLOW PROCESSES
REPRESENTED BY RICHARDS EQUATION
(RESPONSE TO TSPAI 3.18 AIN-1)**

Note Regarding the Status of Supporting Technical Information

This document was prepared using the most current information available at the time of its development. This Technical Basis Document and its appendices providing Key Technical Issue Agreement responses that were prepared using preliminary or draft information reflect the status of the Yucca Mountain Project's scientific and design bases at the time of submittal. In some cases this involved the use of draft Analysis and Model Reports (AMRs) and other draft references whose contents may change with time. Information that evolves through subsequent revisions of the AMRs and other references will be reflected in the license application (LA) as the approved analyses of record at the time of LA submittal. Consequently, the Project will not routinely update either this Technical Basis Document or its Key Technical Issue Agreement appendices to reflect changes in the supporting references prior to submittal of the LA.

APPENDIX A

TECHNICAL BASIS FOR THE WATER-BALANCE PLUG-FLOW MODEL ADEQUATELY REPRESENTING THE NONLINEAR FLOW PROCESSES REPRESENTED BY RICHARDS EQUATION (RESPONSE TO TSPAI 3.18 AIN-1)

This appendix provides a response to the Key Technical Issue (KTI) agreement entitled Total System Performance Assessment and Integration (TSPAI) 3.18 additional information needed (AIN)-1. This agreement relates to providing additional information on the water-balance plug-flow model in the analysis of net infiltration. Net infiltration is defined as the downward water flow (i.e., drainage) below the root zone system.

A.1   KEY TECHNICAL ISSUE AGREEMENT

A.1.1   TSPAI 3.18 AIN-1

Agreement TSPAI 3.18 was reached during the U.S. Nuclear Regulatory Commission (NRC)/U.S. Department of Energy (DOE) Technical Exchange and Management Meeting on TSPAI held August 6 to 10, 2001, in Las Vegas, Nevada. TSPAI KTI subissues 1, 2, 3, and 4 were discussed at the meeting (Reamer 2001).

The wording of the agreement is as follows:

TSPAI 3.18[1]

> Provide a technical basis that the water-balance plug-flow model adequately represents the non-linear flow processes represented by Richard's equation, particularly over the repository where there is thin soil (UZ1.2.1). The DOE will provide a technical basis that the water-balance plug-flow model adequately represents the non-linear flow processes represented by Richard's equation, particularly over the repository where there is thin soil. The technical basis will be documented in an update to the Simulation of Net Infiltration for Modern and Potential Future Climates AMR (ANL-NBS-HS-000032). The AMR is expected to be available to the NRC in FY 2003.

The DOE addressed this and other related KTI agreements in a letter report on January 21, 2003, entitled *KTI Letter Report Response to TSPAI 3.18, 3.21, and 3.23, and TEF 2.13* (Ziegler 2003). The initial response to these agreements used a risk-informed approach, and the response was based on sensitivity studies that showed that the information to be developed in addressing the KTI agreements would not be significant in determining compliance with individual and groundwater protection standards. The NRC reviewed the response and identified three additional risk program elements that would be needed for DOE to make an acceptable case for

---

[1]UZ1.2.1 in this agreement refers to item 2.1 of NRC integrated subissue UZ1 (NRC 2002, Table 1.1-2). This item addresses the NRC concern that there are insufficient data to support the use of a distributed parameter water-balance plug flow approach for net infiltration.

using risk information to address agreement TSPAI 3.18. This resulted in AIN request TSPAI 3.18 AIN-1 (Schlueter 2003a).

The wording of the AIN is summarized as follows (Schlueter 2003a; Schlueter 2003b):

- **Agreement Completion Based on Technical Merit**–Additional technical information is needed to complete agreement TSPAI 3.18 based upon technical merit. Required is either a technical basis showing that the nonlinear flow processes represented by Richards equation have been adequately represented in the current DOE model, or a technical basis demonstrating that a water-balance plug-flow submodel is not underpredicting the net infiltration rate over the repository in comparison with a Richards equation submodel. These information needs apply to DOE sensitivity analyses provided in the response to Agreement TSPAI 3.18.

- **Agreement Completion Based on Low Risk Significance**–The NRC previously relayed to the DOE that additional information is needed when using risk as a basis to complete KTI agreements. The following three additional information needs and clarifications represent risk information elements that need to be addressed when using risk information to address agreements:

  1. Enhanced consideration of the combined effect of uncertainties. The combined effect of uncertainties needs to be evaluated before the individual uncertainties can be dropped from further consideration.

  2. Transparent and traceable documentation that allows the results to be verified independently. The DOE should provide an adequate description of the sensitivity analyses completed.

  3. Information pertaining to the variability in the results. Some measure of how the variability of results changes between the different modeled cases is needed, because only the mean results of the stochastic performance assessment simulations have been presented to date. For example, presentation of the 5th and 95th percentiles of annual dose estimates, in addition to the mean dose estimates, would be a satisfactory way of conveying the variability and uncertainty of performance assessment estimates.

A.1.2   Related Key Technical Issue Agreements

Because the evapotranspiration and lateral flow models are used as submodels in the numerical model for net infiltration predictions and the net infiltration uncertainty analysis, agreement TSPAI 3.18 relates to other agreements discussed in this document. These are KTI agreements TSPAI 3.19 (Appendix B), TSPAI 3.21 (Appendix C), Unsaturated and Saturated Flow under Isothermal Conditions (USFIC) 3.01 (Appendix D), and USFIC 3.02 (Appendix E). Agreements TSPAI 3.23 (which has been closed) and TEF 2.13 are related in that they were previously combined with agreement TSPAI 3.18 in a risk-informed KTI response based on infiltration sensitivity studies (Ziegler 2003). Agreement TEF 2.13 AIN-1 will be addressed separately.

A.2   RELEVANCE TO REPOSITORY PERFORMANCE

KTI agreement TSPAI 3.18 addresses the use of a water-balance plug-flow model to estimate net infiltration rates. The specific issue is whether this model can adequately handle nonlinear flow processes that can be modeled using Richards equation. The NRC has questioned the technical basis for concluding that net infiltration rates will not be underestimated in a model that does not employ the Richards equation representation.

A.3   RESPONSE

This section summarizes the response to KTI agreement TSPAI 3.18, based upon technical merit. This response is based on information available from Yucca Mountain investigations, including the effects of:

- Nonlinear, near-surface processes affecting net infiltration
- Spatial variability on net infiltration and flow in the unsaturated zone
- Heterogeneity of properties of the unsaturated rocks affecting net infiltration.

Simulations of flow through the unsaturated zone at Yucca Mountain, including the determination of net infiltration began in the mid–1980s (Flint, A.L. et al. 2001). The reasons for not using Richards equation then had to do with the lack of parameter values (e.g., for relative permeability and water retention function) and field data for the model calibration at that time.

As an alternative, the watershed-scale, water-balance, plug-flow model with spatially distributed (over the area of watersheds) parameters has been developed for simulations. Consequently, the INFIL numerical code (USGS 2001a) was developed and guided by the results of field observations. The field data collection was performed specifically to support the water-balance model of net infiltration. The model was then calibrated against the results of field observations (e.g., the borehole-measured moisture content and the results of surface runoff measurements (see Appendix C and Sections 4.2 and A.4.3).

Figure A-1 illustrates that net infiltration was determined for the unsaturated zone, using forward simulations with the water-balance model describing flow processes above the bottom of the root zone. The corroborative studies include simulations of percolation in the unsaturated zone below the root system, based on the Richards equation model (BSC 2003a), analysis of borehole temperature measurements (Bodvarsson et al. 2003), chloride (Liu et al. 2003), and calcite (Paces et al. 1996) data, groundwater recharge (Hevesi et al. 2003), neutron logging of moisture content, and environmental tracers based on the age-dating information (USGS 2001b).

The net infiltration flux, calculated from the water balance model, was used as the upper boundary condition to determine the percolation flux within the unsaturated zone using the Richards equation for the present-day, monsoon, and glacial-transition climates (BSC 2003a). Table A-1 summarizes the results of the comparison of water-balance model simulation of net infiltration with those from corroborative experimental investigations and three-dimensional unsaturated zone simulations and reveals agreement among the data (see Sections 4.2 and A.4.4).
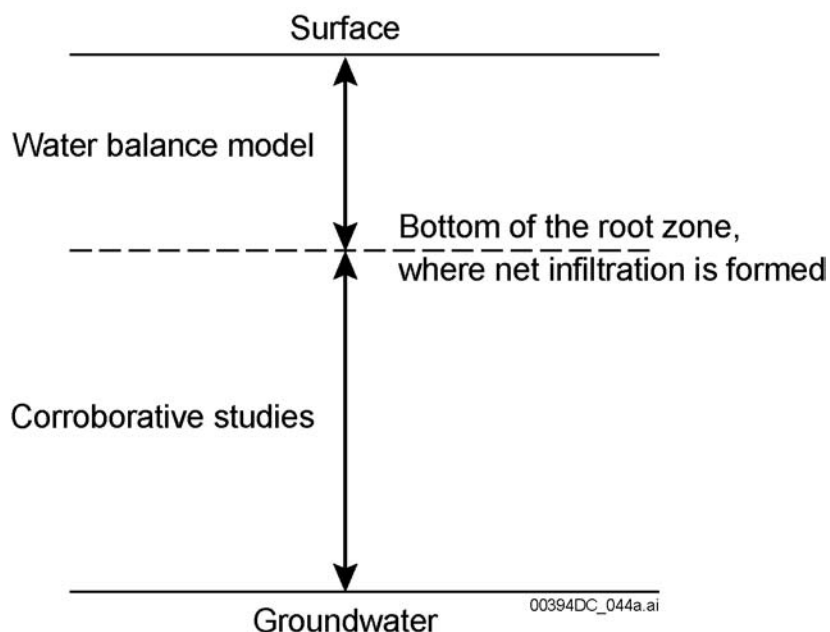
Figure A-1. Schematic Showing Models Used to Determine Net Infiltration above and below the Root Zone

Table A-1. Comparison of the Estimates of Net Infiltration with the Percolation Flux for Present-Day Climatic Conditions, Determined Using Corroborative Experimental Methods and Numerical Modeling Results

Types of Data	Percolation and Infiltration Rates (mm/yr)	Data Source
Temperature measurements in boreholes	0 to 20	Bodvarsson et al. 1999
Chloride in boreholes	0.02 to 5.9	Flint, A.L. et al. 1996
Chloride simulations	0.73 to 10.57	Liu et al. 2003
Calcite data	2 to 20	Xu et al. 2003
Expert evaluation	3.9 to 12.7	CRWMS M&O 1997
Averaged calculated net infiltration for the mean present-day climate state from the water balance model	4.7	USGS 2001b

Because the water-balance model provides reasonable estimations of net infiltration in the shallow subsurface that fit those from multiple corroborative numerical and experimental investigations, there is no need now to initiate simulations of net infiltration in the shallow subsurface using the Richards equation. It is evident that if the Richards equation model applied for the simulation of net infiltration over the Yucca Mountain area, it would have generated reliable estimates of the spatial distribution of net infiltration, comparable to those used as an upper boundary condition in *UZ Flow Models and Submodels* (BSC 2003a; Liu et al. 2003).

The information in this report is responsive to agreement TSPAI 3.18 and the associated AIN (AIN-1). The report contains the information that the DOE considers necessary for NRC to review for closure of this agreement.

A.4 BASIS FOR THE RESPONSE

A.4.1 Introduction

The Richards equation model and the water-balance, water-plug model represent two conceptual approaches that may offer the practical capability for predicting large-scale flow and transport behavior in systems that are dominated by spatially localized flow processes (Pruess et al. 1999). The Richards equation model belongs to a class of detailed process models that describe flows in terms of physical mechanisms (cause and effect relationships) on the scale for which the parameters of this model are determined. The water-balance model relates to a class of phenomenological models that do not require a detailed description of flow media and relevant physical processes. Instead, they directly assess volume- and time-averaged net infiltration, which are based on the volume- and time-averaged water-balance equations.

Three main arguments provide the basis for the response to agreement TSPAI 3.18 regarding a technical basis for the water-balance plug-flow model adequately representing the flow processes, particularly over the repository where there is thin soil: (1) the use of a phenomenological water-balance model is consistent with the type of data available and the intended use of the results of calculations of net infiltration; (2) the parameters of the water-balance model were calibrated using the results of field observations; and (3) the results of predictions were validated using the independent field measurements and modeling investigations.

A.4.2 Water-Balance Equation

Because of the complexity of processes controlling net infiltration (Section 3) and the regional scale of simulation for the Yucca Mountain area, the evaluation of net infiltration is based on a water-balance approach that requires measurements and lumped (distributed) estimates of watershed-scale (or basin-wide averaged over a watershed) precipitation, snowpack depth and density, stream discharge, and evapotranspiration (Lichty and McKinley 1995, pp. 4 to 10; Flint, A.L. et al. 1996). The water-balance model is based on the principle of conservation of mass for water over some arbitrary time interval (e.g., day or year) and volume (area and depth) of the soil. For a watershed area with a depth interval from the surface to the bottom of the root zone (Flint, A.L. et al. 1996, pp. 9 to 11), the water-balance equation is given by (USGS 2001b):

$$P+A+U+W_s+S_s+B_s+L_i+R_{on}-R_{off}-I-E-T-L_o-E_x=0 \qquad \text{(Eq. A-1)}$$

where P is precipitation, A is applied water (human induced), U is upward flow, W_s is the change in soil-water storage, S_s is the change is surface-water storage, B_s is change in biomass water storage, L_i is lateral inflow, R_{on} is surface runon, R_{off} is surface runoff, I is net infiltration (drainage or percolation), E is evaporation, T is transpiration, L_o is lateral outflow, and E_x is water extraction (human induced).

For a simplified conceptual model of flow in the near-surface zone at Yucca Mountain, schematically shown in Figure A-2, taking into account the runon, runoff, and evapotranspiration (ET) (which is the sum of E and T), and neglecting other terms of Equation A-1, net infiltration (I) can be determined by (USGS 2001b):

$$I = P - SF + IR_{on} + SM + SW - SB - ET - R_{off} \qquad \text{(Eq. A-2)}$$

where I is net infiltration, P is precipitation, SF is snowfall, SB is sublimation, SM is snowmelt, SW is change in water-content storage within the root zone, ET is evapotranspiration, IR_{on} is infiltrated surface-water runon, and R_{off} is surface-water runoff generated by excess precipitation, snowmelt, or runon.
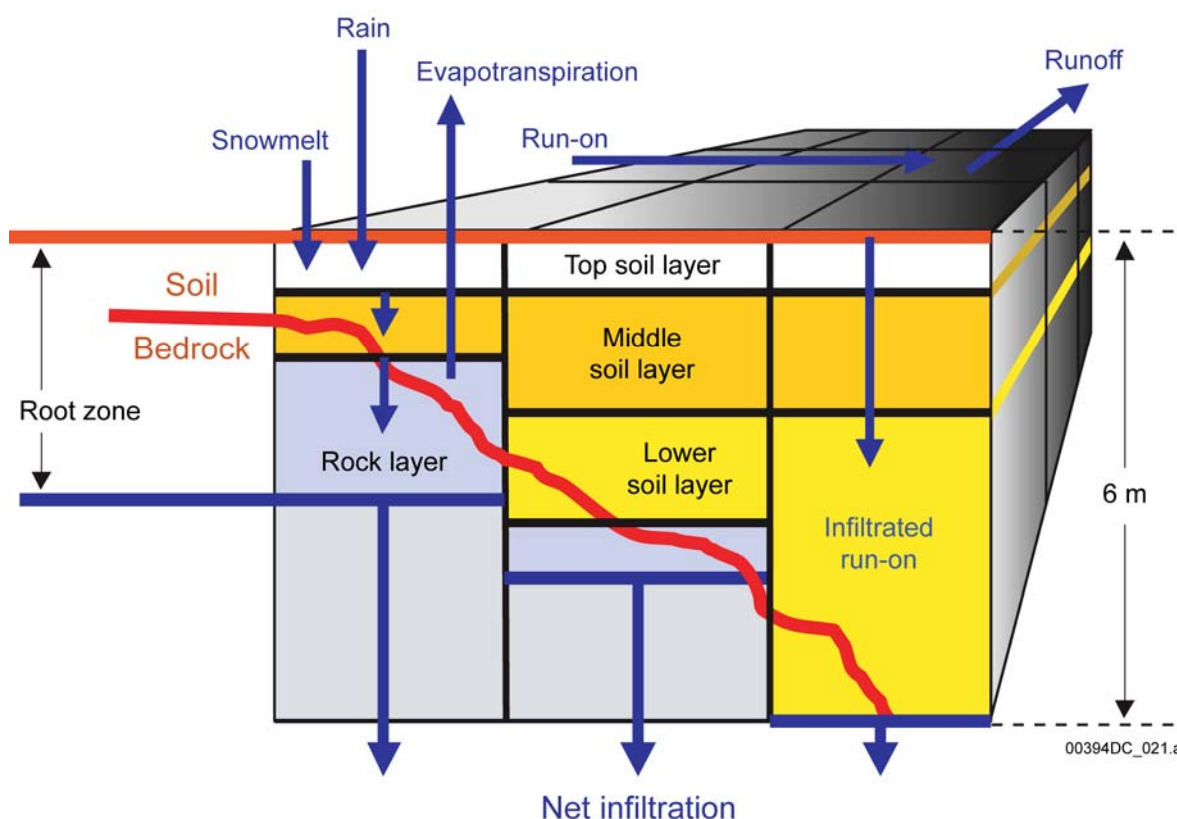
Source: Hevesi et al 2003.

NOTE: Downward arrows, indicating net infiltration, are depicted coming from the bottom of the root zone, shown by horizontal lines. The depth of the root zone increases as the soil–bedrock interface deepens.

Figure A-2. Conceptual Model of Net Infiltration Illustrating the Layered Root-Zone Water-Balance Model of the Death Valley Region, Nevada and California

Figure A-2 depicts a schematic of the vertical profile discretization used for calculations of net infiltration. The left column of Figure A-2 schematically illustrates that for a shallow soil–bedrock interface, the bottom of the root zone extends into the bedrock (the propagation of the root zone into the bedrock was calculated by the USGS (2001b, Equation 17)), and the soil layer is divided into two sublayers (used for calculations of infiltration and evapotranspiration, see the discussion below on the bucket type model). The middle column of Figure A-2 indicates that as the depth to the soil–rock interface increases, the propagation of the root zone into the bedrock

decreases, and the soil layer is divided into three sublayers. The right column of Figure A-2 illustrates that net infiltration is formed at the depth of 6 m, within the soil unit, if the bedrock unit is below the 6 m depth.

The water-balance model used for predictions of net infiltration over the Yucca Mountain area is a phenomenological distributed-type model treating the volume- and time-averaged flow processes for each of the watersheds of the modeling domain. This model also incorporates the concepts of piston-type flow, a multilayer bucket model, and field capacity. For a discussion of the features and uncertainties related to the application of these concepts, see *Simulation of Net Infiltration for Modern and Potential Future Climates* (USGS 2001b, Attachment IV) and Section 4.1.1 of this technical basis document.

A.4.3 Model Calibration

The results of field and modeling investigations over the Yucca Mountain region (USGS 2001b; BSC 2003b, Section 3.2.2) show that the net infiltration rate varies greatly in space and time, depending on storm amplitudes, durations, and frequencies. The model adequately represents the areas with a thin soil layer, which is one of the points of concern of this KTI agreement. For example, as the soil thickness decreases and bedrock crops out, the model adequately reflects that net infiltration increases because fast preferential flow through rock fractures exceeds the depth of evapotranspiration (Flint, L.E. and Flint 1995). Spatial and temporal variation in net infiltration at Yucca Mountain is caused by episodic storm and precipitation events, which occur only every few years (USGS 2001b; Hevesi et al. 2002), as well as the heterogeneous nature of a topsoil layer and topography. In very wet years, infiltration increases to hundreds of millimeters per year during a relatively short time.

Model calibration was based on the comparison of the results of water-balance modeling with those from streamflow measurements that were collected at selected monitoring sites (Flint, A.L. et al. 1996; USGS 2001b). The INFIL model was calibrated using comparisons of simulated streamflow with historical streamflow data from 31 gauging stations in the Death Valley region, and simulated 50-year (1950 to 1999) basinwide average net infiltration with previous estimates of basinwide average recharge for 42 basin areas (defined in previous studies as hydrographic areas and subareas) in the Death Valley region. Model calibration included adjusting the following parameters: bedrock saturated hydraulic conductivity, root density, average storm duration (for summer and winter storms), and soil saturated hydraulic conductivity and wetted area (used to represent stream-channel characteristics).

Data sets used for model calibration are soil hydrologic properties, bedrock hydrologic properties, vertical water-content profiles in soils and bedrock, and meteorological data (Flint, L.E. et al. 1996; Flint, A.L. et al. 1996; USGS 2001b, Table 4-1).

The infiltration model for Yucca Mountain was calibrated using water-content profiles obtained by geophysical logging a network of up to 98 boreholes with neutron-moisture probes at monthly or weekly intervals during 1984 through 1995. The variation of water content over time indicated the importance of thin soils, saturated fracture flow, events of heavy precipitation (or snowmelt), and surface water run-on. For example, the water content versus depth profile measured at borehole USW UZ-N15 (USGS 2001b, Figure 6-4) indicates the occurrence of three major episodes of net infiltration through bedrock in response to wetter than average conditions

during the winters of 1992-1993 and 1994-1995 (Figure 3-8). The USW UZ-N15 site is at a ridge top location in the headwater part of the upper Pagany Wash channel, has relatively thin soils, and based on field observations, received surface-water run-on during the winters of 1992-1993 and 1994-1995. Measurements of water potential using heat dissipation probes at the soil–bedrock contact at a nearby site (USGS 2001b, Figure 6-6) provide evidence that, in exceptionally wet years, infiltration in major drainage areas can increase over a relatively short time. Concentrated flow over short times has the potential to cause rapid fracture flow through welded tuff.

Figure A-3 shows the average net-infiltration rates calculated using changes in measured water-content profiles for the period 1989 to 1995 from a network of monitoring boreholes, compared to depth of alluvium at each borehole. This figure shows the increased net infiltration within topography channels, at ridge tops, and at side slopes.
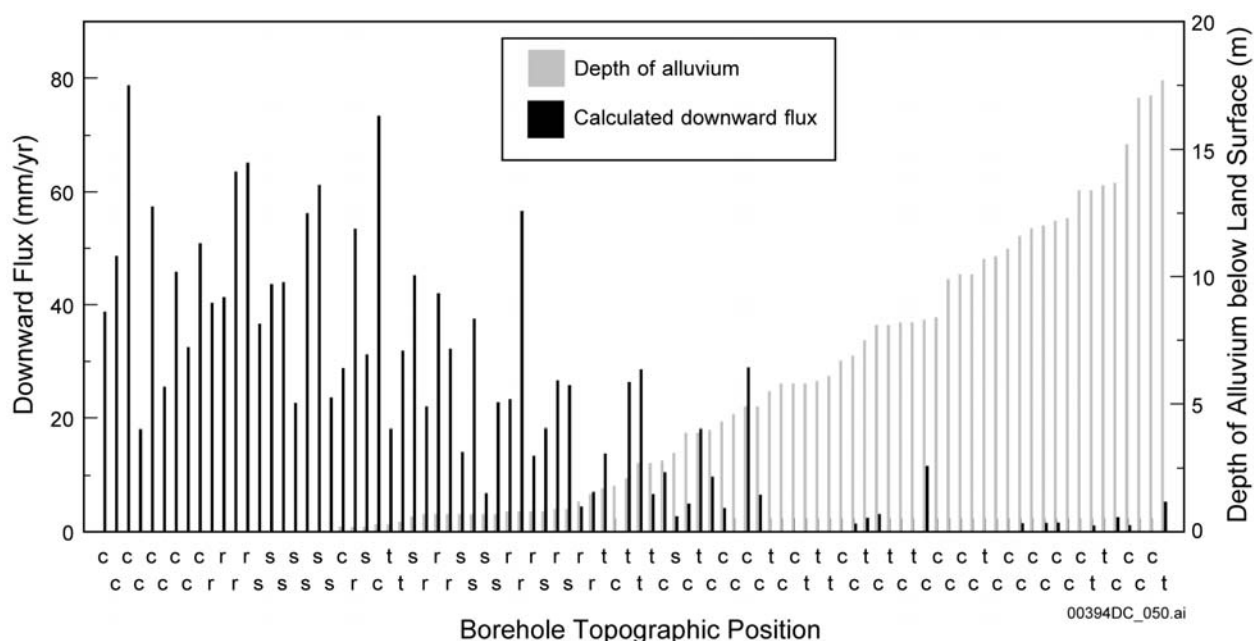
Source: USGS 2001b, Figure 6-5.

NOTE: c = channel; t = terrace; s = side slope; r = ridge top.

Figure A-3. Estimated Average Net Infiltration Rates Calculated Using Changes in Measured Water-Content Profiles Obtained for the Period 1989 to 1995 from a Network of Monitoring Boreholes, Compared to Depth of Alluvium at each Borehole

To confirm that drilling neutron-probe boreholes in the fractured tuffs at Yucca Mountain did not introduce additional fractures or enhanced flow through the existing fracture network, an independent estimate of net infiltration was developed using 1 year of water-potential measurements from heat-dissipation probes near borehole USW UZ-N15. The probes were installed laterally from a small trench that was backfilled. Measurements were made at four depths: 7.0, 15.0, 36.5, and 73.7 cm (the soil–bedrock interface). By early March 1995, within 2 weeks of installation, winter precipitation saturated the soil from the soil–bedrock interface to within 36 cm of the soil surface, and heat-dissipation probes at both 36.5 and 73.7 cm were saturated. The probe at the soil–bedrock interface (73.7 cm) remained saturated until the end of March 1995 and then dried out to less than −10 bars by September 1995. The

probes closer to the surface dried out faster, and the near-surface probes became wetter periodically due to summer precipitation events.

Model calibration using INFIL V2.0 was conducted using streamflow records from five gauging sites on Yucca Mountain that were operational from 1994 through 1995 and included two significant storm events measured during the winter of 1994-1995 (USGS 2001b, Section 6.8).

The wording of TSPAI 3.18 also presents a concern about simulations over the area with thin soils. To address the effect of the soil depth, simulations of net infiltration by means of the stochastic form of the water-balance model (BSC 2003c) included a large range of variations in the soil thickness—a soil depth multiplier SOILDEPM varied from 0.1 to 1.9 with an averaged value of 1 and normal distribution (BSC 2003c). The results of simulations, which are summarized in Appendix E, which also provides ranges of uncertain input parameters, based on *Analysis of Infiltration Uncertainty* (BSC 2003c), show that soil thickness presents the second most important input parameter affecting net infiltration: the correlation coefficient between the soil thickness and net infiltration is –0.493. Three other important parameters affecting net infiltration are precipitation (correlation coefficient is 0.638), potential evapotranspiration (correlation coefficient is –0.341), and bedrock saturated hydraulic conductivity (correlation coefficient is 0.236).

A.4.4   Model Validation

Validation Methods–It is important to provide a validation of net infiltration predictions using the results of different (physically independent) methods. Flint, A.L. et al. (2002) provided a model validation based on the comparison of net infiltration predictions using the water-balance model with those obtained using other experimental methods and numerical calculations, such as:

- Darcian approach using heat and moisture migration equations
- Neutron logging of moisture content
- Recharge estimations using empirical methods
- Environmental tracers based on the age-dating information
- Borehole temperature profiles
- Percolation simulations.

Despite a number of abstractions, the net infiltration rates obtained from numerical simulations using the water-balance model compare reasonably well with those from corroborative experimental and modeling studies (Table A-1), which provides confidence in the results of modeling for the present-day climate conditions.

Validation Using Groundwater Recharge Data–The spatially averaged net-infiltration rates for the nine climate scenarios were compared against estimates of groundwater recharge obtained using independent studies at various locations in the southern Basin and Range Province (Maxey and Eakin 1950; Winograd 1981; Lichty and McKinley 1995; Harrill and Prudic 1998; Dettinger 1989) and are summarized in Section 4.2.2. Hevesi et al. (2003) conducted numerical modeling of net infiltration for the present-day climatic conditions over the area of the Death Valley region

in Nevada and California using four types of models. Hevesi et al. (2003, pp. 96 to 99, Tables 22 and 23) provided a statistical analysis of the results of modeling to compare simulated basinwide average net infiltration and recharge rates to simulated total basinwide net infiltration and recharge volumes. They determined that the simulated net-infiltration volumes are in good agreement with the estimated recharge volumes, and the best fit of simulated and observed data corresponds to the net infiltration model that accounts for streamflow coupled to the root-zone component; this approach was used in the INFIL model for the determination of net infiltration.

Validation Using Chloride Data–The results of simulation of net infiltration for the present-day conditions can be compared with those from calculations based on pore-water chloride data (Liu et al. 2003). To assess the net infiltration distribution, the modeled area was divided into nine regions, according to the available chloride data, as well as hydrogeologic and hydrostructural features. The spatially averaged infiltration flux for each region was calculated from

$$f_w = f_{cl} \left(10^3 \rho / C_{cl} - 1 \right) \qquad \text{(Eq. A-3)}$$

where f_{cl} (in kilograms per second) is the total chloride infiltration flux of the region, C_{cl} (in milligrams per liter) is the average chloride concentration of the region from the chloride data, and ρ (in kilograms per cubic meter) is the aqueous-phase density.

Figure A-4 shows the map of calculated infiltration rates for nine regions from Liu et al. (2003, Figure 4), which is superimposed onto the present-day mean infiltration map simulation from the water-balance model (USGS 2001b). Table A-2 compares the spatially averaged infiltration rates from the water-balance model simulations (USGS 2001b) with those from the chloride data simulations (Liu et al. 2003). The reasonable comparison of area averaged net infiltration rates illustrated in Table A-2 supports the validity of water-balance model calculations of net infiltration.

Table A-2. Averaged Net Infiltration Rates from Water Balance and Chloride Data Simulations

Region	Averaged Net Infiltration (mm/yr)	
	From Water-Balance Simulations	From Chloride Data Simulations
I	10.57	10.57
II	2.31	2.31
III	7.1	7.12
IV	2.43	2.32
V	2.71	3.05
VI	1.14	1.83
VII	1.88	1.88
VIII	0.73	0.73
IX	1.07	1.59
Area averaged	4.58	4.71

Source: Liu et al. 2003, Table 1.

NOTE: Rates are equal to those from the water-balance model estimates because chloride data are not available for Regions I, II, and VIII. Data by region are shown in Figure A-4.
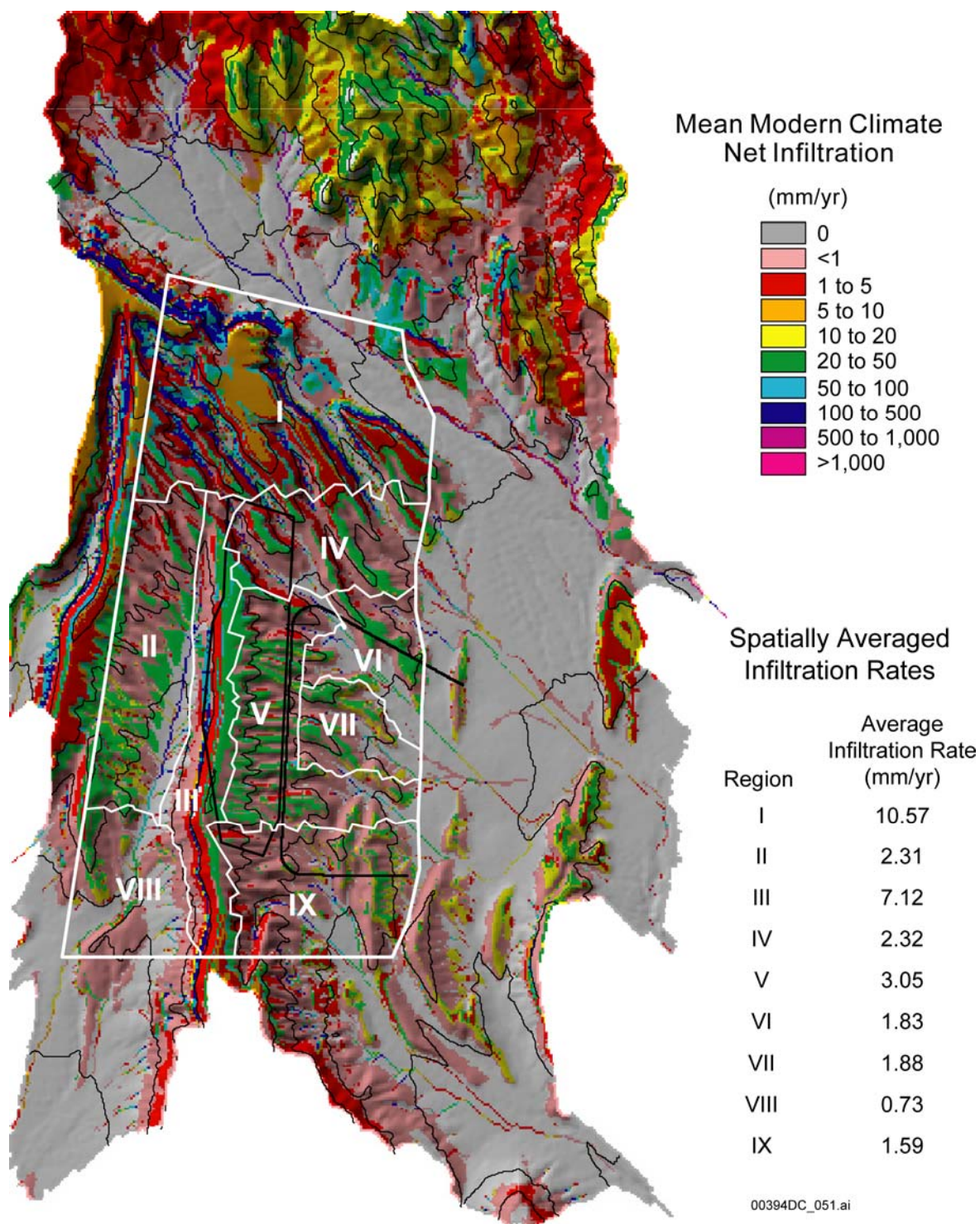
Source: Map of calculated infiltration rates from Liu et al. (2003, Figure 4, Table 1); present-day mean infiltration map from the USGS (2001b, Figure 6-26).

Figure A-4. Map of Calculated Infiltration Rates for Nine Regions Superimposed onto the Present-Day Mean Infiltration Map

Model Expert Elicitation Project–The averaged net infiltration rate of 4.7 mm/yr for the present-day mean climate scenario, obtained from the water-balance model calculations performed by the USGS (2001b) agree reasonably well with the estimated range of mean net infiltration from 3.9 to 12.7 mm/yr, obtained within the scope of the independent *Unsaturated Zone Flow Model Expert Elicitation Project* (CRWMS M&O 1997).

Validation Using Comparison with Modeling Percolation in the Unsaturated Zone–The three-dimensional unsaturated flow model (BSC 2003a) was used for simulations of percolation in the unsaturated zone for the mean, lower-bound, and upper-bound present-day, monsoon, and glacial-transition climates. In these simulations, the net infiltration rates that were estimated in *Simulation of Net Infiltration for Modern and Potential Future Climates* (USGS 2001b) for all nine climate state scenarios were used as upper boundary conditions.

The three-dimensional unsaturated flow model is based on using the calibrated soils and rock properties (BSC 2003d; BSC 2003a). The results of modeling were validated using mountain-scale ambient temperature measurements, gas pressure, chloride, calcite, and strontium data. These data were used to constrain infiltration and percolation flux. The field data (matrix liquid saturations, water potentials, and perched-water elevations) were collected from nine boreholes (USW NRG-7a, USW SD-6, USW SD-7, USW SD-9, UE-25 SD-12, USW UZ-14, UE-25 UZ#16, USW WT-24, and USW G-2) (BSC 2003a, Figure 6.1-1, Table 6.2-1). The water-potential data were also measured from the Enhanced Characterization of the Repository Block tunnel (BSC 2002). Perched-water elevations measured in borehole USW WT-24 and pneumatic data measured in boreholes UE-25 SD-12 and UE-25 UZ#7a were used to validate the unsaturated zone model.

Matching the ambient temperature distribution within the unsaturated zone from field measurements and modeling is important to constrain the percolation flux and infiltration rate (Bodvarsson et al. 2003). Temperature data measured in boreholes USW H-5, USW H-4, and UE-25 WT#18 were used to validate the ambient thermal model. The validation criterion was based on matching the observed values with less than 3°C difference (BSC 2002, Attachment I-1-2-2).

The importance of using chloride data rests on the fact that chloride is present in precipitation, run-on, and runoff waters. The criterion used for validation is that the range of the simulated chloride concentration falls within the range of measured concentrations in the Exploratory Studies Facility (BSC 2002, Attachment I-1-2-3).

The calcite model is validated by comparing one-dimensional simulation results with the results of field measurements. The validation criterion is that the simulated volume fraction of calcite coating for each unsaturated zone model layer fall within the range of measurements for that layer (BSC 2002, Attachment I-1-2-4).

^{14}C data from gas samples provide approximate ^{14}C residence time for pore water in the unsaturated zone. The residence time can be interpreted as the tracer transport time from the ground surface to a depth where the gas sample was collected.

Borehole and Enhanced Characterization of the Repository Block strontium concentrations are used to check the unsaturated zone model strontium modeling results. The criterion for validation is a qualitative agreement between the simulated strontium concentrations and the average of the observations at the same elevation, and agreement with the vertical trends (BSC 2002, Attachment I-1-2-5).

Comparison of the calculated percolation flux through the TSw hydrogeologic unit within the repository footprint (BSC 2003a, Figure 6.6-22, lower panel) with the net infiltration rate (BSC 2003c) shows the ranges of these values are the same.

As an illustration of a close agreement between simulated data from three-dimensional modeling with those determined from field measurements, Figure A-5 shows a reasonable comparison of distributions of saturation and water potentials with depth for borehole USW SD-12.
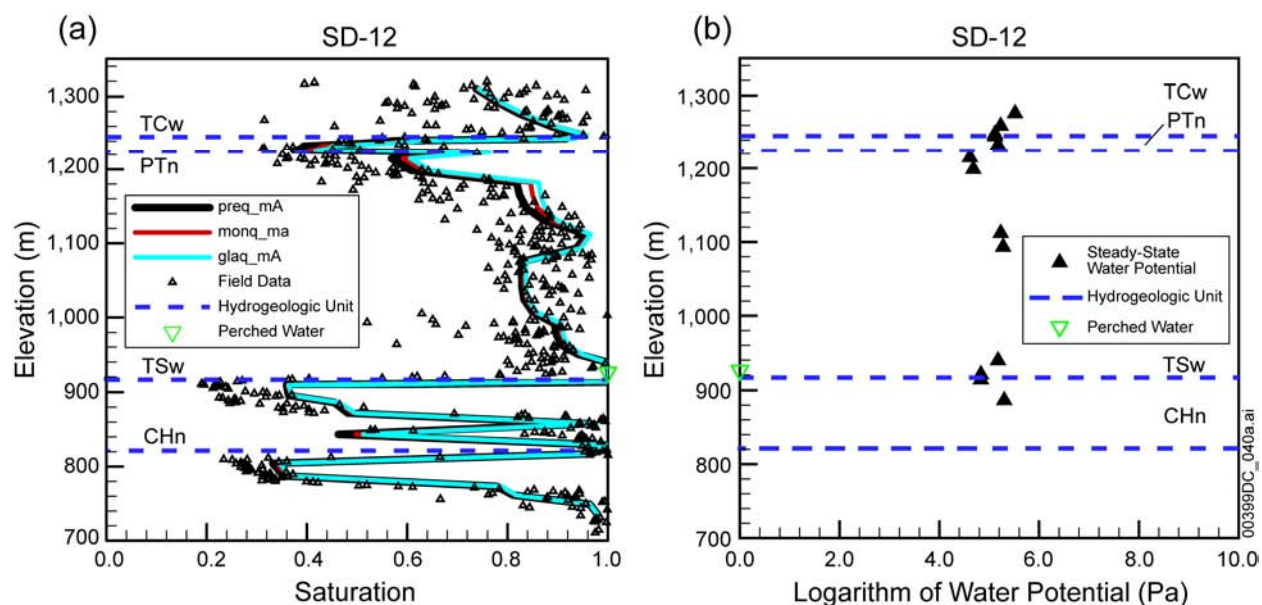
Source: BSC 2003a, Figure 6.8-1.

NOTE: AFP = active fracture parameter.

Figure A-5. Comparison of (a) Simulated Matrix Liquid Saturation and (b) Water Potential with Depth, Using Calibrated Hydraulic Properties with That Obtained Using Modeling for Borehole USW SD-6

Thus, the results of three-dimensional numerical modeling of flow and transport in the unsaturated zone closely agree with the types of data obtained from field measurements in the unsaturated zone (temperature, gas pressure, chloride and calcite concentrations, saturation, water potential, and perched water levels). These agreements confirm the validity of the upper boundary conditions used for modeling, which are obtained from the water-balance calculations of net infiltration rate.

A.4.5 Conclusions

The net infiltration rates obtained from numerical simulations using the water-balance model compare reasonably well with the range of estimated net infiltration rates from corroborative experimental and modeling studies (geochemical and temperature measurements in the unsaturated zone, as well as percolation rate and groundwater recharge) characterizing present-day climate conditions. Thus, multiple lines of evidence from model validation confirm that the water-balance model adequately represents the conceptual model of infiltration in the near-surface zone, spatial variability, and uncertainty of input parameters, and TSPAI 3.18 AIN-1 can be closed.

A.5 REFERENCES

Bodvarsson, G.S.; Boyle, W.; Patterson, R.; and Williams, D. 1999. "Overview of Scientific Investigations at Yucca Mountain—The Potential Repository for High-Level Nuclear Waste." *Journal of Contaminant Hydrology, 38,* (1–3), 3–24. New York, New York: Elsevier. TIC: 244160.

Bodvarsson, G.S.; Kwicklis, E.; Shan, C.; and Wu, Y.S. 2003. "Estimation of Percolation Flux from Borehole Temperature Data at Yucca Mountain, Nevada." *Journal of Contaminant Hydrology, 62–63,* 3–22. New York, New York: Elsevier. TIC: 254205.

BSC (Bechtel SAIC Company) 2002. *Technical Work Plan for: Performance Assessment Unsaturated Zone.* TWP-NBS-HS-000003 REV 02. Las Vegas, Nevada: Bechtel SAIC Company. ACC: MOL.20030102.0108.

BSC 2003a. *UZ Flow Models and Submodels.* MDL-NBS-HS-000006 REV 01. Las Vegas, Nevada: Bechtel SAIC Company. ACC: DOC.20030818.0002.

BSC 2003b. *In Situ Field Testing of Processes.* ANL-NBS-HS-000005 REV 02. Las Vegas, Nevada: Bechtel SAIC Company. ACC: DOC.20031208.0001.

BSC 2003c. *Analysis of Infiltration Uncertainty.* ANL-NBS-HS-000027 REV 01. Las Vegas, Nevada: Bechtel SAIC Company. ACC: DOC.20031030.0003.

BSC 2003d. *Calibrated Properties Model.* MDL-NBS-HS-000003 REV 01. Las Vegas, Nevada: Bechtel SAIC Company. ACC: DOC.20030219.0001.

CRWMS M&O (Civilian Radioactive Waste Management System Management and Operating Contractor) 1997. *Unsaturated Zone Flow Model Expert Elicitation Project.* Las Vegas, Nevada: CRWMS M&O. ACC: MOL.19971009.0582.

Dettinger, M.D. 1989. "Reconnaissance Estimates of Natural Recharge to Desert Basins in Nevada, U.S.A., by Using Chloride-Balance Calculations." *Journal of Hydrology, 106,* 55–78. Amsterdam, The Netherlands: Elsevier. TIC: 236967.

Flint, A.L.; Flint, L.E.; Bodvarsson, G.S.; Kwicklis, E.M.; and Fabryka-Martin, J. 2001. "Evolution of the Conceptual Model of Unsaturated Zone Hydrology at Yucca Mountain, Nevada." *Journal of Hydrology, 247,* ([1–2]), 1–30. New York, New York: Elsevier. TIC: 250932.

Flint, A.L.; Flint, L.E.; Kwicklis, E.M.; Fabryka-Martin, J.T.; and Bodvarsson, G.S. 2002. "Estimating Recharge at Yucca Mountain, Nevada, USA: Comparison of Methods." *Hydrogeology Journal, 10,* (1), 180–240. Berlin, Germany: Springer-Verlag. TIC: 251765.

Flint, A.L.; Hevesi, J.A.; and Flint, L.E. 1996. *Conceptual and Numerical Model of Infiltration for the Yucca Mountain Area, Nevada.* Milestone 3GUI623M. Denver, Colorado: U.S. Geological Survey. ACC: MOL.19970409.0087.

Flint, L.E. and Flint, A.L. 1995. *Shallow Infiltration Processes at Yucca Mountain, Nevada— Neutron Logging Data 1984-93.* Water-Resources Investigations Report 95-4035. Denver, Colorado: U.S. Geological Survey. ACC: MOL.19960924.0577.

Flint, L.E.; Flint, A.L.; Rautman, C.A.; and Istok, J.D. 1996. *Physical and Hydrologic Properties of Rock Outcrop Samples at Yucca Mountain, Nevada.* Open-File Report 95-280. Denver, Colorado: U.S. Geological Survey. ACC: MOL.19970224.0225.

Harrill, J.R. and Prudic, D.E. 1998. *Aquifer Systems in the Great Basin Region of Nevada, Utah, and Adjacent States - Summary Report.* Professional Paper 1409-A. Denver, Colorado: U.S. Geological Survey. TIC: 247432.

Hevesi, J.A.; Flint, A.L.; and Flint, L.E. 2002. *Preliminary Estimates of Spatially Distributed Net Infiltration and Recharge for the Death Valley Region, Nevada–California.* Water- Resources Investigations Report 02-4010. Sacramento, California: U.S. Geological Survey. TIC: 253392.

Hevesi, J.A.; Flint, A.L.; and Flint, L.E. 2003. *Simulation of Net Infiltration and Potential Recharge Using a Distributed-Parameter Watershed Model of the Death Valley Region, Nevada and California.* Water-Resources Investigations Report 03-4090. Sacramento, California: U.S. Geological Survey. TIC: 255193.

Lichty, R.W. and McKinley, P.W. 1995. *Estimates of Ground-Water Recharge Rates for Two Small Basins in Central Nevada.* Water-Resources Investigations Report 94-4104. Denver, Colorado: U.S. Geological Survey. ACC: MOL.19960924.0524.

Liu, J.; Sonnenthal, E.L.; and Bodvarsson, G.S. 2003. "Calibration of Yucca Mountain Unsaturated Zone Flow and Transport Model Using Porewater Chloride Data." *Journal of Contaminant Hydrology, 62–63,* 213–235. New York, New York: Elsevier. TIC: 254205.

Maxey, G.B. and Eakin, T.E. 1950. *Ground Water in White River Valley, White Pine, Nye, and Lincoln Counties, Nevada.* Water Resources Bulletin No. 8. Carson City, Nevada: State of Nevada, Office of the State Engineer. TIC: 216819.

NRC (U.S. Nuclear Regulatory Commission) 2002. *Integrated Issue Resolution Status Report.* NUREG-1762. Washington, D.C.: U.S. Nuclear Regulatory Commission, Office of Nuclear Material Safety and Safeguards. TIC: 253064.

Paces, J.B.; Neymark, L.A.; Marshall, B.D.; Whelan, J.F.; and Peterman, Z.E. 1996. *Letter Report: Ages and Origins of Subsurface Secondary Minerals in the Exploratory Studies Facility (ESF).* Milestone 3GQH450M, Results of Sampling and Age Determination. Las Vegas, Nevada: U.S. Geological Survey. ACC: MOL.19970324.0052.

Pruess, K.; Faybishenko, B.; and Bodvarsson, G.S. 1999. "Alternative Concepts and Approaches for Modeling Flow and Transport in Thick Unsaturated Zones of Fractured Rocks." *Journal of Contaminant Hydrology, 38,* (1–3), 281–322. New York, New York: Elsevier. TIC: 244160.

Reamer, C.W. 2001. "U.S. Nuclear Regulatory Commission/U.S. Department of Energy Technical Exchange and Management Meeting on Total System Performance Assessment and Integration (August 6 through 10, 2001)." Letter from C.W. Reamer (NRC) to S. Brocoum (DOE/YMSCO), August 23, 2001, with enclosure. ACC: MOL.20011029.0281.

Schlueter, J. 2003a. "Review of Documents Pertaining to Agreement Total System Performance Assessment and Integration (TSPAI).3.18 (Status: Need Additional Information)." Letter J. R. Schlueter (NRC) to J.D. Ziegler (DOE/YMSCO), April 30, 2003, with enclosure. ACC: MOL.20030529.0329.

Schlueter, J. 2003b. "Use of Risk as a Basis for Closure of Key Technical Issue Agreements." Letter from J. Schlueter (NRC) to J.D. Ziegler (DOE/YMSCO), January 27, 2003, 0131035890, with enclosure. ACC: MOL.20030227.0018.

USGS (U.S. Geological Survey) 2001a. Software Code: INFIL. V2.0. PC. 10307-2.0-00.

USGS 2001b. *Simulation of Net Infiltration for Modern and Potential Future Climates.* ANL-NBS-HS-000032 REV 00 ICN 02. Denver, Colorado: U.S. Geological Survey. ACC: MOL.20011119.0334.

Winograd, I.J. 1981. "Radioactive Waste Disposal in Thick Unsaturated Zones." *Science, 212,* (4502), 1,457–1,464. Washington, D.C.: American Association for the Advancement of Science. TIC: 217258.

Xu, T.; Sonnenthal, E.; and Bodvarsson, G. 2003. "A Reaction-Transport Model for Calcite Precipitation and Evaluation of Infiltration Fluxes in Unsaturated Fractured Rock." *Journal of Contaminant Hydrology, 64,* (1–2), 113–127. New York, New York: Elsevier. TIC: 254008.

Ziegler, J.D. 2003. "Transmittal of Report Addressing Key Technical Issue (KTI) Agreement Items Total System Performance Assessment and Integration (TSPAI) 3.18, 3.21, and 3.23 and Thermal Effects on Flow (TEF) 2.13", Letter from J.D. Ziegler (DOE) to J.R. Schlueter (NRC), January 21, 2003, with enclosure. ACC: MOL.20030605.0224.

APPENDIX B

**JUSTIFICATION FOR THE EVAPOTRANSPIRATION MODEL
AND ANALOG TEMPERATURE SITE SELECTION
(RESPONSE TO TSPAI 3.19 AIN-1)**

Note Regarding the Status of Supporting Technical Information

This document was prepared using the most current information available at the time of its development. This Technical Basis Document and its appendices providing Key Technical Issue Agreement responses that were prepared using preliminary or draft information reflect the status of the Yucca Mountain Project's scientific and design bases at the time of submittal. In some cases this involved the use of draft Analysis and Model Reports (AMRs) and other draft references whose contents may change with time. Information that evolves through subsequent revisions of the AMRs and other references will be reflected in the License Application (LA) as the approved analyses of record at the time of LA submittal. Consequently, the Project will not routinely update either this Technical Basis Document or its Key Technical Issue Agreement appendices to reflect changes in the supporting references prior to submittal of the LA.

APPENDIX B

JUSTIFICATION FOR THE EVAPOTRANSPIRATION MODEL
AND ANALOG TEMPERATURE SITE SELECTION
(RESPONSE TO TSPAI 3.19 AIN-1)

This appendix provides a response to Key Technical Issue (KTI) agreement Total System Performance Assessment and Integration (TSPAI) 3.19 additional information needed (AIN)-1. This agreement relates to providing additional information on and the technical basis for the use of the evapotranspiration model and analog site temperature data used to predict net infiltration at the site.

B.1   KEY TECHNICAL ISSUE AGREEMENT

B.1.1   TSPAI 3.19

During a series of technical exchanges, the U.S. Nuclear Regulatory Commission (NRC) questioned whether the upper bounds of the U.S. Department of Energy (DOE) net infiltration model were representative of the monsoon, modern, and glacial-transition climates. These concerns were initially discussed during the NRC/DOE Technical Exchange and Management Meeting on Unsaturated and Saturated Flow under Isothermal Conditions (USFIC) held August 16 and 17, 2000, in Berkeley, California (Reamer and Williams 2000a), and the USFIC NRC/DOE Technical Exchange and Management Meeting held October 31 to November 2, 2000, in Albuquerque, New Mexico (Reamer and Williams 2000b). Detailed technical issues were then formulated in writing for TSPAI 3.19, and a cooperative agreement to resolve these issues was reached between the NRC and DOE during the Technical Exchange and Management Meeting on TSPAI held August 6 to 10, 2001, in Las Vegas, Nevada (Reamer 2001). During this meeting, the NRC questioned the use of the evapotranspiration submodel and the adequacy of the analog site temperature data in predicting net infiltration conditions during future climates. The agreement related specifically to evapotranspiration and analog site temperature data (Reamer 2001).

The wording of the agreement is as follows:

TSPAI 3.19[1]

> DOE will provide justification for the use of its evapotranspiration model, and defend the use of the analog site temperature data (UZ1.3.1). DOE will provide justification for the use of the evapotranspiration model, and justify the use of the analog site temperature data. The justification will be documented in an update to the Simulation of Net Infiltration for Modern and Potential Future Climates AMR (ANL-NBS-HS-000032) and the Future Climate Analysis AMR (ANL-NBS-GS-000008). The AMRs are expected to be available to NRC in FY 2003.

---

[1]UZ1.3.1 in this agreement refers to item 3.1 of NRC integrated subissue UZ1 (NRC 2002, Table 1.1-2). This item addresses the NRC concern that the evapotranspiration model adequately represents conditions during future climates at Yucca Mountain.

The DOE performed an initial sensitivity study to provide insight into the role of the net infiltration model in the assessment of postclosure repository performance as a resolution to TSPAI 3.19. The response to TSPAI 3.19 was addressed in a DOE letter report of July 11, 2002, *Response to USFIC 3.01 and TSPAI 3.19* (Ziegler 2002). The study examined the impact of assuming an extreme infiltration flux corresponding to the highest infiltration of the glacial maximum climate. The sensitivity study showed no significant difference between the results of the base case infiltration model and the results for the extreme infiltration model, suggesting that the degree of waste isolation provided by the repository system is not sensitive to the details of the net infiltration model.

In its review of the DOE response to TSPAI 3.19, the NRC indicated that it had a policy encouraging the use of risk assessments and sensitivity analyses to help identify data, models, and barriers that are most important to repository performance (Schlueter 2003). The NRC felt that the DOE could successfully address the agreements using risk information but that the arguments presented by Ziegler (2002) and in *Risk Information to Support Prioritization of Performance Assessment Models* (BSC 2002) were incomplete. The NRC identified three additional risk program elements that are needed for the DOE to make an acceptable case for using risk information to address agreement TSPAI 3.19. First, there needs to be enhanced consideration of the combined effect of uncertainties. These combined uncertainties need to be evaluated before the individual uncertainties can be dropped from further consideration. Second, transparent and traceable documentation needs to be developed that allows the results to be independently verified. The DOE should provide an adequate description of the completed sensitivity analyses. Third, information should be provided pertaining to the variability in the results. Some measure of how the variability of results changes between the different modeled cases is needed, because only the mean results of the stochastic performance assessment simulations have been presented to date. For example, presentation of the 5th and 95th percentiles of annual dose estimates, in addition to the mean dose estimates, would be a satisfactory way of conveying the variability and uncertainty of performance assessment estimates. This resulted in AIN request TSPAI 3.19 AIN-1.

The KTI response provided in the following sections does not attempt to resolve TSPAI 3.19 using the risk-based approach originally proposed by the DOE, nor does it provide the additional risk program elements requested in TSPAI 3.19 AIN-1. (However, the DOE reserves the option of using the risk-based approach in the future.) Rather, this KTI response directly addresses the original NRC concern (i.e., TSPAI 3.19) by clarifying the selection and justifying the use of a modified Priestley–Taylor model and the use of analog site temperature data.

B.1.2 Related Key Technical Issue Agreements

KTI agreements TSPAI 3.18, TSPAI 3.21, USFIC 3.01, and USFIC 3.02 relate to KTI agreement TSPAI 3.19 in that they all address physical processes or model approaches that either influence net infiltration or are used to predict net infiltration at Yucca Mountain. TSPAI 3.18 addresses the technical basis for using a water-balance approach to model net infiltration; TSPAI 3.21 questioned the effect that near-surface lateral flow had on the spatial variability of net infiltration; and USFIC 3.01 and USFIC 3.02 addressed Monte Carlo methods for analyzing infiltration and justifications for parameters used in the analysis of infiltration uncertainty.

Responses to KTI agreements TSPAI 3.18 (Appendix A), TSPAI 3.21 (Appendix C), USFIC 3.01 (Appendix D), and USFIC 3.02 (Appendix E) are provided.

B.2 RELEVANCE TO REPOSITORY PERFORMANCE

The overarching NRC concern is that the DOE infiltration model, its submodels (e.g., evapotranspiration), and the analog site temperature data upon which the models are based may underestimate net infiltration at Yucca Mountain. Net infiltration is used as the upper boundary condition for a hierarchy of numerical models that predict percolation of water through the unsaturated zone, seepage of water into waste emplacement drifts and subsequent corrosion rates for engineered barriers (i.e., drip shields and waste canisters), and transport of radionuclides from the waste canisters to the underlying saturated zone and beyond to the accessible environment. Underestimating net infiltration may result in an underestimation of the potential radiological dose used to assess repository performance.

B.3 RESPONSE

Numerous methods for estimating actual and potential evapotranspiration exist, none of which are globally applicable to all sites, conditions, and circumstances (Linsley et al. 1982, p. 159). Long-term measurements of actual evapotranspiration are rarely made or readily available because of difficulty of measurement and cost and time required to obtain this information. Actual evapotranspiration measurements are typically reserved for calibrating and validating meteorological models, including the Priestley–Taylor model.

Levitt et al. (1996) and Flint and Childs (1991) demonstrated the successful application of the modified Priestley–Taylor equation for modeling evapotranspiration for arid climate and xeric soil conditions, respectively. These studies showed that the Priestley–Taylor model performs reasonably well when the empirical coefficient α, found in the modified Priestley–Taylor equation, is calibrated against soil moisture content (USGS 2001a). These studies showed that the Priestley–Taylor model:

- Can be utilized along with readily measured climate data (solar radiation, temperature, humidity, etc.) to predict evapotranspiration.

- Relies on a simple effective parameter (α) related to soil water content to account for surface resistance to evapotranspiration. Numerous other models contain additional surface resistance coefficients, perhaps lending greater insight into the process of evaporation but can be difficult to measure and data intensive, while providing little improvement in accuracy.

- Can be easily integrated into water balance or physically based unsaturated flow models that also use water content as a primary variable, thus facilitating coupling of different submodels for the net infiltration simulations.

The evapotranspiration submodel used in the simulation of net infiltration at Yucca Mountain was calibrated against water content data obtained from neutron logs performed in site boreholes.

The justification of temperature records for the estimation of evapotranspiration is based on the selection of existing climate analog sites with historical meteorological records (Thompson et al. 1999; USGS 2001a; Sharpe 2003). Records from the existing climate analog sites were available, allowing for the evaluation of evapotranspiration for present-day and future climate scenarios (USGS 2001b). Precipitation and temperature time series records from Nogales and Hobbs meteorological stations were used for simulation of net-infiltration for the upper-bound monsoon climate. The records from Delta, Utah, and Beowawe, Nevada, were selected as representative of the simulation for the lower-bound glacial-transition climate, and the records from Rosalia, Spokane, and St. John, Washington, were selected as representative of the simulation for the upper-bound glacial-transition climate. The locations and a summary of mean annual temperature and precipitation are provided in Tables B-1 and B-2.

The information in this report is responsive to agreement TSPAI 3.19 made between the DOE and NRC. The report contains the information that DOE considers necessary for NRC review for closure of this agreement.

Table B-1. Meteorological Stations Selected to Represent Future Climate States at Yucca Mountain

Climate State	Duration of Climate State	Representative Meteorological Stations	Locations of Meteorological Stations	
Present-Day Interglacial	400 to 600 years	Site and regional meteorological stations	Yucca Mountain region	
Monsoon	900 to 1,400 years	Average Upper Bound: Nogales, Arizona Hobbs, New Mexico	North Latitude 31° 21' 32° 42'	West Longitude 110° 55' 103° 08'
		Average Lower Bound: Site and regional meteorological stations	Yucca Mountain region	
Glacial Transition	8,000 to 8,700 years	Average Upper Bound: Spokane, Washington Rosalia, Washington St. John, Washington	North Latitude 47° 38' 47° 14' 47° 06'	West Longitude 117° 32' 117° 22' 117° 35'
		Average Lower Bound: Beowawe, Nevada Delta, Utah	North Latitude 40° 35' 25" 39° 20' 22"	West Longitude 116° 28' 29" 112° 35' 45"

Source: USGS 2001b.

Table B-2. Mean Precipitation and Temperature at Climate Analog Sites

Climate Regime	Location	Mean Annual Precipitation (mm) for Climate Regime	Mean Annual Temperature (ºC) for Climate Regime
Present-Day Lower Bound	Yucca Mountain region	185.8[a]	Range: 15.1 to 18.2[b]
Present-Day Upper Bound	Yucca Mountain region	265.6[a]	Range: 15.1 to 18.2[b]
Monsoon Lower Bound	Yucca Mountain region	188.5[a]	Range: 15.1 to 18.2[b]
Monsoon Upper Bound	Nogales, Arizona Hobbs, New Mexico	414[c] 418[c]	15.8[c] 16.8[c]
Glacial-Transition Lower Bound	Delta, Utah Beowawe, Nevada	198[c] 220[c]	10.1[c] 8.8[c]
Glacial-Transition Upper Bound	Rosalia, Washington Spokane, Washington St. John, Washington	460[c] 410[c] 433[c]	8.4[c] 8.9[c] 9.1[c]

Source: [a] USGS 2001a, Tables 6-8 and 6-12.
[b] CRWMS M&O 1997, Tables 2-1 and A-10.
[c] USGS 2001a, Tables 6-4, 6-5, and 6-6.

B.4 BASIS FOR THE RESPONSE

B.4.1 Overview of Evapotranspiration Processes

Evapotranspiration is the combined process of evaporation from open water bodies, bare-soil evaporation and transpiration by vegetation (Freeze and Cherry 1979, p. 4). Open water bodies (e.g., lakes, reservoirs, or playas) are not present at Yucca Mountain; therefore, evapotranspiration is primarily limited to bare-soil evaporation and transpiration by plants. Bare-soil evaporation represents the amount of water evaporated from a bare soil surface, which for deep unsaturated soils is limited by the near-surface supply of soil moisture. Transpiration is the uptake and transfer of water to the atmosphere by vegetation. If the soil (or fractured bedrock) becomes drier than what is conceptually referred to as the wilting point, transpiration will not occur even though there may be some residual water in the root zone. Transpiration is much more efficient than bare-soil evaporation in removing water from subsurface soils and fractured bedrock because plant roots typically extend deeper than the near surface dryout zone influenced by bare surface evaporation, and plants can exchange large amounts of soil water with the atmosphere through the process of transpiration.

Actual evapotranspiration is a function of the potential evapotranspiration rate, the availability of water at the ground surface and within the root zone, vegetation characteristics such as timing of plant growth and root density, and the chemical and hydrologic properties of the root zone. (Potential evapotranspiration is an energy-limited rate and is a measure of the ability of the atmosphere to remove water from the surface through the evapotranspiration process assuming unlimited availability of water.) The processes are not independent, but, in general, the primary factors controlling actual evapotranspiration are potential evapotranspiration, soil-water availability, vegetation density, and seasonal vegetation growth. The more saturated the soil (or fractured bedrock) and the denser the vegetation, the closer the actual evapotranspiration rate is to the potential evapotranspiration rate.

After large storm or snowmelt events, water can penetrate deeper and accumulate in the root zone more rapidly than it can be removed by evapotranspiration. This is especially true during winter, when potential evapotranspiration is at a minimum because of shorter days, lower sun angle, and lower air temperatures, and root activity is either diminished or dormant.

The redistribution of water within the root zone affects the actual evapotranspiration rate because bare-soil evaporation extends approximately to depths of only 10 to 30 cm, and the density and growth of roots within the root zone, in general, is typically observed to decrease with depth. The estimate of the depth of bare-soil evaporation is based on field measurements of water potential with depth at Yucca Mountain (USGS 2001a, Figure 6-6A); above a depth of about 20 to 30 cm, the soil is too dry for extraction by plant roots most of the year. The more quickly water redistributes to deeper depths, the greater the potential for net infiltration to occur because the overall susceptibility of water in the root zone to removal by evapotranspiration decreases with depth. At depths greater than the root zone, both vapor and matric potentials can result in upward unsaturated flow or exfiltration back into the root zone, but total water losses from these processes are considered negligible relative to evapotranspiration within the relatively thin root zone. Vapor flow enhanced by barometric pumping and temperature gradients also contributes to the water balance at the site but has been shown to be insignificant relative to precipitation, evapotranspiration, runoff, and net infiltration (USGS 2001a, Section 6.1.4).

The potential evapotranspiration rate is determined by the energy balance and depends primarily on net radiation, air temperature, ground-surface heat flux, the slope of the saturation-vapor density curve, and advective energy from wind (McNaughton and Spriggs 1989; Priestley and Taylor 1972; Flint and Childs 1991). Net radiation depends primarily on solar radiation and surface characteristics, including topography and albedo. For the current climate at Yucca Mountain, the average annual potential evapotranspiration rate is approximately six times greater than the average annual precipitation rate (Hevesi et al. 1994, p. 2,326); thus, on an annual basis, most of the precipitation is removed from the site by evapotranspiration. On a daily basis, however, the precipitation, snowmelt, or surface-water run-on rate can be much higher than the potential evapotranspiration rate. This is especially true during the winter when the potential evapotranspiration rate is at a minimum; the result is net infiltration below the zone of evapotranspiration.

In developing adequate models of evapotranspiration for future climate scenarios, it is important to take into account that solar radiation depends on slope, aspect, elevation, latitude, longitude, and surrounding topography (e.g., blocking ridges, which could change over time). The evapotranspiration model used for predictions with the INFIL model empirically accounts for the combined effects of solar radiation. Redistribution of moisture in the shallow subsurface occurs in response to the total water potential gradients, including the gravitational, capillary, osmotic, and vapor components. The relatively small effects of the vapor movement in unsaturated media on evapotranspiration and evaporation of surface runoff are not taken into account in the U.S. Geological Survey simulations (USGS 2001a). The zone of evapotranspiration is considered only to a depth of 6 m (bottom of the root zone), which could result in underestimating the zone of influence for evapotranspiration and, thus, overestimate infiltration.

For the monsoon climate, the evaluation of evapotranspiration was based on modified root-zone parameters reflecting greater vegetation density and changes in vegetation type for the wetter

climate conditions (USGS 2001a, Section 6.9.4). For the upper-bound monsoon climate, the root-zone weighting parameters were modified to approximate a 40 percent vegetation cover (as compared to 20 percent for present-day climate), and the maximum thickness of the modeled bedrock root-zone layer was increased from 2 to 2.5 m (6.6 to 8.2 ft).

The vegetation characteristics most important for evaluating transpiration are distribution, minimum xylem water potential, and rooting depths (Flint et al. 1996, p. 45).

B.4.2 Direct Measurement of Evapotranspiration

Direct measurement of evapotranspiration is a difficult undertaking, because it requires accurate measurement of various energy balance, mass transfer, or soil water balance parameters. Methods employed to directly measure evapotranspiration include the Bowen ratio (Flint and Childs 1991), weighing lysimeter, and eddy correlation (Levitt et al. 1996). These methods are demanding in terms of accuracy of measurement and not readily amenable to sampling large study areas exhibiting numerous vegetative covers, microclimates, and soil types, such as those found in the 123.7-km^2 area (USGS 2001a, p. 64) of the infiltration model domain.

Evaporation-pans are the most widely used instrument for measuring potential evaporation from surface water reservoirs or saturated soils (Linsley et al. 1982, p. 146). However, the application of pan data to determine actual or potential evapotranspiration from vegetated or bare soils is very limited, especially under arid conditions where soils dry or drain rapidly so that saturated conditions (representative of pan conditions) do not persist for prolonged periods of time. Pan evaporation was measured for several years near Yucca Mountain, using a Class A evaporation pan (Flint et al. 1996, p. 59, Figure 29). Although the data could not be used as a direct measure of potential evapotranspiration, they showed evidence of strong advective effects in the arid environment at Yucca Mountain. The data also indicated considerable spatial-temporal variability in evaporation, with experimentally determined pan evaporation exceeding calculated potential evaporation by about 100 percent. The data also were used to establish the upper limit of available energy for potential evapotranspiration modeling, given that modeled potential evapotranspiration should not exceed pan evaporation. The potential evapotranspiration ranges from a minimum of 500 mm/yr to a maximum of 900 mm/yr, depending mostly on the land-surface slope and aspect. Minimum values of evapotranspiration occur at steep northerly and northeasterly facing slopes, particularly at locations surrounded by blocking topography.

B.4.3 Determination of Potential and Actual Evapotranspiration Using Meteorological Data and Models

Penman (1948) combined the energy balance equation with a physically based mass transfer function describing advection of water vapor and energy above a horizontal surface to derive an equation to compute the evaporation from a thin free-water surface. The utility of Penman's original approach is that it uses standard climatological records of sunshine, temperature, humidity, and wind speed (which are relatively easy to measure) to estimate evaporation, rather than relying on direct and difficult measurements of actual evapotranspiration. However, limiting assumptions and simplifications used by Penman (1948) to model the aerodynamic or mass transfer component of evaporation make the Penman equation only useful for estimating potential evapotranspiration.

Penman's (1948) method was further refined by numerous researchers over the last five decades and has been extended to bare and cropped soil surfaces by introducing surface resistance factors and (or) parameters limiting evapotranspiration from water-supply limited soils. Monteith (1965) modified Penman's original equation using surface resistance factors allowing calculation of actual evapotranspiration from cropped soils. The Penman–Monteith equation, however, requires detailed knowledge of the resistances to heat and water flow at the land surface, making it difficult to apply without having extensive measurements for the resistance parameters (e.g., aerodynamic resistance, bulk stomatal resistance, and active leaf area index). The Penman–Monteith equation is typically applied to extensive cropped soils where water availability is not an issue.

Priestley and Taylor (1972) suggested an alternative, simpler form of the Penman equation that requires a single effective surface resistance parameter (α) as follows (Flint and Childs 1991, p. 248; Levitt et al. 1996, p. 32; USGS 2001a, p. 39, Eq. 8):

$$PET = \alpha \ [s/(s + \gamma) \ (RN - GH) / \lambda] \qquad \text{(Eq. B-1)}$$

where PET is the potential evapotranspiration rate, α is the Priestley–Taylor coefficient, s is the slope of the saturation vapor pressure-temperature curve, γ is the psychometric constant, RN is modeled net radiation, GH is estimated ground-heat flux, and λ is the latent heat of vaporization (λ value of 2.45 MJ/m^2/mm) (Levitt et al. 1996, p. 2, Eq. 2).

The Priestley–Taylor equation includes an empirical scaling term, α, which is multiplied by the energy balance term in the original Penman equation. The Priestley–Taylor method does not utilize the aerodynamic resistance term found in the Penman and Penman–Monteith equation, but rather accounts for advection above the evaporating surface using the single coefficient, α. Flint and Childs (1991, Table 1) report that α values found in the literature range from 0.72 for forests to 1.57 for strongly advective conditions. Measured values of α equal to 1.26 were reported for open-water surfaces, and similar values between 1.18 and 1.29 were reported for wet conditions associated with meadows, forests, irrigated ryegrass, and grass-covered soil at field capacity (Flint and Childs 1991, Table 1). Flint and Childs (1991) found that the coefficient equaled 0.9 when the water content of the loamy soil evaluated at their field site in southwestern Oregon was near field capacity. From this literature review, Flint and Childs (1991) concluded that this range of values was applicable to Yucca Mountain.

Calculation of actual evapotranspiration from potential evapotranspiration for soil-water-limited cases, which commonly occur in arid regions, can be accomplished using the Priestley–Taylor equation and an empirical relation redefining α as a function of soil water content ($\alpha' = f(\theta)$) (Flint and Childs 1991, Eq. 5; Levitt et al. 1996, Eq. 14 and 15). The modified Priestley–Taylor equation is used in the DOE net infiltration model to predict actual evapotranspiration as summarized in Section B.4.5 (see *Simulation of Net Infiltration for Modern and Potential Future Climates* (USGS 2001a, p. 39, Section 6.4.4) for complete details).

B.4.4 Case Studies Demonstrating the Successful Use of the Modified Priestley–Taylor Equation for Xeric Soil and Arid Climate Conditions

Flint and Childs (1991) performed an evapotranspiration study on a partially vegetated clearcut site in southwest Oregon near Wolf Creek northeast of Grants Pass. The site soils ranged from 0.48 to 0.7 m in depth overlying a steeply dipping, south-facing, weathered bedrock slope. Vegetation at the reforested site covered 81 percent of the surface area and consisted primarily of shrubs, perennial forbs, and annual species. Continuous climate measurements, including air temperature, precipitation, dew point temperature, and net radiation, were made, along with periodic measurement of soil water content and temperature. The modified Priestley–Taylor model was calibrated by estimating the coefficient, α', from actual evapotranspiration results determined using the Bowen ratio method (Flint and Childs 1991, Eq. 2) and climate data. The α' values were then calibrated against daily estimates of relative soil water saturations obtained from a mass balance water budget model. Flint and Childs (1991) calculated a relation between α' and relative saturations using regression analysis, allowing the Priestley–Taylor coefficients derived from Bowen ratios to be expressed directly in terms of soil water contents. The Priestley–Taylor model-derived soil water contents were then validated against independent measurements of field water contents (Flint and Childs 1991, Figure 3). The long-term trend in the observed water content data was reproduced reasonably well, indicating that the Priestley-Taylor equation, coupled with an effective α' value directly related to relative soil saturation, can be used to predict actual evapotranspiration.

Levitt et al. (1996) performed a second more extensive study of evapotranspiration at the Area 5 Radioactive Waste Management Site at the Nevada Test Site. The site is located north of Mercury, Nevada, within the Frenchman Flat basin in the same south-central part of the Great Basin section of the Basin and Range physiographic province as Yucca Mountain. Similar climate conditions, vegetation types, size and spacing, soil types, and evapotranspiration rates are expected, given the relative proximity of Frenchman Flat to Yucca Mountain (37 km).

A thorough literature review performed by Levitt et al. (1996) revealed that seven types of evapotranspiration models appeared to be applicable to the arid environment susceptible to bare-soil evaporation, including:

1. The Penman–Monteith model (Monteith 1965)
2. The Shuttleworth–Wallace model (Shuttleworth and Wallace 1985)
3. The Priestley–Taylor model (Priestley and Taylor 1972)
4. The advection-aridity model (Brutsaert and Stricker 1979)
5. The aerodynamic profile
6. The sensible heat-flux based model (Albertson et al. 1995)
7. The square-root-of-time (bare-soil evaporation) model.

The models were calibrated with actual evapotranspiration data determined primarily using weighing lysimeters (with and without vegetation) and, to a lesser extent, using the Bowen ratio and eddy correlation data and methods. The results of the study indicated that the Penman–Monteith and Priestley–Taylor models performed well under a variety of conditions for both short-term (daily) and long-term (71-day) hourly data sets, and the adjusted square-root-of-time model for bare-soil evaporation worked well for long-term data sets. These three models

required inputs of soil water content to improve their performance. The sensible heat-flux model did not require soil water content as an input and performed reasonably well for predicting sensible heat-fluxes. The remaining three models (Shuttleworth–Wallace, advection-aridity, and aerodynamic) did not produce reasonable matches to the long-term or short-term hourly data sets and, therefore, were not acceptable for application at Yucca Mountain.

B.4.5 Implementation of the Priestley–Taylor Evapotranspiration Model at Yucca Mountain

The DOE infiltration model for Yucca Mountain (INFIL V2.0; USGS 2001c) and its associated submodels use a water-balance approach and meteorological input to produce lumped (distributed) estimates of basinwide (averaged over a watershed) net infiltration (USGS 2001a). INFIL V2.0 performs a daily simulation of net infiltration using 253,597 model cells that are 30 by 30 m each, comprising a watershed model domain centered on the Yucca Mountain site. The daily water balance consists of simulating precipitation, snowmelt, sublimation, actual and potential evapotranspiration, changes in water content in the root zone, net infiltration, and surface water runoff (run-on). Potential evapotranspiration is modeled hourly for each daily water balance using estimates of incoming solar radiation and accounting for reduced solar radiation caused by blocking terrain. The model is driven by daily estimates of climate input data, which also serve to carry the INFIL V2.0 simulation through the time domain.

Actual evapotranspiration was simulated using the modified Priestley–Taylor equation given by Flint and Childs (1991):

$$ET^k = \alpha' \cdot \text{PET}^k$$

$$\alpha' = \sum_i \, \{\text{wgt}_i \cdot [a^k (1-\exp(b^k \cdot \text{relsat}_i{}^k))]\} \qquad \text{(Eq. B-2)}$$

where ET^k is total root-zone evapotranspiration for grid cell k and PET^k is the adjusted clear-sky simulated equilibrium potential evapotranspiration for grid cell k. (The PET was calculated using a α value of 1.0, which is needed to represent the nonadvective component of the energy balance.) The term $\text{relsat}_i{}^k$ is the relative saturation calculated for a soil layer i within the grid cell k; and a^k and b^k are the Priestley–Taylor model coefficients for grid cell k, which are used as soil- and rock-type input parameters. In INFIL simulations (USGS 2001a), the a and b coefficients were different for various climate scenarios for different soils and rocks. The dynamic weighting (wgt_i) factor is used to increase the root activity effect within the wettest layer. For the topsoil, the bare-soil evaporation term is added to the transpiration term. The coefficients of a equal to 1.04 (for bare soils) and a b value equal to −10 were used in simulations provided in *Simulation of Net Infiltration for Modern and Potential Future Climates* (USGS 2001a). To evaluate the net infiltration uncertainty for the glacial-transition climate, the coefficient a was taken to range from 0.54 to 1.54 (with a mean of 1.04), and b was from −0.10 to −19.9 (with a mean of −10) (BSC 2003). Simulation of net infiltration was performed using a and b coefficients selected from their respective probability distributions (within the range of the 1 to 99th percentile).

Potential evapotranspiration was simulated using the Priestley–Taylor equation (Priestley and Taylor 1972), which is a simpler form of the Penman equation with an effective surface

resistance parameter, α (Flint and Childs 1991, p. 248; Levitt et al. 1996, p. 32; USGS 2001a, p. 39, Eq. 8):

$$\text{PET}_d^k = \alpha \cdot [s/(s+\gamma)_d^k \cdot (\text{RN}_d^k - \text{GH}_d^k)/\lambda] \qquad \text{(Eq. B-3)}$$

where PET_d^k is the potential evapotranspiration rate on day d for grid cell k, α is the Priestley–Taylor coefficient, s is the slope of the saturation vapor pressure-temperature curve; γ is the psychometric constant; RN is modeled net radiation; GH is estimated ground-heat flux, and λ is the latent heat of vaporization (λ value of 2.45 MJ/m^2/mm, Levitt et al. 1996, p. 2, Eq. 2).

For wet conditions having freely evaporating surfaces, α is often set to 1.26 (Priestley and Taylor 1972; Flint and Childs 1991). For dry conditions, available moisture becomes the limiting factor controlling actual evapotranspiration, and α can be modeled as an empirical scaling function, α', using a relative saturation term, as defined in Equation B-1 (Flint and Childs 1991). In the root-zone water-balance submodel, α' is defined as an empirical function of relative saturation within the root zone. For days with precipitation, the modeled clear-sky potential evapotranspiration rate was reduced by approximately 25 percent due to cloud cover that exists whenever it rains. The assumption is that the energy for evapotranspiration is reduced in the presence of clouds (associated with precipitation) and, the more rain there is, the less evapotranspiration there is.

The $s/(s+\gamma)$ term is modeled as a function of average daily air temperature by using the following equation from Flint et al. (1996):

$$s/(s+\gamma)_d^k = -13.281 + 0.083864 \cdot TA_d^k - 0.00012375 \cdot (TA_d^k)^2 \qquad \text{(Eq. B-4)}$$

where TA_d^k is the average daily air temperature on day d for grid cell k, in Kelvin. This equation was defined using parameter values obtained from a regression of data from Campbell (1977, Table A.3), and indicates the relative effect of air temperature on potential evapotranspiration, which varies for different temperature ranges. In Figure B-1, the solution of Equation B-3 is compared with selected values taken from Campbell (1977, Table A.3) to illustrate the greater relative change in the $s/(s+\gamma)$ term for low air temperatures (in the range −5°C to 5°C) as compared to higher temperatures (25°C to 35°C). For example, a decrease in air temperature from 5°C to 0°C results in a 17 percent reduction in $s/(s+\gamma)$ and, thus, potential evapotranspiration, while a decrease in air temperature from 35°C to 30°C causes only a 5 percent reduction in the $s/(s+\gamma)$ term.
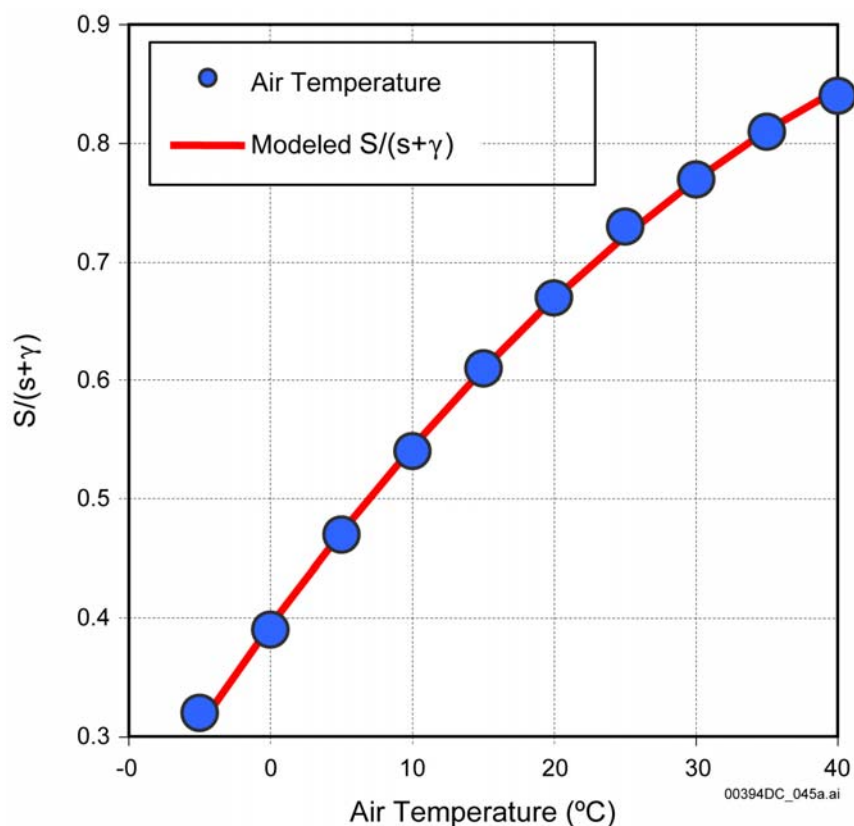
Source: USGS 2001a, Figure 6-8.

NOTE: Data are from Campbell 1977, Table A.3.

Figure B-1.   Relative Effect of Air Temperature Change on the Modeled $s/(s+\gamma)$ Term of the Priestley–Taylor Equation Used for Estimating Potential Evapotranspiration

Using the INFIL V2.0 code (USGS 2001c), evapotranspiration is simulated for each root-zone layer using a dynamic root-zone weighting function and a modified Priestley–Taylor equation. Evapotranspiration is simulated only for days with air temperature greater than 0°C.

To account for seasonal changes in the solar trajectory, as well as terrain effects across model elements, SOLRAD, a submodel in INFIL V2.0, calculates solar position on an hourly basis from sunrise to sunset as a function of the day of year and geographic position of each grid cell (Flint and Childs 1987). Terrain effects (blocking ridges) on incoming solar radiation are modeled using topographic parameters calculated from the digital elevation model and included as input in the geospatial parameter file. Topographic parameters include grid cell slope, aspect, and 36 blocking ridge angles that define shading effects and reductions in skyview for every 10° in the horizontal plane, starting with the Universal Transverse Mercator northing axis as the 0° azimuth. Shading causes a reduction in direct beam radiation, and diminished skyview decreases diffuse radiation. These effects can become important in rugged mountainous terrain.

The minimum xylem water potential used to calculate the lower limit of plant-available water was −6,000 kPa (about 60 bar) which was assumed to be equivalent to the wilting point of

vegetation. The dynamic weighting was based on calculated relative saturations for each root-zone layer and the relative distribution of water (based on saturation) throughout all layers.

B.4.5.1   Calibration of the Evapotranspiration Submodel and INFIL Model

Changes in water-content profiles through time, measured in boreholes located in active channels with thick soils, were used to develop and calibrate the modified Priestley–Taylor evapotranspiration submodel (Hevesi et al. 1994). Initial calibration of the net infiltration model was conducted in 1996 using INFIL V1.0 (Flint et al. 1996; USGS 2001d) and consisted of a generalized (site-wide) calibration of the modified Priestley–Taylor model coefficients. INFIL V1.0 was calibrated by comparing measured time-series water-content profiles from the network of neutron-monitoring boreholes described by the U.S. Geological Survey (USGS 2001a, Section 6.3.4) to simulated water-content data (Flint et al. 1996). At selected neutron boreholes, water-content data were summed for the soil profile and compared to the model simulation for the same time period by using the developed site precipitation record. The match of the simulated and measured volumetric water content was improved by varying the *a* and *b* coefficient values in the modified Priestley–Taylor equation (Eq. B-2), which adjusted the evapotranspiration calculations of the simulated water content to better match the measured water content. Simulated water content compared well with measured water content, which indicated that the water-balance technique used in the model to calculate simulated net infiltration could correctly maintain the proper soil moisture. This is important for accurate determination of when the water-storage capacity of the soil was exceeded and ponding at the soil–bedrock interface had occurred, which controls the calculation of net infiltration.

INFIL V1.0 did not account for infiltration from surface water runoff in channels, making it necessary to increase precipitation input to the net infiltration model to obtain a good match with the borehole water-content profiles, particularly during wet years. Therefore, INFIL V1.0 was modified to include stream-routing (i.e., runoff and run-on) resulting in INFIL V2.0 (USGS 2001c). The calibration approach for the INFIL V2.0 net infiltration model differed from that for the 1996 model. Model calibration using INFIL V2.0 was conducted using the coefficients *a* and *b* from calibration of INFIL V1.0 and stream-flow records from five gauging sites on Yucca Mountain. The gauging sites were operational from 1994 through 1995 and included two significant storm events measured during the winter of 1994 to 1995.

B.4.5.2   Results of Simulations

For the present-day climate, the simulated evapotranspiration varies over the Yucca Mountain area, reflecting the distribution of precipitation, local terrain, and surface-water flow effects (Figure B-2). For example, evapotranspiration from 140 to 160 mm/yr occurs along the southern and southeastern sections of the model domain, and from 220 to 240 mm/yr for higher elevations receiving greater precipitation. Minimum evapotranspiration of less than 100 mm/yr occur at steep north-facing side slopes and areas with minimal soil cover, the west-facing slope of Solitario Canyon, and the rugged terrain in the northern part of Yucca Wash. Maximum evapotranspiration of 240 mm/yr and higher are indicative of locations with a high volume or high frequency of infiltrated surface-water run-on, particularly immediately downgradient from areas receiving higher precipitation, as well as rugged terrain conducive to runoff generation, such as the northern part of Yucca Wash.

For the mean glacial-transition climate, the spatial distribution of evapotranspiration is different from that for the present-day conditions, showing the importance of changes in precipitation, root-zone water-storage capacity, and infiltrated surface-water run-on (Figure B-3). Minimum evapotranspiration rates are less than 100 mm/yr on steep side slopes with thin soil cover, and maximum rates are close to 600 mm/yr in active channel locations. Maximum evapotranspiration rates for the glacial-transition climate (600 mm/yr) are less than those for the present-day climate (700 mm/yr), which is caused by the effect of a cooler future glacial-transition climate.

B.4.5.3   Summary of Sensitivity Analysis

The sensitivity analysis of uncertain input parameters, including the potential evapotranspiration and coefficients *a* and *b*, revealed the negative correlation between these parameters and net infiltration (Section 6, Appendix D) (BSC 2003). This analysis showed that the correlation between net infiltration and parameters of the evapotranspiration model decrease in the following order of importance: potential evapotranspiration (correlation coefficient is −0.34), coefficient *a* (−0.18), and coefficient *b* (−0.1). Among 12 uncertain parameters that were investigated, potential evapotranspiration is the third most sensitive parameter.

B.4.6   Analog Site Meteorological Stations and Temperature Records

For the next 10,000 years, each climate regime was represented by existing meteorological stations. Data from the meteorological stations were used to determine precipitation and temperature records, which were used as inputs to the infiltration model (see Section 4). For each of the climate scenarios (present-day, monsoon, and glacial transition), the lower-bound, mean, and upper-bound states were considered (see Table B-1).
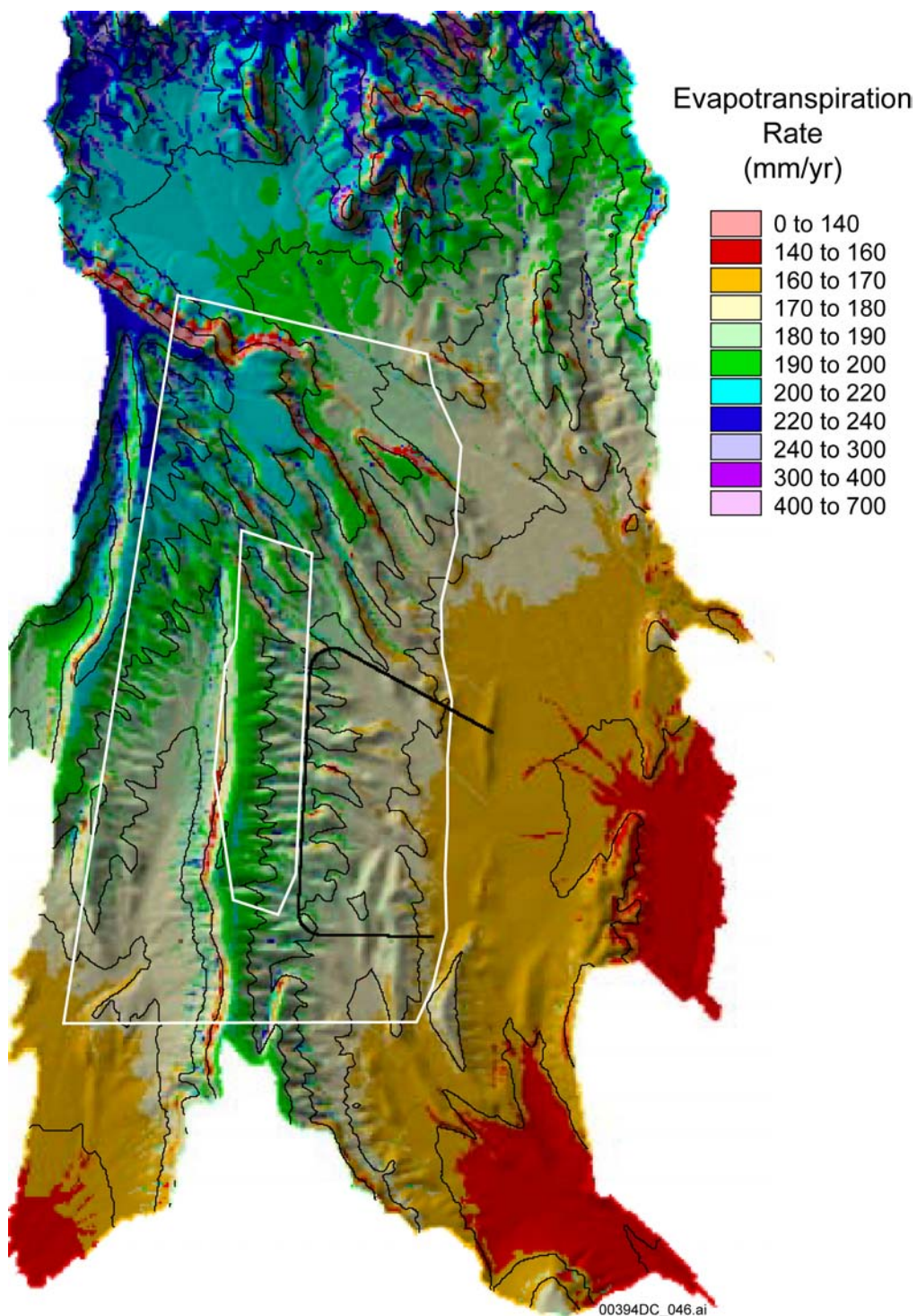
Source: USGS 2001a, Figure 6-24.

Figure B-2.   Estimated Evapotranspiration for the Mean Modern Climate Scenario

Mean Glacial
Transition Climate
Evapotranspiration
Rate
(mm/yr)

	0 to 200
	200 to 260
	260 to 280
	280 to 290
	290 to 300
	300 to 320
	320 to 340
	340 to 400
	400 to 600

00394DC_047.ai
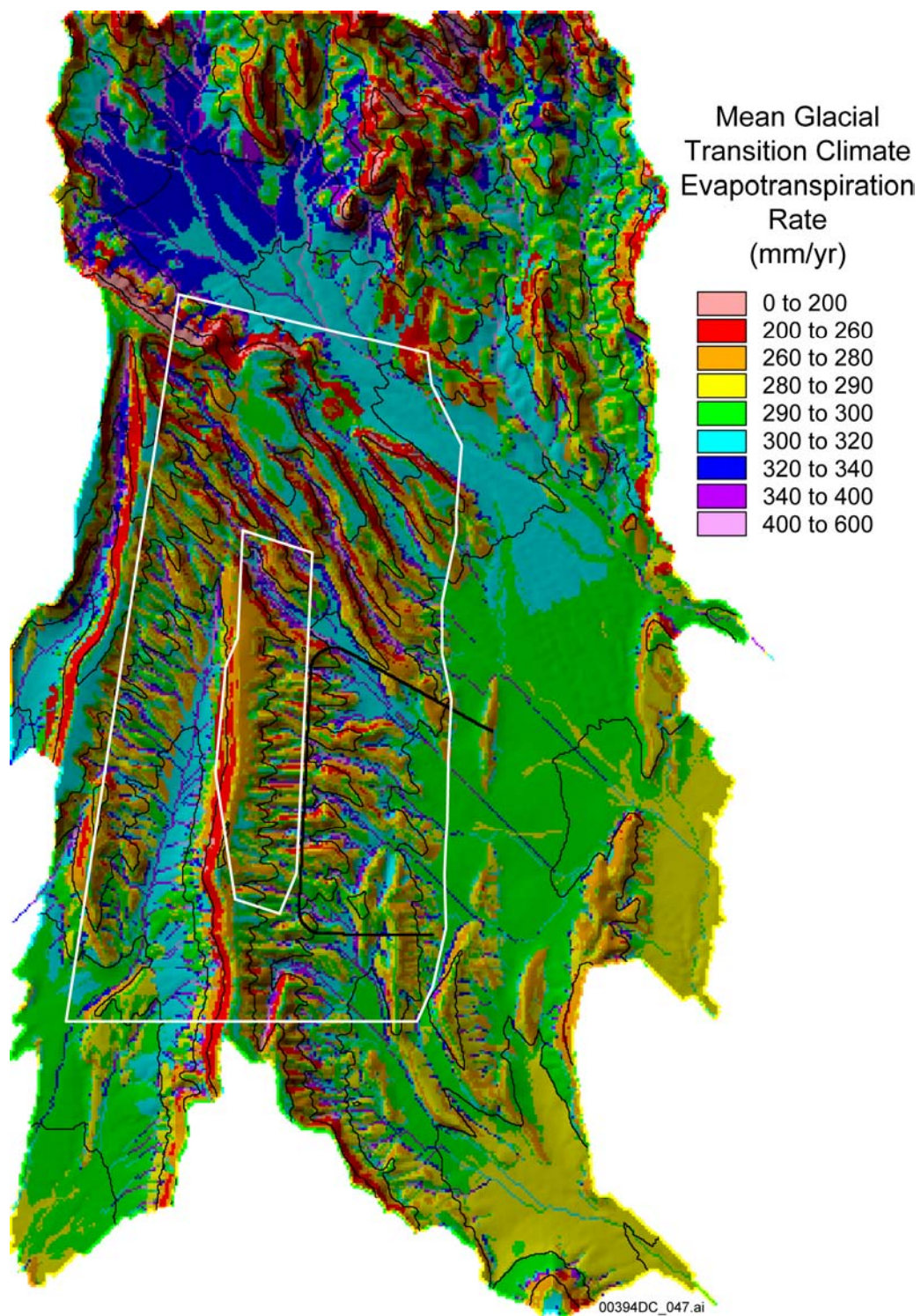
Source: USGS 2001a, Figure 6-34.

Figure B-3. Evapotranspiration for the Mean Glacial-transition Climate Scenario

Present-day meteorological data for the upper and lower bounds come from available stations in the region, including project and nonproject data (USGS 2001a). The present-day climate scenario was characterized using the results of observations conducted from 1980 to 1995, with results from the Nevada Test Site Station 4JA 100-year stochastic simulation. To represent the lower-bound present-day climate scenario, the driest 10-year period (from 1980 to 1990) from the 100-year observations at the 4JA precipitation station was used. Note that the 4JA Station is located at the elevation of 1,044 m (within the Nevada Test Site) (USGS 2001a, Table 6-3). To characterize the upper-bound present-day climate scenario, the average data for the 1980 to 1995 observations at the Nevada Test Site Station Area 12 Mesa (located within the northern boundary of the Nevada Test Site known as Rainier Mesa) were used. These data were intended to represent the wetter conditions resulting from the enhanced El Niño Southern Oscillation activity.

Within the region in the United States that experiences a strong summer monsoon, there are two meteorological stations with long-term records needed to identify the monsoon climate upper bound: Hobbs, New Mexico, and Nogales, Arizona. These two stations were selected to minimize the influence of local meteorological phenomena on the input to the infiltration model. The lower-bound monsoon climate scenario was defined as being equivalent to the mean present-day climate scenario (USGS 2001a).

Selecting upper- and lower-bound glacial-transition climate from meteorological stations required identifying sites with cool winter wet seasons, and warm to cool and dry summers (i.e., areas north of the summer rain regime) (USGS 2001b, Section 6.6.2). Further, the analog sites needed to lie on the east side of large mountain ranges and, hence, in the rain shadow of those ranges. Based on the ostracod assemblage, the absence of cold Canadian-like climate implies the upper-bound analog should lie within the contiguous United States. The mean annual temperature for the glacial-transition climate should be no colder than and preferably warmer than 8ºC. The analog stations should be in the semiarid west (USGS 2001b, p. 73).

The meteorological stations representing the lower-bound glacial-transition climate should be in a place where mean annual temperature is higher than for the upper bound, and, thus, these stations would be south of the upper-bound localities (USGS 2001b, Section 6.6.2). The mean annual temperature should, however, be lower than that for the Owens Lake Basin at present, so that effective moisture is higher, consistent with a full and overflowing lake. The stations should have a lower mean annual precipitation than the upper-bound sites, because the record from the Owens Lake Basin shows episodes of either saline diatoms or ostracodes, implying less surface flow in the Owens River. However, the absence of abundant saline taxa implies effective moisture is higher than at present, reflecting cooler than present mean annual temperature rather than high mean annual precipitation (USGS 2001b, p. 74). Thus, the lower-bound glacial-transition meteorological sites may have mean annual precipitation values similar to or even lower than present-day Owens Lake Basin (USGS 2001b, p. 74). As with the upper-bound meteorological sites, the region should be winter-precipitation dominated, north of the summer rain regime, and have some or all of the ostracod or diatom species found in the fossil record at Owens Lake. Inspection of meteorological sites that fit lower-bound glacial-transition conditions revealed that there were few choices available (USGS 2001b, Section 6.6.2). The sets of meteorological data that fit all of these criteria and also have long and complete records were found at Delta, Utah, and Beowawe, Nevada.

The upper-bound meteorological stations were selected in an area where the polar front currently resides through most or all of the winter season and where its average position resides most of the year (USGS 2001b, Section 6.6.2). Given the above qualifying conditions, the upper-bound glacial-transition meteorological site was selected in the northwestern United States, east of the Cascades, a high mountain range. The area falls within a rain shadow, as does Yucca Mountain. The regional mean annual precipitation is winter-precipitation dominated and is under the influence of the polar front during the winter, as well as other times throughout the year. Furthermore, unlike localities farther north in Canada, the region does not experience extended dominance by extremely cold, Arctic high pressure, typical of the cold, full-glacial periods. Based on meteorological-station data from eastern Washington state, three stations were selected for the upper-bound glacial-transition climate: Spokane, Rosalia, and St. John (see Figure 2-2). These three stations are close to each other but do not have identical records, presumably reflecting local differences in mean annual precipitation and mean annual temperature. As in other cases, selection of multiple meteorological stations was intended to minimize local effects on the climate parameters used as input to the infiltration model.

The temperature data were used as inputs to the INFIL net infiltration model. For each of the climate scenarios (present-day, monsoon, and glacial transition), the lower-bound, mean, and upper-bound states were considered (see Table B-1).

Average daily air temperature, in degrees Celsius, if not provided in the daily climate input file, was calculated internally by INFIL V2.0 (Flint et al. 1996, Equation 20):

$$T = T1\text{-}T2 \{\sin[(D/366)*2\pi + 1.3]\} \tag{Eq. B-5}$$

where T is modeled daily air temperature (°C), D is day of year number, $T1$ is mean annual air temperature (°C), and $T2$ is mean seasonal variation of average daily air temperatures above the mean during summer and below the mean during winter (the 0.5 amplitude of the sine wave). $T1$ and $T2$ were calculated as 17.3°C and 11.74°C, respectively, based on measured air temperature data from Yucca Mountain (USGS 2001a, Section 6.4.2). The mean temperature given by Sharpe (2003) is 13.4°C.

For the glacial-transition climate, the temperature record was taken from the Tule Lake, California, meteorological station (DTN: GS000308311221.010).

B.4.7   Conclusions

Flint and Childs (1991) and Levitt et al. (1996) showed that the modified Priestley–Taylor equation could be used to predict actual evapotranspiration for xeric soils and arid climate conditions, respectively. An empirical relation between the Priestley–Taylor coefficient, α', and soil water content allowed the Priestley–Taylor method to be used to produce reasonable short-term and long-term estimates of evapotranspiration for water supply–limited soils (Levitt et al. 1996).

The modified Priestley–Taylor method was selected for use because:

- Like the Penman and Penman–Monteith methods (and numerous other meteorological models), it relies on meteorological data to estimate evapotranspiration. Historical

climatological records of sunshine, temperature, humidity, etc., are typically available for relatively long time periods, allowing long-term evaluation of evapotranspiration. In comparison, direct measurements of actual evapotranspiration are difficult to make and are rarely performed for extended periods, so that historical records are typically incomplete and not readily amenable for validating meteorological models and evaluating past, present, or future evapotranspiration trends.

- Unlike the Penman approach, the Priestley–Taylor method is not limited to predicting evaporation from a freewater surface representative of the maximum potential evapotranspiration rate. Rather, it can be used to predict actual evapotranspiration from vegetated and bare-soil surfaces under soil moisture–deficit conditions. Measurement of actual rather than maximum evapotranspiration is desirable. Actual evapotranspiration rates, reflective of soil moisture-deficit conditions, are less than potential evaporation rates resulting in greater net infiltration below the root zone for a given precipitation rate. In turn, increased net infiltration will produce shorter and, therefore, more conservative estimates of groundwater transport times through the unsaturated zone.

- Unlike the Penman–Monteith method, the Priestley–Taylor method uses only one effective parameter (α) representing either surface resistances to heat and water flow at the evaporating surface, water supply–limited evaporation, or both. This simplification has the advantage that it does not require measurement of individual surface resistance parameters (e.g., aerodynamic resistance, bulk stomatal resistance, and active leaf area index), which can be difficult, time consuming, and impractical to make, given the different microclimates, types of plant-cover, and numerous soils found in the net infiltration model domain, with little improvement in the reliability of results. However, the disadvantage of using one effective resistance parameter is that it does not lend insight into the nature of other processes that can control evapotranspiration.

The INFIL model used by DOE to predict net infiltration at Yucca Mountain is based, in part, on an evapotranspiration submodel. The evaporation submodel uses the modified Priestley–Taylor equation, which was calibrated against water content data obtained from neutron logs performed in site borings. The modified form of the Priestley–Taylor equation produces reasonable results when calibrated against field data and site observations.

Meteorological data (including temperature) are used as input to the Priestley–Taylor model to estimate evapotranspiration. A broad range of climate scenarios that could potentially occur at Yucca Mountain in the future, including a wetter monsoon and a cooler glacial-transition period relative to today (USGS 2001b), were identified and used to select representative analog sites. Selection of analog sites was limited by the relatively small number of representative meteorological stations to choose from and by the availability of long-term meteorological records needed to calibrate models used to estimate evapotranspiration and net infiltration (Thompson et al. 1999; USGS 2001b; Sharpe 2003). Historical meteorological records were obtained from available sources, allowing for the evaluation of evapotranspiration for present-day and future climate scenarios and their upper and lower bounds.

B.5 REFERENCES

B.5.1 Documents Cited

Albertson, J.D.; Parlange, M.B.; Katul, G.G.; Chu, C.-R.; Stricker, H.; and Tyler, S. 1995. Sensible Heat Flux from Arid Regions: A Simple Flux-Variance Method." *Water Resources Research*, *31*, (4), 969–973. Washington, D.C.: American Geophysical Union. TIC: 252318.

Brutsaert, W. and Stricker, H. 1979. "An Advection-Aridity Approach to Estimate Actual Regional Evapotranspiration." *Water Resources Research*, *15*, (2), 443–450. Washington, D.C.: American Geophysical Union. TIC: 255551.

BSC (Bechtel SAIC Company) 2002. *Risk Information to Support Prioritization of Performance Assessment Models.* TDR-WIS-PA-000009 REV 01 ICN 01. Las Vegas, Nevada: Bechtel SAIC Company. ACC: MOL.20021017.0045.

BSC 2003. *Analysis of Infiltration Uncertainty.* ANL-NBS-HS-000027 REV 01. Las Vegas, Nevada: Bechtel SAIC Company. ACC: DOC.20031030.0003.

Campbell, G.S. 1977. *An Introduction to Environmental Biophysics.* New York, New York: Springer-Verlag. TIC: 238256.

CRWMS M&O (Civilian Radioactive Waste Management System Management and Operating Contractor) 1997. *Engineering Design Climatology and Regional Meteorological Conditions Report.* B00000000-01717-5707-00066 REV 00. Las Vegas, Nevada: CRWMS M&O. ACC: MOL.19980304.0028.

Flint, A.L. and Childs, S.W. 1987. "Calculation of Solar Radiation in Mountainous Terrain." *Agricultural and Forest Meteorology, 40,* (3), 233–249. Amsterdam, The Netherlands: Elsevier. TIC: 225242.

Flint, A.L. and Childs, S.W. 1991. "Use of the Priestley–Taylor Evaporation Equation for Soil Water Limited Conditions in a Small Forest Clearcut." *Agricultural and Forest Meteorology, 56,* (3–4), 247–260. Amsterdam, The Netherlands: Elsevier. TIC: 241865.

Flint, A.L.; Hevesi, J.A.; and Flint, L.E. 1996. *Conceptual and Numerical Model of Infiltration for the Yucca Mountain Area, Nevada.* Milestone 3GUI623M. Denver, Colorado: U.S. Geological Survey. ACC: MOL.19970409.0087.

Freeze, R.A. and Cherry, J.A. 1979. *Groundwater.* Englewood Cliffs, New Jersey: Prentice-Hall. TIC: 217571.

Hevesi, J.A.; Flint, A.L.; and Flint, L.E. 1994. "Verification of a 1-Dimensional Model for Predicting Shallow Infiltration at Yucca Mountain." *High Level Radioactive Waste Management, Proceedings of the Fifth Annual International Conference, Las Vegas, Nevada, May 22-26, 1994. 4,* 2323–2332. La Grange Park, Illinois: American Nuclear Society. TIC: 210984.

Levitt, D.G.; Sully, M.J.; and Lohrstorfer, C.F. 1996. *Modeling Evapotranspiration from Arid Environments: Literature Review and Preliminary Model Results.* Las Vegas, Nevada: Bechtel Nevada. TIC: 254273.

Linsley, R.K., Jr.; Kohler, M.A.; and Paulhus, J.L.H. 1982. *Hydrology for Engineers.* 3rd Edition. McGraw-Hill Series in Water Resources and Environmental Engineering. New York, New York: McGraw Hill. TIC: 234716.

McNaughton, K.G. and Spriggs, T.W. 1989. "An Evaluation of the Priestley and Taylor Equation and the Complementary Relationship Using Results from a Mixed-Layer Model of the Convective Boundary Layer." *Estimation of Areal Evapotranspiration, Proceedings of an International Workshop Held During the XIXth General Assembly of the International Union of Geodesy and Geophysics at Vancouver, British Columbia, Canada, 9-22 August, 1987. 177,* 89–104. Wallingford, United Kingdom: International Association of Hydrological Sciences. TIC: 245925.

Monteith, J.L. 1965. "Evaporation and the Environment." *The State and Movement of Water n Living Organisms*, *XIXth Symposium. Society for Experimental Biology. 19*, 205–234. Cambridge, United Kingdom: Cambridge University Press. TIC: 235937.

NRC (U.S. Nuclear Regulatory Commission) 2002. *Integrated Issue Resolution Status Report.* NUREG-1762. Washington, D.C.: U.S. Nuclear Regulatory Commission, Office of Nuclear Material Safety and Safeguards. TIC: 253064.

Penman, H. L. 1948. "Natural Evaporation from Open Water, Bare Soil and Grass." *Proceedings of the Royal Society of London. A193*, 120-146. London, United Kingdom: The Royal Society. TIC: 225252.

Priestley, C.H.B. and Taylor, R.J. 1972. "On the Assessment of Surface Heat Flux and Evaporation Using Large-Scale Parameters." *Monthly Weather Review, 100,* (2), 81–92. Washington, DC: U.S. Department of Commerce. TIC: 235941.

Reamer, C.W. 2001. "U.S. Nuclear Regulatory Commission/U.S. Department of Energy Technical Exchange and Management Meeting on Total System Performance Assessment and Integration (August 6 through 10, 2001)." Letter from C.W. Reamer (NRC) to S. Brocoum (DOE/YMSCO), August 23, 2001, with enclosure. ACC: MOL.20011029.0281.

Reamer, C.W. and Williams, D.R. 2000a. Summary Highlights of NRC/DOE Technical Exchange and Management Meeting on Unsaturated and Saturated Flow Under Isothermal Conditions. Meeting held August 16–17, 2000, Berkeley, California. Washington, D.C.: U.S. Nuclear Regulatory Commission. ACC: MOL.20001201.0072.

Reamer, C.W. and Williams, D.R. 2000b. Summary Highlights of NRC/DOE Technical Exchange and Management Meeting on Unsaturated and Saturated Flow Under Isothermal Conditions, October 31–November 2, 2000, Albuquerque, New Mexico. Washington, D.C.: U.S. Nuclear Regulatory Commission. ACC: MOL.20001128.0206.

Schlueter, J. 2003. "Use of Risk as a Basis for Closure of Key Technical Issue Agreements." Letter from J. Schlueter (NRC) to J.D. Ziegler (DOE/YMSCO), January 27, 2003, 0131035890, with enclosure. ACC: MOL.20030227.0018.

Sharpe, S. 2003. *Future Climate Analysis—10,000 Years to 1,000,000 Years After Present.* MOD-01-001 REV 01. Reno, Nevada: Desert Research Institute. ACC: MOL.20030407.0055.

Shuttleworth, W.J. and Wallace, J.S. 1985. "Evaporation from Sparse Crops - An Energy Combination Theory." *Quarterly Journal of the Royal Meteorological Society*, *111*, 839–855. Berkshire, United Kingdom: Royal Meteorological Society. TIC: 235943.

Thompson, R.S.; Anderson, K.H.; and Bartlein, P.J. 1999. *Quantitative Paleoclimatic Reconstructions from Late Pleistocene Plant Macrofossils of the Yucca Mountain Region.* Open-File Report 99-338. Denver, Colorado: U.S. Geological Survey. ACC: MOL.19991015.0296.

USGS (U.S. Geological Survey) 2001a. *Simulation of Net Infiltration for Modern and Potential Future Climates*. ANL-NBS-HS-000032 REV 00 ICN 02. Las Vegas, Nevada: BSC. ACC: MOL.20011119.0334.

USGS 2001b. *Future Climate Analysis.* ANL-NBS-GS-000008 REV 00 ICN 01. Denver, Colorado: U.S. Geological Survey. ACC: MOL.20011107.0004.

USGS 2001c. Software Code: INFIL. V2.0. PC. 10307-2.0-00.

USGS 2001d. Software Code: INFIL. V1.0. PC. 10127-1.0-00.

Ziegler, J.D. 2002. "Transmittal of Information Addressing Key Technical Issue (KTI) Agreement Items Unsaturated and Saturated Flow Under Isothermal Conditions (USFIC) 3.01, and Total System Performance Assessment and Integration (TSPAI) 3.19." Letter from J.D. Ziegler (DOE/YMSCO) to J.R. Schlueter (NRC), July 11, 2002, 0715023334, OL&RC:TCG-1372, with enclosure. ACC: MOL.20020918.0029.

B.5.2   Data, Listed by Data Tracking Number

GS000308311221.010. Developed Daily Climate Data from Tule Lake, California Used for Infiltration Uncertainty Analysis. Submittal date: 03/07/2000.

APPENDIX C

**NEAR-SURFACE LATERAL FLOW EFFECTS ON NET INFILTRATION
(RESPONSE TO TSPAI 3.21 AIN-1)**

Note Regarding the Status of Supporting Technical Information

This document was prepared using the most current information available at the time of its development. This Technical Basis Document and its appendices providing Key Technical Issue Agreement responses that were prepared using preliminary or draft information reflect the status of the Yucca Mountain Project's scientific and design bases at the time of submittal. In some cases this involved the use of draft Analysis and Model Reports (AMRs) and other draft references whose contents may change with time. Information that evolves through subsequent revisions of the AMRs and other references will be reflected in the License Application (LA) as the approved analyses of record at the time of LA submittal. Consequently, the Project will not routinely update either this Technical Basis Document or its Key Technical Issue Agreement appendices to reflect changes in the supporting references prior to submittal of the LA.

APPENDIX C

NEAR-SURFACE LATERAL FLOW EFFECTS ON NET INFILTRATION
(RESPONSE TO TSPAI 3.21 AIN-1)

This appendix provides a response to Key Technical Issue (KTI) agreement Total System Performance Assessment and Integration (TSPAI) 3.21 additional information needed (AIN)-1. This agreement relates to providing additional information on the effects of near-surface lateral flow in the analysis of net infiltration.

C.1   KEY TECHNICAL ISSUE AGREEMENT

C.1.1   TSPAI 3.21 AIN-1

Agreement TSPAI 3.21 was reached during the U.S. Nuclear Regulatory Commission (NRC)/U.S. Department of Energy (DOE) Technical Exchange and Management Meeting on TSPAI held August 6 through 10, 2001, in Las Vegas, Nevada. TSPAI KTI subissues 1, 2, 3, and 4 were discussed at that meeting (Reamer 2001).

The wording of the agreement is as follows:

TSPAI 3.21[1]

> Demonstrate that effects of near surface lateral flow on the spatial variability of net infiltration are appropriately considered (UZ1.5.1). DOE will demonstrate that effects of near surface lateral flow on the spatial variability of net infiltration are appropriately considered in an update to the Simulation of Net Infiltration for Modern and Potential Future Climates AMR (ANL-NBS-HS-000032) and UZ Flow Models and Submodels AMR (MDL-NBS-HS-000006). These AMRs are expected to be available to NRC in FY 2003.

The DOE addressed this agreement and other KTI agreements in a letter report on January 21, 2003, entitled *KTI Letter Report Response to TSPAI 3.18, 3.21, and 3.23, and TEF 2.13* (Ziegler 2003). The initial response to these agreements used a risk-informed approach, and the response was based on sensitivity studies that showed the information to be developed in addressing the KTI agreements would not be significant in determining compliance with individual and groundwater protection standards. The NRC reviewed the response and identified three additional risk program elements that are needed for DOE to make an acceptable case for using risk information to address agreement TSPAI 3.21. This resulted in AIN request TSPAI 3.21 AIN-1 (Schlueter 2003a).

---

[1]UZ1.5.1 in this agreement refers to item 5.1 of NRC integrated subissue UZ1 (NRC 2002, Table 1.1-2). This item addresses the NRC concern that the effect of lateral surface or near-surface flow on net infiltration may be underestimated.

The wording of the TSPAI 3.21 AIN-1 is summarized as follows (Schlueter 2003a, Schlueter 2003b):

- **Agreement Completion Based on Technical Merit**–Additional technical information is needed to complete TSPAI 3.21 based upon technical merit. To complete TSPAI 3.21, DOE could provide the information originally requested in the text of the agreement. For example, net infiltration estimates from portions of the DOE submodel could be compared to estimates obtained using a smaller (e.g., watershed-scale) model that treats overland and near-surface lateral flow using more physically based numerical approaches. A second approach utilizing a technical basis would be to use the multiple lines of field evidence to quantitatively evaluate the range of uncertainty for present-day net infiltration above the repository area and demonstrate that this uncertainty is reasonably bounded by the net infiltration estimates used in total system performance assessments.

- **Agreement Completion Based on Low Risk Significance**–The NRC previously relayed to the DOE that additional information is needed when using risk as a basis to complete KTI agreements. The following three AINs and clarifications represent risk information elements that need to be addressed when using risk information to address agreements:

  1. Enhanced consideration of the combined effect of uncertainties. The combined effect of uncertainties needs to be evaluated before the individual uncertainties can be dropped from further consideration.

  2. Transparent and traceable documentation that allows the results to be verified independently. The DOE should provide an adequate description of the sensitivity analyses completed.

  3. Information pertaining to the variability in the results. Some measure of how the variability of results changes between the different modeled cases is needed, because only the mean results of the stochastic performance assessment simulations have been presented to date. For example, presentation of the 5th and 95th percentiles of annual dose estimates, in addition to the mean dose estimates, would be a satisfactory way of conveying the variability and uncertainty of performance assessment estimates. These information needs apply to DOE sensitivity analyses provided in the response to TSPAI 3.18.

C.1.2 Related Key Technical Issue Agreements

KTI agreements TSPAI 3.23 and TEF 2.13 are related in that they were previously combined with agreements TSPAI 3.18 and TSPAI 3.21 in a risk-informed KTI response based on infiltration sensitivity studies (Ziegler 2003). TSPAI 3.23 was closed by the NRC on the basis of the initial response. TEF 2.13 will be addressed in a separate technical basis document on unsaturated zone flow.

C.2 RELEVANCE TO REPOSITORY PERFORMANCE

The issues that underlie this KTI agreement pertain to the representation of the unsaturated zone flow system. Specifically, these issues are related to shallow infiltration and near-surface lateral flow contributing to the estimation of net infiltration. The direct impact of these issues is on the performance of the unsaturated zone.

TSPAI 3.21 pertains to the effects of near-surface lateral flow on the spatial variability of net infiltration. Lateral flow is modeled to occur as precipitation exceeds the infiltration capacity of a soil column, resulting in surface flow of water to a lower elevation. The effect of lateral flow will be in the areal distribution of infiltration rates.

This issue is related to the estimation of net infiltration, and net infiltration is a major factor in determining the seepage rate of water into the repository. Thus, there will be consequences for other potential barriers, such as effects on chemical environments and corrosion rates of the drip shield, waste package, and waste form, and effects on flow rates in the unsaturated zone and saturated zone beneath the repository.

C.3 RESPONSE

Although *Simulation of Net Infiltration for Modern and Potential Future Climates* (USGS 2001a) was not revised in 2003, it is reasonable to argue that lateral flow is indirectly considered in the net infiltration model and that processes not directly captured in the model are of lesser importance to model performance. This section summarizes the response to KTI agreement TSPAI 3.21, based upon technical merit of field evidence and modeling results. A risk-informed approach was not used to address the response, as provided to the NRC by Ziegler (2003) and as outlined in the AIN (Schlueter 2003a). This approach is valid because, while lateral flow of infiltrating water is common in hillslope soils, it is a transient process generally occurring at short time scales and spatial scales smaller than the 30-by-30-m gridblocks used for estimating net infiltration at Yucca Mountain. As a result, the effect on spatial variability of net infiltration would not be expected to be significant, as any influence should likely be contained within the redistribution portion of the infiltration model within the 30-by-30-m gridblocks. The basis for this response (Section C.4) will demonstrate the following points:

- Lateral subsurface flow may influence the redistribution of moisture and, therefore, infiltration; however, this process most likely occurs within the 30-by-30-m gridblocks.

- Lateral subsurface flow redistribution of water is accounted for indirectly in the water-balance model as mass is conserved at the spatial and temporal scales in the model.

- The potential influence of lateral flow would be expected to be a small percentage change in net infiltration, which is a small total volume of water relative to precipitation.

- Any influence of lateral redistribution on net infiltration would be expected to be secondary to the dominant factors of precipitation, soil moisture storage, evapotranspiration, and gravity drainage in preferential flow pathways.

- Infiltrating water diverted laterally (as subsurface flow) within the soil will experience greater time for evapotranspiration (particularly in depositional valley regions) as the dominant flow vector is upward for a majority of the year. This would suggest that net infiltration estimates not accounting for lateral flow should overestimate water volumes and could, therefore, be a conservative assumption.

These points are reasonable, based on several calculations, model results, and field evidence of specific conditions at the site (USGS 2001a). Each of these points will be discussed in the following sections.

The information in this report is responsive to agreement TSPAI 3.21 and the associated AIN (AIN-1). The report contains the information that DOE considers necessary for NRC review for closure of this agreement.

C.4 BASIS FOR THE RESPONSE

Lateral subsurface flow of infiltrating water is common in hillslope soils and, for the most part, results from slope, vertical anisotropy in soil hydraulic conductivity, or lateral preferential flow pathways (e.g., root channels and macrofauna burrows) (Campbell et al. 2002; Newman et al. 1998; Tsuboyama et al. 1994). As a result of these mechanisms, continuous lateral flow generally occurs at length scales smaller than 10^3 m. This length-based limitation to continuous lateral flow results from the large spatial variability in vertical preferential flow pathways, soil layering, hydraulic conductivities, and topography.

At Yucca Mountain, net infiltration is estimated using the INFIL model (Flint et al. 1996; USGS 2001a) from the first 6 m (on average) as a boundary condition for percolation represented in the unsaturated zone flow in *UZ Flow Models and Submodels* (BSC 2003a). The net infiltration is estimated using water-balance equations in the model discussed in Section C.4.2.1 for base units of 30-by-30-m gridblocks. In this situation, explicitly modeling lateral flow in the soil would not be expected to greatly change the net infiltration estimated from such a large grid water-balance model.

A separate flow-routing routine is included in INFIL V2.0 for lateral surface runoff. The model fully accounts for lateral diversion of surface water as infiltration excess overland flow, or when precipitation exceeds the saturated hydraulic conductivity of the surface soil layer. Surface flow-routing will be discussed in the following sections; however, as it is accounted for in the model, a majority of the following discussion focuses on lateral subsurface flow.

The following sections introduce the site-specific infiltration model developed for Yucca Mountain, focusing on model components relating to lateral subsurface flow and redistribution. Using this background information as the basis for this KTI response, it will be demonstrated that, while lateral flow is not explicitly considered in net infiltration modeling, the water-balance model indirectly accounts for the process (on average) through redistribution and mass conservation. The influence of lateral redistribution on net infiltration is expected to be secondary to the dominant factors of precipitation, soil moisture storage, evapotranspiration, and gravity drainage in preferential flow pathways. Therefore, as near-surface lateral flow is not expected to be significant between the 30-by-30-m gridblocks and is accounted for within the

gridblocks as redistribution, the occurrence of lateral subsurface flow is expected to be rare. As such, the potential influence of lateral flow would likely be only a small percentage change in total infiltration. A small change in total infiltration would amount to only a small volume of water relative to the net infiltration estimates.

C.4.1 Site Characteristics Related to Infiltration and Lateral Flow

Yucca Mountain is located within a transition zone between the northern boundary of the Mojave Desert and the southern boundary of the Great Basin Desert (Flint et al. 1996, pp. 43 to 44). The topography is characterized by isolated, long and narrow, roughly north-south-trending mountain ranges and broad intervening valleys. The topography at Yucca Mountain includes ridgetops (about 7 percent), side slopes (about 47 percent, including footslopes), terraces (about 44 percent), and channels (about 2 percent) (Flint et al. 1996, pp. 38 and 39). The ridgetops generally are flat to gently sloping, with soils 0.5 to 2 m (1.6 to 6.6 ft) thick. Side slopes are characterized by a very thin soil cover, underlain by densely welded or highly fractured bedrock. North-facing mountain side slopes comprise 8 percent of the area and soil depths are typically shallow (10 to 36 cm) to bedrock. Permeability is moderate to moderately rapid, with a moderate to rapid runoff potential. These soils are well drained and have low available water-holding capacity. The majority of the mountain side slopes (27 percent) occur on south-, east-, and west-facing slopes and on moderately sloping alluvial deposits below side slopes. These soils are shallow (10 to 51 cm) to bedrock or to thin duripan over bedrock. They are well to excessively drained and have moderately rapid to rapid hydraulic conductivity and runoff potential, as well as a very low available water-holding capacity. These side-slope soils are the most likely locations with the potential for lateral subsurface flow. Terraces and channels are located at lower elevations of primary washes and have thin soil cover in the upper washes and thick soils farther down. The surface elevations above the site of the repository are approximately 1,400 m. The locations of Yucca Mountain watersheds are shown in Figure C-1.

Yucca Mountain is located in the Amargosa River drainage basin, which is the major tributary drainage area to Death Valley. In exceptionally wet years or following a major storm, streamflow from Yucca Mountain can extend from local drainages to the Amargosa River and then to Death Valley. The Amargosa River and its tributaries are ephemeral streams (i.e., they are dry most of the time), with rarely occurring flow that is in direct response to precipitation and generally not continuing for more than 1 day (USGS 2001a). Along short distances, groundwater discharges at springs into the channel system. Surface water flows have been monitored at numerous sites in the Yucca Mountain region.
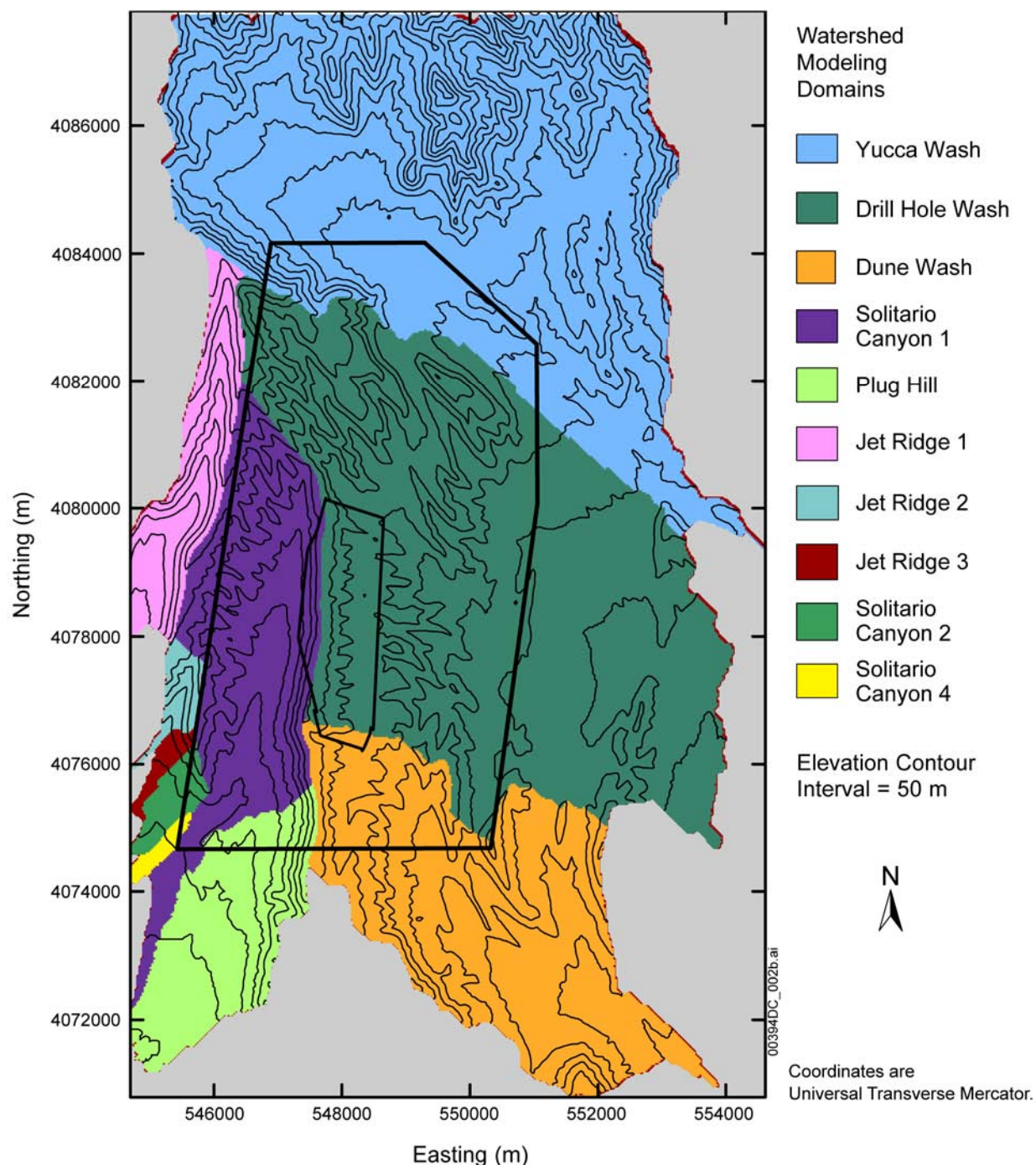
Source: USGS 2001a, Figure 6-12.

Figure C-1.   Location of 10 Watershed Model Domains Included in the Composite Watershed Model
Area Overlying the Area of the Unsaturated Zone Flow and Transport Model

A soil survey of Midway Valley (the location of the North Portal facilities) and the ridges to the
west (Resource Concepts 1989) and a more general soil survey of the entire Yucca Mountain
region identified 17 soil series and seven map units (Resource Concepts 1989). Yucca Mountain
soils are derived from underlying volcanic rocks and mixed alluvium dominated by volcanic

material and, in general, have low water-holding capacities. A detailed description of the soils at Yucca Mountain can be found in Section 1.5.

C.4.2   Net Infiltration Water-Balance Model

C.4.2.1   Daily Water and Energy Balance

The INFIL V2.0 model algorithm consists of three main loops for performing a daily simulation of net infiltration over all model cells comprising a watershed model domain. Figure C-2 illustrates the general model algorithm and the primary loop (day-of-year loop), which is driven by the daily climate input file and carries the simulation through the time domain. Nested within the primary loop is a grid cell loop for performing a daily water-balance calculation at each grid cell location and within each layer of the root zone. The root zone was subdivided into layers based on the estimated maximum depth of bare-soil evaporation and an estimated variation in root density. In general, the layering represents a decrease in root density, with increased depth in the root zone, particularly at locations with thick soils (greater than 6 m). The daily root zone water balance consists of simulating precipitation, snowmelt, sublimation, evapotranspiration, changes in water content for each root zone layer, net infiltration, and runoff generation. Nested within the water balance loop is an hourly loop for modeling potential evapotranspiration based on the simulation of incoming solar radiation and effects on total solar radiation due to blocking ridges using the SOLRAD submodel in INFIL V2.0 and the routine BLOCKR7 (Flint et al. 1996; USGS 2001a).

After the completion of the water balance loop, a surface-water flow-routing subroutine is called if runoff was generated at any grid cell. Surface-water flow is routed at the end of the day as a time-independent (instantaneous) total daily flow depth across each grid cell. The routing algorithm connects all grid cells horizontally using surface-water flow-routing parameters included in the geospatial parameter input file. Surface-water flow is coupled to the water balance calculation by allowing surface water to infiltrate into downstream grid cells according to the available root zone storage capacity, soil hydraulic conductivity, and estimates for effective surface-water flow area and streamflow duration. The infiltrated water is added to the grid cell's antecedent root zone water-content term used in the following day's water balance calculation. The surface-water flow depth routed across the grid cell defining the outflow location of the watershed is converted to a daily mean discharge flow rate, in cubic feet per second, which can be compared to measured streamflow for model calibration.

Based on the flow chart in Figure C-2, the model tends to overestimate net infiltration by not considering (1) upward moisture movement due to drying upper layers and (2) lateral subsurface flow that could be held longer in the soil and, therefore, experience greater evapotranspiration. However, it is also true that the model tends to underestimate net infiltration by not accounting for (1) the downward movement of water when soils are at less than moisture-holding capacity and (2) how subsurface lateral flow could enhance downward preferential flow. However, given the dominance of evapotranspiration in this system, the last two points causing underestimation of net infiltration would be expected to be of lesser importance than the first two points, resulting in an overestimation of net infiltration by the INFIL model.
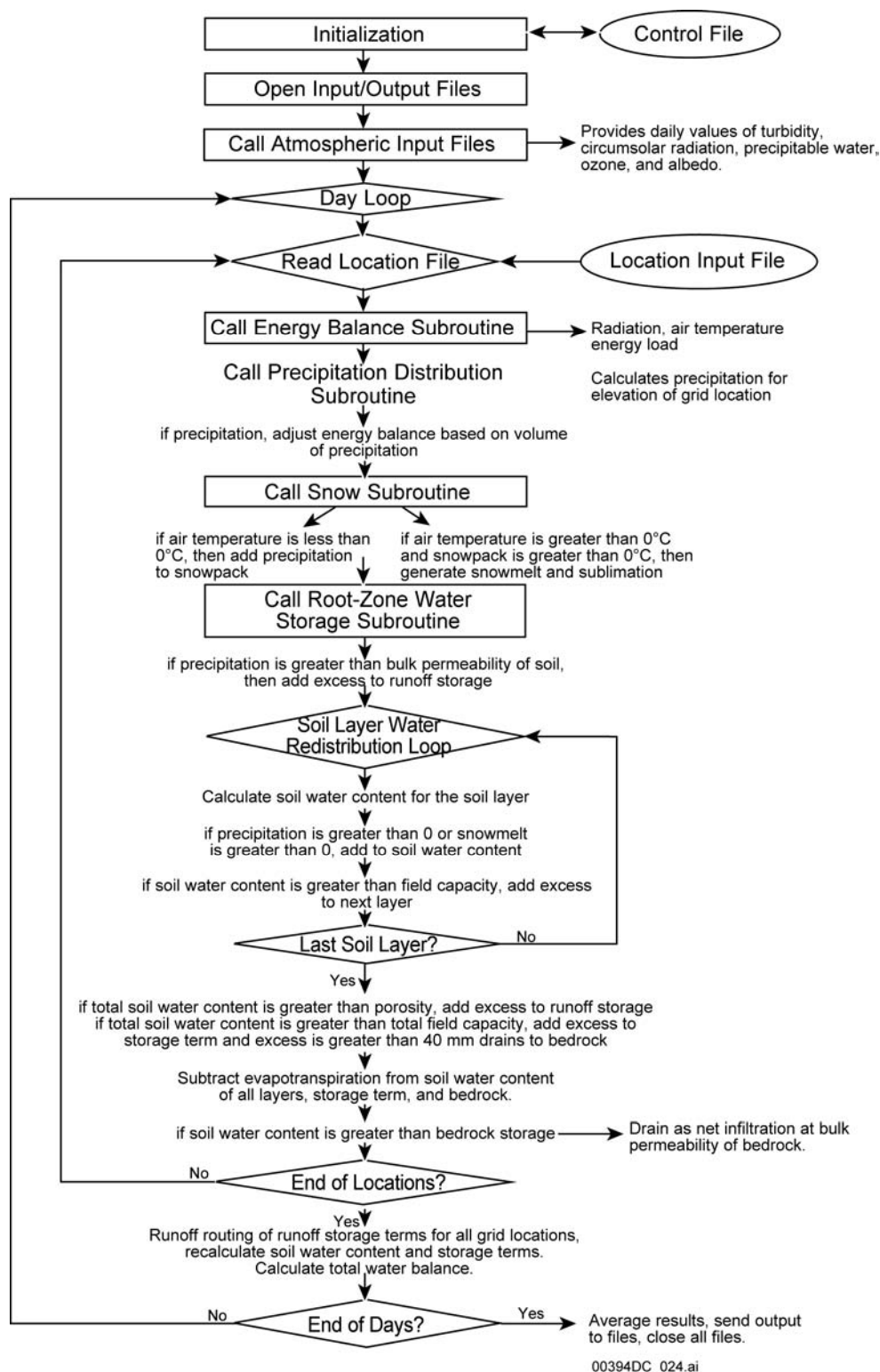
Source: USGS 2001a, Figure 6-7.

Figure C-2. Flow Chart of the Model Algorithm Used for Simulating Net Infiltration

Time-averaged net-infiltration rates are calculated by accumulating the simulated daily net infiltration amounts obtained at the end of the daily water balance loop. Time-averaged rates also are calculated for the remaining components of the water balance (precipitation, snowmelt, sublimation, evapotranspiration, infiltrated run-on, root zone water-content change, and runoff) for all model grid cells and are included in the main output file used for developing the net infiltration results. The time-averaged rates for all components of the water balance simulated at each grid cell are averaged over the watershed model domain and compared against the time-averaged watershed outflow to check the consistency of the simulated water balance for the entire watershed.

Output from INFIL V2.0 also includes spatially averaged daily water balance terms for all components of the water balance. The daily output indicates the average inflow, outflow, and change in storage rates over the area of the watershed being simulated. The spatially averaged daily water balance is compared against the simulated daily outflow to provide a water balance check for each day simulated. The simulated daily water balance rates are averaged over time and compared against the spatially averaged water balance rates simulated at each grid cell as an additional method of checking the consistency of the simulated water balance for the entire watershed.

C.4.2.2 Root Zone Submodel: Infiltration, Percolation, and Redistribution

Water infiltrating and percolating through the multilayered root zone system is modeled as a cascading flow process. Downward percolation is modeled as a forward cascade initiated by adding the total volume of water infiltrating the top layer of the root zone to the antecedent water content of the layer. The new water content is calculated using the layer thickness and compared against the field capacity defined by the grid cell soil type. The volume of water exceeding the field capacity becomes downward percolation that is added to the antecedent water content of the underlying layer, and the new water content of the underlying layer is compared against the field capacity of that layer. If the potential percolation volume exceeds the saturated soil hydraulic conductivity or the saturated bulk bedrock hydraulic conductivity of the underlying layer, the downward percolation rate is set equal to the saturated hydraulic conductivity of the underlying layer, and the excess water volume is added to a temporary storage term for the overlying layer. The process is repeated for each soil and bedrock layer in the root zone (in the case of the model used in this analysis and modeling activity, a maximum of three soil layers and one bedrock layer were used) until the bottom layer is reached, which completes the forward cascade.

The volume of water that has percolated into the bottom bedrock layer (which may be zero if the field capacity of an overlying layer was not exceeded) is compared against the effective root zone storage capacity of the bedrock. If a bedrock layer exists in the root zone, the effective root zone storage capacity of the bedrock layer is calculated based on the estimated root zone depth, the estimated soil depth, and the estimated effective fracture porosity of the rock type. The volume of water exceeding the bedrock storage capacity is the potential net-infiltration volume.

For thick soils, there is no bedrock layer in the root zone. The thickness of the bedrock root zone layer is set to zero, the effective fracture porosity for the bottom bedrock layer becomes zero, and all water exceeding the field capacity of the bottom soil layer (the third soil layer) is potential net

infiltration unless limited by the saturated bulk hydraulic conductivity of the underlying soil or bedrock.

C.4.2.3 Surface-Water Flow

Starting with the bottom root zone layer, a reverse cascade is performed to determine if runoff is generated. The volume of water in the temporary storage term is compared against the total storage capacity of each layer defined by the porosity (or effective fracture porosity in the case of bedrock) and layer thickness. If the volume of water in the temporary storage term exceeds the storage capacity, the excess water is added to the temporary storage term of the overlying layer. The process is repeated until the top layer is reached, completing the reverse cascade. The volume of water in the temporary storage term exceeding the storage capacity of the top layer is added to the potential runoff volume calculated for that grid cell. The final runoff volume is calculated following the simulation of evapotranspiration from the root zone.

At the completion of the root zone water balance loop, the surface-water flow submodel is called if the runoff accumulation term is greater than zero (at least one grid cell has generated runoff). The submodel uses an instantaneous flow routing method to perform an efficient time-independent simulation of surface-water flow. The purpose of the routing algorithm is to calculate the lateral redistribution of water throughout the watershed domain and to allow for the infiltration of surface water as it is routed. The surface water flow routing algorithm is fully coupled with the algorithm used to calculate infiltration into the root zone. The instantaneous flow routing method assumes that the duration of surface water flow at Yucca Mountain is less than 24 hours, which is generally supported by the available streamflow records and field observations (USGS 2001a). For the purpose of calculating daily net infiltration, it is not necessary to perform surface water flow routing at time steps less then the daily water balance, especially when streamflow events are known to be episodic and have durations of less than 24 hours (at least for current climate conditions) (USGS 2001a, p. 42).

Saturated conditions along the active channel are assumed for estimated storm durations of 2 hours for summer storms and 12 hours for winter storms. Positive pressure heads are assumed to be negligible and are not included in the calculation of infiltration volumes. The increase in water content for each layer in the root zone is stored and included in the following day's root zone water balance calculation.

C.4.3 Evidence of Vertical Preferential Flow

Part of the reason that lateral subsurface flow is not continuous over large spatial scales is that it can be short-circuited by vertical preferential flow. There is evidence of vertical preferential flow pathways in the surface soils at Yucca Mountain. Figure C-3 contains water content profiles for a single location measured over time (1993 to 1995). There is clear evidence of vertical zones of deeper water penetration in the first 6 m. Reoccurring preferential flow pathways like these have the potential to short-circuit lateral flow. This short-circuiting does have the potential to increase preferential flow with increasing lateral flow. This possibility has not been experimentally examined. It is possible, however, that the model calibration accounts for this preferential flow occurring within the 30-by-30-m gridblocks.

An additional aspect demonstrated by this figure is the periodic infiltration that is stalled at a given depth. The moisture disappears moving toward the right. This suggests drying of the soil without deeper vertical infiltration. This redistribution process appears to occur on an annual to semiannual timescale, suggesting water flowing laterally locally could potentially undergo redistribution after the gradient created by falling precipitation decreases.
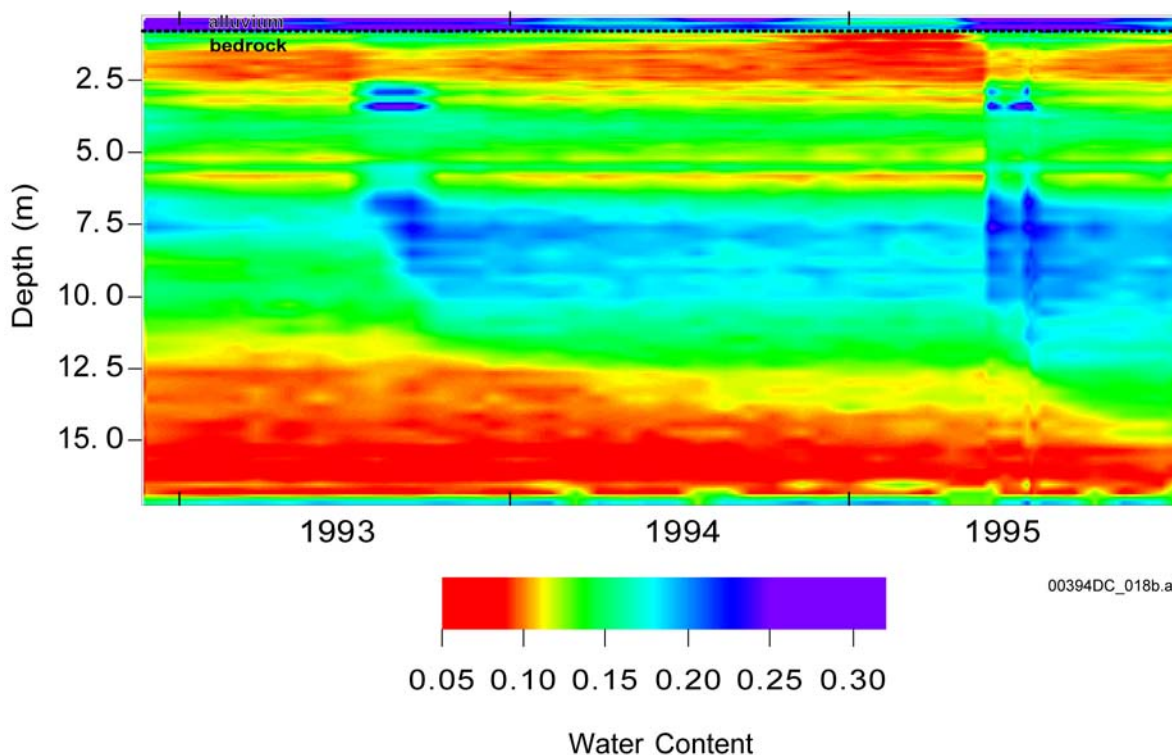
Source: USGS 2001a, Figure 6-4.

Figure C-3. Measured Water-Content Profiles at Borehole USW UZ-N15 for 1993 to 1995

C.4.4 Net Infiltration Boundary Condition

Net infiltration estimates made with the INFIL model are on average less than 10 percent of total annual precipitation under modern climate conditions. Figure C-4 presents predicted net infiltration under modern climate and future climate scenarios made with different models for different annual precipitation levels. Even under the most extreme climate conditions, the net infiltration is still less than 30 percent of precipitation due to water losses to evaporation and soil moisture storage. Under these conditions, even a large lateral flow component would not be expected to alter the net infiltration volumes.
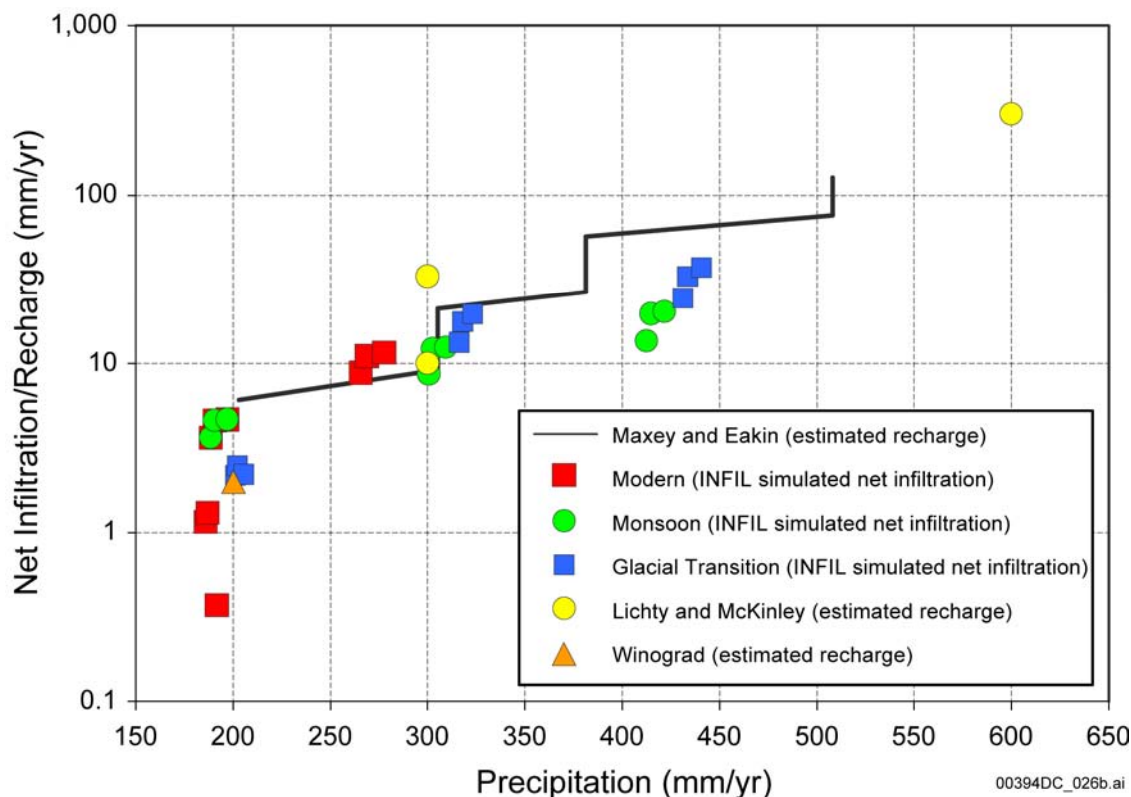
Source: USGS 2001a, Figure 6-41.

Figure C-4. Comparison of INFIL V2.0 Simulated Average Net-Infiltration Rates with an Estimate of the Average Holocene Recharge Rate for the Saturated Zone at Yucca Mountain and with Estimates of Recharge in the Southern Great Basin Obtained Using Alternative Methods

The unsaturated zone model uses net infiltration rates as surface water recharge boundary conditions. The net infiltration rates consist of present-day and future scenarios, determined by studies of modern and future climates (USGS 2001a; USGS 2001b). Nine net infiltration maps are implemented with the unsaturated zone model and its submodels and are documented in *Future Climate Analysis* (USGS 2001b) and *Simulation of Net Infiltration for Modern and Potential Future Climates* (USGS 2001a) for climate and infiltration models. They include present-day (modern), monsoon, and glacial transition—three climatic scenarios, each of which consists of lower-bound, mean, and upper-bound rates. The nine infiltration rates are summarized in Table C-1 for average values over the model domain. The unsaturated zone model is concerned primarily with steady-state flow under each infiltration scenario, while in the climate models, reference to future climates means climates are expected to act sequentially over the modeled period: present day, monsoon, and then glacial transition for specific periods.

Table C-1. Infiltration Rates Averaged over the Unsaturated Zone Model Domain

Scenario	Lower-Bound Infiltration (mm/yr)	Mean Infiltration (mm/yr)	Upper-Bound Infiltration (mm/yr)
Present-Day/Modern	0.24	4.21	10.79
Monsoon	4.21	11.95	19.69
Glacial Transition	1.93	18.64	35.34

Source: BSC 2003b, Table 6-4.

As shown in Table C-1, the average rate over the model domain for the present-day mean infiltration with the unsaturated zone model grid is 4.21 mm/yr (BSC 2003b), which is considered as a base-case infiltration scenario. The use of the lower- and upper-bound infiltration values is intended to cover the uncertainties associated with the infiltration for each climate. The two future climatic scenarios, the monsoon and glacial-transition periods, are used to account for possible climate-induced changes in precipitation and net infiltration. The glacial transition has higher infiltration rates except for the lower-bound case.

Comparison of results from the mean present-day climate conditions to the mean monsoon climate conditions indicates significant changes in the overall water balance, including net infiltration. While average annual precipitation for mean monsoon conditions is about 60 percent greater than that for mean present-day conditions, net infiltration is about 140 percent greater for the monsoon climate. This change in the overall water balance could be caused by the significantly greater infiltration of surface-water run-on during the monsoon climatic conditions (i.e., infiltrated surface-water run-on for mean monsoon conditions is about 155 percent greater than that for mean present-day conditions). Furthermore, the greater influence of infiltrated surface-water run-on in channels is apparent in the substantially greater average annual outflow as streamflow associated with the monsoon climate (i.e., average annual outflow for mean monsoon conditions is 25 times that for mean present-day conditions). Under monsoon conditions, snowfall and surface-water run-on in channels will increase. For the mean monsoon climate scenario, average precipitation is 309.3 mm/yr, average outflow as streamflow is 13.2 mm/yr, and average net infiltration is estimated to be 11.95 mm/yr. For the upper-bound monsoon climate, average precipitation is 421.6 mm/yr, outflow as streamflow is 25.1 mm/yr, and net infiltration is 19.69 mm/yr over the area of the repository.

The greater net infiltration rates are within the higher elevation areas with higher precipitation and thinner soils (USGS 2001a, Section 6.11.1). Figure C-5 illustrates the spatial distribution of precipitation, and Figure C-6 demonstrates the net infiltration for the mean present-day climate. Net infiltration of greater than 100 mm/yr occurs throughout the steep, northeast facing slope of The Prow, caused by the combined effect of high precipitation, reduced evapotranspiration, frequent surface-water run-on at the area of very thin soils, and the high permeability of nonwelded bedrock. High net infiltration also occurs in the upper channels of Solitario Canyon and Drill Hole Wash, Pagany Wash, and Abandoned Wash. Maximum net infiltration of more than 100 mm/yr occurs within isolated areas on side slopes and in channels with thin soils and high-permeability bedrock. However, total net infiltration within the domain of the unsaturated zone flow and transport model is dominated by the lower rates of 1 to 20 mm/yr on side slopes and ridgetops, which make up much of the unsaturated zone flow and transport model domain.
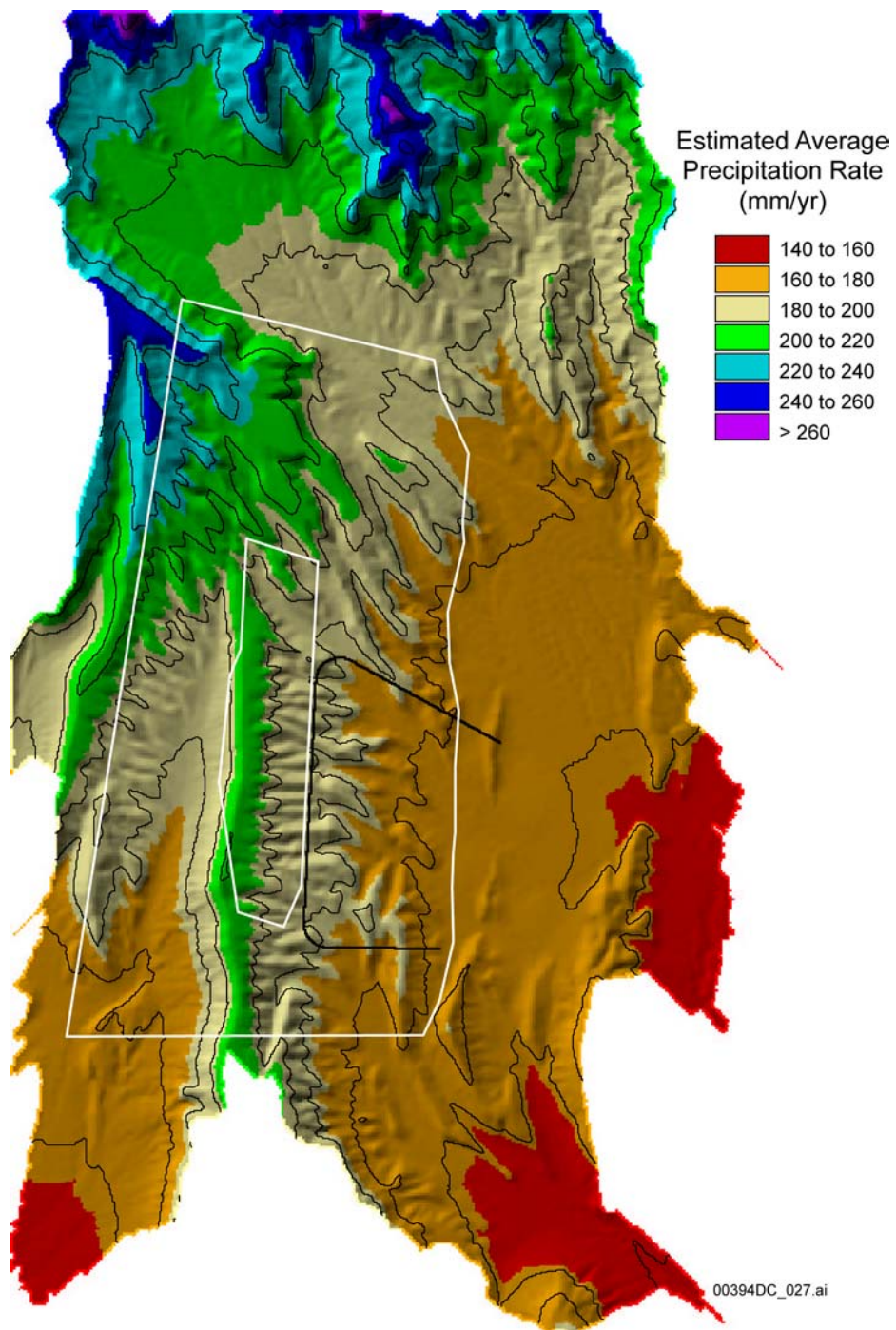
Source: USGS 2001a, Figure 6-23.

Figure C-5. Estimated Precipitation for the Mean Modern Climate Scenario

Mean Modern Climate
Net Infiltration (mm/yr)

⬜	0
🟪	< 1
🟥	1 to 5
🟧	5 to 10
🟨	10 to 20
🟩	20 to 50
🟦	50 to 100
🟦	100 to 500
🟪	500 to 1,000
🟪	>1,000

N

00394DC_028a.ai
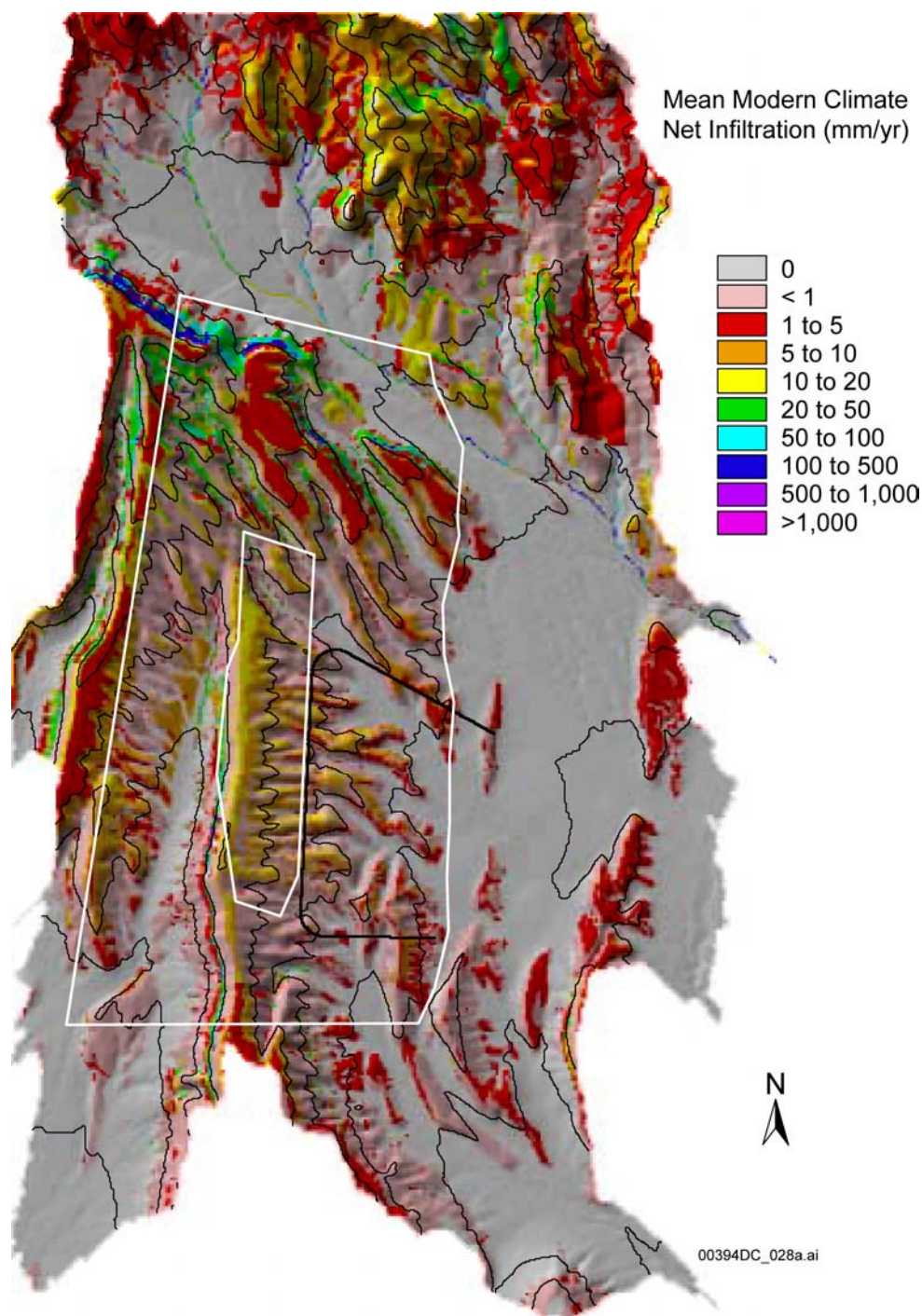
Source: USGS 2001a, Figure 6-26.

Figure C-6. Estimated Net Infiltration for the Mean Modern Climate Scenario

There is a high correlation between the precipitation and net infiltration maps in Figures C-5 and C-6. As net infiltration is on average less than 10 percent of the total precipitation, a majority of the net infiltration estimates for the domains overlying the repository experience less than 10 mm/yr net infiltration. As mentioned, the lateral surface runoff, lower evapotranspiration, higher precipitation, and soils of higher hydraulic conductivity contribute to a small zone of

greater net infiltration on the western side slope. This illustrates the relative dominance of these factors on overall net infiltration.

Figure C-6 also demonstrates the relatively low spatial variability in net infiltration using the 30-by-30-m gridblock size. These factors suggest that if significant lateral subsurface flow were to occur, it would decrease the net infiltration in the ridgetops and increase the amount of water in the valleys. This would not be likely to increase net infiltration in the valleys, however, as the soils tend to be thicker with great storage capacity, with more opportunity for redistribution and evapotranspiration to result in losses. Therefore, on side slopes, the lack of explicit lateral flow in the infiltration model, if the lateral flow was significant enough to surpass the 30-by-30-m gridblocks, could be considered a conservative assumption.

C.4.5   Relationships to Lateral Flow

The details discussed in the previous sections and in *Simulation of Net Infiltration for Modern and Potential Future Climates* (USGS 2001a) provide evidence for the points made in Section C.3. The following sections address some of the specific relationships between lateral flow and the net infiltration estimate for Yucca Mountain.

C.4.5.1   Lateral Flow in Relation to Gridblock Size

Lateral subsurface flow would not be expected to exceed the 30-by-30-m gridblocks, in most cases, based on the following analysis. Given a land surface slope of approximately 4° to 6°, the sine of the gravity vector is 0.07 to 0.10. The saturated hydraulic conductivity of the alluvium soil units 7 and 5 (USGS 2001a, Attachment IV, Table IV-4) is 5.6×10^{-6} m/s to 6.7×10^{-6} m/s, and the porosity is 35 percent. Hydraulic conductivity values of the soils range from 3.8×10^{-5} to 6.7×10^{-6} m/s, and the porosity ranges from 28.1 to 37.0 percent (USGS 2001a, Attachment IV, Table IV-4). Using Darcy's equation and assuming fully saturated flow in a lateral downslope direction with a perched system at the bedrock–alluvium contact that parallels the soil surface, the distance that lateral flow would travel in 30 days is approximately 3 to 6 m, thereby not moving beyond the 30-by-30-m gridblock area. If the slope were 45°, the distance would be an order of magnitude greater (USGS 2001a, p. 17); however, as the maximum slope value is 47° (USGS 2001a, p. IX-5) and a majority of the slope values are less than 30° (USGS 2001a, Figure IX-1), most lateral flow would not be likely to occur on a scale greater than 30 m. However, in areas with high hydraulic conductivity and high slope, isolated lateral flow beyond the minimum 30-m scale is possible. Given the other model components and the limited number of locations where this could occur, the total volume of that lateral flow is not likely to be significant.

According to Hatton (1998), one-dimensional, distributed-parameter, water-balance models are appropriate for use unless the excess rainfall generates overland flow (which, in this case, is accommodated by flow routing in INFIL V2.0) or with the development of saturated conditions in soil profiles on slopes. The above calculation, and the fact that slopes have very thin soil cover and the underlying fractured bedrock has a relatively high saturated hydraulic conductivity, negate this as a significant concern. On the other hand, if water were to move from one gridblock downslope to the next gridblock at the soil–bedrock contact in a three-dimensional model configuration, this volume would be additive and would continue downslope until the

slope was reduced, resulting in a shorter lateral travel distance. The total slope would only be affected in the uppermost and lowermost gridblocks. The contribution of this type of lateral flow to the spatial variability of net infiltration is expected to be insignificant relative to the spatial resolution required for the site-scale unsaturated zone groundwater flow model.

C.4.5.2   Lateral Flow as Redistribution within Gridblocks

As discussed in Section C.4.2.2, redistribution processes are accounted for in a general sense within the 30-by-30-m gridblocks using a cascading time-step approach. Any lateral subsurface flow processes that might have occurred within a given gridblock would be included in the net infiltration estimate for that particular gridblock. As such, the minimum spatial resolution of the model is 30 by 30 m. In addition, the water-balance equation is solved on a daily time scale, which is longer than the average streamflow (and thus storm) duration (USGS 2001a).

With this minimum resolution, lateral flow processes would not be expected to significantly alter the spatial and temporal variability of net infiltration. Lateral flow is rapid within the storm process, generally occurring at smaller than hillslope scale (10^3 m). It is reasonable to assume that the spatial and temporal variability caused by lateral flow is not an issue at the spatial and temporal resolution of the Yucca Mountain infiltration model. Lateral flow that occurs at a larger scale than the 30-by-30-m gridblock is addressed in Section C.4.5.3.

C.4.5.3   Side-Slope Soil Depth and Lateral Flow

As the side slopes and footslopes comprise about 47 percent of the Yucca Mountain area, these slopes have the greatest potential for lateral flow. Of this 47 percent area, approximately 27 percent is composed of the south-, west-, and east-facing slopes. In addition, these are shallow, well-drained slopes, some underlain with fractured bedrock and some with relatively cemented bedrock. Within the repository footprint, the greatest subsurface lateral flow is expected to occur at its western boundary, where the net infiltration rates are generally highest (Figure C-6). If lateral flow were to occur at a scale larger than the 30-by-30-m gridblock size, then it would likely occur as flow at the bedrock–soil interface in these slopes (Scanlon et al. 1999; Newman et al. 1998). The most likely result of such lateral flow would be redistribution of water from slopes to the valley regions.

However, net infiltration estimates in the valleys are very low (some essentially zero). This result occurs due to the depth of the soils and the corresponding soil moisture storage capacity (USGS 2001a). Given that evapotranspiration dominates the flux direction of water for a majority of the year, the deeper soils prevent infiltration to the bedrock as more time is allowed for losses to the atmosphere. Water stored in the soil that remains longer than the storm is more likely to eventually move upward under the evaporative gradient. This is shown by the drying pattern in Figure C-3.

Under these conditions, ignoring lateral flow on the slopes at Yucca Mountain is a conservative assumption. This is because water that would have been lost to lateral flow and evapotranspiration in the deep valley soils is assumed to contribute to the net infiltration volume estimate. Therefore, if significant lateral flow did occur on these slopes, it would only decrease

net infiltration beneath the soils on those slopes and not change estimates of net infiltration in the valleys.

C.4.6   Conclusions

This document has demonstrated that lateral flow of infiltrating water at Yucca Mountain is a process generally occurring at a scale smaller than the gridblocks used for estimating net infiltration. Using Darcy's equation and assuming fully saturated flow in a lateral downslope direction with a perched system at the bedrock–alluvium contact that parallels the soil surface, the distance that lateral flow would travel in 30 days is approximately 3 to 6 m under low slope conditions, thereby not moving beyond the minimum gridblock area. Lateral subsurface flow redistribution of water is accounted for indirectly in the water-balance model as mass is conserved and spatial and temporal resolution are relatively large. The potential influence of lateral flow that does occur would likely be a small percent change in net infiltration, which is a small total volume of water relative to precipitation. Any influence of lateral redistribution on net infiltration would be expected to be secondary to the dominant factors of precipitation, soil moisture storage, evapotranspiration, and gravity drainage in preferential flow pathways.

C.5   REFERENCES

BSC (Bechtel SAIC Company) 2003a. *UZ Flow Models and Submodels.* MDL-NBS-HS-000006 REV 01. Las Vegas, Nevada: Bechtel SAIC Company. ACC: DOC.20030818.0002.

BSC 2003b. *Analysis of Infiltration Uncertainty.* ANL-NBS-HS-000027 REV 01. Las Vegas, Nevada: Bechtel SAIC Company. ACC: DOC.20031030.0003.

Campbell, C.G.; Ghodrati, M.; and Garrido, F. 2002. "Using Time-Domain Reflectometry to Characterize Shallow Solute Transport in an Oak Woodland Hillslope in Northern California, USA." *Hydrological Processes, 16,* 2921–2940. TIC: 255447.

Flint, A.L.; Hevesi, J.A.; and Flint, L.E. 1996. *Conceptual and Numerical Model of Infiltration for the Yucca Mountain Area, Nevada.* Milestone 3GUI623M. Denver, Colorado: U.S. Geological Survey. ACC: MOL.19970409.0087.

Hatton, T. 1998. *Catchment Scale Recharge Modelling.* Part 4 of the *Basics of Recharge and Discharge*. Zhang, L ed. Collingwood, Victoria, Australia: CSIRO Publishing. TIC: 247711.

Newman, B.D; Campbell, A.R.; and Wilcox, B.P. 1998. "Lateral Subsurface Flow Pathways in a Semiarid Ponderosa Pine Hillslope." *Water Resources Research, 34*, (12), 3,485–3,496. Washington, D.C.: American Geophysical Union. TIC: 252308.

NRC (U.S. Nuclear Regulatory Commission) 2002. *Integrated Issue Resolution Status Report.* NUREG-1762. Washington, D.C.: U.S. Nuclear Regulatory Commission, Office of Nuclear Material Safety and Safeguards. TIC: 253064.

Reamer, C.W. 2001. "U.S. Nuclear Regulatory Commission/U.S. Department of Energy Technical Exchange and Management Meeting on Total System Performance Assessment and Integration (August 6 through 10, 2001)." Letter from C.W. Reamer (NRC) to S. Brocoum (DOE/YMSCO), August 23, 2001, with enclosure. ACC: MOL.20011029.0281.

Resource Concepts 1989. *Soil Survey of Yucca Mountain Study Area, Nye County, Nevada.* NWPO EV 003-89. Carson City, Nevada: Resource Concepts. TIC: 206227.

Scanlon, B.R.; Langford, R.P.; and Goldsmith, R.S. 1999. "Relationship between Geomorphic Settings and Unsaturated Flow in an Arid Setting." *Water Resources Research, 35*, (4), 983– 999. Washington, D.C.: American Geophysical Union. TIC: 252295.

Schlueter, J.R. 2003a. "Review of Documents Pertaining to Agreement Total System Performance Assessment and Integration (TSPAI).3.21 (Status: Need Additional Information)." Letter from J.R. Schlueter (NRC) to J.D. Ziegler (DOE/ORD) May 9, 2003, with enclosure. ACC: MOL.20030603.0305.

Schlueter, J. 2003b. "Use of Risk as a Basis for Closure of Key Technical Issue Agreements." Letter from J. Schlueter (NRC) to J.D. Ziegler (DOE/YMSCO), January 27, 2003, with enclosure. ACC: MOL.20030227.0018.

Tsuboyama, Y.; Sidle, R.C.; Noguchi, S.; and Hosoda, I. 1994. "Flow and Solute Transport through the Soil and Macropores of a Hillslope Segment." *Water Resources Research, 30*, (4), 879–890. Washington, D.C.: American Geophysical Union. TIC: 252320.

USGS (U.S. Geological Survey) 2001a. *Simulation of Net Infiltration for Modern and Potential Future Climates.* ANL-NBS-HS-000032 REV 00 ICN 02. Denver, Colorado: U.S. Geological Survey. ACC: MOL.20011119.0334.

USGS 2001b. *Future Climate Analysis.* ANL-NBS-GS-000008 REV 00 ICN 01. Denver, Colorado: U.S. Geological Survey. ACC: MOL.20011107.0004.

Ziegler, J.D. 2003. "Transmittal of Report Addressing Key Technical Issue (KTI) Agreement Items Total System Performance Assessment and Integration (TSPAI) 3.18, 3.21, and 3.23 and Thermal Effects on Flow (TEF) 2.13." Letter from J.D. Ziegler (DOE/ORD) to J.R. Schlueter (NRC), January 21, 2003, 0122035753, OLA&S:TCG-0379, with enclosure. ACC: MOL.20030605.0224.

INTENTIONALLY LEFT BLANK

APPENDIX D

**MONTE CARLO ANALYSIS OF INFILTRATION UNCERTAINTY
(RESPONSE TO USFIC 3.01 AIN-1)**

Note Regarding the Status of Supporting Technical Information

This document was prepared using the most current information available at the time of its development. This Technical Basis Document and its appendices providing Key Technical Issue Agreement responses that were prepared using preliminary or draft information reflect the status of the Yucca Mountain Project's scientific and design bases at the time of submittal. In some cases this involved the use of draft Analysis and Model Reports (AMRs) and other draft references whose contents may change with time. Information that evolves through subsequent revisions of the AMRs and other references will be reflected in the License Application (LA) as the approved analyses of record at the time of LA submittal. Consequently, the Project will not routinely update either this Technical Basis Document or its Key Technical Issue Agreement appendices to reflect changes in the supporting references prior to submittal of the LA.

APPENDIX D

MONTE CARLO ANALYSIS OF INFILTRATION UNCERTAINTY
(RESPONSE TO USFIC 3.01 AIN-1)

This appendix provides a response to the Key Technical Issue (KTI) agreement entitled Unsaturated and Saturated Flow under Isothermal Conditions (USFIC) 3.01 additional information needed (AIN)-1. This agreement relates to providing documentation sources and schedule for the Monte Carlo analysis of infiltration uncertainty.

D.1   KEY TECHNICAL ISSUE AGREEMENT

D.1.1   USFIC 3.01 AIN-1

Agreement USFIC 3.01 was reached during the U.S. Nuclear Regulatory Commission (NRC)/U.S. Department of Energy (DOE) Technical Exchange and Management Meeting on USFIC on October 31 to November 2, 2000 (Reamer and Williams 2000a), in Albuquerque, New Mexico. USFIC Subissue 3, Present-Day Shallow Groundwater Infiltration, was discussed at that meeting.

At the NRC/DOE Technical Exchange and Management Meeting on USFIC in August 2000 in Berkeley, California (Reamer and Williams 2000b), and the follow-up Technical Exchange and Management Meeting (Reamer and Williams 2000a), the NRC was concerned that the representations of the upper bounds of the infiltration model for the present-day, monsoon, and glacial-transition climates would underestimate infiltration and, therefore, underestimate dose. The NRC indicated that one approach would be to perform Monte Carlo analyses, similar to those performed for the glacial-transition climate in *Analysis of Infiltration Uncertainty* (CRWMS M&O 2000), and to base upper-bound infiltration estimates for each climate on, for example, the upper 90th percentile (Reamer and Williams 2000a).

In the October/November 2000 technical exchange, the DOE agreed to provide documentation sources and a schedule for the Monte Carlo analyses for analyzing infiltration (Reamer and Williams 2000a). The DOE initial plan to address the NRC concerns included the following elements: (1) developing an upper-bound infiltration case based on the Monte Carlo analysis for the glacial-transition climate; the upper bound was to be based on the 90th percentile case from the Monte Carlo analysis and new weighting factors for the lower bound, mean, and upper bound cases was to be based on the previously documented methodology (CRWMS M&O 2000); (2) develop upper-bound infiltration cases for the monsoon and present-day climates by proportional scaling based on the average infiltration ratio between the upper bound and mean cases for the glacial-transition climate; and (3) incorporate the new infiltration maps and weighting factors into the models that support total system performance assessment (TSPA) for the license application. The NRC agreed with the approach of the Monte Carlo analysis and the use of the 90th percentile.

The wording of the agreement is as follows:

USFIC 3.01

> Provide the documentation sources and schedule for the Monte Carlo method for analyzing infiltration. DOE will provide the schedule and identify documents expected to contain the results of the Monte Carlo analyses in February 2002.

The DOE submitted the initial response to this agreement in July 2002 (Ziegler 2002), using results of risk sensitivity studies as an alternative approach to meeting the agreement. Results of the sensitivity studies showed that postclosure performance objectives would be met and that the information that would be developed to address USFIC 3.01 is not important to the repository performance. NRC staff subsequently provided review comments on the DOE initial response to USFIC 3.01 and identified three additional risk program elements that are needed as part of DOE's initiative to address KTI agreements by providing risk information in lieu of other information originally agreed upon (Schlueter 2003). This resulted in AIN request USFIC 3.01 AIN-1 (Schlueter 2003).

The wording of the AIN can be summarized as follows:

- The following three AINs and clarifications represent risk information elements that need to be addressed when using risk information to address agreements:

    1. Enhanced consideration of the combined effect of uncertainties. The combined effect of uncertainties needs to be evaluated before the individual uncertainties can be dropped from further consideration.

    2. Transparent and traceable documentation that allows the results to be verified independently. The DOE should provide an adequate description of the sensitivity analyses completed.

    3. Information pertaining to the variability in the results. Some measure of how the variability of results changes between the different modeled cases is needed, because only the mean results of the stochastic performance assessment simulations have been presented to date. For example, presentation of the 5th and 95th percentiles of annual dose estimates, in addition to the mean dose estimates, would be a satisfactory way of conveying the variability and uncertainty of performance assessment estimates.

D.1.2   Related Key Technical Issue Agreements

KTI agreement USFIC 3.02 is related to USFIC 3.01 in that they both concern the infiltration uncertainty analysis. USFIC 3.02 requires DOE to provide additional justification of the technical basis for the parameters used in the infiltration uncertainty analysis. A response to agreement USFIC 3.02 is provided in Appendix E.

D.2 RELEVANCE TO REPOSITORY PERFORMANCE

The infiltration model provides estimates of infiltration flux that are used as top boundary conditions in the development of unsaturated zone flow fields in TSPA (Wu et al. 1997; BSC 2003a). The infiltration uncertainty analysis using the Monte Carlo method provides the weighting factors for the glacial-transition climate that are applied to the unsaturated zone flow fields in TSPA. In addition, the Monte Carlo analyses provide quantitative and qualitative information that supports the description of the surficial soils and topography, one of the natural barriers to downward infiltration. The use of the net infiltration weighting factors developed for the glacial-transition climate for the 10,000-year compliance period provides additional conservatism in TSPA for the license application, needed to avoid underestimating net infiltration and the potential radiological dose used to assess repository performance.

D.3 RESPONSE

This response presents the technical information related to agreement USFIC 3.01 and the associated AIN (AIN-1). Thus, the AIN asking for a risk-based approach is not applicable for this response. The report contains the information that the DOE considers necessary for NRC review for closure of this agreement.

Goals of Investigations–*Analysis of Infiltration Uncertainty* (BSC 2003b) was prepared to (1) develop uncertain input parameter distributions, (2) evaluate the net infiltration distribution over the repository footprint, and (3) determine weighting factors for net infiltration (i.e., the probabilities of the range of net infiltration rates) for the lower-bound, mean, and upper-bound glacial-transition climates. These calculations were performed using infiltration rate maps developed in *Simulation of Net Infiltration for Modern and Potential Future Climates* (USGS 2001a), which were based on meteorological data from analog sites (USGS 2001b) and spatially averaged values (USGS 2001a).

The glacial-transition climate was selected for assessing infiltration uncertainty because it would dominate most of the 10,000 years of the Yucca Mountain performance period and the 20,000-year TSPA calculation period (USGS 2001a). The calculations for the net infiltration distribution of the present-day and monsoon climates were performed in *Simulation of Net Infiltration for Modern and Potential Future Climates* (USGS 2001a). The weighting factors developed for the glacial-transition climate were used because the glacial-transition climate is wetter than the present-day and monsoon climates.

Types of Uncertainties Considered–Two types of uncertainty in the evaluation of net infiltration were considered: epistemic and aleatoric uncertainties. Epistemic uncertainty arises from lack of knowledge about parameters, because the data are limited, or because alternative interpretations of the available data exist. This type of uncertainty can be reduced because the state of knowledge about the processes and parameters can be improved by further characterization and data collection. As a consequence, epistemic uncertainty can also be referred to as reducible uncertainty.

Aleatoric uncertainty arises from the existence of spatial and temporal variability or randomness of heterogeneous subsurface media, affecting flow processes and model parameters. This type of

uncertainty cannot be reduced through further testing and data collection; consequently, this type of uncertainty is also referred to as irreducible uncertainty. It can typically be accounted for using geostatistical approaches (e.g., using appropriate probability distribution functions) (Rechard 1996, p. 4-3) with the range of values and a distribution type of model input parameters.

In general, uncertain input parameters are assigned using known site characterization data, expert judgment, and analog site data records. Because both epistemic and aleatoric uncertainties are incorporated into models, the resulting uncertainty is considered as combined epistemic-aleatoric uncertainty.

The upper limit of the 99th percentile for the uncertain input parameters exceeds that (90th percentile) which was discussed at the NRC/DOE Technical Exchange and Management Meeting on USFIC in August 2000 in Berkeley, California (Reamer and Williams 2000b), in order to cover a larger range of the net infiltration distribution (BSC 2003b).

Types of Uncertain Parameters–The net infiltration uncertainty analysis for the glacial-transition climate was performed to assess a combined effect of 12 uncertain input parameters, which are characterized with corresponding probability density functions. Parameters selected for development of uncertainty distributions include effective bedrock porosity, bedrock root-zone thickness, soil depth, precipitation, potential evapotranspiration, bulk bedrock saturated hydraulic conductivity, soil saturated hydraulic conductivity, two parameters associated with bare-soil evaporation, and effective surface-water flow area (BSC 2003b, Section 4.1.1). Two additional parameters related to sublimation and melting of snow cover were included for the glacial-transition climate (BSC 2003b, Section 4.1.1). The mean values for these 12 uncertain parameters are summarized in Tables D-1 and D-2.

Table D-1. Types of Uncertain Input Parameters for Glacial-Transition Climate

Parameter Identifier	Parameter
BRPERM	Bedrock bulk saturated hydraulic conductivity (multiplier)
BRPOROS	Bedrock effective root-zone porosity
BRZDEPTH	Bedrock root-zone thickness
ETCOEFFA	First coefficient in expression for evapotranspiration
ETCOEFFB	Second coefficient in expression for evapotranspiration
FLAREA	Surface flow runoff area
POTETMUL	Daily evapotranspiration (multiplier)
PRECIPM	Daily precipitation (multiplier)
SNOPAR1	Snow-melt parameter
SOILDEPM	Soil zone thickness (multiplier)
SOILPERM	Soil saturated hydraulic conductivity (multiplier)
SUBPAR1	First term ("A1") in snow loss (sublimation) equation for temperature regime below freezing (i.e., $Tk \leq 0.0°C$)

Source: BSC 2003b, Table 6-1.

Table D-2. Uncertain Input Parameter Distributions Used for the Simulation of Net Infiltration for Glacial-Transition Climate

Parameter Identifier	Mean	Low Range	High Range	Distribution Type	Units
BRPERM	1.00	0.10	10.0	Lognormal	None
BRPOROS	0.009	0.002	0.024	Normal	None
BRZDEPTH	1.50	0.00	3.00	Normal	Meters
ETCOEFFA	-10.0	-0.10	-19.9	Normal	None
ETCOEFFB	1.04	0.54	1.54	Normal	None
FLAREA	0.25	0.01	0.49	Normal	None
POTETMUL	1.00	0.60	1.40	Normal	None
PRECIPM	1.00	0.60	1.40	Normal	None
SNOPAR1	1.78	0.78	2.78	Uniform	None
SOILDEPM	1.00	0.10	1.90	Normal	None
SOILPERM	1.00	0.10	10.0	Lognormal	None
SUBPAR1	0.10	0.00	0.20	Uniform	None

Source: BSC 2003b, Table 6-2.

NOTE: Parameter identifiers are defined in Table D-1.

Repository Footprint–A set of four contiguous rectangles (Figure D-1) was used to approximate the repository footprint. The repository footprint coordinates required to assess the spatially averaged infiltration rate were taken from the Universal Transverse Mercator coordinates supplied by *Repository Design, Repository/PA IED Subsurface Facilities* (BSC 2003c) and shown in Figure D-1. (Note that the repository footprint was modified in 2003 and is different from that used in *Analysis of Infiltration Uncertainty* (CRWMS M&O 2000) and in *Simulation of Net Infiltration for Modern and Potential Future Climates* (USGS 2001a).) However, the modification to the footprint does not impact the resulting statistical parameters of the net infiltration distribution analysis.
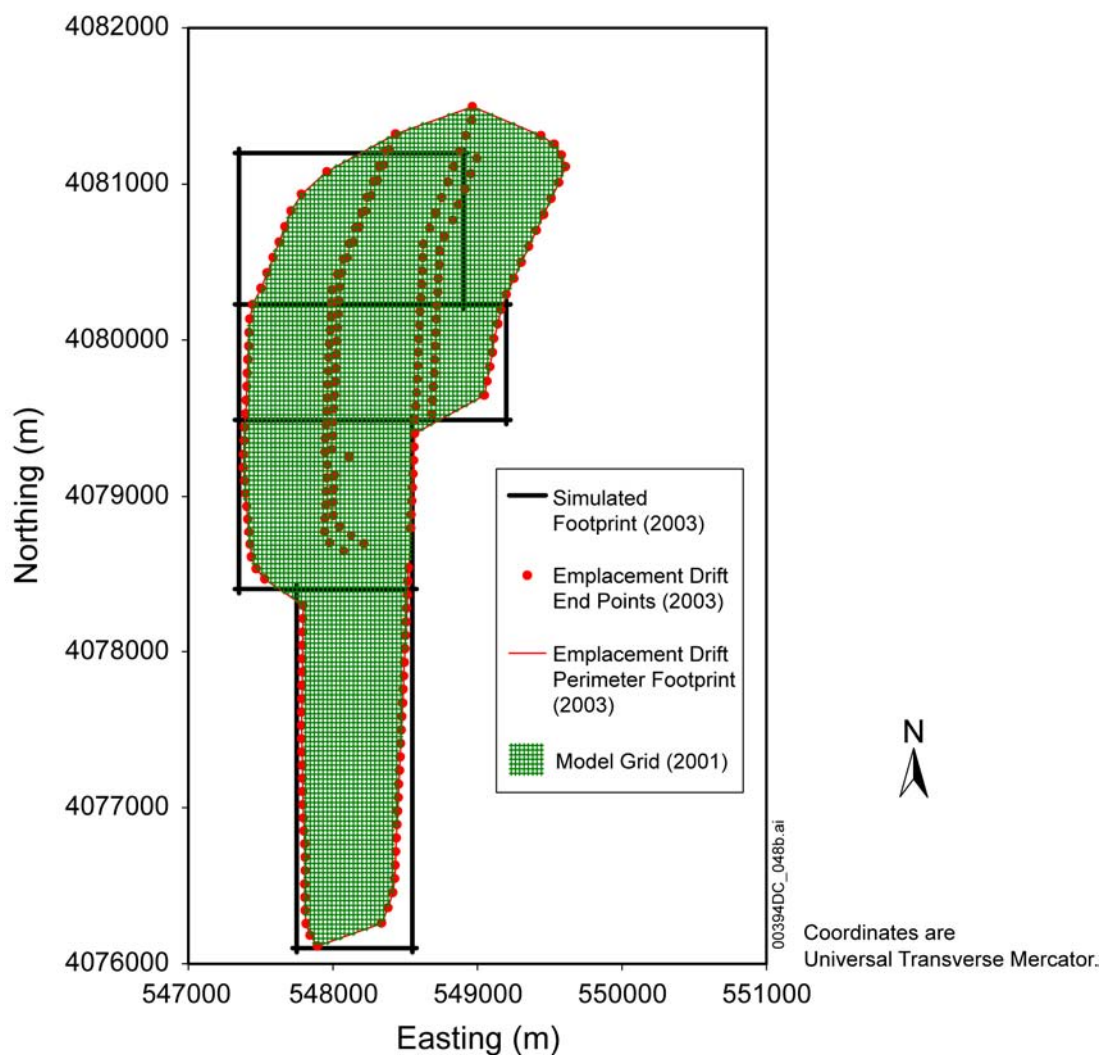
Source: BSC 2003b.

NOTE: The simulated footprint is from *Analysis of Infiltration Uncertainty* (BSC 2003b) and was used in uncertainty analysis of infiltration. UTM coordinates were supplied by *Repository Design, Repository/PA IED Subsurface Facilities* (BSC 2003c). The original coordinates, in Nevada state plane coordinates (central zone) with meters as units, were converted to UTM coordinates using EARTHVISION V5.1 (STN: 10174-5.1-00). The repository perimeter schematic and emplacement drift end points are from *Repository Design, Repository/PA IED Subsurface Facilities* (BSC 2003d). The model grid from *Simulation of Net Infiltration for Modern and Potential Future Climates* (USGS 2001a) was superimposed onto the 2003 repository perimeter. The schematic is for illustrative purposes only. The northeast portion of the repository was not included in calculations because of the lack of input data for this area, which, however, did not affect the estimations of the spatially averaged net infiltration over the repository footprint (see BSC 2003b, Section 6.1.3 and Attachment IV).

Figure D-1. Modeled Region and Repository Footprint

A detailed description of watersheds covering the repository footprint and used for simulations can be found in *Simulation of Net Infiltration for Modern and Potential Future Climates* (USGS 2001a) and *Analysis of Infiltration Uncertainty* (BSC 2003b).

The inputs required for this calculation are the infiltration rate maps calculated by the U.S. Geological Survey for the lower-bound, mean, and upper-bound glacial-transition climates (BSC 2003a, Section 6.1.4). These infiltration rate maps contain the net infiltration rate data per grid cell over the region containing the modeled repository footprint. The numerical information employed to calculate the mean spatial net infiltration for each analog climate is restricted to those grid cells that fall within the multirectangular region used to approximate the repository footprint. These calculated means are combined with the output net-infiltration uncertainty-distribution to determine weighting factors, which are the probabilities of the range of net infiltration (BSC 2003b).

The information in this report is responsive to agreement USFIC 3.01 and the associated AIN (AIN-1). The report contains the information that the DOE considers necessary for NRC review for closure of this agreement.

D.4 BASIS FOR THE RESPONSE

D.4.1 Net Infiltration Distribution

The uncertainty analysis was performed based on the results of simulation of net infiltration using the INFIL VA_2.a1 code (SNL 2001), which is a modified version of the U.S. Geological Survey code INFIL V2.0 (USGS 2001c). The Latin Hypercube statistical technique was used to generate 100 realizations (simulations) of the spatial distribution of net infiltration over the repository area. Uncertain input parameters used for these simulations are presented in Tables D-1 and D-2. Precipitation and temperature data, which characterized the glacial-transition climate, were represented by the data set of the Tule Lake meteorological station (see Figure 3-5).

The results of this analysis are shown in Figures D-2 and D-3. Figure D-2 shows a frequency histogram of the net infiltration rate from the uncertainty analysis (for the modeling domain, including the contingency area—the southern extension of repository footprint), which also displays the mean values obtained from the U.S. Geological Survey simulations (USGS 2001a). The weighting factors, which were estimated from the cumulative distribution function, are 0.22, 0.40, and 0.38 for the lower-bound, mean, and upper-bound glacial-transition climate infiltration maps, respectively. Figure D-3 shows a frequency histogram of the net infiltration rate from the uncertainty analysis for the modeling domain excluding the contingency area, using weighting factors of 0.24, 0.41, and 0.35 for the lower-bound, mean, and upper-bound glacial-transition climate infiltration maps, respectively.

D.4.2 Correlation Analysis

The results of the correlation analysis between the net infiltration distribution and uncertain input parameters are presented in Table D-3 and Figure D-4. These results show that the parameters with the greatest impact to net infiltration are precipitation and bedrock permeability (with positive correlation coefficients) and soil depth and daily potential evapotranspiration (with negative correlation coefficients).

00394DC_033a.ai
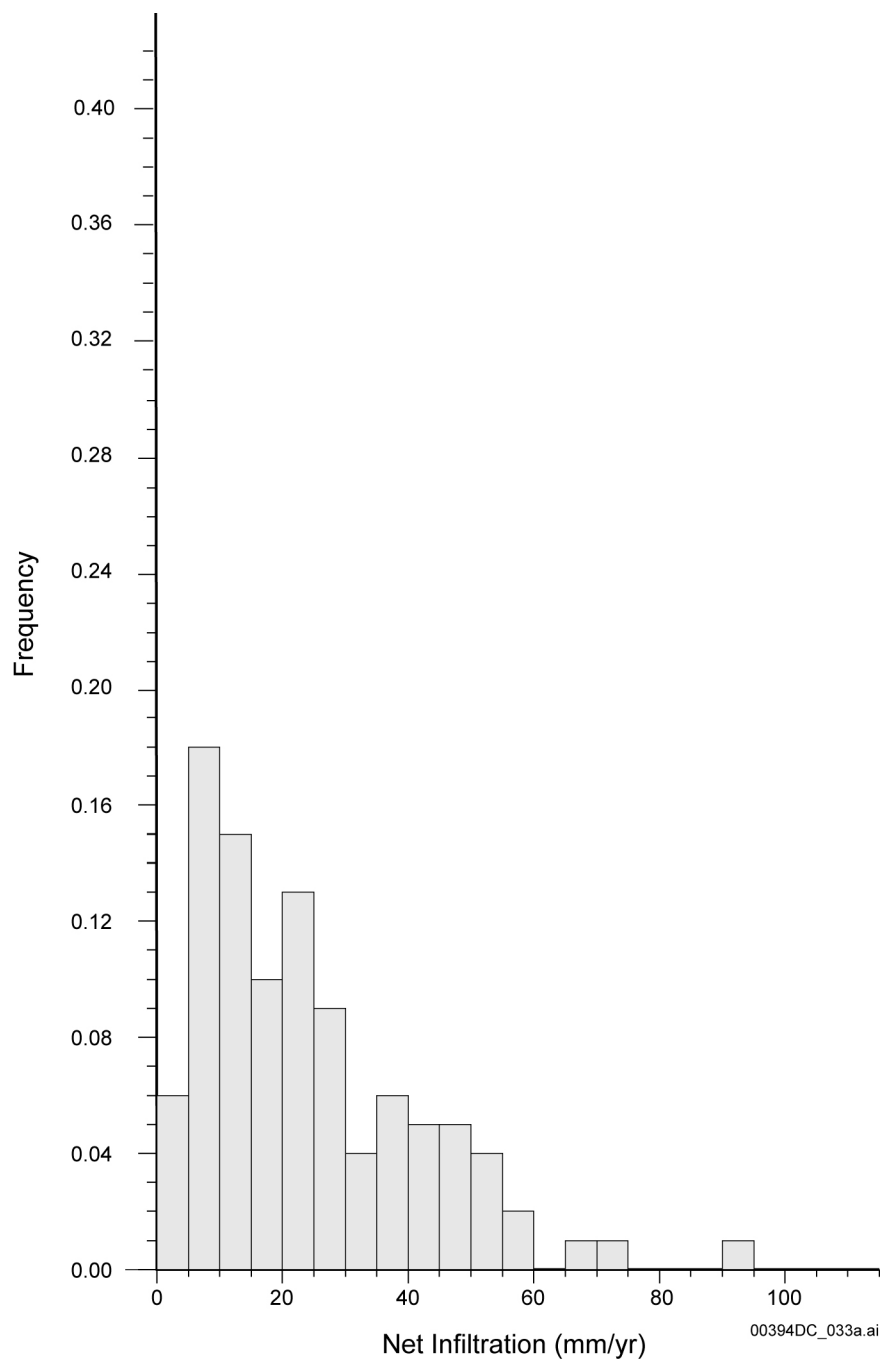
Source: BSC 2003b, Figure 6-2a.

Figure D-2.   Histogram of Average Annual Infiltration and Weighting Factors for Glacial-Transition Climate (Including Contingency Area)

00394DC_035a.ai

Source: BSC 2003b, Figure 6-3a.

Figure D-3.   Histogram of Average Annual Infiltration and Weighting Factors for Glacial-Transition
Climate (Excluding Contingency Area)

Source: BSC 2003b, Table 6-8.

Figure D-4.   Correlation Coefficients between Net Infiltration and Uncertain Input Parameters Used for Simulations of Net Infiltration for the Glacial-Transition Climate (for the Flow Domain, Including the Contingency Area)

Table D-3.   Results of the Correlation Analysis of Parameters Used in Calculation of Net Infiltration for the Glacial-Transition State for the Repository Domain Approximation, Including the Contingency Area

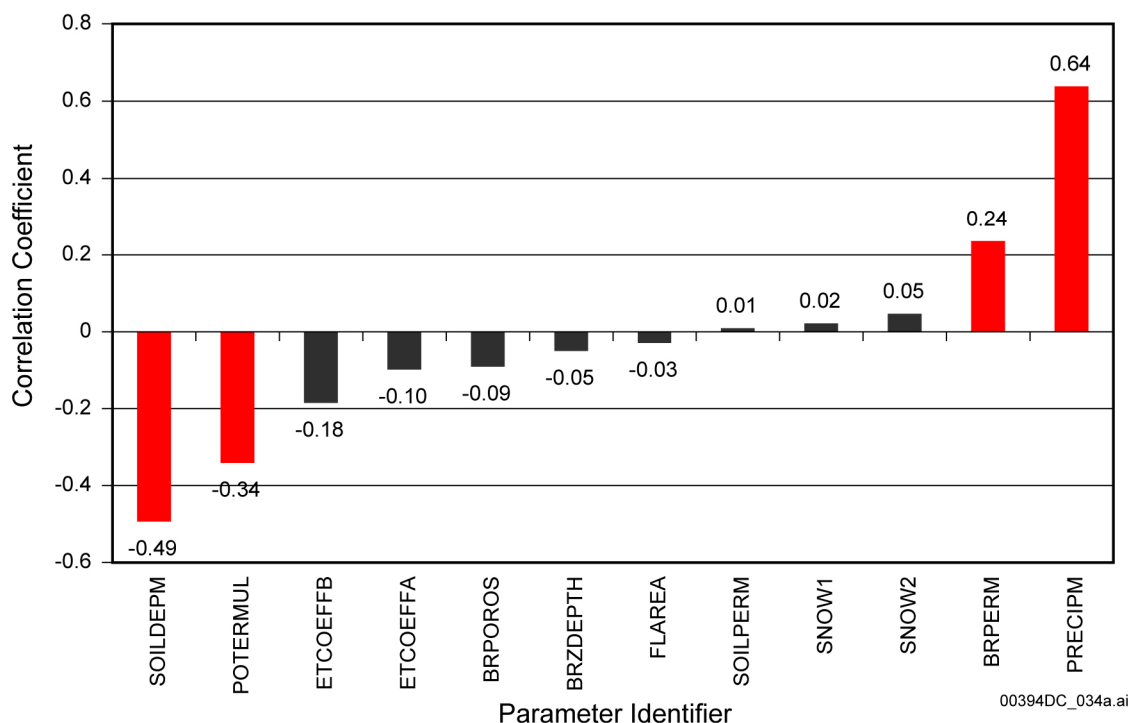|	BRPOROS	BRZDepth	soildepm	precipm	potermul	brperm	soilperm	etcoeffa	etcoeffb	flarea	snow1	snow2	Net Infiltration
BRPOROS	1	-0.0117	-0.46	0.0047	-0.0014	-0.0106	-0.0985	0.0004	0.0063	0.0036	0.0471	0.0099	-0.091
BRZDepth	-0.0117	1	-0.0126	0.0102	0.0093	0.0551	-0.1101	-0.0006	-0.0059	0.0041	-0.016	-0.0104	-0.0496
soildepm	-0.0046	-0.0126	1	-0.0091	-0.0008	0.0143	0.0322	0.0091	0.0068	-0.0067	-0.0225	0.0154	-0.4931
precipm	0.0047	0.0102	-0.0091	1	-0.0024	-0.0398	-0.0277	0.0075	0.001	0.0083	0.0121	-0.0302	0.638
potermul	-0.0014	0.0093	-0.0008	-0.0024	1	-0.027	-0.0887	0.0036	0.0099	-0.0098	-0.0035	-0.0215	-0.3409
brperm	-0.0106	0.0551	0.0143	-0.0398	-0.027	1	0.0016	0.0053	-0.0452	0.0291	0.076	0.0049	0.2358
soilperm	-0.0985	-0.1101	0.0322	-0.0277	-0.0887	0.0016	1	0.0017	-0.069	-0.0139	0.0209	0.0173	0.009
etcoeffa	0.0004	-0.0006	0.0091	0.0075	0.0036	0.0053	0.0017	1	0.0156	0.0112	-0.0185	-0.0114	-0.098
etcoeffb	0.0063	-0.0059	0.0068	0.001	0.0099	-0.0452	-0.069	0.0156	1	0.0019	0.0141	-0.017	-0.1849
flarea	0.0036	0.0041	-0.0067	0.0083	-0.0098	0.0291	-0.0139	0.0112	0.0019	1	-0.0428	0.0111	-0.0294
snow1	0.0471	-0.016	-0.0225	0.0121	-0.0035	0.076	0.0209	-0.0185	0.0141	-0.0428	1	0.0087	0.0217
snow2	0.0099	-0.0104	0.0154	-0.0302	-0.0215	0.0049	0.0173	-0.0114	-0.017	0.0111	0.0087	1	0.0467
Net Infiltration	-0.091	-0.0496	-0.4931	0.638	-0.3409	0.2358	0.009	-0.098	-0.1849	-0.0294	0.0217	0.0467	1

Source: Net infiltration rate data are from *Analysis of Infiltration Uncertainty* (BSC 2003b, Table 6-5). Correlation coefficients of net infiltration with the 12 uncertain input parameters are from *Analysis of Infiltration Uncertainty* (BSC 2003b, Table 6-8).

D.4.3 Conclusions

The combined effects of the 12 uncertain input parameters were assessed using the Latin Hypercube Sampling method (which is a modified Monte Carlo technique) using 100 realizations.

Analysis of Infiltration Uncertainty (BSC 2003b) describes the procedure used for selecting the ranges and probability density functions for uncertain input parameters. To obtain a wide range of net infiltration, the parameter ranges were selected to account for two types of uncertainty: epistemic (which arises from lack of knowledge about parameters, because the data are limited or because alternative data interpretations exist) and aleatoric (which cannot be reduced because the state of knowledge about the processes and parameters cannot be improved by further characterization and data collection).

The variability of net infiltration uncertainty was accounted for by using the range of values between the 1st and 99th percentile (for lognormal and normal distributions), which contain nearly the entire range of the actual distribution. Moreover, the calculations performed with no correlation between input parameters enhanced the range of calculated uncertainty.

The net infiltration weighting factors determined in *Analysis of Infiltration Uncertainty* (BSC 2003b) will be applied to unsaturated zone flow fields in TSPA, as outlined in the *Total System Performance Assessment License Application Methods and Approach* (BSC 2002, Section 3.1) as a general method for the treatment of uncertainty.

D.5 REFERENCES

D.5.1 Documents Cited

BSC (Bechtel SAIC Company) 2002. *Total System Performance Assessment-License Application Methods and Approach.* TDR-WIS-PA-000006 REV 00. Las Vegas, Nevada: Bechtel SAIC Company. ACC: MOL.20020923.0175.

BSC 2003a. *UZ Flow Models and Submodels.* MDL-NBS-HS-000006 REV 01. Las Vegas, Nevada: Bechtel SAIC Company. ACC: DOC.20030818.0002.

BSC 2003b. *Analysis of Infiltration Uncertainty.* ANL-NBS-HS-000027 REV 01. Las Vegas, Nevada: Bechtel SAIC Company. ACC: DOC.20031030.0003

BSC 2003c. *Repository Design, Repository/PA IED Subsurface Facilities.* 800-IED-EBS0-00402-000-00B. Las Vegas, Nevada: Bechtel SAIC Company. ACC: MOL.20030109.0146.

BSC 2003d. *Repository Design, Repository/PA IED Subsurface Facilities.* 800-IED-EBS0-00401-000-00C. Las Vegas, Nevada: Bechtel SAIC Company. ACC: ENG.20030303.0002.

CRWMS M&O (Civilian Radioactive Waste Management System Management and Operating Contractor) 2000. *Analysis of Infiltration Uncertainty.* ANL-NBS-HS-000027 REV 00. Las Vegas, Nevada: CRWMS M&O. ACC: MOL.20000525.0377.

Reamer, C.W. and Williams, D.R. 2000a. Summary Highlights of NRC/DOE Technical Exchange and Management Meeting on Unsaturated and Saturated Flow Under Isothermal Conditions, October 31 – November 2, 2000, Albuquerque, New Mexico. Washington, D.C.: U.S. Nuclear Regulatory Commission. ACC: MOL.20001128.0206.

Reamer, C.W. and Williams, D.R. 2000b. Summary Highlights of NRC/DOE Technical Exchanges and Management Meeting on Unsaturated and Saturated Flow under Isothermal Conditions, August 16-17, 2000, Berkeley, California. Washington, D.C.: U.S. Nuclear Regulatory Commission. ACC: MOL.20001201.0072.

Rechard, R.P. 1996. *An Introduction to the Mechanics of Performance Assessment Using Examples of Calculations Done for the Waste Isolation Pilot Plant Between 1990 and 1992.* SAND93-1378 Revised. Albuquerque, New Mexico: Sandia National Laboratories. TIC: 245715.

Schlueter, J.R. 2003. "Use of Risk as a Basis for Closure of Key Technical Issue Agreements." Letter from J.R. Schlueter (NRC) to J.D. Ziegler, (DOE), January 27, 2003, 0131035890, with attachment. ACC: MOL.20030227.0018.

SNL (Sandia National Laboratories) 2001. *Software Code: INFIL.* VA_2.a1. DEC Alpha, OpenVMS V7.2-1. 10253-A_2.a1-00.

USGS (U.S. Geological Survey) 2001a. *Simulation of Net Infiltration for Modern and Potential Future Climates.* ANL-NBS-HS-000032 REV 00 ICN 02. Denver, Colorado: U.S. Geological Survey. ACC: MOL.20011119.0334.

USGS 2001b. *Future Climate Analysis.* ANL-NBS-GS-000008 REV 00 ICN 01. Denver, Colorado: U.S. Geological Survey. ACC: MOL.20011107.0004.

USGS 2001c. *Software Code: INFIL.* V2.0. PC. 10307-2.0-00.

Wu, Y.S.; Ritcey, A.C.; Ahlers, C.F.; Mishra, A.K.; Hinds, J.J.; and Bodvarsson, G.S. 1997. *Providing Base-Case Flow Fields for TSPA-VA: Evaluation of Uncertainty of Present-Day Infiltration Rates Using DKM/Base-Case and DKM/Weeps Parameter Sets.* Milestone SLX01LB2. Berkeley, California: Lawrence Berkeley National Laboratory. ACC: MOL.19980501.0475.

Ziegler, J.D. 2002. "Transmittal of Information Addressing Key Technical Issue (KTI) Agreement Items Unsaturated And Saturated Flow Under Isothermal Conditions (USFIC) 3.01, and Total System Performance Assessment and Integration (TSPAI) 3.19." Letter from J.D. Ziegler (DOE) to J.R. Schlueter (NRC), July 11, 2002, 0715023334, with attachment. ACC: MOL.20020918.0029.

D.5.2 Software Codes

EARTHVISION V5.1. STN: 10174-5.1-00.

APPENDIX E

**PARAMETERS OF INFILTRATION UNCERTAINTY ANALYSIS
(RESPONSE TO USFIC 3.02 AIN-1)**

Note Regarding the Status of Supporting Technical Information

This document was prepared using the most current information available at the time of its development. This Technical Basis Document and its appendices providing Key Technical Issue Agreement responses that were prepared using preliminary or draft information reflect the status of the Yucca Mountain Project's scientific and design bases at the time of submittal. In some cases this involved the use of draft Analysis and Model Reports (AMRs) and other draft references whose contents may change with time. Information that evolves through subsequent revisions of the AMRs and other references will be reflected in the License Application (LA) as the approved analyses of record at the time of LA submittal. Consequently, the Project will not routinely update either this Technical Basis Document or its Key Technical Issue Agreement appendices to reflect changes in the supporting references prior to submittal of the LA.

APPENDIX E

PARAMETERS OF INFILTRATION UNCERTAINTY ANALYSIS
(RESPONSE TO USFIC 3.02 AIN-1)

This appendix provides a response to the Key Technical Issue (KTI) agreement entitled Unsaturated and Saturated Flow under Isothermal Conditions (USFIC) 3.02, additional information needed (AIN)-1. This agreement relates to providing additional information on the technical basis for parameters used in the infiltration uncertainty analysis.

E.1   KEY TECHNICAL ISSUE AGREEMENT

E.1.1   USFIC 3.02 AIN-1

Agreement USFIC 3.02 was reached during the U.S. Nuclear Regulatory Commission (NRC)/U.S. Department of Energy (DOE) Technical Exchange and Management Meeting on USFIC on October 31 to November 2, 2000 (Reamer and Williams 2000a), in Albuquerque, New Mexico. USFIC Subissue 3, Present-Day Shallow Groundwater Infiltration, was discussed at that meeting.

At the NRC/DOE Technical Exchange and Management Meeting on USFIC in August 2000 in Berkeley, California (Reamer and Williams 2000b), the NRC questioned the values assigned by the DOE to the weight-multipliers for upper-bound mean annual infiltration in the analyses conducted as part of the infiltration uncertainty analysis supporting the total system performance assessment (TSPA) for site recommendation, which is documented in *Total System Performance Assessment for the Site Recommendation* (CRWMS M&O 2000a). At the Technical Exchange and Management Meeting on October 31 to November 2, 2000 (Reamer and Williams 2000a), the NRC also requested justification of parameters used in *Analysis of Infiltration Uncertainty* (CRWMS M&O 2000b, Table 4-1) and specifically noted that bedrock permeability estimates need to be reconciled with observations from Alcove 1 and Pagany Wash experiments. At the latter meeting, the NRC also requested documentation of the infiltration tests conducted at Alcove 1 and Pagany Wash. In these meetings, the DOE indicated that there were typographic errors in *Analysis of Infiltration Uncertainty* (CRWMS M&O 2000b, Table 4-1) that would be corrected in a revision of that report and agreed to provide additional justification of the parameters and documentation of the tests.

The wording of the agreement is as follows:

USFIC 3.02

> Provide justification for the parameters in Table 4-1 of the Analysis of Infiltration Uncertainty AMR (for example, bedrock permeability in the infiltration model needs to be reconciled with Alcove 1 results/observations). Also, provide documentation (source, locations, tests, test results) for the Alcove 1 and Pagany Wash tests. DOE will provide justification and documentation in a Monte Carlo analysis document. The information will be available in February 2002.

The DOE submitted the initial response to this agreement in November 2002 (Ziegler 2002), including (1) justification of parameters used in *Analysis of Infiltration Uncertainty* (CRWMS M&O 2000b) based on data and other information available at the time of its preparation; (2) documentation of Alcove 1 and Pagany Wash test data that were not available at the time of its preparation; and (3) additional results of a recent TSPA sensitivity study showing that postclosure performance objectives would be met and that the information to be developed to address USFIC 3.02 would not be significant in determining compliance with regulatory standards. NRC staff subsequently provided review comments on the DOE initial response. This resulted in AIN request USFIC 3.02 AIN-1 (Schlueter 2003a).

The wording of the AIN is summarized as follows:

- The DOE report provided both technical information to address the topic of the USFIC 3.02 agreement and results of TSPA simulations that illustrated the lack of sensitivity of dose to very high net infiltration rates. Agreement USFIC 3.02 can be satisfactorily resolved using either a technical approach or a risk-informed approach.

- **Agreement Completion Based on Technical Merit:**

  (1) Additional support of values in the parameter distribution table for glacial-transition climates (CRWMS M&O 2000b, Table 4-1) is needed. This information would include the technical bases for reducing the parameter ranges and changing the mean values from those used for the modern climate. Model self-consistency was also inferred as a justification for changing parameter distributions for the glacial-transition climate. Transparency or clarification of the model self-consistency argument and basis are needed.

  (2) Alcove 1 test documentation needs to be complete.

- **Agreement Completion Based on Low Risk Significance:**

  Guidance on the use of risk information to complete agreements was provided by NRC in its letter to DOE titled, "Use of Risk as a Basis for Closure of Key Technical Issue Agreements," dated January 27, 2003 (Schlueter 2003b). It is expected that the following information would be presented: (i) combined effect of uncertainty associated with agreements addressed with risk information; (ii) transparency of changes made to implement the sensitivity analyses and explanation of the results, and (iii) details on the distribution of simulation results.

E.1.2   Related Key Technical Issue Agreements

KTI agreement USFIC 3.01 is related to USFIC 3.02 in that they both relate to the infiltration uncertainty analysis. USFIC 3.01 requires DOE to provide schedule and documentation for the Monte Carlo analysis for infiltration. A response to agreement USFIC 3.01 is provided in Appendix D.

E.2 RELEVANCE TO REPOSITORY PERFORMANCE

The infiltration model provides estimates of infiltration flux, which are used as top boundary conditions in the development of unsaturated zone flow fields in TSPA. The infiltration uncertainty analysis using the parameters described herein provides the weighting factors for the glacial-transition climate that are applied to the unsaturated zone flow fields in TSPA. In addition, the infiltration uncertainty analysis provides quantitative and qualitative information that supports the description of the surficial soils and topography, one of the natural barriers to downward infiltration. The use of the net infiltration weighting factors developed for the glacial-transition climate for the 10,000-year compliance period provides additional conservatism in TSPA for the license application, needed to avoid underestimating net infiltration and the potential radiological dose used to assess repository performance.

E.3 RESPONSE

This response provides information on the topic of USFIC 3.02 based on the technical merit of the evaluation of net infiltration uncertainty, which is different from the initial response, so that the issues identified in the AIN for the risk-informed approach are no longer relevant.

The wording of the AIN refers to the initial issue of *Analysis of Infiltration Uncertainty* (CRWMS M&O 2000b, Table 4-1). This report was superseded (BSC 2003a) and the current response is based on the revised analysis (BSC 2003a, Table 6-3). The names and types of the 12 uncertain parameters selected as input parameters for the evaluation of infiltration uncertainty are given in Table E-1. The distribution ranges and types of 10 uncertain parameters for the present-day and monsoon climate scenarios are given in Table E-2. These data were used as the basis for assigning the input parameters for the glacial-transition climate scenario, which are given in Table E-3.

Table E-1. Description of Uncertain Input Parameters for Glacial-Transition Climate

Parameter Identifier	Parameter
BRPERM	Bedrock bulk saturated hydraulic conductivity (multiplier)
BRPOROS	Bedrock effective root-zone porosity
BRZDEPTH	Bedrock root-zone thickness
ETCOEFFA	First coefficient in expression for evapotranspiration
ETCOEFFB	Second coefficient in expression for evapotranspiration
FLAREA	Surface flow runoff area
POTETMUL	Daily evapotranspiration (multiplier)
PRECIPM	Daily precipitation (multiplier)
SNOPAR1	Snow-melt parameter
SOILDEPM	Soil zone thickness (multiplier)
SOILPERM	Soil saturated hydraulic conductivity (multiplier)
SUBPAR1	First term ("A1") in snow loss (sublimation) equation for temperature regime below freezing (i.e., Tk $\leq$ 0.0°C)

Source: BSC 2003a, Table 6-1.

Table E-2. Uncertain Input Parameter Distributions for Present-Day and Monsoon Climates

Parameter Identifier	Mean	Low Range	High Range	Distribution Type	Units
BRPERM	1.00	0.10	10.0	LOGNORMAL	NONE
BRPOROS	0.009	0.002	0.024	NORMAL	NONE
BRZDEPTH	1.00	0.00	2.00	NORMAL	METERS
ETCOEFFA	-10.0	-0.10	-19.9	NORMAL	NONE
ETCOEFFB	1.04	0.54	1.54	NORMAL	NONE
FLAREA	0.50	0.01	0.99	NORMAL	NONE
POTETMUL	1.00	0.60	1.40	NORMAL	NONE
PRECIPM	1.00	0.60	1.40	NORMAL	NONE
SOILDEPM	1.00	0.10	1.90	NORMAL	NONE
SOILPERM	1.00	0.10	10.0	LOGNORMAL	NONE

Source: BSC 2003a, Table 6-2.

NOTE: Parameter identifiers are defined in Table E-1.

Table E-3. Uncertain Input Parameter Distributions Used for the Simulation of Net Infiltration for Glacial-Transition Climate

Parameter Identifier	Mean	Low Range	High Range	Distribution Type	Units
BRPERM	1.00	0.10	10.0	LOGNORMAL	NONE
BRPOROS	0.009	0.002	0.024	NORMAL	NONE
BRZDEPTH	1.50	0.00	3.00	NORMAL	METERS
ETCOEFFA	-10.0	-0.10	-19.9	NORMAL	NONE
ETCOEFFB	1.04	0.54	1.54	NORMAL	NONE
FLAREA	0.25	0.01	0.49	NORMAL	NONE
POTETMUL	1.00	0.60	1.40	NORMAL	NONE
PRECIPM	1.00	0.60	1.40	NORMAL	NONE
SNOPAR1	1.78	0.78	2.78	UNIFORM	NONE
SOILDEPM	1.00	0.10	1.90	NORMAL	NONE
SOILPERM	1.00	0.10	10.0	LOGNORMAL	NONE
SUBPAR1	0.10	0.00	0.20	UNIFORM	NONE

Source: BSC 2003a, Table 6-3.

NOTE: Parameter identifiers are defined in Table E-1.

The parameters BRPOROS, BRZDEPTH, ETCOEFFA, ETCOEFFB, SNOPAR1, and SUBPAR1 were defined using actual values. The remaining input parameters were defined using multipliers to assign the range of corresponding parameters in the Monte Carlo simulations of net infiltration. Distribution functions for the input parameters were selected based on results from prior studies (e.g., BSC 2003b, Section 6.2.1, p. 50) or based on the distribution type of the actual data set (e.g., fracture porosity and precipitation) and literature data.

Upper and lower bounds for the BRPOROS, BRZDEPTH, SOILDEPM, PRECIPM, POTETMUL, BRPERM, SOILPERM, FLAREA, ETCOEFFB, and SNOPAR1 parameters were

assigned based on the limits of the physical values for these parameters, taking into account that SUBPAR1 could not be negative, ETCOEFFA could not be positive, and BRPOROS and FLAREA range between 0 and 1. Two correlations between parameters were considered: one between the soil-depth parameter SOILDEPM and the bedrock-rooting-depth parameter BRZDEPTH; and one between the precipitation-rate multiplier PRECIPM and the potential-evapotranspiration multiplier POTETMUL. SOILDEPM and BRZDEPTH are inversely correlated, by definition, through Equation 17 in *Simulation of Net Infiltration for Modern and Potential Future Climates* (USGS 2001a, pp. 50 to 51) for deterministic model simulations. To provide a conservative estimation of the range of net infiltration, zero pair-wise correlation was used between all input parameters, so that the uncorrelated parameters could vary independently of one another (BSC 2003a).

The information in this report is responsive to agreement USFIC 3.02 and the associated AIN (AIN-1). The report contains the information that the DOE considers necessary for NRC review for closure of this agreement.

E.4 BASIS FOR THE RESPONSE

E.4.1 Parameter Distributions Developed for the Present-Day and Monsoon Climate Scenarios

Effective Bedrock Porosity–BRPOROS was assigned a range from 0.002 to 0.024 (to represent the maximum effective fracture porosity) with a mean value of 0.009 and a normal distribution. To assign the range of BRPOROS, the first 12 bedrock porosities reported in *Analysis of Hydrologic Properties Data* (BSC 2003b, Table 7) were used, and the data were analyzed using the *W* test of Shapiro and Wilk (Gilbert 1987, pp. 158 to 160) to accept the hypothesis of the normal distribution of porosity. This range of values is narrower than the input used for model simulations presented in the previous version of *Analysis of Infiltration Uncertainty* (CRWMS M&O 2000b). This new range uses actual bedrock fracture porosity for all exposed rock units as shown in the Cross-Drift as-built geologic cross section in *Geology of the ECRB Cross Drift-Exploratory Studies Facility, Yucca Mountain Project, Yucca Mountain, Nevada* (Mongano et al. 1999, Drawings OA-46-345 and OA-46-346). The BRPOROS range is the same for present-day (and monsoon) and glacial-transition climate scenarios.

Soil Thickness–The multiplier SOILDEPM was used to uniformly scale estimates of soil depth across all model grid cells. A deviation of ±0.9 (±90%) with a normal distribution was used to define the lower- and upper-bound estimates of 0.1 and 1.9 for SOILDEPM. This distribution captures the large uncertainty in estimates of the soil depth across the model domain, and it is consistent with the data used in the INFIL V2.0 (USGS 2001b) and VA_2.a1 (SNL 2001) models and the soil-thickness data from *State Soil Geographic (STATSGO) Data Base, Data Use Information* (USDA 1994) in the vicinity of Yucca Mountain.

Bedrock Root-Zone Thickness–BRZDEPTH is expected to vary with climate, with lower values for drier climates and higher values for wetter climates, as discussed by Wirth et al. (1999). For the present-day climate scenario, BRZDEPTH ranges from 0 to 2 m with a mean of 1 m and a normal distribution. The thickness of the root zone in bedrock is calculated using Equation 17 of *Simulation of Net Infiltration for Modern and Potential Future Climates* (USGS

2001a, Section 6.7.2) with the soil-depth-class map using the INFIL V2.0 (USGS 2001b) model (BSC 2003a, Section 6.1.2.2). The root zone thickness in bedrock decreases as the thickness of soil increases. The root density in bedrock is only a small fraction of the root density in a soil layer (USGS 2001a, Section 6.8.3, p. 56). This range for BRZDEPTH is narrower than that used in *Analysis of Infiltration Uncertainty* (CRWMS M&O 2000b).

For the uncertainty analysis, the values of SOILDEPM and BRZDEPTH were sampled independently (no correlation) to capture the large uncertainty in bedrock rooting depth. The ranges used in this uncertainty analysis are likely to be larger (with shallower values of bedrock rooting depth) than would be found over the repository footprint.

Precipitation and Potential Evapotranspiration–The PRECIPM and POTETMUL distribution ranges were left unchanged (±0.4 about the mean). As described in *Analysis of Infiltration Uncertainty* (BSC 2003a, Section 6.1.2.1), the multiplier range of ±0.4 was consistent with the ranges of mean annual precipitation between the upper and lower climate bounds for modern, monsoon, and glacial-transition climates used in *Simulation of Net Infiltration for Modern and Potential Future Climates* (USGS 2001a, Table 6-19).

The distribution of precipitation using the PRECIPM parameter was consistent with the observed variability in estimated average annual precipitation for the Yucca Mountain area (French 1983; Hevesi et al. 1992) and with the ranges of mean annual precipitation between the upper and lower climate bounds. For example, the mean annual precipitation during the mean present-day climate is 197 mm, which is 41% lower than the mean annual precipitation for the upper-bound present-day climate of 278 mm (USGS 2001a, Table 6-10). The range of multipliers between the lower and upper bounds of potential evapotranspiration for present-day (and monsoon) climates is expected to be the same as the range between the lower and upper bounds of precipitation for each climate. Development of a daily present-day precipitation input file for the model calibration and simulations was based on available precipitation records from monitoring sites within the study area and in the proximity of Yucca Mountain. A 100-year daily climate input file for the present-day climate scenario was based on precipitation records from the Nevada Test Site Stations 4JA and Area 12 Mesa, which are summarized in Table 4-2, based on *Simulation of Net Infiltration for Modern and Potential Future Climates* (USGS 2001a).

Bedrock and Soil Permeability–For BRPERM, the upper- and lower-bound values were set to be plus or minus 1.0 orders of magnitude (plus or minus a multiplier of 10) around the mean value (where the mean value is defined by BRPERM equal to 1), with the total range of 2 orders of magnitude. This range is consistent with the expected range of hydraulic conductivities reported by Freeze and Cherry (1979, p. 31), who report that permeability in most geologic formations has a standard deviation in the range of 0.5 to 1.5 (log K) and shows total heterogeneous variations of 1 to 2 orders of magnitude. This range in standard deviation of permeability reported by Freeze and Cherry (1979, p. 31) is consistent with the average standard deviation of 0.57 for the exposed units (top 12 layers) of fracture permeability data reported in *Analysis of Hydrologic Properties Data* (BSC 2003b, Table 7). This range for BRPERM is narrower than the input used for model simulations presented in the previous version of *Analysis of Infiltration Uncertainty* (CRWMS M&O 2000b). This new range is considered to be a less conservative but more realistic range of effective bedrock permeability than was previously used.

Tiva Canyon Tuff Permeability Data–Different estimates of bulk-bedrock saturated hydraulic conductivities (or permeabilities) were used to justify the range of ±1.0 (log K) for BRPERM for the upper lithophysal unit of Tiva Canyon Tuff (TCw hydrogeologic unit). The sources for these estimates are as follows:

- Bulk-bedrock hydraulic conductivity for the upper lithophysal unit of Tiva Canyon Tuff, which was taken from the results of calibration of the INFIL model in *Simulation of Net Infiltration for Modern and Potential Future Climates* (USGS 2001a, pp. IV-11 to IV-15, Table IV-3)

- Infiltration rate data reported for the Alcove 1 experiments (Guertal 2001a; Guertal 2001b)

- Air-permeability data reported by LeCain (1998).

The saturated hydraulic conductivity (K) value for the upper lithophysal unit (Tpcpul) reported in *Simulation of Net Infiltration for Modern and Potential Future Climates* (USGS 2001a, Table IV-3) is 1.13 mm/day. This value of K corresponds to an intrinsic permeability (k) of 1.33×10^{-15} m^2. The hydraulic conductivities used in the INFIL model (SNL 2001) and reported in *Simulation of Net Infiltration for Modern and Potential Future Climates* (USGS 2001a, Table IV-3) are equal to the calculated value of bulk-bedrock saturated hydraulic conductivity for 250-µm-aperture fractures filled with infill materials, as described by Flint, A.L. et al. (1996).

The analysis of the results of the Alcove 1 infiltration test (the description of the test is given in Section 6.4.4) shows that the infiltration flux ranged from 0 to 30 mm/day, which corresponds to the permeability value of 3.54×10^{-14} m^2 (assuming a unity hydraulic gradient) from February 19, 1999, to December 15, 1999 (Flint, A.L. et al. 2000). The infiltration flux range of 18 to 25 mm/day, which corresponds to the permeability value of 2.12×10^{-14} to 2.95×10^{-14} m^2, was maintained from September 21, 1999, to October 15, 1999. In both the Phase I (from March 8, 1998, to December 4, 1998) and the Phase II (from January 29, 1999, to June 20, 2000) tests, water application was controlled so that no surface runoff occurred (BSC 2003a, Section 6.1.2.4).

The permeability values determined from Phase II of the Alcove 1 infiltration experiments basically encompasses the upper bound (+1 for log K) of the multiplier BRPERM.

The air-injection tests were conducted using horizontal boreholes in Alcove 1 (drilled from the alcove and situated below surface covers) to determine air permeabililty, but their results were not used in simulations of net infiltration for the following reasons. For the Tpcpul unit air permeability, LeCain (1998) reported a mean of the natural log of K of 2.772 (16.0×10^{-12} m^2) for boreholes RBT#1, RBT#2, and RBT#3. This permeability estimate is approximately four orders of magnitude larger than that reported in *Simulation of Net Infiltration for Modern and Potential Future Climates* (USGS 2001a, Table IV-3) and three orders of magnitude higher than that from the Alcove 1 infiltration test. Permeabilities for open fractures without filling are greater than those for filled fractures with the same aperture (Flint, A.L. et al. 1996, Table 2) and are not realistic for simulations of infiltration. For these reasons, the permeability values

measured by air injection at Alcove 1 were not suitable for use in the simulations described in *Analysis of Infiltration Uncertainty* (BSC 2003a).

The lower range of the multiplier BRPERM of 1.0 (log K) is consistent with the range of flux rates calculated for matrix and filled fractures reported by Flint, A.L. et al. (1996, Table 2).

A range of two orders of magnitude (-1.0 (log K)) was also assigned to SOILPERM. This distribution for SOILPERM is considered to be representative of both field-scale variability within mapped soil types and uncertainty in estimated values provided by Flint, A.L. et al. (1996, Table 4), who report that soil saturated hydraulic conductivity ranges from 5.6×10^{-6} to 3.8×10^{-5} m/s. Although this range is narrower than that assigned for SOILPERM, the two orders of magnitude distribution of SOILPERM was considered appropriate because the soils at Yucca Mountain have a relatively high percentage of coarse material (grain sizes greater than 2 mm) with very high permeability. However, the soils can also contain layers cemented with calcium carbonate (Flint, A.L. et al. 1996, p. 39), which have a much lower permeability. This approach to the selection of SOILPERM provides conservatism in predictions of net infiltration.

A lognormal distribution was assigned to conductivity multipliers BRPERM and SOILPERM based on the literature sources (e.g., Freeze and Cherry 1979, pp. 30 to 31) and the distribution of the first 12 fracture permeabilities reported in *Analysis of Hydrologic Properties Data* (BSC 2003b, Table 7, p. 50).

Evapotranspiration Coefficients A and B–To represent the large uncertainty in evapotranspiration estimates, mainly caused by the variability in vegetation, large ranges with normal distributions for ETCOEFFA (± 9.9) and ETCOEFFB (± 0.5) were selected. The mean values for both parameters (-10.00 for ETCOEFFA and 1.04 for ETCOEFFB) are consistent with values reported by Flint and Childs (1991). However, the bare-soil coefficients α and β of Flint and Childs (1991) are renamed ETCOEFFB and ETCOEFFA, respectively, in *Simulation of Net Infiltration for Modern and Potential Future Climates* (USGS 2001a) and in this document. These coefficients are used in the modified Priestley-Taylor evapotranspiration equation as described by Flint and Childs (1991) and Levitt et al. (1996).

Surface Flow Runoff Area–The FLAREA parameter defines the fraction of each grid cell of the infiltration model, which is affected by overland flow and channel flow during the routing of runoff. For the present-day climate, overland flow processes are considered to be the primary component of surface water flow, with FLAREA ranging ± 0.49 from 0.01 to 0.99 representing a high degree of both spatial and temporal variability (only values between 0 and 1 are valid for FLAREA), along with a mean value of 0.5 and a normal distribution. The mean value of 0.5 was determined from the model calibration conducted by matching streamflow records (USGS 2001a, Section 6.8).

E.4.2   Parameter Distributions for the Glacial-Transition Climate Scenario

For the glacial-transition climate scenario, in addition to 10 input parameters considered for the present-day and modern climate, two parameters, characterizing a snowmelt (SNOPAR1) and sublimation (SUBPAR1), were added to utilize the snow module in the infiltration model (USGS

2001a). In total, the 12 uncertain input parameters were used for the evaluation of the net infiltration uncertainty.

For the glacial-transition climate, the BRZDEPTH and FLAREA distributions were modified (in comparison with those for the present-day and monsoon climate) to take into account the changes in a root zone, channel characteristics, which could occur during the glacial-transition climate state. To take into account the expected changes in precipitation during the glacial-transition climate, a Tule Lake precipitation time series data set was used (while the PRECIPM parameter was left unchanged from that for the present-day and monsoon climate). Other uncertain input parameters for the glacial-transition climate were kept the same, as described in Section E.4.1.

Bedrock Root-Zone Thickness–The mean value for BRZDEPTH was increased from 1 to 1.5 m, and the distribution range was increased from ±1 m to ±1.5 m. The increase in BRZDEPTH was selected because the root zone thickness in fractured bedrock should increase as precipitation increases. A range of 0 to 3 m is consistent with the expected range of bedrock rooting depth for the glacial-transition climate, using *Simulation of Net Infiltration for Modern and Potential Future Climates* (USGS 2001a, Section 6.7.2, Equation 17).

Precipitation–The PRECIPM distribution range for the glacial-transition climate was left unchanged (±0.4 about the mean) from that for the present-day and monsoon climates. Based on the data in *Simulation of Net Infiltration for Modern and Potential Future Climates* (USGS 2001a, Table 6-19), the mean annual precipitation during the mean glacial-transition climate is 323 mm, which is 39% higher than the minimum annual precipitation for the lower-bound glacial-transition climate (198 mm) and 41% lower than the maximum annual precipitation for the upper-bound glacial-transition climate (455 mm). However, the Tule Lake precipitation data set used for the glacial-transition climate for the analysis of infiltration uncertainty (USGS 2001a; BSC 2003a) is not the same as that used for predictions of net infiltration in *Simulation of Net Infiltration for Modern and Potential Future Climates* (USGS 2001a). The mean annual precipitation from the Tule Lake data set is 278 mm (calculated from daily data), while that used in *Simulation of Net Infiltration for Modern and Potential Future Climates* (USGS 2001a) is 323 mm. If the two extreme highest and lowest annual precipitation totals from the 49-year Tule Lake data set are not used, then the mean annual precipitation rate of 278 mm/yr is 39% higher than the minimum annual precipitation rate (169 mm/yr) and 42% lower than the maximum annual precipitation rate (394 mm). Therefore, the use of a multiplier of ±0.4 about the mean is approximately the same as that used in *Simulation of Net Infiltration for Modern and Potential Future Climates* (USGS 2001a).

Surface Flow Runoff Area–The range of the FLAREA input distribution was narrowed from ±0.49 about the mean to ±0.24 about the mean, and the mean was reduced from 0.5 to 0.25. The new distribution was defined by a lower-bound value of 0.01 (same as for present-day climate) and an upper-bound value of 0.49 (about one-half that used for present-day climate). The reason for these changes was that a greater proportion of total surface water flow for the wetter glacial-transition climate would occur as channelized streamflow, as opposed to widespread overland flow. A supporting assumption was also made that drainage networks would be better established for a wetter climate, and surface features would include better-defined rill features on side slopes and in headwater areas of drainages, which, in turn, would serve to better concentrate

overland flow. The reduction in FLAREA from the present and monsoon climates to the glacial-transition climate is conservative for TSPA infiltration calculations, because the change will have the effect of increasing infiltration. Furthermore, the infiltration model is relatively insensitive to the value of the uncertain parameter FLAREA.

Snowmelt and Sublimation–For the glacial-transition climate, the parameters SNOPAR1 and SUBPAR1 were added to the set of input parameters to utilize the snow module of the infiltration model. A uniform distribution was used for both parameters, with SNOPAR1 defining the snowmelt rate and SUBPAR1 defining the sublimation rate (SNOPAR1 is equivalent to "A" in Equation 7, and SUBPAR1 is equivalent to "A1" in Equation 6 of USGS 2001a, p. 38). A uniform distribution was selected for both parameters because of a lack of data defining input distributions. The mean value of 1.78 for SNOPAR1 was based on the temperature-index expression for light, open forest during April (Sierra Nevada, California) obtained from Maidment (1993, Table 7.3.7). The upper-bound value of 2.78 and the lower-bound value of 0.78 were defined using an assumed distribution range of ±1.0, based on a qualitative assessment of various temperature-index expressions provided by Maidment (1993, Table 7.3.7).

Because of the lack of literature references needed to assess the effect of temperature on sublimation and advective processes (saltation and turbulent diffusion) and the effect of wind direction and speed, a model was developed using an assumed energy-index expression. The energy for sublimation–advection is defined using the adjusted potential evapotranspiration rate (USGS 2001a, p. 38). This sublimation–advection model assumes no snow accumulation caused by advection (snowdrifts). Given a conceptual understanding that sublimation (including saltation and turbulent diffusion) of snow is a component of the snowpack water balance, the parameter was assigned a range so that it would be small compared to the snowmelt parameter. To be conservative (i.e., to generate higher infiltration in the simulation results), the mean percentage of snowpack loss resulting from sublimation–advection was assumed to be considerably less than the maximum values of 34 to 41% indicated by field studies (Maidment 1993, p. 7.8). Therefore, a value of 0.10 with a range of ±0.10 was assigned to the SUBPAR1 parameter.

E.4.3   Alcove 1 Test

E.4.3.1   Goals of the Test and Site Location

The Alcove 1 test was designed to characterize the surface-to-drift flow and transport processes, including infiltration, percolation, seepage, fracture–matrix interaction, and flow diversion within the fractured Tiva Canyon Tuff over a large area in the range of 20 to 30 m. The test area is adequate to obtain information to support models for describing field-scale flow and transport processes in the unsaturated zone. The test was conducted by the U.S. Geological Survey in 1998 to 2000.

Alcove 1 is located near the North Portal of the Exploratory Studies Facility in the upper lithophysal zone of the Tiva Canyon Tuff (Figure E-1). The alcove is about 30 m below the ground surface and was constructed for collecting seepage water originating from the infiltration plot located at the ground surface.
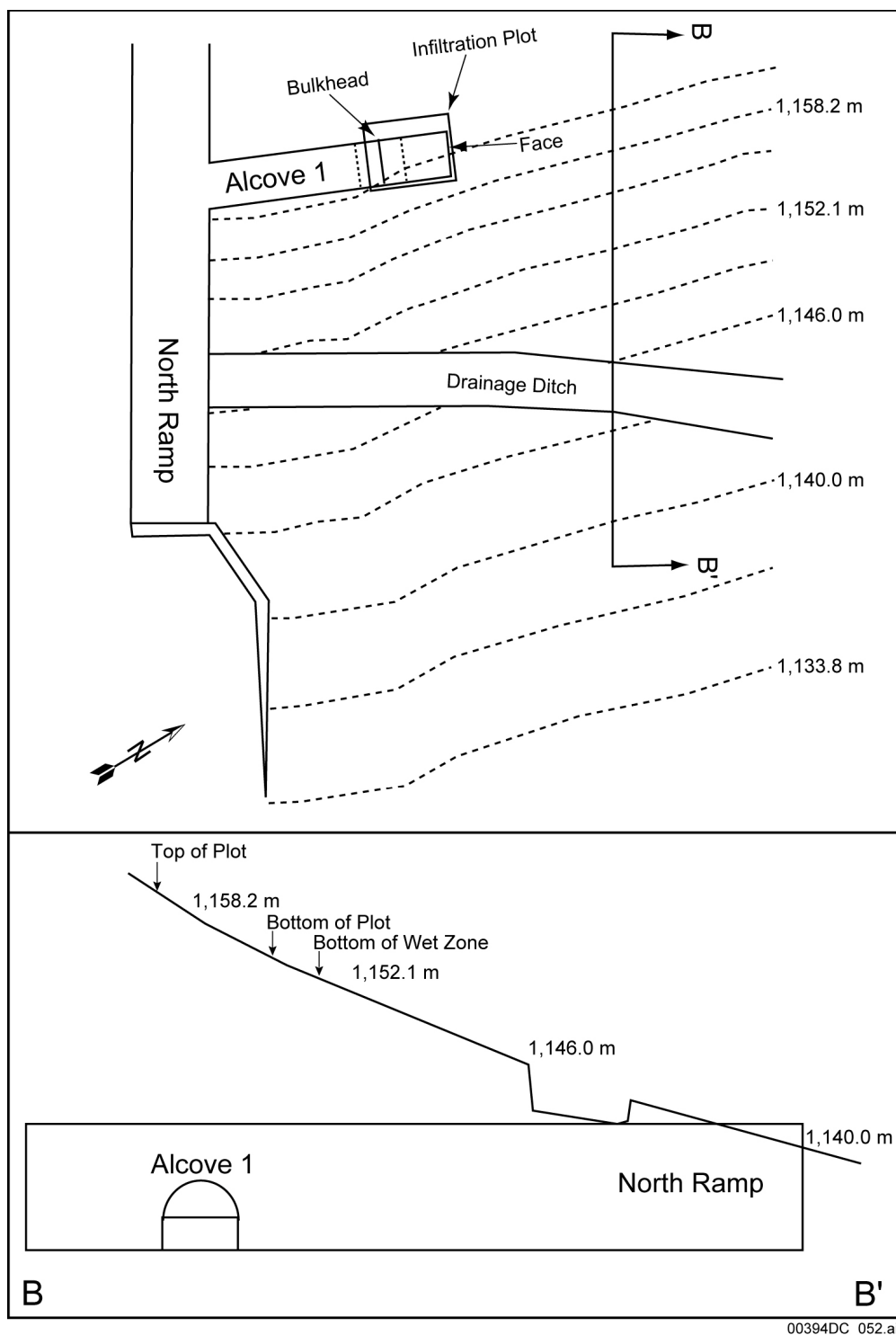
Source: BSC 2003c, Figure 6.12.5-1.

Figure E-1. Schematic Illustration of Alcove 1 Test Site inside the Exploratory Studies Facility North Portal

E.4.3.2   Test Design

Alcove 1 is about 5.5 m high, 5.8 m wide, and 37 m long. To minimally perturb the underground environment, a bulkhead was installed near the face of the alcove to isolate the alcove from the ESF. The bulkhead is intended to raise the relative humidity and reduce evaporation from the wall of the alcove so that dripping from the alcove ceiling and walls could be observed.

The size of the infiltration plot was 7.9×10.6 m (area of 83.7 m^2). Water was supplied to a plot through an irrigation drip tubing, with 490 drippers uniformly distributed over the infiltration plot. The plot is located directly above the alcove. The test was conducted from March 9, 1998, to August 13, 1998. The infiltration test consisted of two phases: Phase I, from March 9, 1998, to December 4, 1998; and Phase II, from February 19, 1999, to June 20, 2000.

To collect seepage water from the entire ceiling of the alcove, a water collection system consisting of 432 relatively small containers (trays) of the size 0.3×0.3 m (1-ft^2) was installed just below the ceiling of the alcove over the area of 40.2 m^2. Seepage monitoring was performed from May 5, 1998, to August 27, 1998 (Phase I), and from February 19, 1999, to December 15, 1999.

During the late stage of Phase II, a conservative tracer, LiBr, was introduced into the infiltrating water. Prior to application, the LiBr solution was prepared in a tank. Tracer data were collected in Alcove 1 from May 9, 2000, to July 5, 2000.

E.4.3.3   Data Available

The environmental conditions and the results of Alcove 1 infiltration tests are summarized in *In Situ Field Testing of Processes* (BSC 2003c, Table 4.1-12b, Table 6.12.5-1, Section 6.12.5.1) and by Liu et al. (2003).

The infiltration and seepage data from Phase I and infiltration and tracer data from Phase II are stored in the Automated Technical Data Tracking system (BSC 2003c). The following types of data are available:

- Pulse flow meter data for infiltration on surface, Phase I, March 9, 1998, to December 4, 1998 (DTN: GS990108312242.006)

- Seepage data for water collected in Alcove 1, Phase I, May 5, 1998, to September 27, 1998 (DTN: GS000308312242.002)

- Pulse flow meter data for infiltration on surface, Phase II, February 19, 1999, to June 20, 2000 (DTN: GS000808312242.006)

- Infiltration and seepage rates, as well as tracer concentrations, Phase II, February 19, 1999, to December 15, 1999 (DTN: GS000399991221.003)

- Tracer data for water collected in Alcove 1, Phase II, May 9, 1999, to July 5, 2000 (DTN: GS001108312242.009).

Although a complete summary of the Alcove 1 infiltration test was not provided in *In Situ Field Testing of Processes* (BSC 2003c) because the data have not been verified for use as direct input in analysis or modeling studies, the data will not change the analysis performed in *Analysis of Infiltration Uncertainty* (BSC 2003a) and by Liu et al. (2003). The supporting information is provided below.

Infiltration Rate–Figure E-2 shows a plot of the applied infiltration rate as a function of time. Infiltration rates in Phase I exhibited a greater degree of temporal variability than those in Phase II. The temporal variability of infiltration rate generally resulted from time-dependent flow processes and water redistribution within the fractured rock (Bodvarsson et al. 2001).
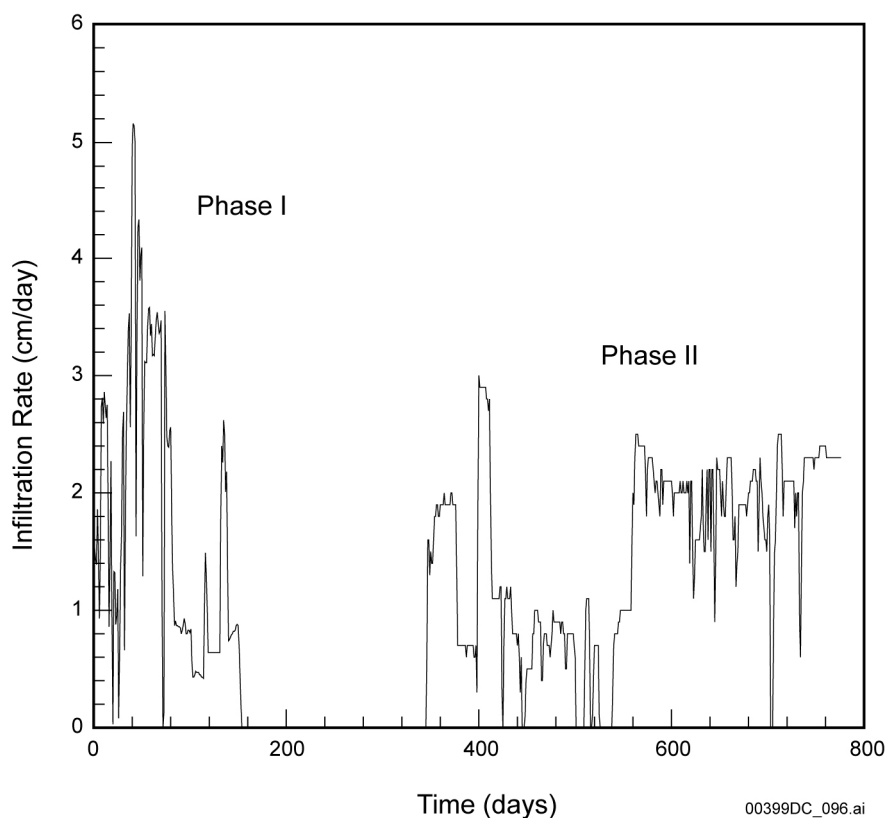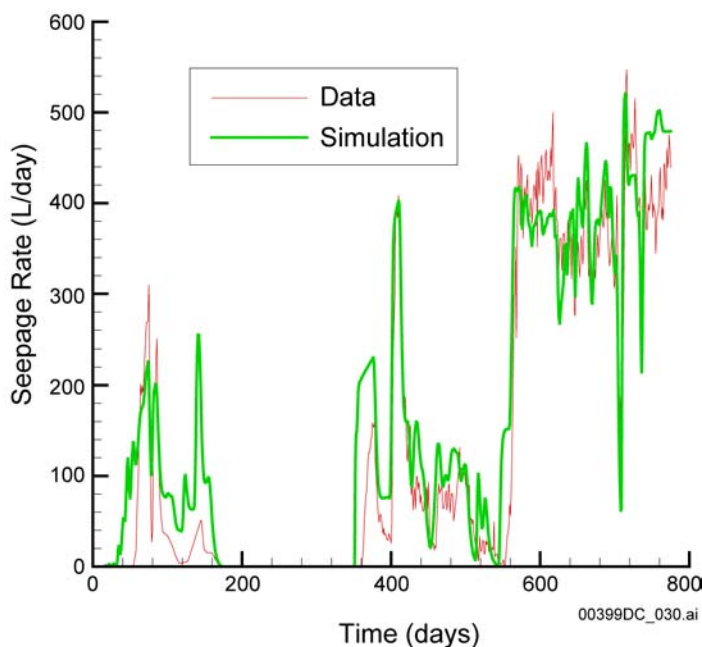

Source: Liu et al. 2003, Figure 1.

Figure E-2. Infiltration Rates Applied during the Alcove 1 Infiltration Test

The Alcove 1 infiltration rate of up to 30 mm/day is orders of magnitude smaller than that evaluated for the Tiva Canyon fractured rock from air-injection tests in boreholes drilled from the interior of the alcove with hydraulic conductivity values ranging from 1.69×10^2 to 7.20×10^4 mm/day and the geometric mean of 1.36×10^4 mm/day (BSC 2003c, p. 6.12-31). This difference in hydraulic conductivities can be explained by the fact that the near-surface fractures are filled with soils or other infill material, and the overall infiltration rate and hydraulic conductivity are controlled by the low permeability filling material. At depths below the zone of soil influence, fractures are open, with much higher hydraulic conductivity values. It is also possible that the Tpcpul units above Alcove 1 are not subject to the same structural stresses as

the Tpcpul units above the repository because of proximity to the edge of Yucca Mountain and, therefore, contain more open fractures.

Seepage Rate–A seepage rate was approximated by dividing the amounts of total seepage, collected during a given time interval (about 1 day), by the corresponding time interval. Figure E-3 presents the plot of seepage rate for both phases of the test from field observations and modeling results.
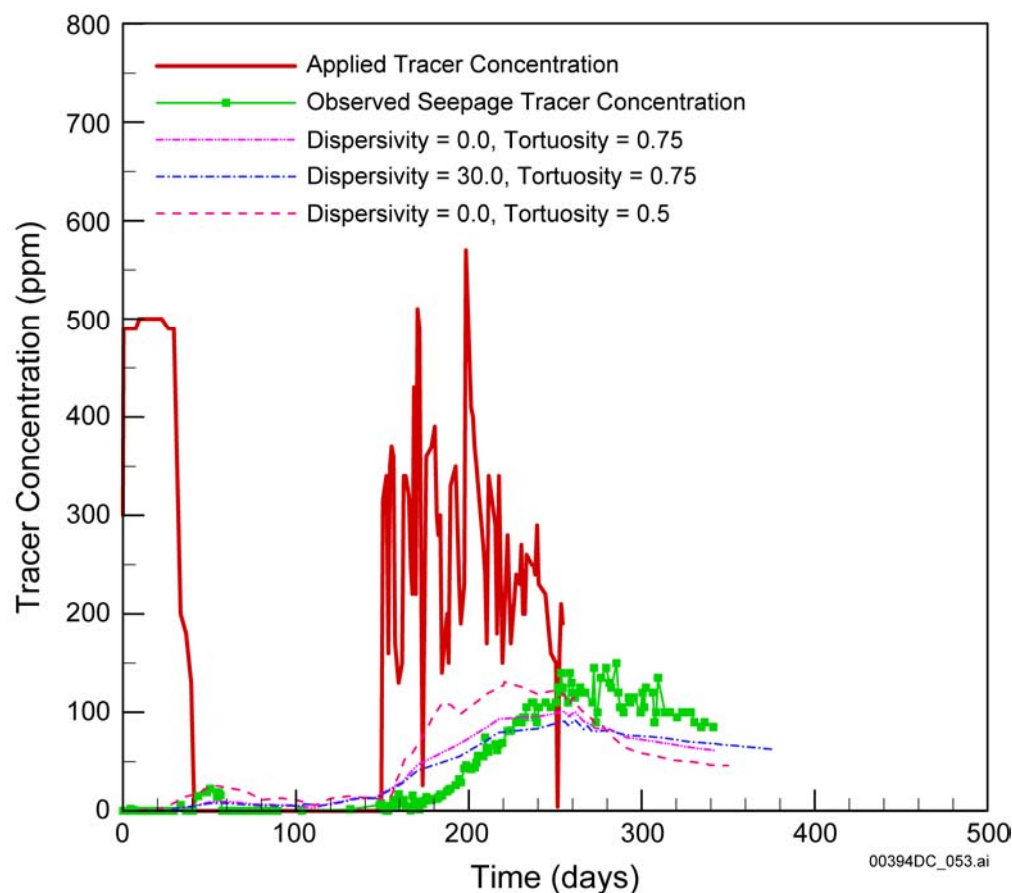

Source: Liu et al. 2003, Figure 4.

Figure E-3.   Seepage Rate Data from Observations and Model Calibration for Phase I, and Observations and Prediction for Phase II

The seepage rate can also be expressed as a percentage of the infiltrating water applied at the surface. The calculated seepage rate depends on the area chosen for comparison and the time of observations. The results show that 2.9% of the total applied water seeped into Alcove 1; 6.1% of the water applied above the collection area seeped into Alcove 1; 5.4% of the total applied water seeped into Alcove 1 after the rock above Alcove 1 was wetted; and 11.1% of the water applied above the collection area seeped into Alcove 1 after the rock above Alcove 1 was wetted (BSC 2003c, p. 6.12-31).

Tracer Data–Tracer concentrations in seepage water were obtained by analyzing the seepage water collected during each time interval. The tracer concentrations are average values for the corresponding time intervals. Figure E-4 presents the bromide concentration from field observations and modeling results.

Source: Liu et al. 2003, Figure 7.

NOTE: Zero time corresponds to May 18, 1999, the time of introducing the tracer.

Figure E-4. Observed and Simulated Bromide Concentrations

Results of Modeling–Both Phase I and Phase II observed data were used for calibration of hydraulic parameters of fractured tuff. Table E-4 lists rock hydraulic properties, which were used as inputs into the model of Liu et al. (2003), including fracture spacing, fracture and matrix permeabilities, porosities, van Genuchten parameters, and the parameter of the active fracture model, γ. The fracture porosity and spacing were estimated from the fracture map obtained in the ESF. Fracture permeability was estimated based on air-injection tests performed at the Alcove 1 site (LeCain 1997). The van Genuchten (1980) parameters for the fracture continuum were estimated using fracture permeability and frequency data (Sonnenthal et al. 1997). The matrix properties are taken from L.E. Flint (1998).

Table E-4. Hydrologic Properties of Fractured Tuff

Property	Fracture			Matrix		
	Initial Estimate	First Calibration	Second Calibration	Initial Estimate	First Calibration	Second Calibration
Porosity	0.01	0.028	0.03	0.164[a]	0.164	0.164
Vertical permeability (m^2)	2.29×10^{-11}	2.90×10^{-11}	3.08×10^{-11}	1.2×10^{-15}	3.64×10^{-16}	1.01×10^{-15}
Horizontal permeability (m^2)	2.29×10^{-11}	3.14×10^{-11}	2.99×10^{-11}	1.2×10^{-15}	9.35×10^{-16}	3.42×10^{-16}
α (Pa^{-1})	2.37×10^{-3}	2.07×10^{-3}	2.34×10^{-3}	7.12×10^{-6}	1.84×10^{-5}	1.90×10^{-5}
m	0.633[a]	0.633	0.633	0.346[a]	0.346	0.346
Fracture spacing (m)	0.377[a]	0.377[a]	0.377[a]	–	–	–
Residual saturation	0.01[a]	0.01[a]	0.01[a]	0.06[a]	0.06	0.06
γ	0.15	0.28	0.21	–	–	–

Source: Liu et al. 2003, Table 1.

NOTE: [a] These properties are fixed during model calibrations.

Comparisons between experimental and modeling results for the infiltration rate (Figure E-2), seepage rate (Figure E-3), and tracer concentration (Figure E-4) show that the continuum modeling approach captures essential features of flow and transport processes observed from the test (Liu et al. 2003). The modeling results, based on the LiBr tracer data, show that matrix diffusion may have significantly affected the overall solute transport in unsaturated fractured rocks. The tracer data can be used to estimate effective fracture–matrix interface areas.

E.4.4   Conclusions

This report provides the response on the topic of USFIC 3.02 based on the technical merit of the evaluation of net infiltration uncertainty. The revision of *Analysis of Infiltration Uncertainty* (BSC 2003a) provides additional support for uncertain input parameter distributions used for the glacial-transitional climate, including the technical bases for changes to the mean and parameter ranges from those used for the present-day climate. The available test data (source, locations, tests, test results) for Alcove 1, which are required by USFIC 3.02 AIN-1, are summarized in *Analysis of Infiltration Uncertainty* (BSC 2003a), *In Situ Field Testing of Processes* (BSC 2003c), and by Liu et al. (2003). The results of analyses of Alcove 1 infiltration and air-injection experiments (BSC 2003a; BSC 2003c; Liu et al. 2003) are in agreement with other data for the TCw fractured tuff unit. The Alcove 1 data were used for corroboration in evaluating the distribution range of permeability for the net infiltration uncertainty analysis (BSC 2003a). Although a complete summary of the Alcove 1 testing has not been conducted, the data analysis is not expected to change the results provided in *Analysis of Infiltration Uncertainty* (BSC 2003a) and by Liu et al. (2003). Therefore, the results presented in this response (Liu et al. 2003; BSC 2003a; BSC 2003c) are considered sufficient for closure of USFIC 3.02.

E.5   REFERENCES

E.5.1   Documents Cited

Bodvarsson, G.S.; Liu, H.H.; Ahlers, C.F.; Wu, Y-S.; and Sonnenthal, S. 2001. "Parameterization and Upscaling in Modeling Flow and Transport in the Unsaturated Zone of Yucca Mountain." Chapter 11 of *Conceptual Models of Flow and Transport in the Fractured Vadose Zone.* Washington, D.C.: National Academy Press. TIC: 252777.

BSC (Bechtel SAIC Company) 2003a. *Analysis of Infiltration Uncertainty.* ANL-NBS-HS-000027 REV 01. Las Vegas, Nevada: Bechtel SAIC Company. ACC: DOC.20031030.0003.

BSC 2003b. *Analysis of Hydrologic Properties Data.* MDL-NBS-HS-000014 REV 00. Las Vegas, Nevada: Bechtel SAIC Company. ACC: DOC.20030404.0004.

BSC 2003c. *In Situ Field Testing of Processes.* ANL-NBS-HS-000005 REV 02. Las Vegas, Nevada: Bechtel SAIC Company. ACC: DOC.20031208.0001.

CRWMS M&O (Civilian Radioactive Waste Management System Management and Operating Contractor) 2000a. *Total System Performance Assessment for the Site Recommendation.* TDR-WIS-PA-000001 REV 00 ICN 01. Las Vegas, Nevada. CRWMS M&O. ACC: MOL.20001220.0045.

CRWMS M&O 2000b. *Analysis of Infiltration Uncertainty*. ANL-NBS-HS-000027 REV 00. Las Vegas, Nevada. CRWMS M&O. ACC: MOL.20000525.0377.

Flint, A.L. and Childs, S.W. 1991. "Use of the Priestley-Taylor Evaporation Equation for Soil Water Limited Conditions in a Small Forest Clearcut." *Agricultural and Forest Meteorology, 56,* (3-4), 247-260. Amsterdam, The Netherlands: Elsevier. TIC: 241865.

Flint, A.L.; Flint, L.E.; Hevesi, J.A.; D'Agnese, F.A.; and Faunt, C.C. 2000. "Estimation of Regional Recharge and Travel Time Through the Unsaturated Zone in Arid Climates." *Dynamics of Fluids in Fractured Rock, [Papers Selected from a Symposium held at Ernest Orlando Lawrence Berkeley National Laboratory on February 10-12, 1999].* Faybishenko, B.; Witherspoon, A.; and Benson, S.M.; eds. Geophysical Monograph 122. Pages 115-128. [Washington, D.C.]: American Geophysical Union. TIC: 254272.

Flint, A.L.; Hevesi, J.A.; and Flint, L.E. 1996. *Conceptual and Numerical Model of Infiltration for the Yucca Mountain Area, Nevada*. Milestone 3GUI623M. Denver, Colorado: U.S. Geological Survey. ACC: MOL.19970409.0087.

Flint, L.E. 1998. *Characterization of Hydrogeologic Units Using Matrix Properties, Yucca Mountain, Nevada.* Water-Resources Investigations Report 97-4243. Denver, Colorado: U.S. Geological Survey. ACC: MOL.19980429.0512.

Freeze, R.A. and Cherry, J.A. 1979. *Groundwater.* Englewood Cliffs, New Jersey: Prentice-Hall. TIC: 217571.

French, R.H. 1983. "Precipitation in Southern Nevada." *Journal of Hydraulic Engineering, 109*, (7), 1023-1036. New York, New York: American Society of Civil Engineers. TIC: 238300.

Gilbert, R.O. 1987. *Statistical Methods for Environmental Pollution Monitoring*. New York, New York: John Wiley & Sons. TIC: 252619.

Guertal, W. 2001a. Seepage into Alcove 1. Scientific Notebook SN-USGS-SCI-108-V1. ACC: MOL.20011219.0325.

Guertal, W. 2001b. Seepage into Alcove 1. Scientific Notebook SN-USGS-SCI-108-V2. ACC: MOL.20011219.0326.

Hevesi, J.A.; Flint, A.L.; and Istok, J.D. 1992. "Precipitation Estimation in Mountainous Terrain Using Multivariate Geostatistics. Part II: Isohyetal Maps." *Journal of Applied Meteorology, 31*, (7), 677-688. Boston, Massachusetts: American Meteorological Society. TIC: 225248.

LeCain, G.D. 1997. *Air-Injection Testing in Vertical Boreholes in Welded and Nonwelded Tuff, Yucca Mountain, Nevada.* Water-Resources Investigations Report 96-4262. Denver, Colorado: U.S. Geological Survey. ACC: MOL.19980310.0148.

LeCain, G.D. 1998. *Results from Air-Injection and Tracer Testing in the Upper Tiva Canyon, Bow Ridge Fault, and Upper Paintbrush Contact Alcoves of the Exploratory Studies Facility, August 1994 through July 1996, Yucca Mountain, Nevada*. Water-Resources Investigations Report 98-4058. Denver, Colorado: U.S. Geological Survey. ACC: MOL.19980625.0344.

Levitt, D.G.; Sully, M.J.; and Lohrstorfer, C.F. 1996. *Modeling Evapotranspiration from Arid Environments: Literature Review and Preliminary Model Results.* Las Vegas, Nevada: Bechtel Nevada. TIC: 254273.

Liu, H-H.; Haukwa, C.B.; Ahlers, C.F.; Bodvarsson, G.S.; Flint, A.L.; and Guertal, W.B. 2003. "Modeling Flow and Transport in Unsaturated Fractured Rock: An Evaluation of the Continuum Approach." *Journal of Contaminant Hydrology, 62–-63,* 173–188. New York, New York: Elsevier. TIC: 254205.

Maidment, D.R., ed. 1993. *Handbook of Hydrology*. New York, New York: McGraw-Hill. TIC: 236568.

Mongano, G.S.; Singleton, W.L.; Moyer, T.C.; Beason, S.C.; Eatman, G.L.W.; Albin, A.L.; and Lung, R.C. 1999. *Geology of the ECRB Cross Drift-Exploratory Studies Facility, Yucca Mountain Project, Yucca Mountain, Nevada.* [Deliverable SPG42GM3]. Denver, Colorado: U.S. Geological Survey. ACC: MOL.20000324.0614.

Reamer, C.W. and Williams, D.R. 2000a. Summary Highlights of NRC/DOE Technical Exchange and Management Meeting on Unsaturated and Saturated Flow Under Isothermal Conditions, October 31 – November 2, 2000, Albuquerque, New Mexico. Washington, D.C.: U.S. Nuclear Regulatory Commission. ACC: MOL.20001128.0206.

Reamer, C.W. and Williams, D.R. 2000b. Summary Highlights of NRC/DOE Technical Exchange and Management Meeting on Unsaturated and Saturated Flow under Isothermal Conditions, August 16-17, 2000, Berkeley, California. Washington, D.C.: U.S. Nuclear Regulatory Commission. ACC: MOL.20001201.0072.

Schlueter, J.R. 2003a. "The U.S. Nuclear Regulatory Commission Review of the U.S. Department of Energy Documents Pertaining to Agreement Unsaturated and Saturated Flow under Isothermal Conditions (USFIC).3.02 (Status: Additional Information Needs) and Agreement Total System Performance Assessment and Integration (TSPAI).3.22 (Status: Additional Information Needs)." Letter from J.R. Schlueter (NRC) to J.D. Ziegler, (DOE), February 26, 2003, 030436305, with attachment. ACC: MOL.20030424.0627.

Schlueter, J. 2003b. "Use of Risk as a Basis for Closure of Key Technical Issue Agreements." Letter from J. Schlueter (NRC) to J.D. Ziegler (DOE/YMSCO), January 27, 2003, 0131035890, with enclosure. ACC: MOL.20030227.0018.

SNL (Sandia National Laboratories) 2001. *Software Code: INFIL.* VA_2.a1. DEC Alpha, OpenVMS V7.2-1. 10253-A_2.a1-00.

Sonnenthal, E.L.; Ahlers, C.F.; and Bodvarsson, G.S. 1997. "Fracture and Fault Properties for the UZ Site-Scale Flow Model." Chapter 7 of *The Site-Scale Unsaturated Zone Model of Yucca Mountain, Nevada, for the Viability Assessment.* Bodvarsson, G.S.; Bandurraga, T.M.; and Wu, Y.S., eds. LBNL-40376. Berkeley, California: Lawrence Berkeley National Laboratory. ACC: MOL.19971014.0232.

USDA (U.S. Department of Agriculture) 1994. *State Soil Geographic (STATSGO) Data Base, Data Use Information.* Miscellaneous Publication Number 1492. Washington, D.C.: U.S. Department of Agriculture, Natural Resources Conservation Service, National Soil Survey Center. TIC: 249639.

USGS (U.S. Geological Survey) 2001a. *Simulation of Net Infiltration for Modern and Potential Future Climates.* ANL-NBS-HS-000032 REV 00 ICN 02. Denver, Colorado: U.S. Geological Survey. ACC: MOL.20011119.0334.

USGS 2001b. *Software Code: INFIL.* V2.0. PC. 10307-2.0-00.

van Genuchten, M.T. 1980. "A Closed-Form Equation for Predicting the Hydraulic Conductivity of Unsaturated Soils." *Soil Science Society of America Journal, 44,* (5), 892-898. Madison, Wisconsin: Soil Science Society of America. TIC: 217327.

Wirth, S.; Brown, T.; and Beyeler, W. 1999. *Native Plant Uptake Model for Radioactive Waste Disposal Areas at the Nevada Test Site*. SAND98-1789. Albuquerque, New Mexico: Sandia National Laboratories. TIC: 254423.

Ziegler, J.D. 2002. "Transmittal of Report Addressing Key Technical Issue (KTI) Agreement Item Unsaturated and Saturated Flow Under Isothermal Conditions (USFIC) 3.02." Letter from J.D. Ziegler (DOE) to J.R. Schlueter (NRC), November 22, 2002, 1125025275, with attachment. ACC: MOL.20030213.0112.

E.5.2 Data, Listed by Data Tracking Number

GS000308312242.002. Phase 1 of Water Collection in Alcove 1 from 05/05/98 to 08/27/98. Submittal date: 03/01/2000.

GS000399991221.003. Preliminary Alcove 1 Infiltration Experiment Data. Submittal date: 03/10/2000.

GS000808312242.006. Pulse Flow Meter Data for the Alcove 1 Infiltration Experiment from 02/19/99 to 06/20/00. Submittal date: 09/07/2000.

GS001108312242.009. Tracker Data for the Alcove 1 Infiltration Experiment, Phase II 05/09/99 to 07/05/00. Submittal date: 11/07/2000.

GS990108312242.006. Pulse Flow Meter Data for the Alcove 1 Infiltration Experiment from 03/08/98 to 12/04/98. Submittal date: 01/29/1999.